

AD-A055 642

AIR FORCE INST OF TECH WRIGHT-PATTERSON AFB OHIO SCH--ETC F/G 17/5  
A THEORETICAL ANALYSIS OF CHANGES IN THERMAL SIGNATURES CAUSED --ETC(U)  
DEC 77 J T SMALL  
AFIT/GEP/PH/77-12

UNCLASSIFIED

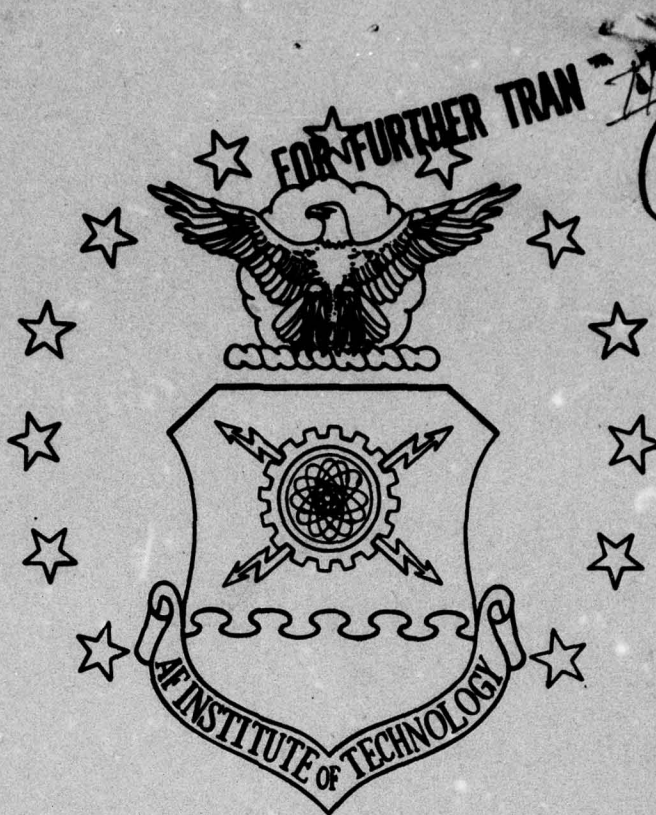
NL

1 OF 3  
ADA  
055642



AD No. \_\_\_\_\_  
DDC FILE COPY

AD A055642



This document has been approved  
for public release and its  
distribution is unlimited.

UNITED STATES AIR FORCE  
AIR UNIVERSITY  
AIR FORCE INSTITUTE OF TECHNOLOGY  
Wright-Patterson Air Force Base, Ohio

78 06 15 069



## **DISCLAIMER NOTICE**

**THIS DOCUMENT IS BEST QUALITY  
PRACTICABLE. THE COPY FURNISHED  
TO DDC CONTAINED A SIGNIFICANT  
NUMBER OF PAGES WHICH DO NOT  
REPRODUCE LEGIBLY.**

GEP/PH/77-12

(1)

AD A055642

DDC  
JUN 21 1978  
RECEIVED  
F

AD No. —

DDC FILE COPY

(6)

A THEORETICAL ANALYSIS OF CHANGES  
IN THERMAL SIGNATURES CAUSED BY  
PHYSICAL AND CLIMATOLOGICAL FACTORS.

THESIS

(11) Dec 77

(14)

AFIT/GEP/PH/77-12

(10)

John T. Small, Jr.  
Capt USAF

(12) 272p

(9) Master's thesis,

Approved for public release; distribution unlimited

78 06 15 069

Ø12 225

JOB

A THEORETICAL ANALYSIS OF CHANGES  
IN THERMAL SIGNATURES CAUSED BY  
PHYSICAL AND CLIMATOLOGICAL FACTORS

THESIS

Presented to the Faculty of the School of Engineering  
of the Air Force Institute of Technology  
Air University  
in Partial Fulfillment of the  
Requirements for the Degree of  
Master of Science

by

John T. Small, Jr., B.A.

Capt

USAF

Graduate Engineering Physics

December 1977



### Preface

This analysis was designed to help answer some questions about thermal signatures. It was a tremendous challenge to me, since I had to begin in an area of Engineering Physics with which I was totally unfamiliar. Now, after gathering together a few basic facts, and building on them with a little curiosity and a lot of time, it is very pleasing to see a result that works, and seems to make sense, albeit with a few rough edges here and there, and maybe a question or two about accuracy.

I would like to thank my thesis advisor, Capt Philip Nielsen, because without him I would undoubtedly still be lost among the trees trying to figure out how to solve the ground conduction equation. Additionally I am very grateful to Lt Col Carl Case, who sponsored this topic, for he has been especially generous with his time and extremely helpful with his suggestions and questions.

Most important, though I would like to thank my wife, Letha, who has encouraged and helped me when she could throughout the whole project, and especially in the last few hectic weeks.

John T. Small, Jr.

ACCESSION for	
WHS	Write Section <input checked="" type="checkbox"/>
DDC	B-41 Section <input type="checkbox"/>
RECEIVED	<input type="checkbox"/>
JUL 1964	
BY	
DISTRIBUTION/AVAILABILITY CODES	
SPECIAL	
A	23 EL

## Contents

	<u>Page</u>
Preface . . . . .	11
List of Figures . . . . .	v
List of Tables. . . . .	viii
Notation. . . . .	ix
Abstract. . . . .	xi
I. Introduction. . . . .	1
Background . . . . .	1
The Problem. . . . .	1
Purpose and Scope of the Study . . . . .	2
II. Theory . . . . .	4
Energy Balance . . . . .	4
Insolation. . . . .	5
Atmospheric Thermal Radiation . . . . .	6
Thermal Radiation of Objects. . . . .	8
Evaporative Heat Transfer . . . . .	9
Convection . . . . .	9
Conduction . . . . .	10
III. Models . . . . .	11
Sun Model . . . . .	11
Atmospheric Thermal Radiation Model . . . . .	13
Air Temperature Model . . . . .	13
Ground Model. . . . .	13
Tank Model. . . . .	17
Leaf Model. . . . .	19
IV. Computer Considerations. . . . .	23
Input Data. . . . .	23
Standard Conditions . . . . .	24
Plot Identification Numbers . . . . .	25
V. Results . . . . .	26
Diurnal Temperature Curves. . . . .	26
Delta-T Curves. . . . .	27
Parameter Sensitivity Curves and Analysis . . . . .	28
VI. Conclusions and Recommendations. . . . .	55

## Contents

	<u>Page</u>
Bibliography . . . . .	57
Appendix A: Comparison of Ground Conduction Model to Analytical Solution Using Sinusoidal Input. . . . .	59
Appendix B: Computer Programs TEMPS and DELTA . . . . .	65
Appendix C: Plots from Program TEMPS for all Parameters . . . . .	87
Appendix D: Plots from Program DELTA for all Parameters . . . . .	209
Appendix E: Sample Target/Background Physical Characteristics .	254
Vita . . . . .	257



# List of Figures

<u>Figure</u>		<u>Page</u>
1	The Solar Spectrum; outside the earth's atmosphere, at 14,000 ft. altitude, and at sea level . . . . .	6
2	Spectral radiance of clear sky from Elk Park, Colorado, several elevations . . . . .	7
3	Spectral radiance of clear sky from Cocoa Beach, Florida, several elevations . . . . .	7
4	Variation of the spectral radiance of the zenith sky with ambient air temperature . . . . .	8
5	The spectral radiance of the sky covered with cirrus clouds at several elevations . . . . .	8
6	Spectral radiance of black body sources at various temperatures as a function of wavelength . . . . .	9
7	Energy balance terms for the ground model . . . . .	14
8	Verification of Eq. (11) . . . . .	15
9	The concept of energy impulse solution to the simplified basic heat conduction equation. . . . .	17
10	Energy balance terms for the tank model. . . . .	18
11	Energy balance terms for the leaf model. . . . .	19
12	Verification of Eq. (17) . . . . .	21
13	Explanation of Plot Set Numbers. . . . .	25
14	Sample Diurnal Temperature Curve for Summer Conditions at 50° Latitude . . . . .	26
15	Sample Delta-T Plot. . . . .	28
16	Changes in Daytime Delta-T caused by variations in mean temperature. . . . .	30
17	Changes in Nighttime Delta-T caused by variations in mean temperature. . . . .	31
17(a)	Key to Curves in Figs. 18(a) to 19(k), including "Standard" Parameter Values. . . . .	32
18	Parameter Analysis; Daytime. . . . .	33
19	Parameter Analysis; Nighttime. . . . .	44

<u>Figure</u>		<u>Page</u>
20	Graph of analytical solution for semi-infinite slab heat conduction equation (Ref21:76). . . . .	60
21	Eq.(14) solution to semi-infinite slab problem, With DT=.25 . . . . .	61
22	Eq.(14) solution to semi-infinite slab problem, With DT=.02 . . . . .	62
23	TEMPS solution with DT=.25. . . . .	63
24	TEMPS solution with DT=.15. . . . .	64
25	Basic Temperature Plots of Mean Temp. . . . .	88
26	Basic Temperature Plots of Absolute Humidity. . . . .	99
27	Basic Temperature Plots of Wind . . . . .	110
28	Basic Temperature Plots of Sun Strength . . . . .	121
29	Basic Temperature Plots of Ground Reflectivity. . . . .	132
30	Basic Temperature Plots of Ground <b>Emissivity</b> . . . . .	143
31	Basic Temperature Plots of Ground Diffusivity . . . . .	154
32	Basic Temperature Plots of Target Reflectivity. . . . .	165
33	Basic Temperature Plots of Target <b>Emissivity</b> . . . . .	176
34	Basic Temperature Plots of Target Thickness. . . . .	187
35	Basic Temperature Plots of A.C. Velocity . . . . .	198
36	Delta-T Plots for Mean Temp . . . . .	210
37	Delta-T Plots for Absolute Humidity . . . . .	214
38	Delta-T Plots for Wind . . . . .	218
39	Delta-T Plots for Sun Strength. . . . .	222
40	Delta-T Plots for Ground Reflectivity . . . . .	226
41	Delta-T Plots for Ground <b>Emissivity</b> . . . . .	230
42	Delta-T Plots for Ground Diffusivity. . . . .	234

<u>Figure</u>		<u>Page</u>
43	Delta-T Plots for Target Reflectivity. . . . .	238
44	Delta-T Plots for Target Emissivity. . . . .	242
45	Delta-T Plots for Target Thickness . . . . .	246
46	Delta-T Plots for A. C. Velocity . . . . .	250
47	Typical Reflectance of Water Surface, Snow, Dry Soil, and Vegetation . . . . .	256



## List of Tables

<u>Table</u>		<u>Page</u>
I.	Parameters for Cloud Types . . . . .	12
II.	Standard Climatic Conditions for Three Model Locations. . . . .	24
III.	Parameter Identification Numbers . . . . .	25
IV.	Summary of Parameter Strengths for Eleven Hypothetical, Geographic, and Climatic Conditions. . .	55
V.	Overall Day and Night Parameter Strength Rating. . . .	56
VI.	Sample Target/Background Characteristics . . . . .	255

### Notation

$A(\text{Temp})$	Portion of Grashof Number that represents buoyancy of fluid
$C_d$	Heat Transfer due to conduction
$C_p$	Thermal Heat Capacity at constant pressure ( $\text{Cal}/\text{gm}^\circ\text{C}$ )
CTEMPA	Computer variable for air temperature
CTEMPI	Component used in calculating the air temperature
$C_v$	Heat Transfer due to convection
$C_{v,\text{in}}$	Heat convection inside the tank model
$C_{v,\text{out}}$	Heat Convection outside the tank model
$D$	Diffusivity ( $\text{cm}^2/\text{min}$ )
$\Delta T$	Temperature difference between two objects
$\delta$	Ratio of molecular weights also sun declination angle
$\epsilon$	<b>Emissivity</b> , or small time increment
$E$	Net energy deposited on a surface ( $\text{cal}/\text{cm}^2\text{-min}$ )
$E_v$	Total energy in a volume $V$ of substance
$E_{\text{net}}$	Net energy stored in an impulse in time $dt$
$E_{\text{surf}}$	Energy per unit volume at the surface of the ground
$E_{\text{sat}}$	Saturated water vapor pressure (millibars)
$e_s$ or $e_a$	Vapor pressure at earth's surface or in the air ( <b>respectively</b> )
$\phi$	Latitude in degrees
$\mu$	Viscosity of the air
$h_c$	Heat transfer coefficient (general)
$h_{c,\text{force}}$	Heat transfer <b>coefficient</b> due to forced convection
$h_{c,\text{free}}$	Heat transfer <b>coefficient</b> due to free convection

K	VonKarmon's constant (.41)
$^{\circ}\text{K}$	Degrees Kelvin
LE	Energy loss due to evaporation of moisture
Pr	Prandtl number (Approximately = .72 for air)
R	Total radiation of a body
$R_1$	Thermal radiation gain due to surrounding radiating objects
$R_o$	Thermal radiation loss of objects
RH	Relative Humidity (0 to 100%)
Re	Reynolds number
RSOIL	Reflectivity of the soil
S	Insolation due to Sun at earth's surface corrected for clouds and orientation angle
$S_t$	Atmospheric Thermal radiation
$S_p$	Total sun's energy on an object which is perpendicular to the sun's rays
$S_o$	Insolation on an object oriented parallel to the ground (uncorrected for clouds)
$\rho$	Density of an object
$\rho_a$	Density of the air
$\theta$	Time
$\sigma$	Stefan-Boltzmann constant
u	velocity of the air (cm/sec)
x	distance in cm
$Z_a$	Sensor height (for measuring wind or temperature)
$Z_o$	Roughness parameter (about .025 cm for smooth surfaces)



Abstract

An investigation of the thermal signatures of natural objects is undertaken. Using the principle of energy balance, diurnal temperature models are developed for the ground, a vehicle (such as a tank), and the leaves of a tree. These models are included in a computer program designed to simulate daily variations in conductive, radiative, and convective heat transfer processes.

Environmental conditions are changed by altering the program inputs, which include; latitude, day, wind speed, mean air temperature, cloud type, total insolation, absolute and relative humidity, atmospheric pressure, and particulate concentration. The program is iterated for several values of a single parameter such as one of the environmental inputs, or one of 21 physical characteristics of the models (for example; ground reflectivity, tank thickness, or leaf transpiration rate). There are two types of output from the program; simultaneous plots of the temperatures of all the models for a 30-hour period, and curves representing 24-hour periods of the temperature difference ( $\Delta T$ ) between the tank and the ground. The effects of changing a parameter are analyzed by comparing the various  $\Delta T$  curves.

In this study, 11 scenarios (representing three geographic locations and a variety of climatic conditions) are used to examine the following parameters; mean temperature, absolute humidity, wind speed, cloud cover, ground/target reflectivity and emissivity, ground diffusivity, target thickness, and tank air conditioning velocity. Analysis of the  $\Delta T$  curves indicates that overall, the ground emissivity appears to affect the temperatures the most, while the amount of insolation affects them the least.

A THEORETICAL ANALYSIS OF CHANGES  
IN THERMAL SIGNATURES CAUSED BY  
PHYSICAL AND CLIMATOLOGICAL FACTORS

I. Introduction

Background

Although thermal imaging systems have been used since the 1940's, accurate ways of predicting the thermal signatures of target backgrounds have not been developed (Ref 1:267). Modern infrared imaging devices can detect the temperature differences between objects such as trees, fields, roads, tanks and trucks, and can convert these thermal contrast differences into a visual display on a screen. Because such equipment is an integral part in the development of new missile systems like the Air Force Imaging Infrared Maverick and the Army Hellfire, it is important to have an understanding of what environmental factors drive the temperature differences of the objects detected by these infrared devices. A knowledge of the physics behind thermal signatures can increase the insight into what infrared images should look like under various conditions. This insight should be helpful not only to scientists gathering data on infrared image characteristics, but also to system operators trying to identify particular targets.

The Problem

In spite of the accuracy of current infrared systems, incorrect target signature prediction has still caused problems. For example, in one test of the Maverick missile, inaccurate aiming occurred, even

though the crew-members had studied videotapes of infrared images made in Western Europe. These tests were monitored by the Office of the Assistant Chief of Staff for Studies and Analysis, Air Force Headquarters, Washington, D.C.. After reviewing the results, a member of that office, Lt Col Carl Case, suggested that a study be started to investigate the physical processes of thermal heating, with the premise that a better understanding of the physics involved may lead to better prediction of target signature characteristics under varying environmental conditions.

Unfortunately, current work on thermal signatures has been restricted to very specific areas, and has been concentrated on a single item such as a tank (Ref 2), or the ground (Ref 3; Ref 4). There does not seem to be a study using several items in a scenario to determine how their interrelated temperature differences would change under a variety of environments.

#### Purpose and Scope of the Study

This analysis applies heat transfer principles in a computer model to determine the key driving factors behind the daily and seasonal temperature differences of various objects and their backgrounds. The models that are developed simulate heat transfer processes at the surfaces of the ground, a tank, and the leaf of a deciduous tree. The study is kept very general, since specific results have only limited applicability and may require lengthy, detailed, computer coding. By relying on a theoretical, physical appraisal, as opposed to a complex mathematical solution, the output of the analysis will be a series of graphs showing how thermal signatures vary with certain general parameters (to be described later) rather than a precise method of predicting temperatures at specific times.



Two computer programs will be used. The first program (TEMPS) calculates and graphs a 30 hour, diurnal temperature profile of the air temperature, and the tank, ground, and tree models. The second program (DELTA) computes the same temperature cycles and plots out the difference between the tank and the ground temperature from the 6th to the 30th hour.

Both programs are set up to iterate four times in each run, and a selected parameter is varied for each iteration. The tank/ground temperature difference ( $\Delta T$ ) is noted at the 14th and 24th hour (representing times of high and low heat-loading, respectively) for all values of the various parameters. These data are then graphically compared and analyzed to determine the relative effect that each parameter has on  $\Delta T$ .

## II. Theory

The temperature of an object arises primarily due to the kinetic energy of its molecules. In a natural setting, this energy is distributed through a complex energy balance with the environment. This balance changes continually, depending upon the object itself, its location, the time of year, the time of day, and the existing meteorological conditions.

### Energy Balance

If the amount of random, or thermal energy per volume of substance can be determined, then the temperature of the object can be calculated through the relation:

$$T = \frac{E_v}{\rho C_p V} \quad (1)$$

where  $E_v$  is the thermal energy contained in a volume  $V$  of material with density  $\rho$  and a thermal heat capacity at constant pressure,  $C_p$ . Because of the complex interrelationships of internal and external factors it is extremely difficult to determine the precise amount of energy flow into and out of an object at a specific time. As a result, determining exact temperatures from the net energy remaining with the object is also difficult.

However, by setting up an equation which represents the energy flow of various heat transfer processes (Ref 5:3), a model can be generated to determine the relative significance of those processes. The above technique is used in the models of this study and the fol-

lowing energy balance equation is assumed:

$$E = S + S_t + R_i - R_o - LE \pm C_v \pm C_d \quad (2)$$

(All terms in gram-calories per  $\text{cm}^2$  per min)

Where  $E$  = the net energy being deposited at the surface  
 $S$  = the solar insolation (direct, scattered and reflected)  
 $S_t$  = incident thermal radiation from the atmosphere  
 $R_i$  = thermal radiation gain due to surrounding objects  
 $R_o$  = thermal radiation loss of the object  
 $LE$  = energy loss due to evaporation of moisture from surface  
 $C_v$  = energy loss (gain) due to free or forced convection  
 $C_d$  = energy loss (gain) due to thermal conduction.

In all cases the convention of a plus sign means flow into the body.

Other terms that represent such processes as heat generated by internal sources (a running engine, for example) can be added to Eq (2), but will not be included explicitly in the models of this study. (An "engine" can be simulated by assuming a higher interior temperature). Because of various conditions, some terms in Eq (2) may not be used in certain models. Descriptions of the energy balance terms and their associated heat transfer processes follows.

#### Insolation (S)

The main thermal energy supply to objects on the earth comes from the sun. The sun's radiation can be approximated by a  $6000^\circ \text{K}$  black body, and at the outer edge of the earth's atmosphere it has an intensity of about  $2.0 \text{ cal/cm}^2\text{-min}$  (Ref 6). After propagating through



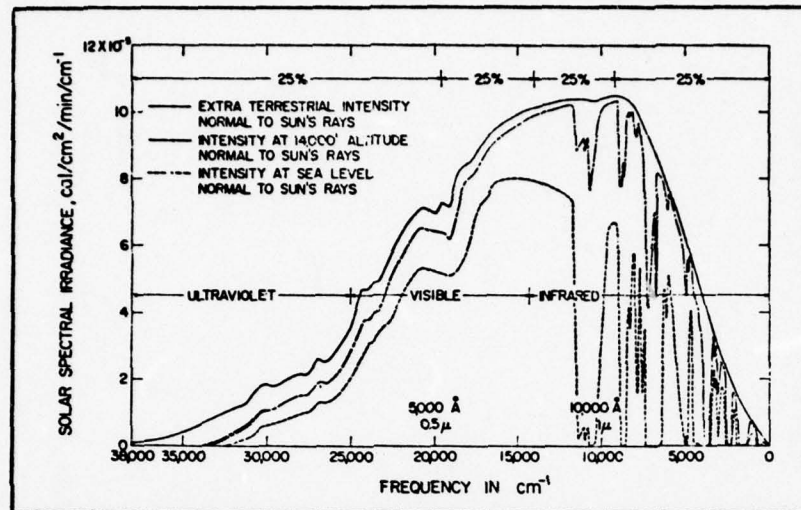


Fig. 1. The solar spectrum; outside the earth's atmosphere, at 14,000 ft altitude, and at sea level (Ref 5:49)

the atmosphere, however, absorption and scattering has reduced it by one half, and the spectral characteristics are modified considerably. Figure 1 shows that the largest part of incident energy is in the visible and near infrared region, thus, for radiation heat purposes, the spectral properties of objects at these wavelengths are critical.

The amount of scattering and absorption is further related to the distance of transmission through the atmosphere and this depends on the time of year and time of day for each point on the globe. Hence, to arrive at the amount of solar energy impinging upon an object at a certain time, some of the factors that must be known are; latitude, astronomical (or sun) time, amount of water vapor in the atmosphere (a key absorber in the infrared), amount of particulate matter in the air (a cause of scattering) and the type and amount of cloud cover.

#### Atmospheric Thermal Radiation ( $S_t$ )

The atmosphere absorbs and scatters the sunlight which passes

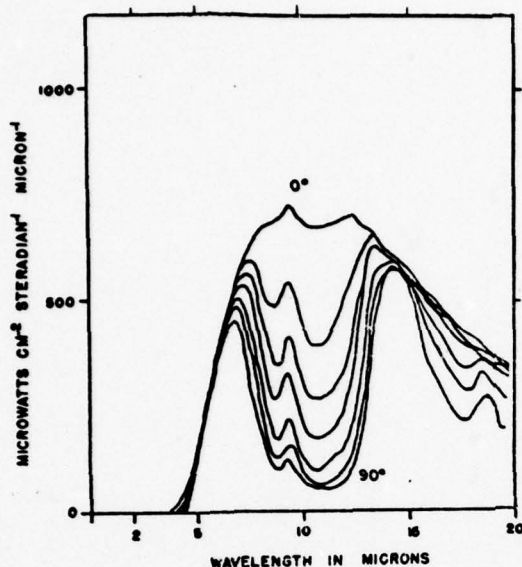


Fig. 2. Spectral radiance of clear sky from Elk Park, Colorado, several elevations. (Ref 7:1315)

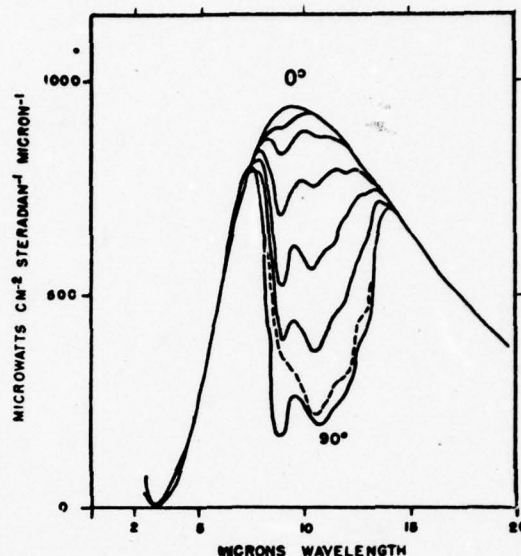


Fig. 3. Spectral radiance of clear sky from Cocoa Beach, Florida, several elevations. (Ref 7:1316)

through it. Additionally the molecules re-radiate thermally at long wavelengths (8-12 microns) like a grey body with an emissivity that depends on the amount of gasses (particularly water vapor and carbon dioxide) present. The sky radiance is highly dependent upon the elevation angle, since the effective thickness of the atmosphere is least when measured directly overhead. The influence of the climate and elevation angle is shown in Figs. 2 and 3, where the drier air in Fig. 2 exhibits a lower peak. Since the molecular activity depends greatly upon the temperature, the ambient air temperature also has a strong influence on the radiance, as shown in Fig. 4. The presence of clouds (Fig. 5) primarily tends to increase the amount of radiance in the zenith direction, which also increases the total amount of sky thermal radiation received by the earth.

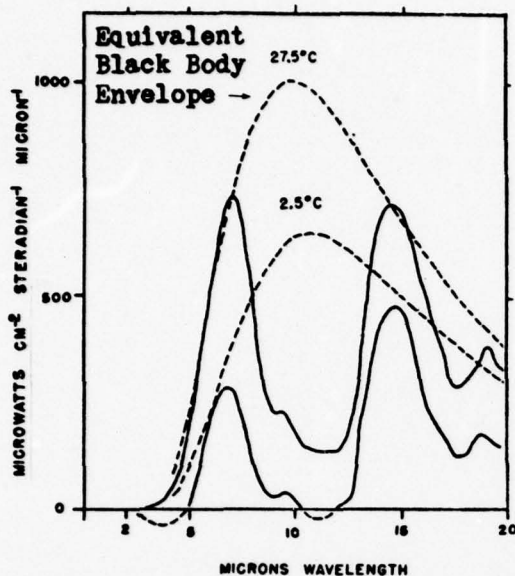


Fig. 4. Variation of the spectral radiance of the zenith sky with ambient air temperature (Ref 7:1316)

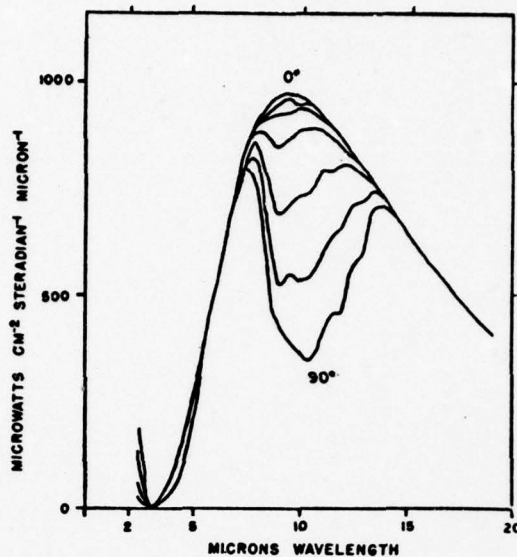


Fig. 5. The spectral radiance of the sky covered with cirrus clouds at several elevations. (Ref 7:1318)

#### Thermal Radiation of Objects ( $R_i$ and $R_o$ )

All objects above absolute zero give off thermal radiation due to Random, molecular activity. The total amount of radiation given off is determined by the Stefan-Boltzmann law

$$R = \epsilon \sigma T^4 \quad (3)$$

Where  $\epsilon$  is the emissivity of the object which characterizes its emission compared to that of a perfect black body,  $\sigma$  is the Stefan-Boltzmann constant of  $7.93 \times 10^{-9}$  cal per  $\text{cm}^2$  per  $^\circ\text{K}^4$  per minute ( $5.67 \times 10^{-5}$  erg per  $\text{cm}^2$  per  $^\circ\text{K}^4$  per second) and  $T$  is the temperature of the object in  $^\circ\text{K}$ . The spectral distribution of thermal radiation is governed by the Planck radiation law and the wavelength of peak emission for most natural objects is in the 8 to 10 micron region as shown in Fig. 6. The constant loss of energy by thermal radiation is one of



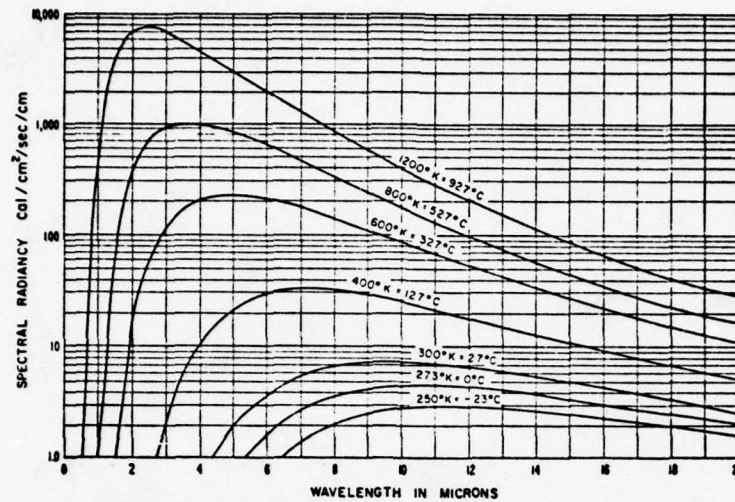


Fig. 6. Spectral radiance of black body sources at various temperatures as a function of wavelength (Ref 3:62).

the major, natural mechanisms for temperature regulation in objects.

$R_0$  represents the outgoing thermal radiation of the object considered and  $R_i$  is the incoming thermal radiation due to other nearby thermal sources other than the atmosphere.

#### Evaporative Heat Transfer ( $LE$ )

When one gram of water is converted from liquid to vapor, approximately 600 calories of heat is needed. Thus, the evaporation process that occurs at the surface of a leaf, or at the top of the soil is capable of removing a significant amount of thermal energy, and reducing the temperature at the surface. The amount of evaporation is governed by natural factors such as the diffusion resistance. This term characterizes the rate of fluid transport to the surface, and since its value can vary greatly, so can the quantity of evaporative cooling.

#### Convection ( $C_v$ )

Convection is a method of heat transfer caused by the mixing of

fluids of different temperatures (and hence different densities). During convection, the flow of heat across a temperature gradient is generally enhanced because the fluids on each side of the gradient are mixed in the process. There are two types of convection, free convection, where the movement is caused by the temperature-related buoyancy of the air, and forced convection, where a large-scale mass movement, such as wind, is involved. Both types of convective heat transfer depend on the shape and orientation of the object, as well as the temperature difference between it and the surroundings.

#### Conduction ( $C_d$ )

Heat transfer by conduction depends on the direct exchange of kinetic energy between molecules. The rate of this transfer is highly dependent upon the physical makeup (thermal conductivity) of the substance and the temperature difference across the conducting path. Hence the contribution of conduction to the overall energy balance may vary widely.

It is assumed that the time dependence of conductive heat transfer follows the classic heat equation (Ref 8:III-18)

$$\frac{dI}{d\theta} = D \frac{\partial^2 I}{\partial X^2} \quad (4)$$

Where  $I$  is the temperature,  $X$  is the distance below the surface,  $\theta$  is the time, and  $D$  is the thermal diffusivity.

Simplifying the geometry of the models will allow the use of a one dimensional solution to Eq (4). Thin, highly conductive objects will reach equilibrium quickly so Eq (4) will not be necessary. In such cases temperature can be determined by energy balance alone.

### III. Models

In order to analyze the effect that various physical parameters and climatological conditions have on Delta-T (the temperature difference of an object relative to its background) it is necessary to develop models for at least two different media. Because of the military interest in using infrared systems for tank detection, the models used are intended to give a rough representation of tank thermal signatures. These models encompass; the ground, a tank, and the leaves of a deciduous tree. Each of these will be discussed in this section; however, first will come a description of some other models needed to simulate the sun's strength, the atmospheric thermal radiation, and the air temperature.

#### Sun Model

The solar zenith angle, with respect to the normal at the earth's surface,  $z$ , can be calculated from the following equation (Ref 3:58):

$$\cos(z) = \sin(\phi)\sin(\delta) + \cos(\phi)\cos(\delta)\cos(h) \quad (5)$$

Where  $\phi$  is the latitude (+ is north),  $\delta$  is the sun's declination, and  $h$  is the sun's hour angle. The angle  $\phi$  is given as one of the inputs to the computer program, and  $\delta$  is calculated from a curve fit of the data in the Air Almanac (Ref 9) using:

$$\delta = \left[ \frac{\text{Day}}{183} \times 52.88 \right] - 26.44 \quad (\text{for: } 0 \leq \text{Day} \leq 183) \quad (6a)$$

$$\delta = 26.44 - \left[ \frac{\text{Day}}{365} \times 52.88 \right] \quad (\text{for: } 184 \leq \text{Day} \leq 365) \quad (6b)$$

Where Day is the Julian date.



The hour angle is assumed to be set so that 12:00 noon occurs when  $h = 90^\circ$ . Thus, there is no correction for local time (longitude).

The strength of the sun on a flat surface at the ground and perpendicular to the sun's rays is calculated using an equation developed after Brooks (Ref 10:264):

$$S_p = 2.0 \exp \left[ -.089 \left[ \frac{pm}{1013} \right]^{.75} -.174 \left[ \frac{wm}{20} \right]^{.6} -.083 [dm]^{.9} \right] \quad (7)$$

cal /cm<sup>2</sup>-min

Where  $p$  = air pressure (mb)

$w$  = total precipitable water vapor in the atmosphere in the zenith direction (mm)

$d$  = concentration of particulate matter (particles/cm<sup>3</sup>)

$m \approx$  secant of the zenith angle.

To correct this value for a horizontal surface,  $S_p$  is multiplied by the result of Eq. (5);  $S_0 = S_p \cos(z)$ . A final adjustment for the amount of insolation comes from the effect of clouds, and is contained in an empirical formula by Haurwitz (Ref 11:112):

$$S = S_0 \left[ \frac{a}{94.4} \right] \exp \left[ -m(b-.059) \right] \quad (8)$$

Where  $m$  is the secant of the zenith angle,  $a$ , and  $b$  are parameters based on cloud type (See Table I).

Table I  
Parameters for Cloud Types (Ci, cirrus; Cs, cirrostratus; Ac, altocumulus; As, altostratus; Sc, stratocumulus; St, stratus; Ns, nimbostratus)

	Ci	Cs	Ac	As	Sc	St	Ns	Fog
$a$	82.2	87.1	52.5	39.0	34.7	23.8	11.2	15.4
$b$	.079	.148	.112	.063	.104	.159	-.167	.028

(From Ref 3:56)

### Atmospheric Thermal Radiation Model

As previously mentioned, there are many variables affecting the thermal radiation of the atmosphere. Complex, analytical solutions have been developed for this problem, but they require detailed data for the calculations. For this study, a simple empirical formula, developed by Ångström for a clear sky is used (Ref 12):

$$S_t = \sigma T^4 (0.81 - .2411 \times 10^{-.052 ea}) \quad (9)$$

Where  $ea$  is the partial pressure of water vapor at ground level in millibars (calculation of  $ea$  will be discussed later).

### Air Temperature Model

An exact model for daily air temperatures is difficult due to the effects of such meteorological conditions as winds and fronts. Nevertheless an arbitrary diurnal cycle was chosen using the temperature profiles noticed in the literature (Ref 13:78; Ref 14:109; Ref 15:43-46). Care was taken to attempt to preserve the times of occurrence of maximum and minimum temperatures.

$$CTEMPA = CTEMP1 + 10 \sin\left(\pi\left(1.05 + \frac{t}{12}\right)\right) + 2.5 \sin\left(\pi\left(1.5 + \frac{t}{12}\right)\right) \quad (10)$$

Where  $CTEMPA$  is the air temperature in  $^{\circ}C$  at time,  $t$ ,  $CTEMP1$  is a "DC" term to shift the temperature according to the season and latitude, and  $t$  is the time of day, in hours, since midnight.

### Ground Model

The ground is assumed to be a barren, semi-infinite slab, composed of thermally homogeneous and isotropic soil. This simplifies the ground heat conduction solution, so that, providing the energy balance

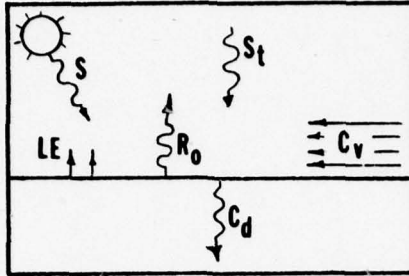


Fig. 7. Energy balance terms for the ground model.

remains uniform along the boundary, the direction of heat flow will be one dimensional. Figure 7 identifies the energy balance terms that are assumed to be significant for the ground model.

The insolation ( $S$ ) and atmospheric long-wave radiation ( $S_t$ ) are equal to the values computed from their respective models, depending on the time of day and conditions. The rate of thermal heat loss ( $R_0$ ) from the surface is based upon Eq. (3), using the ground temperature calculated in the previous program time increment and an emissivity that is set at the beginning of the computer run.

Use of analytical convective heat transfer equations for the ground model fail due to a dependence upon the "characteristic length" (the dimension of the object in the direction of flow; which is infinite for the ground model). Van Bavel (Ref 17:85) was also unable to derive an applicable ground model formula. Thus, the forced convection coefficients in this study are from an empirical formula, Eq (11), based on convection data over a flat surface (Ref 18:538). The free convection coefficient also comes from Eq (11), with the wind speed set at zero. This value was checked by inserting it in a standard equation (Ref 16:296) and solving for the characteristic length. The resulting dimension of 85 cm is large compared to typical data (Ref 16) and so for the "infinite" ground it appears that the empirical formula is also



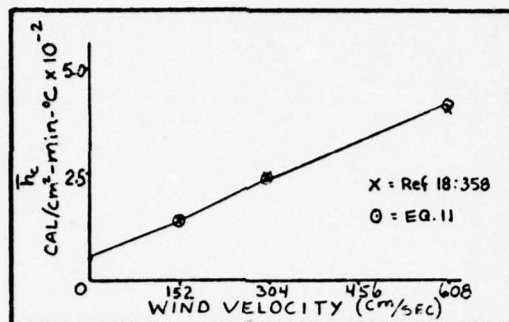


Fig. 8. Verification of Eq. (11)

a reasonable approximation for free convection. The formula used is;

$$\bar{h}_c = \left[ 1.8 + \left[ \frac{[\text{Speed} - 152.4]}{304.8} \right] (2.4) - \left[ \frac{[\text{Speed} - 152.4]}{1371.6} \right]^2 (2.6) \right] (8.136 \times 10^{-3}) \quad (11)$$

$\text{Cal/cm}^2\text{-min-}^\circ\text{C}$

Where Speed is the velocity of the air over the surface.

The expression for (1E) is used from Van Bavel (Ref 17:7)

$$1E = (L) \frac{\rho_a \delta k^2 u}{P [\ln(Z_a/Z_0)]^2} (60(es - ea)) \quad (12)$$

$\text{Cal/cm}^2\text{-min}$

Where  $L$  = Latent heat of Vaporization ( $\approx 600 \text{ Cal/gm}$ )

$\rho_a$  = Density of air ( $\text{gm/cm}^3$ )

$k$  = Von Karman's Constant (.41)

$\delta$  = Water/air molecular weight ratio (.622)

$u$  = Velocity of air ( $\text{cm/sec}$ )

$P$  = Atmospheric pressure (mb)

$Z_a$  = Air sensor height (100 cm)

$Z_0$  = Roughness length (.025 cm)

$es/ea$  = Water vapor pressure at ground/air (mb)

$Z_a$  was arbitrarily chosen to be 100 cm as a representative height at which temperature can be measured, the value for  $Z_0$  is from Van Bavel

(Ref 17:85) and is representative of bare soil. Saturated vapor pressure ( $e_{sat}$ ) is calculated from an empirical formula by Brunt (Ref 19:104):

$$e_{sat} = \text{Exp} \left[ \left[ \frac{1}{273} - \frac{1}{T_{sat}} \right] (5423) \right] (e_o) \quad (\text{mb}) \quad (13)$$

Where  $T_{sat}$  is the temperature of the saturated vapor in  $^{\circ}\text{K}$  and  $e_o$  is the water vapor pressure of saturated air at  $0^{\circ}\text{C}$  (6.1071 mb). This vapor pressure must then be corrected for relative humidity using the following (Ref 20:162):

$$e_a = e_{sat}(\text{RH}/100) \quad (14)$$

Where RH is the relative humidity from 0 to 100%. An expression similar to Eq (14) is used for  $e_s$  except that instead of relative humidity the moisture content of the ground (in percent by weight) is substituted for RH.

At this point in the model all the energy terms for the ground are summed ( $S + S_f - R - [E \pm C_v]$ ) to give a net flow of energy ( $E_{net}$  in  $\text{cal}/\text{cm}^2\text{-min}$ ) which is then used to calculate the amount of thermal heat conduction. Carslaw and Jaeger (Ref 21) have developed many analytical solutions to heat conduction; however, most of the input heat fluxes are explicit functions of time. Because of the activity of clouds and winds, the net heat flux into the ground may not be a smooth, continuous, curve, so an approximation to the solution can be assumed as follows:

Eq (4) becomes:

$$\frac{I}{\theta} \approx \frac{I}{x^2} D$$

Yielding:

$$x \approx \sqrt{D\theta} \quad (13)$$

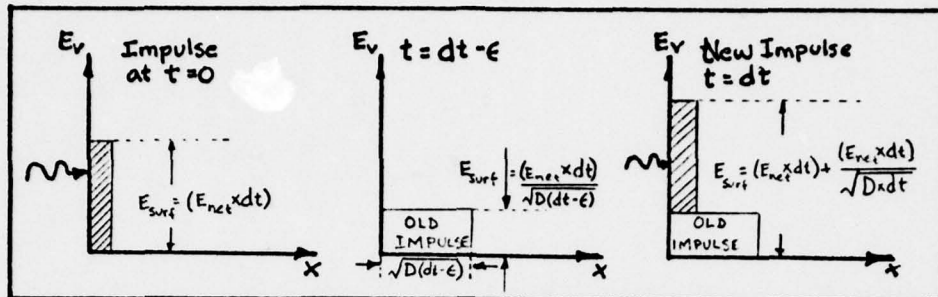


Fig. 9. The concept of the energy impulse solution to the simplified basic heat conduction equation.

Eq. (13) represents an approximate distance,  $\lambda$  that a heat wave will travel through a medium with diffusivity,  $D$  in a time  $\theta$ .

If the net energy flow,  $E_{net}$  is "stored up" and deposited as an impulse every "dt" minutes, then each impulse will diffuse into the soil between intervals (see Fig. 9). This will cause a net "piling-up" of energy at the surface. The net amount of energy that remains at the surface after  $N$  impulses can be expressed as:

$$E_{surf} = \sum_{m=1}^{N-1} \frac{[E_{net}(dt)]}{\sqrt{D(m(dt))}} + [E_{net}(dt)] \quad (14)$$

This net energy gain is then used in Eq (1) to calculate the net temperature difference at the earth's surface. Eq. (14) has been tested against the analytical solution for a sinusoidal heat flux input (Ref 21:76) with good results (see Appendix A). The computer ground model has one additional computation included to allow for the reverse flow of energy when the sub-terrainian temperature is greater than at the surface.

#### Tank Model

The tank model consists of a hollow, rectangular box assumed to be made of iron, 3 in (7.62 cm) thick. The height of the box is



considerably smaller than the length or width so that the heat flux contribution from the sides is considered to be negligible. The top of the box facing the sky is the surface of primary interest for temperature considerations. Although the bottom surface receives long-wave radiation from the ground, it is assumed that this heats the lower surface, causing it to radiate, but only enough to approximately balance the radiation from the heated upper surface. (Under high heat-loading this simplification may cause the computed temperature of the upper surface to be erroneously high). The dominant heat factors considered are shown in Fig. 10.

The thickness of the skin is such that it reaches equilibrium within the time increments of the overall program (usually 15 minutes). This can be verified by solving Eq (13) for  $\theta$  and using the diffusivity of iron and substituting  $\lambda = 7.62$  cm. In this case,  $\theta$  turns out to be about 8 minutes for the heat wave to travel through the skin.

The computations for  $S$ ,  $S_t$ ,  $R_o$  and  $C_{v,out}$  are the same as for the ground model. The addition of the term  $C_{v,in}$  is to include the simulation of heat exchange with the atmosphere inside the tank. The

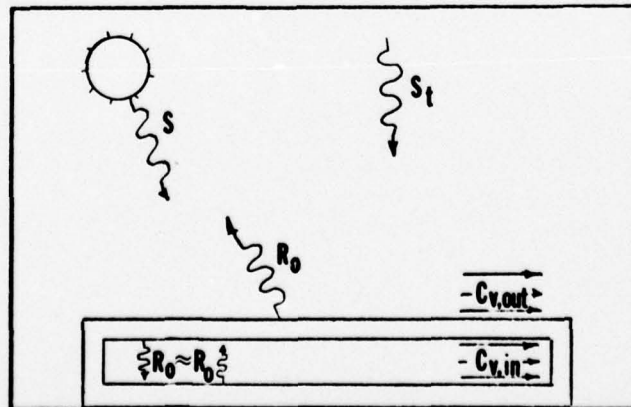


Fig. 10. Energy balance terms for the tank model.

atmosphere is assumed to be air conditioned at  $27^{\circ}\text{C}$ , and is kept moving at a velocity of 447 cm/sec. Although this model appears to be extremely simplified, it roughly parallels a very successful technique used by the Army Night Vision Laboratories, where the temperature signatures of tanks and trucks are area-weighted to arrive at a single, overall  $\Delta I$  that is then used to characterize each vehicle (Ref 22). Computation of  $C_{v,in}$  is the same as for  $C_{v,out}$ , using Eq. (11).

#### Leaf Model

The leaf model is assumed to be a flat plate that is suspended parallel to the ground and is fully exposed to the sky and ground for the complete 30 hour cycle. This would be typical of an outer leaf located on a lower branch of a tree. The thickness is small, so that a time independent solution is valid. Figure 11 indicates what are considered to be the primary heat transfer terms for the leaf. Note that both sides make significant contributions to the energy balance equation.

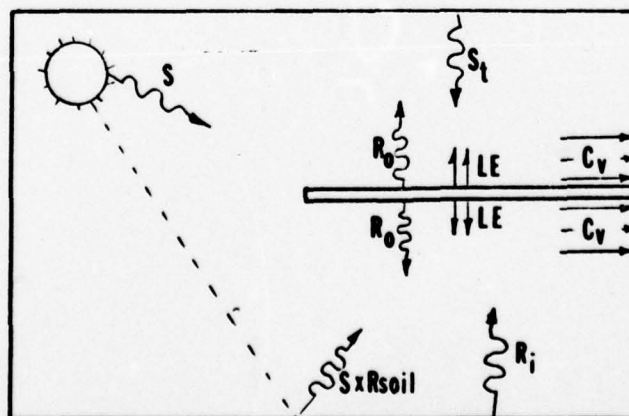


Fig. 11. Energy balance terms for the leaf model.

The upper surface of the leaf receives the direct portion of insolation ( $S$ ) and the atmospheric thermal radiation ( $S_t$ ). The lower surface intercepts not only the thermal radiation of the ground ( $R_g$ ), but also a portion of the insolation that has been reflected off the ground ( $S \times \text{Reflectivity of the Ground}$ ).

Outgoing energy from the leaf's top and bottom sides leaves in the form of thermal radiation ( $R_o$ ), evaporation through transpiration ( $LE$ ) and convection ( $C_v$ ). The processes of all the heat exchange terms are the same as in the previous models, except for small differences in the convection and evaporation terms.

The geometry of a leaf is such that it applies to the basic equations for heat transfer by convection. Thus a distinction must be made between the free and forced convection regimes. The heat transfer coefficient for free convection over a flat plate is (Ref 5:100)

$$\bar{h}_{c,free} = \frac{\text{Const}}{L} (\text{Gr} (\text{Pr}))^{.25} \quad (15)$$

Where  $L$  is the characteristic length of the plate (leaf),  $\text{Pr}$  is the Prandtl number of the air ( $\approx .72$  for temperatures between 0 and 100  $^{\circ}\text{C}$ ), and  $\text{Gr}$  is the Grashof number.

But 
$$\text{Gr} = A(\text{Temp}) (\Delta T)(L)^3 \quad (16)$$

Where  $A(\text{Temp})$  is a buoyancy term that is a function of the temperature and pressure. A curve-fit relation for the values of  $A(\text{Temp})$  has been included in the program using data from Kreith (Ref 16:595):

$$A(\text{Temp}) = 2.04 \left[ \frac{2.03 - [.007 (\text{Ctempa})]}{[.145 + [.0009 (\text{Ctempa})]]^2} \right] \quad (17)$$



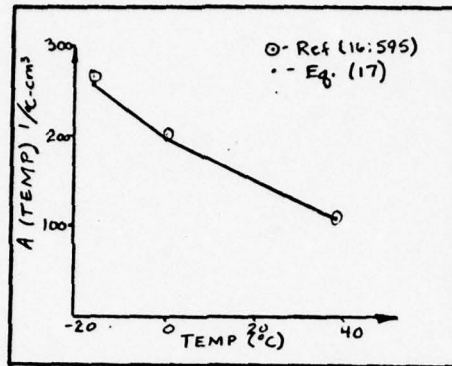


Fig. 12. Verification of Eq. (17)

Agreement for Eq. (17) is shown in Fig. 12. Using the results of Eq. (17) leaves the following relationship for free convection;

$$\bar{h}_{c,free} = \text{Const} \left[ \frac{A(\text{Temp}) (\Delta T) (\text{Pr})}{L} \right]^{.25} \quad (18)$$

For forced convection, the heat transfer coefficient is related by (Ref 16:296):

$$\bar{h}_{c,force} = \frac{\text{Const}}{L} (\text{Re})^{.5} (\text{Pr})^{.33} \quad (19)$$

Where Re is the Reynolds number and is computed from;

$$\text{Re} = \frac{\rho_a u L}{\mu} \quad (20)$$

Where  $\mu$  is the absolute viscosity of the air (gm/cm-sec) and  $u$  is the air velocity (cm/sec). Using the ideal gas law to calculate  $\rho_a$  and a curve-fit equation for  $\mu$ , fitted to within .5% of a set of tables (Ref 18:11) for temperatures between 240 and 330 °K, the forced convection coefficient is then computed (once the air temperature, air velocity and leaf dimension are known) using;

$$\bar{h}_{c,force} = (\text{Constant}) (\text{Pr})^{.33} \left[ \frac{u \rho_a}{\mu L} \right]^{.5} \quad (21)$$

The program compares the values of  $\bar{h}_{c,free}$  and  $\bar{h}_{c,force}$  and the higher of the two is used for computation.

Evaporation (lf) at the leaf surface is accomplished through transpiration, which depends upon the quantity of water pumped to the leaf's surface, and is controlled by the plant's physiology. In this process, moisture reaches the outside of the leaf through pore-like cells, called stomata. "Guard cells", at the opening of these pores, act as valves to regulate how fast the water reaches the surface, where evaporation (and hence cooling) can take place. The amount of water transported can vary from 0 to 0.001 gm/cm<sup>2</sup>-min (Ref 25,994), depending upon the type of plant, its "health", and the heat-loading conditions. The model in this study is designed to follow the leaf temperature cycles indicated by Gates (Ref 24,82).

The transpiration rate is very near zero at night, and if winds are light, the leaf can cool down below the air temperature by radiation alone. After sunrise, the heat-loading increases, as does the leaf temperature, and transpiration starts when the leaf temperature reaches the air temperature. This condition is maintained by regulating the transpiration rate to provide sufficient cooling moisture. If the heat-load demand exceeds a preset maximum transpiration rate, the leaf temperature will rise above the air temperature to an equilibrium based on energy balance. Later in the day, transpiration decreases as the heat-loading goes down and the leaf temperature reaches the air temperature. Eventually, at night, the transpiration rate drops to zero, and the leaf temperature is again controlled by energy balance.

#### IV. Computer Considerations

In general, both of the programs used (See Appendix B) do the same computations, their basic difference being that program TEMPS plots out the original temperature curves for the air, tank, ground and leaf models, and program DELTA plots the temperature difference between the target (tank) model and the ground model. The programs are set up to vary one parameter over a range of four values for each run. The programs must be changed slightly when a different parameter is selected. These changes amount to altering the input reading cards so that they are set up for the proper variable and putting the proper title name into some of the graph commands.

##### Input Data

Input can be read-in either by cards or by terminal. All input is unformatted, since a list directed read command is used. The organization for the input variables is shown in Appendix B. The number of runs is controlled by the variable NGRAPHS. There must be one complete set of data cards (11 cards total) for each run. These cards set up the initial conditions concerning the location, climate and physical make-up of the models, such as reflectivity and emissivity.

A single run (NGRAPHS = 1) with program TEMPS will produce a set of four graphs of basic, 30-hour temperature profiles. The same single run with program DELTA will give a single graph with four curves corresponding to the tank-ground  $\Delta T$ 's of the graphs in program



TEMPS. These curves will start at the 6th hour because this minimizes the initial transient conditions inherent in the model. These transients arise since the algorithm sets all relevant temperatures at the value of the air temperature in order to start the calculations.

### Standard Conditions

This study focuses on three hypothetical geographic areas with different climatic conditions. The first is a northern continental region, the second, a mid-latitude coastal area and the third is a mid-latitude desert location. The effects of changing certain parameters at each place are investigated under a variety of climates designed to simulate winter (with and without snow), spring, and summer. Table II summarizes the assumed standard conditions for each location and season.

Table II  
Standard Climatic Conditions for Three Model Locations

Location	Latitude	Season	Temp	Precip. H <sub>2</sub> O Vapor (mm)	Rel Hum (%)	Sun (%)	Dust (part /cm <sup>3</sup> )
Continental	50	Winter(Snow)	-1.0	2.0	80	50	0.50
		Winter(No Snow)	-1.0	2.0	80	50	0.50
		Spring	7.5	3.0	72	50	1.00
		Summer	17.0	4.0	66	50	1.00
Coastal	32	Winter(Snow)	9.0	1.0	70	50	1.00
		Winter(No Snow)	9.0	1.0	70	50	1.00
		Spring	20.0	3.0	67	50	2.00
		Summer	27.0	4.5	64	50	2.50
Desert	20	Winter	15.0	0.4	40	70	0.25
		Spring	24.0	0.6	30	70	0.25
		Summer	32.0	0.9	20	85	0.50

(Ref 20; Ref 23)

### Variables

Not all of the 31 variables which are read as input were able to be examined. Other than the changes in location and climate already mentioned, 11 other separate parameters were run through the

program. Each of these parameters was given a number to simplify organizing the graph sets that were generated. Table III lists the parameters, their computer variable name, their corresponding identification number, and the total range of values used in the study.

Table III  
Parameter Identification Numbers

I.D. #	Range of Values	Parameter	Variable Name
1	-7 - +8 (C°)	Mean Temperature	MEANTEMP
2	.16 - 7.2 (mm)	Absolute Humidity	WATER
3	0 - 401 (cm/sec)	Wind	SPEED
4	25 - 120 (%)	Percent Sunshine	CLOUD
5	0.08 - 1.00	Ground Reflectivity	RSOIL
6	.475 - 1.00	Ground Emissivity	ESOIL
7	.09 - .54 (cm <sup>2</sup> /s)	Ground Diffusivity	DSOIL
8	.09 - .54	Target Reflectivity	RTANK
9	.35 - .98	Target Emissivity	ETANK
10	1.9 - 9.5 (cm)	Target Thickness	TTANK
11	0 - 536 (cm/sec)	Internal A. C. Velocity	SPEEDGI

#### Plot Identification Numbers

On each plot, or set of plots, a specific three-number key has been used to identify the variable being examined, the latitude corresponding to one of the three locations and the Julian day that the run is simulating. Figure 3 shows the organization of this system.

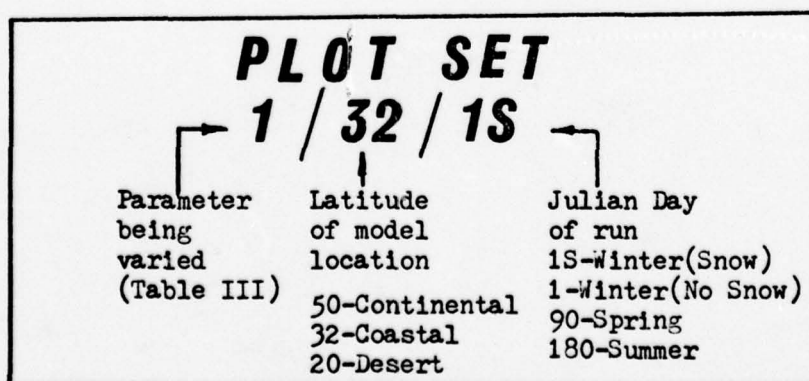


Fig. 13. Explanation of  
Plot Set Numbers

## V. Results

### Diurnal Temperature Curves

A single run of program TEMPS results in four diurnal temperature plots (one plot is shown in Fig. 14). All The temperatures are started near the air temperature, but, by the fifth hour, each curve takes on its own profile. The repetition of the curves at 6 and 30 hours indicates that the initial transient condition damps out within a day. The peak tank and ground temperatures in Fig. 14 (simulating summer) occur about two hours after the time of maximum insolation (at 14 hours, versus

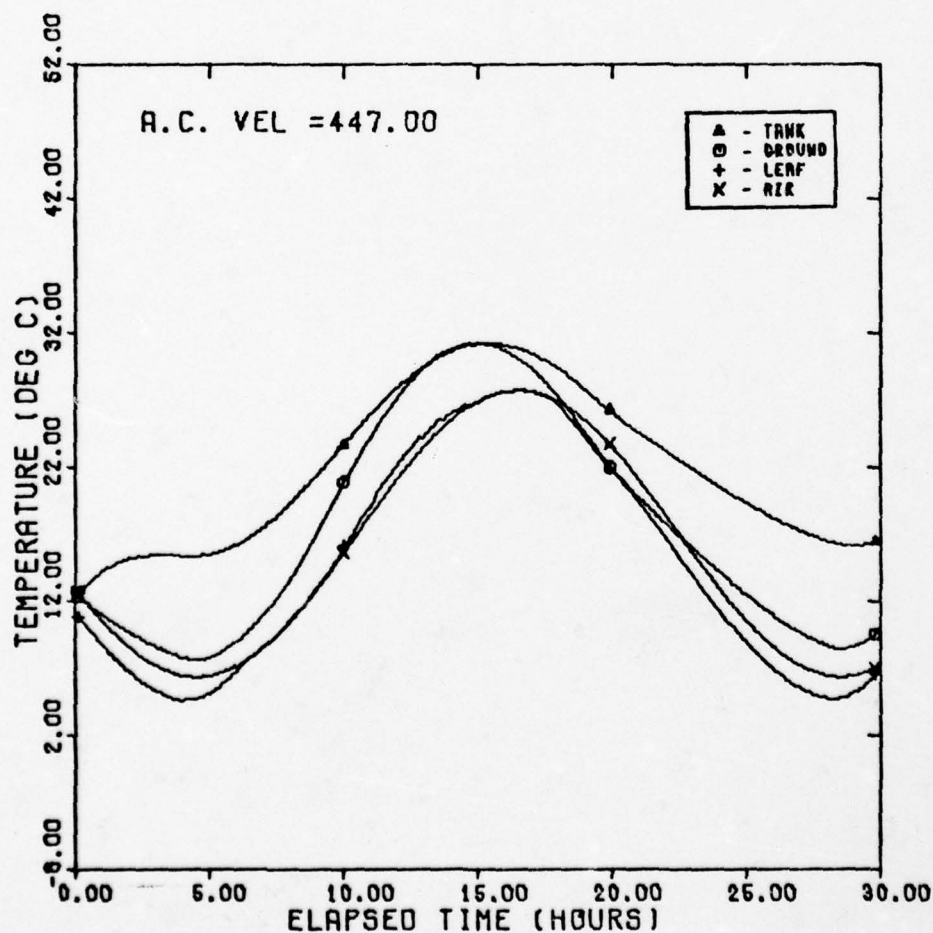


Fig. 14. Sample Diurnal Temperature Curve for Summer Conditions at 50° Latitude.



12 hours). The leaf temperature also increases above the air temperature, slightly, between 10 and 14 hours. This indicates that the leaf is transpiring at its maximum rate and that its temperature is being determined by energy balance. This profile parallels nicely the theoretical curves proposed by Gates (Ref 24:82). At night the leaf temperature stays below the air temperature, an indication of the high amount of outward radiation ( $R_0$ ) occurring at both surfaces. Were it not for the wind warming the leaf by convection, this temperature drop would be more severe (as in Plot Set 3/20/280). The ground; however, stays slightly warmer due to the reverse heat flux from inside the earth, and the tank is warmer still, mainly due to the imposed internal temperature being constant at 28°C. (The significance of this effect is shown in Plot Set 11/50/1). The remaining diurnal plots are located in Appendix C.

#### $\Delta I$ Curves

Figure 15 shows a sample  $\Delta I$  plot, where the target emissivity has been varied. From this graph it can be seen that in general, decreasing the target emissivity in the summer at northern latitudes tends to increase the  $\Delta I$  between the target and the ground. Another characteristic that can be deduced is that all the curves appear to have minima near the time of peak heat-loading (14.00 hours) and maxima when heat-loading is the lowest in the early morning. This, too, is probably caused by the preset internal temperature of the tank at 28°C. This point can be emphasized by noticing the lack of regularity in the  $\Delta I$  plots for Plot Set 11/50/180. Note too that the equal spacing of the curves in Fig. 15 seems to show a linear relationship between the emissivity and  $\Delta I$  for this computer model. Additional  $\Delta I$  curves are in Appendix D.

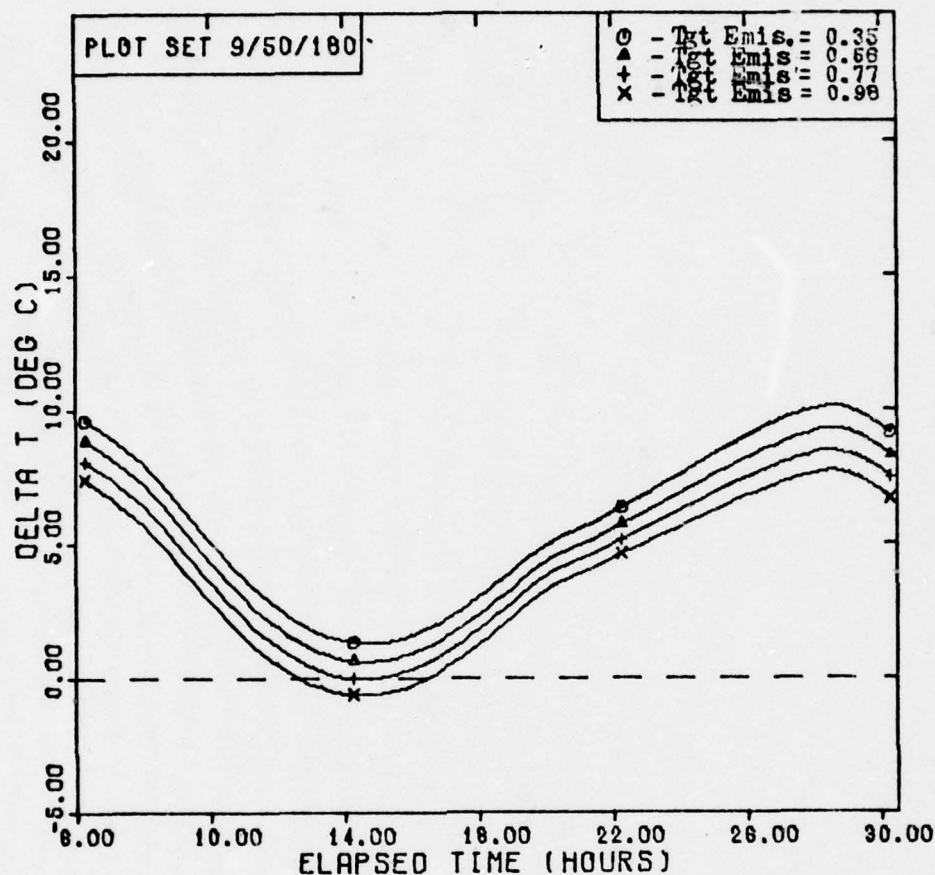


Fig. 15. Sample Plot.

#### Parameter Sensitivity Curves and Analysis

All of the parameters that were varied, except the mean temperature, were altered around a "standard value" so that a normalized, multiplicity constant could be used to compare the relative changes brought about by each parameter. In order to compare these changes, the same two selected times (14 and 24 hours) were used as data points for each parameter. By graphing the multiplicity value against the observed  $\Delta T$ , the effects of all parameters can be displayed on a single graph for each set of seasons and latitudes. These plots are additionally separated into day and night categories, plus the target and ground/en-

Environmental parameters are plotted separately to improve clarity.

The first two groups of curves (Fig. 16 and Fig. 17) indicate the results that occurred when the mean temperatures were raised and lowered above the standard values. Figure 16 represents the sample values taken in the day. All of the curves appear to have the same negative correlation. Moreover, the even spacing of most of the curves indicates that the same, apparently linear, relationship exists for all the seasons, and the effect of the season is just an upward, or downward shift. It is interesting to note the fairly large shift between the snow and no-snow lines on the top two graphs. It seems that the changing of the reflectivity of the ground also has a strong effect in shifting the curves. The smaller spacing for the 50° latitude example is apparently due to the lower insolation at that latitude.

The curves in Fig. 17 have all shifted upward during the nighttime when compared to Fig. 16. This is because the heated tank exhibits a stronger signature when the night air is colder. The other relationships mentioned for Fig. 16 still seem to hold, except that the effects due to the snow are greatly reduced at night when there is no insolation.

Figures 18 (a) through 18 (k) represent the analysis of parameters 2 through 11 (as listed in Table III) during the daytime. The graphs are organized with a single season and latitude combination on each page. The left-hand curves are those that result from the ground/environment parameters, and the right-hand curves are for those parameters pertaining to the target. Comments on each curve will be made on each individual page. The same type of organization will apply for Figures 19 (a) through 19 (k) which include the analysis made on the parameters during the nighttime.



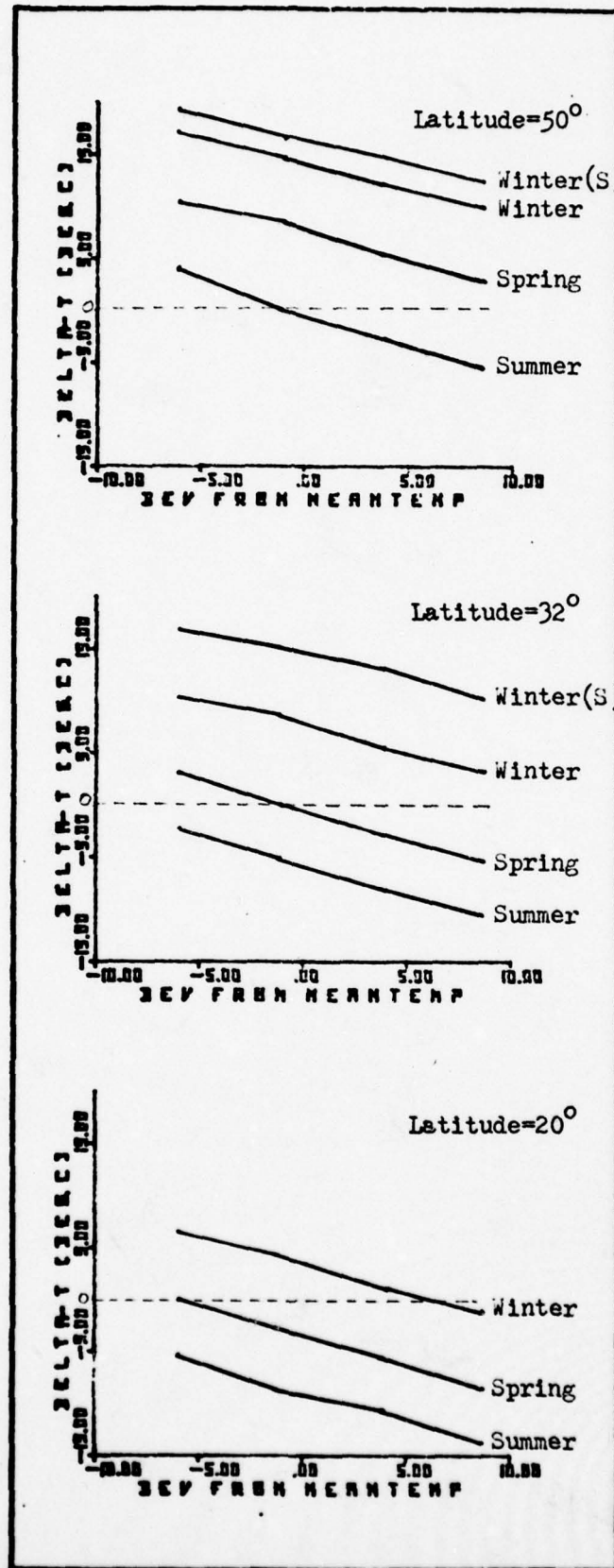


Fig. 16. Changes in daytime  $\Delta T$  caused by variations in mean temperature.

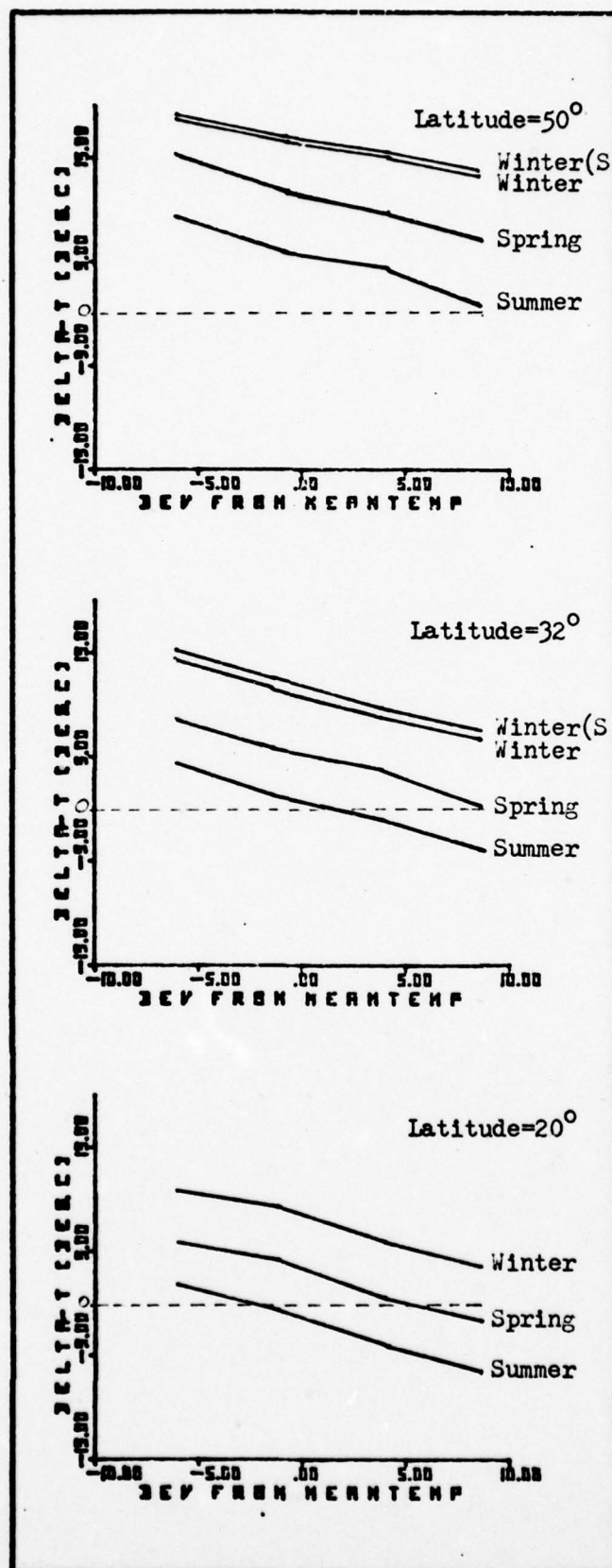


Fig. 17. Changes in nighttime  $\Delta T$  caused by variations in mean temperature

<u>Identifying Letter</u>	<u>Parameter</u>	<u>"Standard" Value</u>
a	- Absolute Humidity	See Table II for appropriate latitude and time
b	- Wind	223 cm/sec
c	- Percent Sunshine	See Table II for appropriate latitude and time
d	- Ground Reflectivity	20°---.3 32°&50°---.2(no snow) or .95(snow)
e	- Ground Emissivity	.95
f	- Ground Diffusivity	.3 cm <sup>2</sup> /min
g	- Target Reflectivity	.3
h	- Target Emissivity	.7
i	- Target Thickness	7.62 cm
j	- Internal A. C. Velocity	447 cm/sec

Fig. 17(a). Key to curves in Figs. 18(a) to 19(k), including "standard" parameter values.



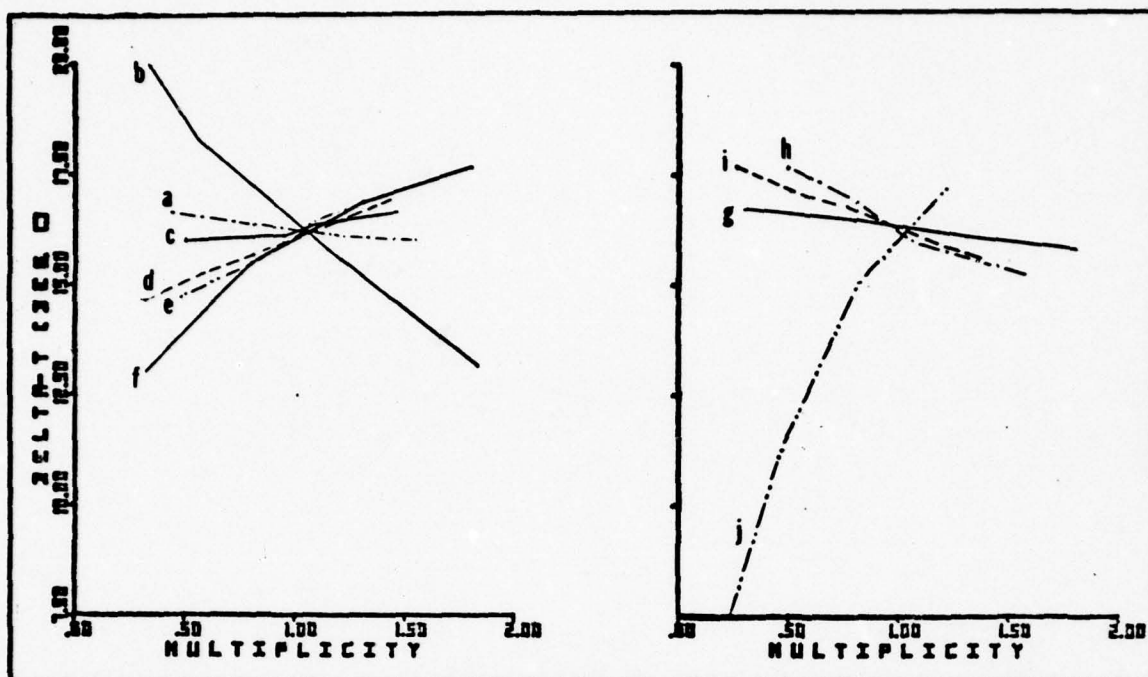


Fig. 18(a). Parameter Analysis; Daytime  
Season: Winter (S); Latitude:  $50^{\circ}$ .

The most sensitive external parameter is the wind (b). This is primarily due to the large temperature difference caused by the heated tank sitting over the cold ground in winter. Even a slight breeze starts to cool the tank off, bringing its temperature closer to the snow-covered earth. However, as the wind velocity increases above standard its effect appears to become less sensitive as seen by the gradual decrease in slope. The diffusivity has an opposite correlation, but a word of caution, the values used here may not be appropriate for the actual diffusivity values of the snow. Ground reflectivity has some variance and this may span the range of old to new snow. Interior convection is very critical, a stagnant interior decreases the temperature difference a great deal even though the inside air may be warm.

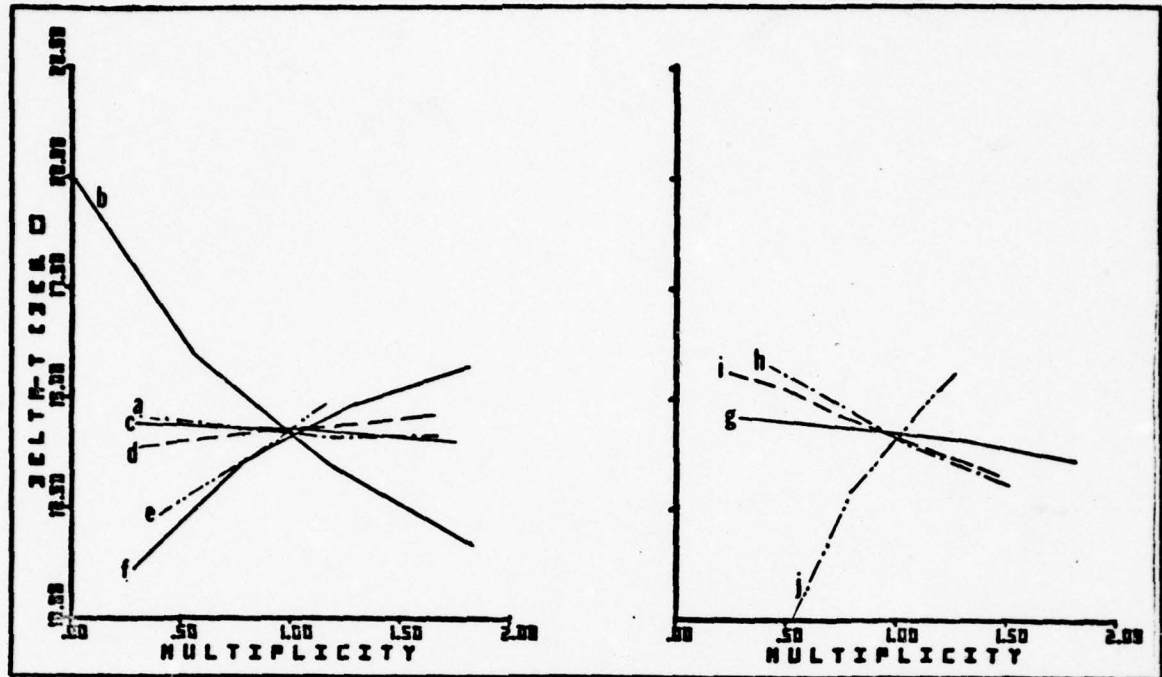


Fig. 18(b). Parameter Analysis; Daytime  
Season: Winter; Latitude:  $50^{\circ}$ .

The relationships in this figure are very close to those on the previous figure except that the standard temperature is shifted down by about 3 degrees when there is no snow on the ground. (This shift is similar to the one shown in Figures 16 and 17). One apparent change with the external parameters is that the dependence on the amount of sunshine has changed from slightly positive to slightly negative. This is probably due to the increased amount of heat that the soil is picking up, causing it to stay warmer for a longer period of time. The ground reflectivity seems to be even less sensitive in this regime. Interior and exterior convective processes still dominate as the most sensitive parameters.

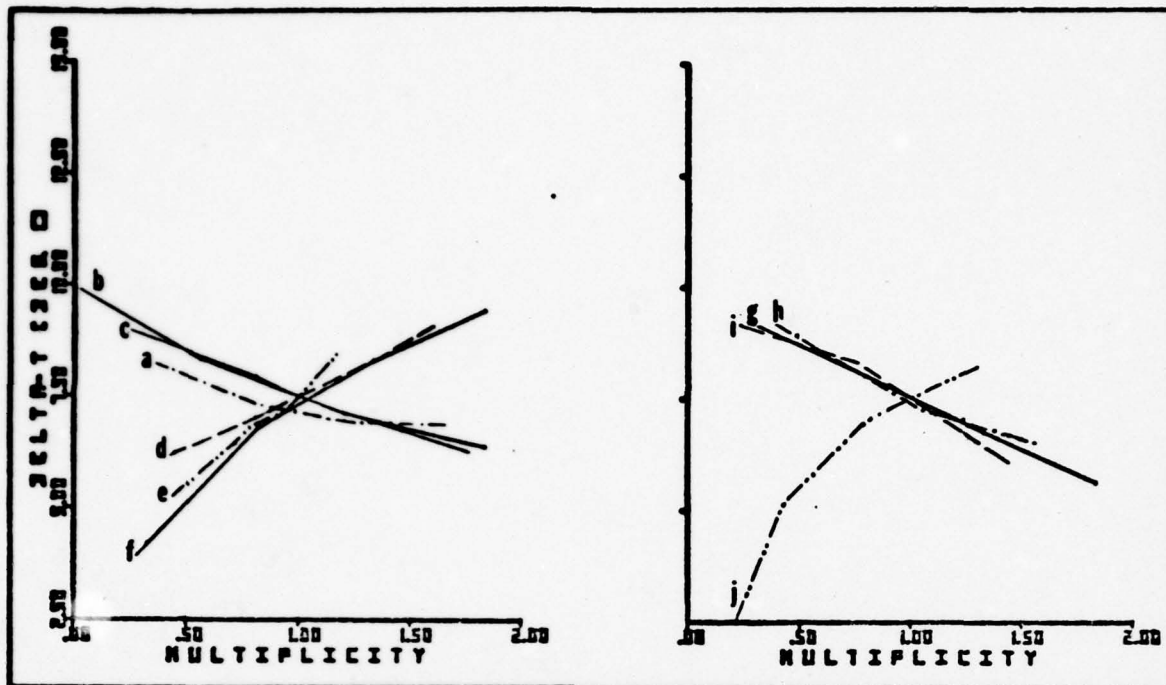


Fig. 18(c). Parameter Analysis; Daytime  
Season: Spring; Latitude:  $50^{\circ}$

The strength of the wind parameter has begun to fall off as the temperature of the tank gets closer to the ground temperature. In this spring example, the relative change brought about by the absolute humidity, the wind and the amount of sunshine are practically the same. The effect of the diffusivity is about the same, as is the ground emissivity ; however the ground reflectivity seems to be getting more important, and this is probably due to the increased amount of insolation at this time of year. The effects of target reflectivity, emissivity and thickness all appear to have about the same relative merit with a negative correspondence. The value of the internal heat transfer by convection still remains the strongest parameter of them all.



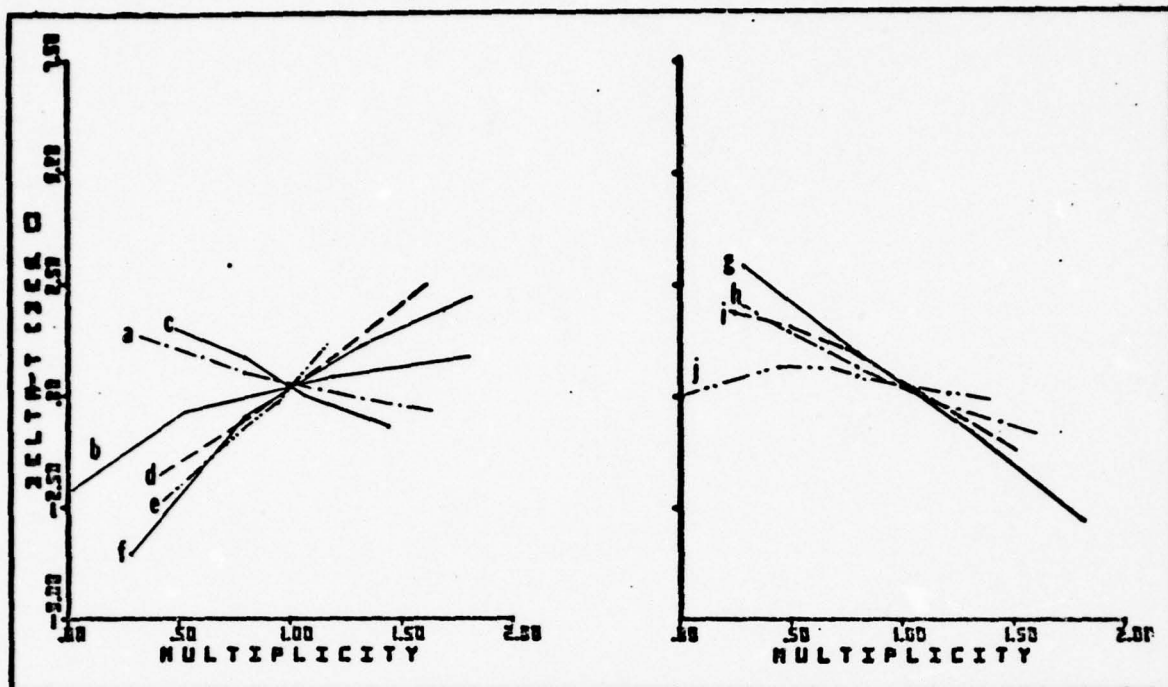


Fig. 18(d). Parameter Analysis; Daytime  
Season: Summer; Latitude:  $50^{\circ}$

During the summer, the most notable change is that the importance of the internal heat exchange (j) falls off drastically, this is primarily because the daytime temperatures are becoming closer to the assumed  $28^{\circ}\text{C}$  of the inside of the tank. At the same time the target reflectivity is becoming increasingly important with the higher values of insolation. The wind (b) now has a positive correlation because the temperature of the tank is getting warmer than the air temperature and increased values of the wind velocity tend to cool it down and drive the temperature difference toward zero. The relative strength of the other climate and ground factors appear to remain about the same.

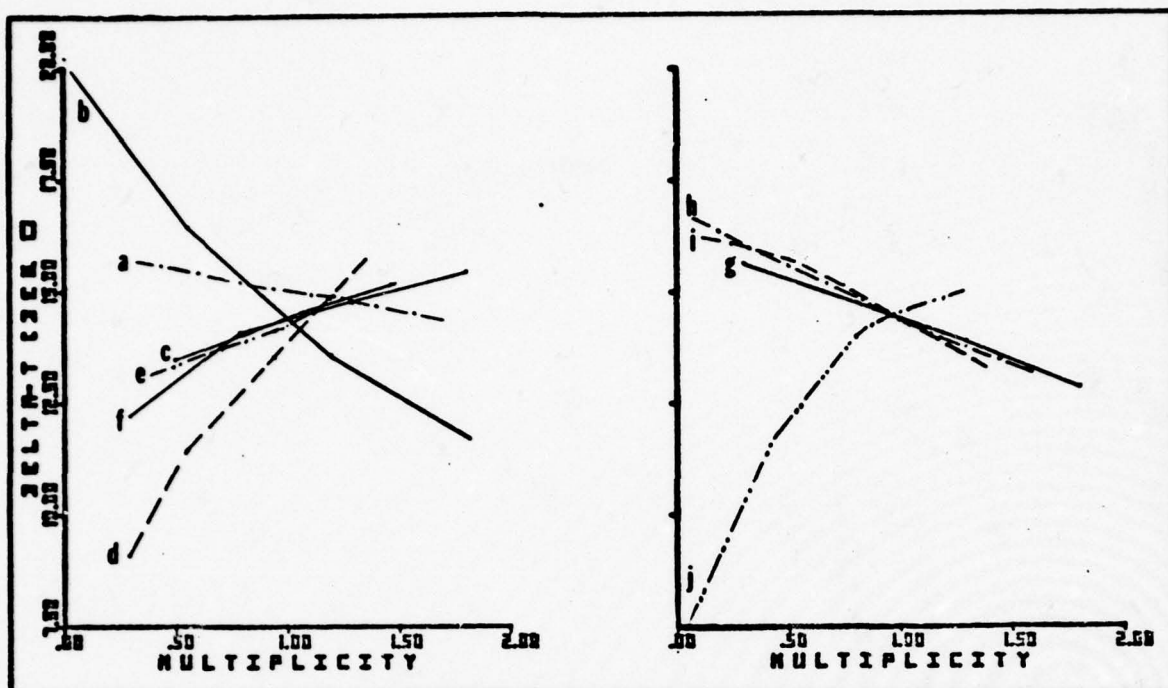


Fig. 18(e). Parameter Analysis; Daytime  
Season: Winter(S) Latitude:  $32^{\circ}$

In the mid-latitude winter with a snow-covered ground the outside wind still is the most sensitive factor, but not nearly as strong as was the case at  $50^{\circ}$  latitude. The ground reflectivity has a much stronger influence at  $32^{\circ}$  however and this is quite likely due to the greater amount of insolation. From this fact it is apparent that the different reflectivity of the snow (old versus new) in the lower latitudes may be able to change the values of Delta-T by as much as 35 to 50 percent. A similar situation could occur at higher latitudes in early spring. The other external factors have a relatively "standard" appearance as far as significance goes. The rate of convective transfer inside the tank is the key internal factor, although slightly less important than at  $50^{\circ}$  with a snow covered ground. This is due to the warmer air temperature most likely.

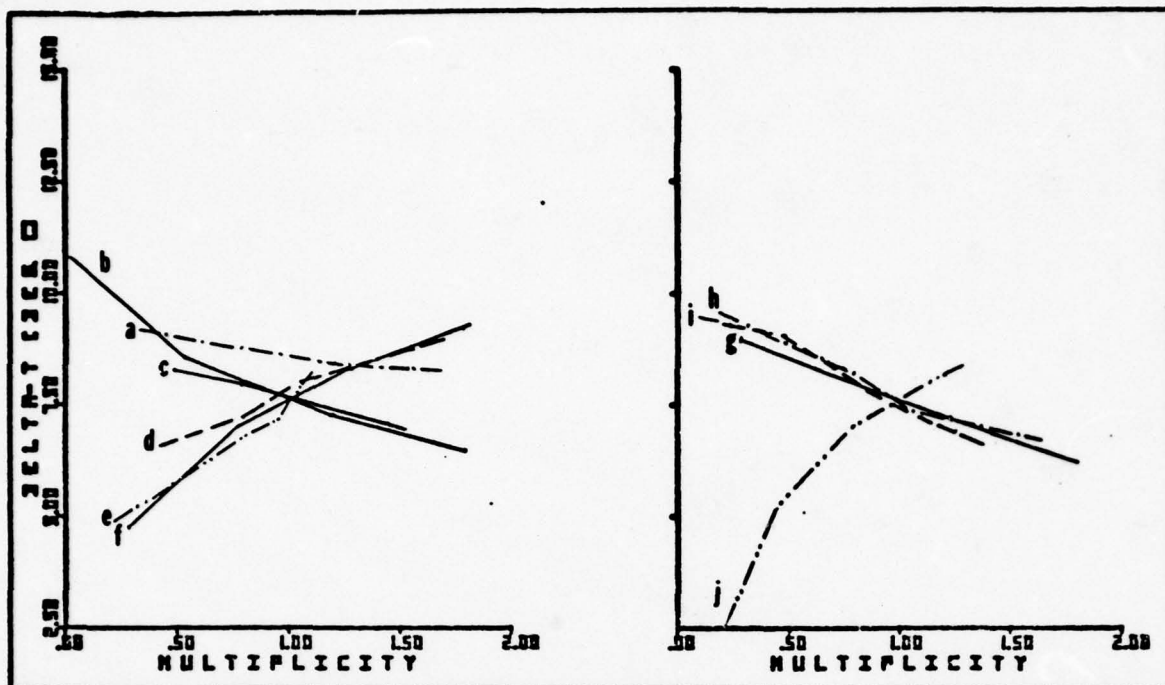


Fig. 18(f). Parameter Analysis; Daytime  
Season: Winter; Latitude:  $32^{\circ}$ .

Without snow, the ground absorbs more solar energy and hence is warmer during the daytime, thus the Delta-T is lower in this instance and the effects of the wind (b) and the ground reflectivity (d) have become less significant. Because the ground is absorbing more energy, the diffusivity and emissivity have become more sensitive, since they are apparently acting as regulators for the energy flow into and out of the ground. Very little change has occurred with the internal parameters, in fact, the convective heat transfer appears to be as important as it was when there was snow on the ground.



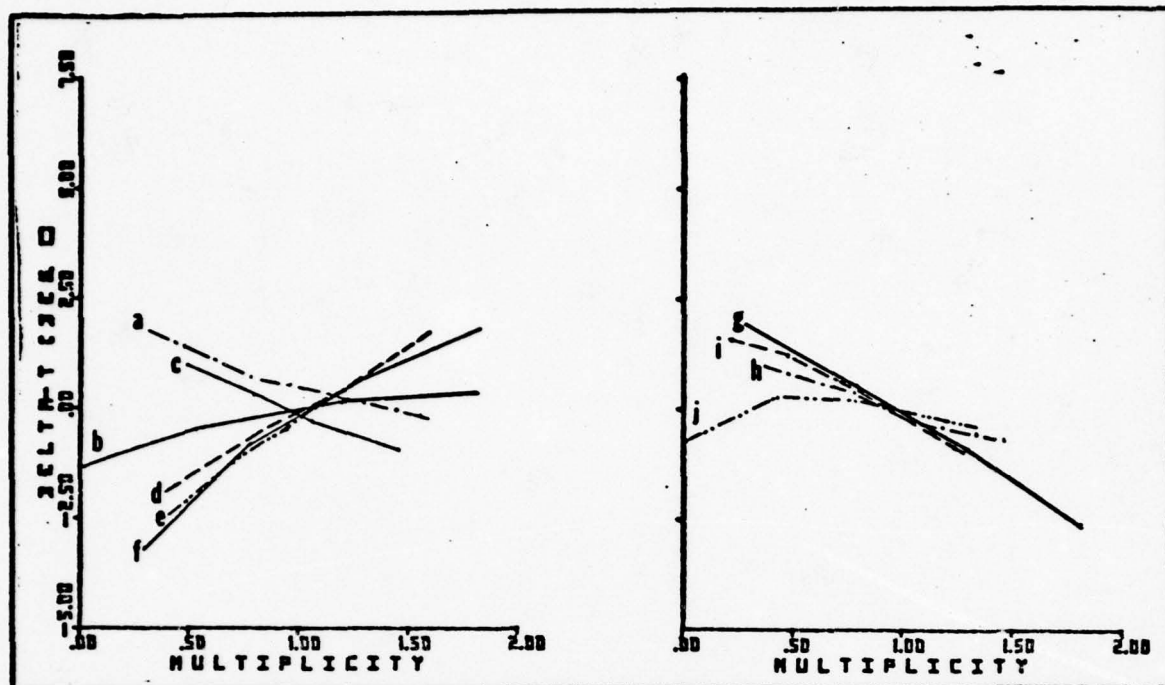


Fig. 18(g). Parameter Analysis; Daytime  
Season: Spring; Latitude:  $32^{\circ}$

As the year goes on and the air temperature warms up, the cooling effect of the wind on the tank becomes a warming effect, as shown in the change in slope of curve (b) compared to the winter. The negative slope for the amount of sunshine (c) indicates that with increased insolation, the ground heats up more than the tank. A similar effect occurs when the absolute humidity (a) is increased. The increased spring-time air temperature causes the internal heat convection term to become much less effective, since the interior tank temperature is closer to the air temperature. The emissivity of the tank is less important now, due to a higher percentage of insolation versus atmospheric radiation (as compared to the winter heat-load).

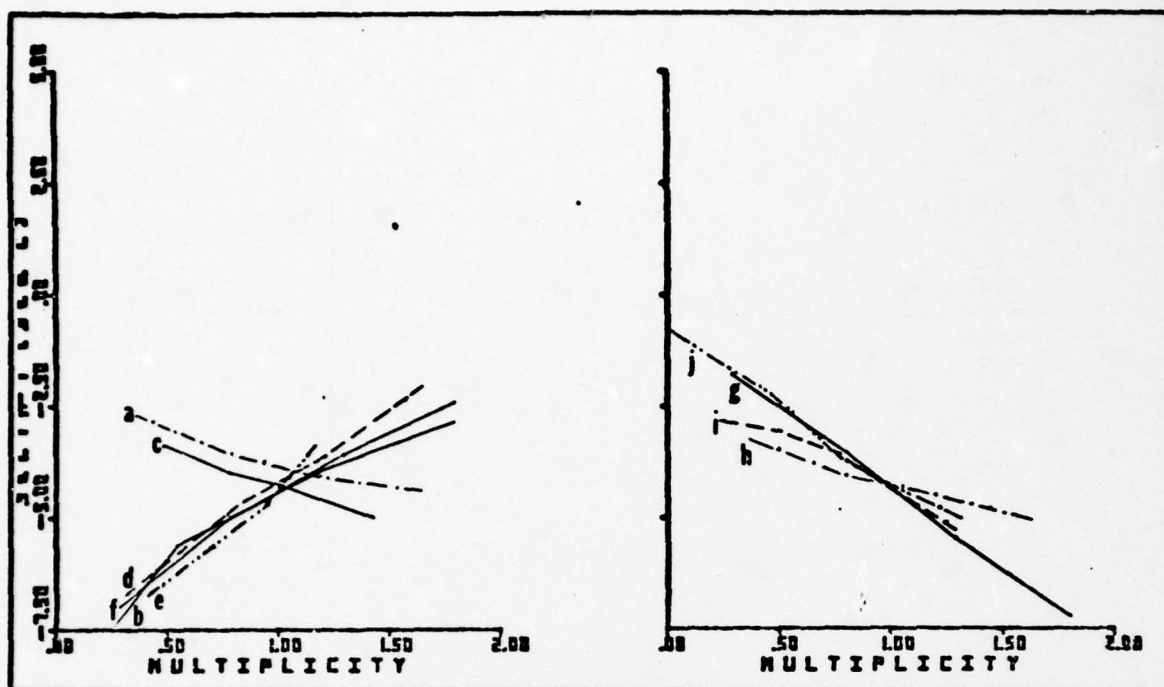


Fig. 18(h). Parameter Analysis; Daytime  
Season: Summer; Latitude:  $32^{\circ}$ .

With maximum insolation, the factors that tend to cause heat-gain in the ground are showing a strong positive correlation, this includes the emissivity, reflectivity and diffusivity. Additionally, as the wind velocity decreases outside, the ground heats up more than the tank causing the value of the Delta-T to become more negative. The negative slope on the internal A.C. velocity term shows that during the middle of the day the inside of the tank is cooler than the ground and cooling the inside shows up as causing the Delta-T value to become more negative. An explanation of why increasing the tank thickness causes the Delta-T to become more negative (the tank skin is cooler) may be that due to the increased heat storage capability, the peak tank temperature shifts to a time that increases the temperature difference at the 14 hour point.

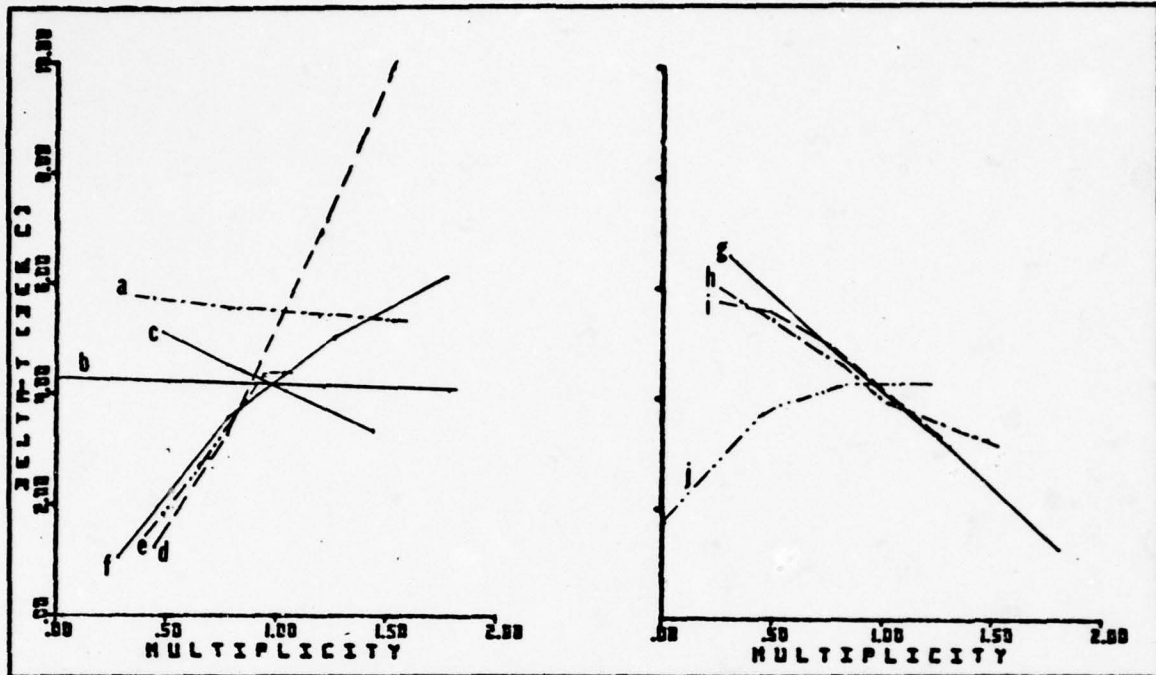


Fig. 18(i). Parameter Analysis; Daytime  
Season: Winter; Latitude:  $20^{\circ}$ .

The first noticeable part of the winter curves in the desert is that the wind has very little effect upon the thermal signature. On the contrary, the **soil reflectivity is of much greater importance, now,** compared to the other two latitudes in winter. This is probably due to the greater amount of insolation for the time of year. **More** evidence of the relatively strong insolation **is** the importance of the ground's diffusivity and emissivity. The negative slope on the sun strength curve (c) shows that as the insolation is increased the heating of the soil is greater than the tank, causing a decrease in the Delta-T despite the fact that the reflectivity of the soil is higher in this model than the others (assuming that it is desert sand). With higher air temperature and insolation, the tank emissivity, thickness, and reflectivity are more important, while the internal convection is less important than at the other latitudes studied.



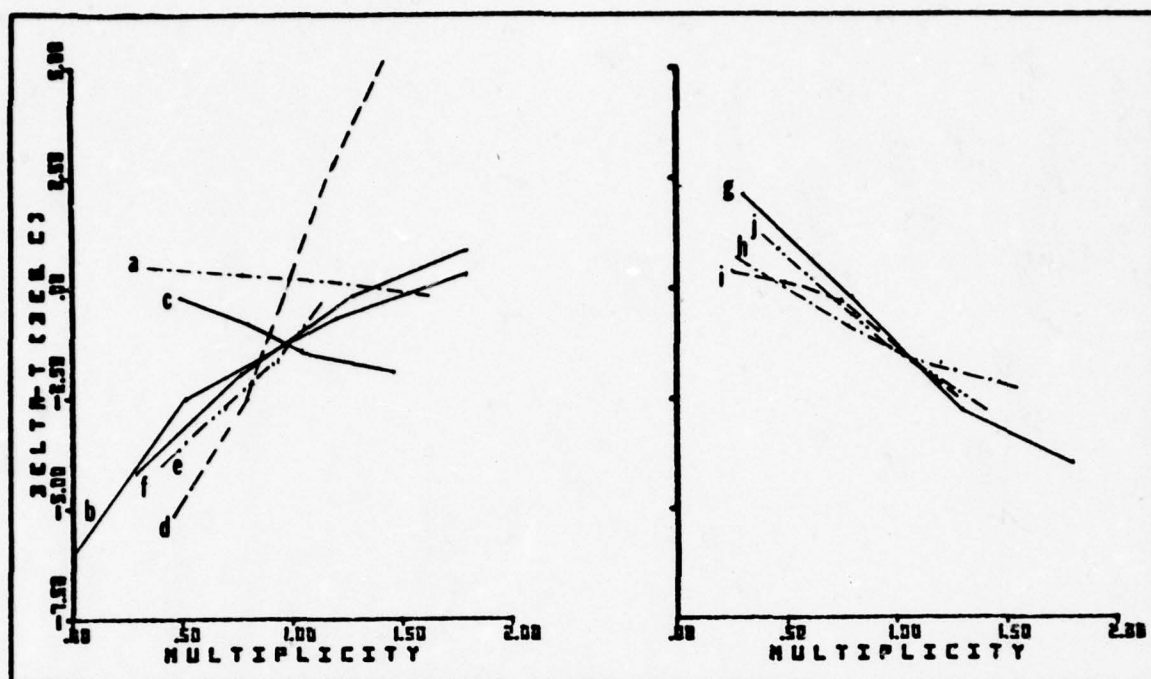


Fig. 18(j). Parameter Analysis; Daytime  
Season: Spring; Latitude:  $20^{\circ}$ .

As the intensity of the insolation increases from winter to spring, the importance of the soil reflectivity increases also. A strong positive slope on the wind term indicates that cooling of the sand by a breeze can change the value of the temperature difference by a great deal. The other external parameters are similar to the winter case. The action of the internal convection term now tends to cool the outside of the tank and thus when it is increased the magnitude of Delta-T also decreases. The slope of the target reflectivity has become slightly more negative, which is indicative of the increase in solar insolation over the winter.

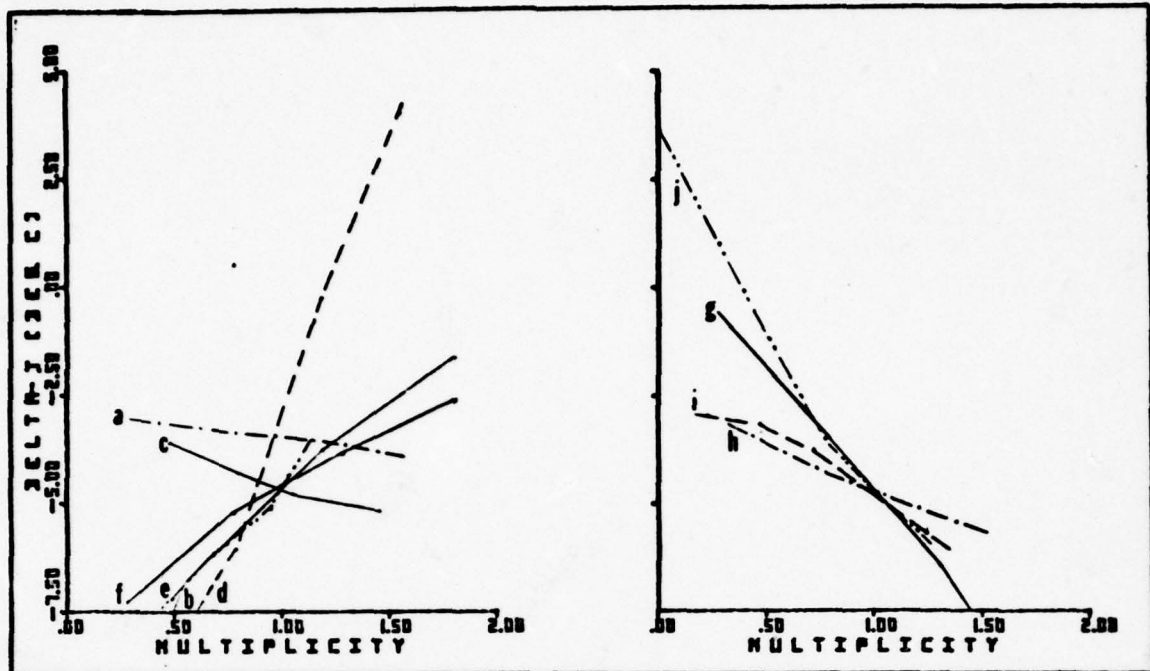


Fig. 18 (k). Parameter Analysis; Daytime  
Season: Summer; Latitude: 20°.

Under maximum insolation the extreme sensitivity of the ground reflectivity is readily apparent; a 100% change in the reflectivity can mean a 200% change in the Delta-T value. At the same time, the cooling effect of the wind on the soil has also become a bit more important, while the relative slopes of the other 4 external factors have remained about the same. The cooling effect of the internal air conditioning is at a maximum and the difference between having it off and having it on can mean a 170% difference in the Delta-T value. The importance of the reflectivity of the tank has also become more important with the increased heat-load of the summer.

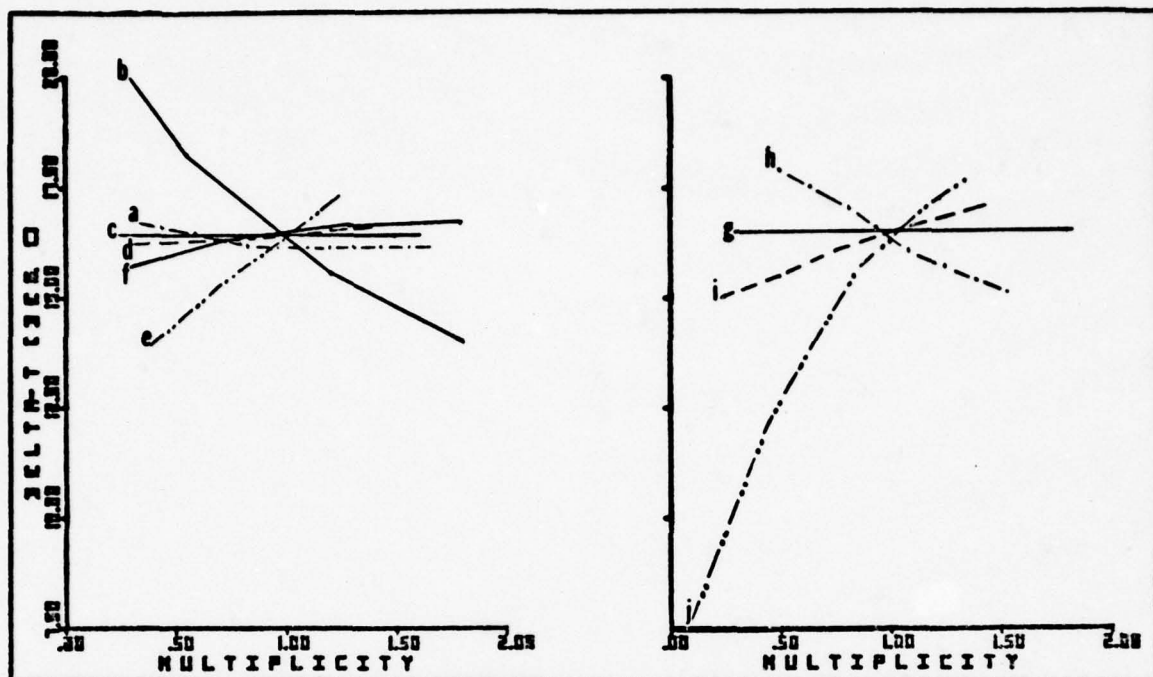


Fig. 19(a). Parameter Analysis; Nighttime  
Season: Winter(Snow); Latitude;  $50^{\circ}$ .

The two most important external factors at night appear to be the wind and the **emissivity** of the snow, the former is because of the cooling of the tank that will occur as the wind velocity increases, the latter is due to the fact that thermal radiation from the sky and snow comprise the major energy balance at the snow's surface. Except for the target reflectivity, the internal terms appear to have more significance at night. Again, because of the importance of thermal radiation at night, the **emissivity** plays an important role in the target signature. The positive correlation with thickness is presumably an indication of the gradual release of the energy stored up within the skin of the tank.



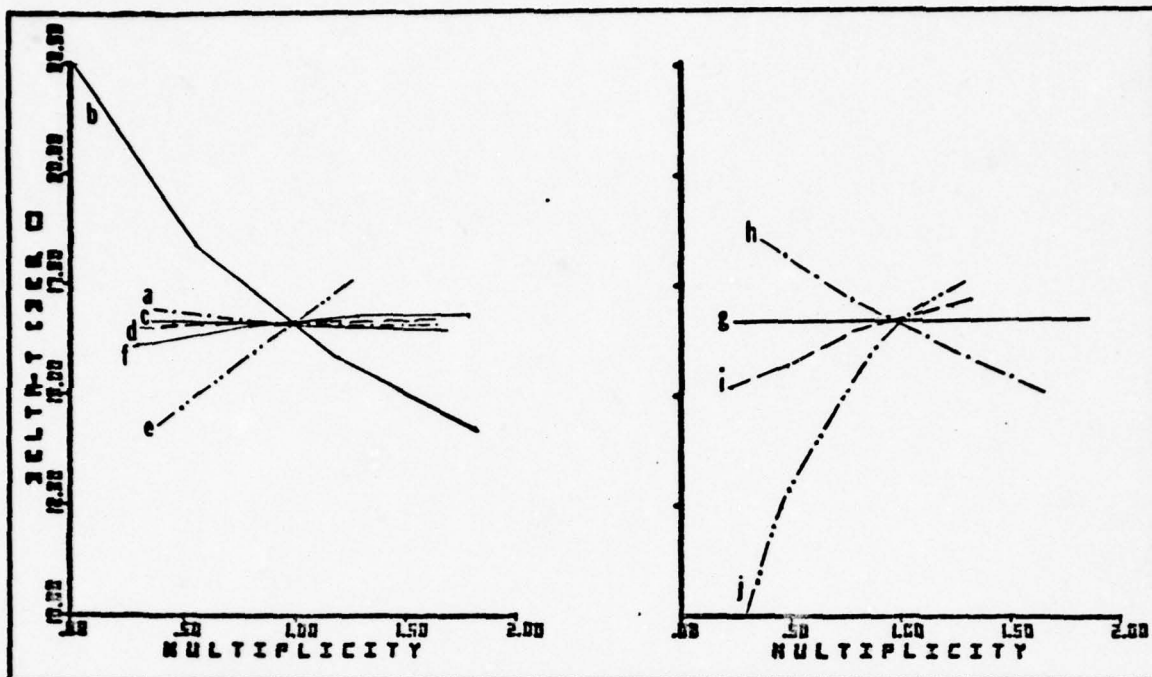


Fig. 19(b). Parameter Analysis; Nighttime  
Season: Winter; Latitude:  $50^{\circ}$ .

There is no apparent change in the energy balance relationships using a scenario without snow under the same conditions as in Fig. 19(a). The graphs do look a bit different, but this is due primarily to a change of scale between the two.

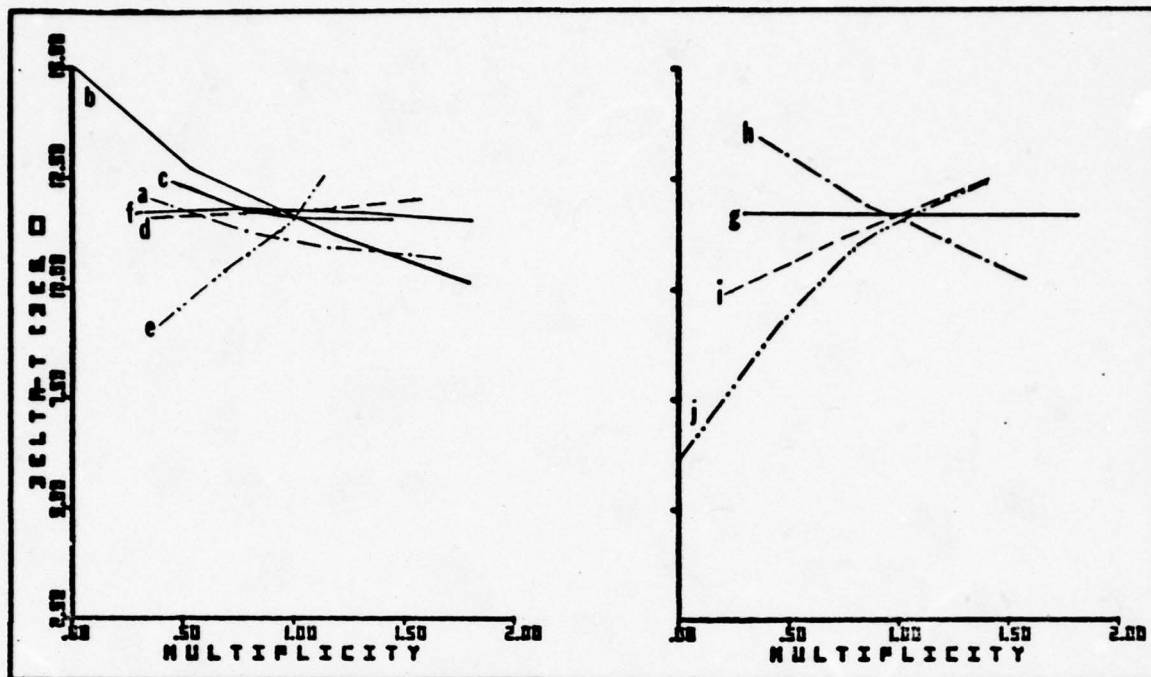


Fig. 19(c). Parameter Analysis; Nighttime  
Season: Spring; Latitude:  $50^{\circ}$

With Spring, the importance of the wind begins to decrease as the air temperature and tank temperature begin to coincide. The ground emissivity has about the same effect as in the winter, but the diffusivity appears to be even less sensitive, even though the day time heat-loading is more at this time. It is interesting to note that the intensity of the sun seems to have some effect, only if it is reduced below the normal value. It seems that with less sun strength, the ground collects less energy, is cooler at night, and the Delta-T is thus increased. The only significant change with the target parameters is that the strong changes due to the convective transfer are beginning to ebb, primarily due to the smaller difference between the air temperature and the target.

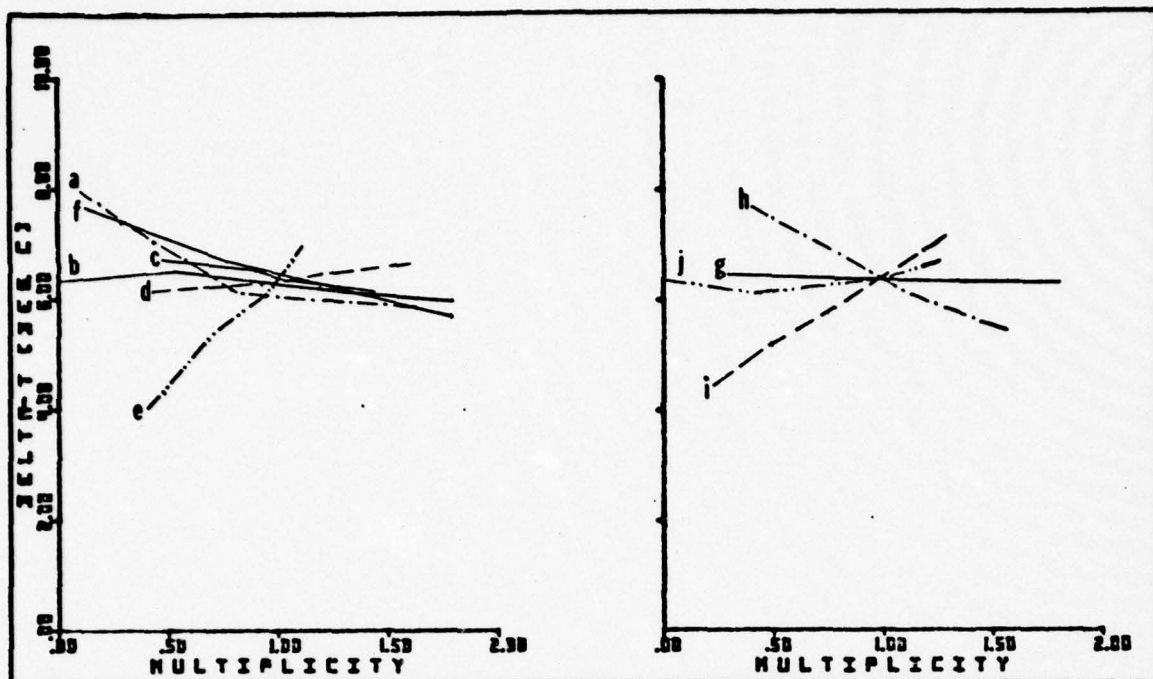


Fig. 19(d). Parameter Analysis; Nighttime  
Season: Summer; Latitude:  $50^{\circ}$ .

The effects of the ground's emissivity and reflectivity do not seem to have changed much, and the convection term has nearly zeroed out in the summer night. There is still a slight negative correlation between the variation of the sun's intensity, but not as much as in the spring. The biggest change is due to the diffusivity and the absolute humidity. Apparently, with a lower diffusivity there is less energy stored deep in the soil to allow it to be warmer at night (the heat radiates away faster causing the nighttime minimum to occur at a different time). The decrease in the absolute humidity will tend to decrease the long-wave radiation at night, but during the day it would have caused an increase in the insolation, so that the net effect is that the tank receives more energy in the day, than the soil receives at night, thus the Delta-T is increased. The convection inside the tank causes little change now, but the thickness becomes more important, as there is more solar energy available to store up during the day.



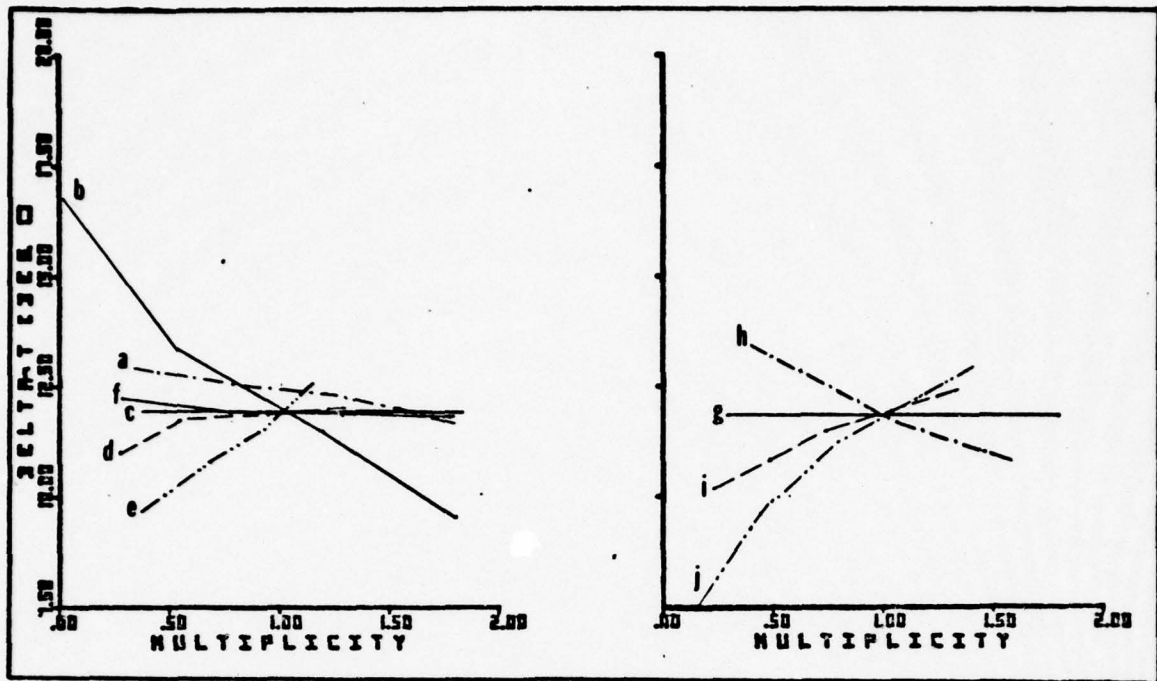


Fig. 19(e). Parameter Analysis; Nighttime  
Season: Winter (Snow); Latitude:  $32^{\circ}$ .

The ground emissivity and wind curves are similar to those for the spring at latitude  $50^{\circ}$ , and the absolute humidity curve has a small negative slope as was the earlier case. There are only very slight effects due to changes in the diffusivity and the amount of sun insolation. There is an interesting dip in the reflectivity curve for values less than about .6 of the normal value; however, this is even a bit low for a reflectivity for old snow. The graph of the internal parameters is similar to the other night plots in the winter, with strong influences due to convection, thickness and emissivity .

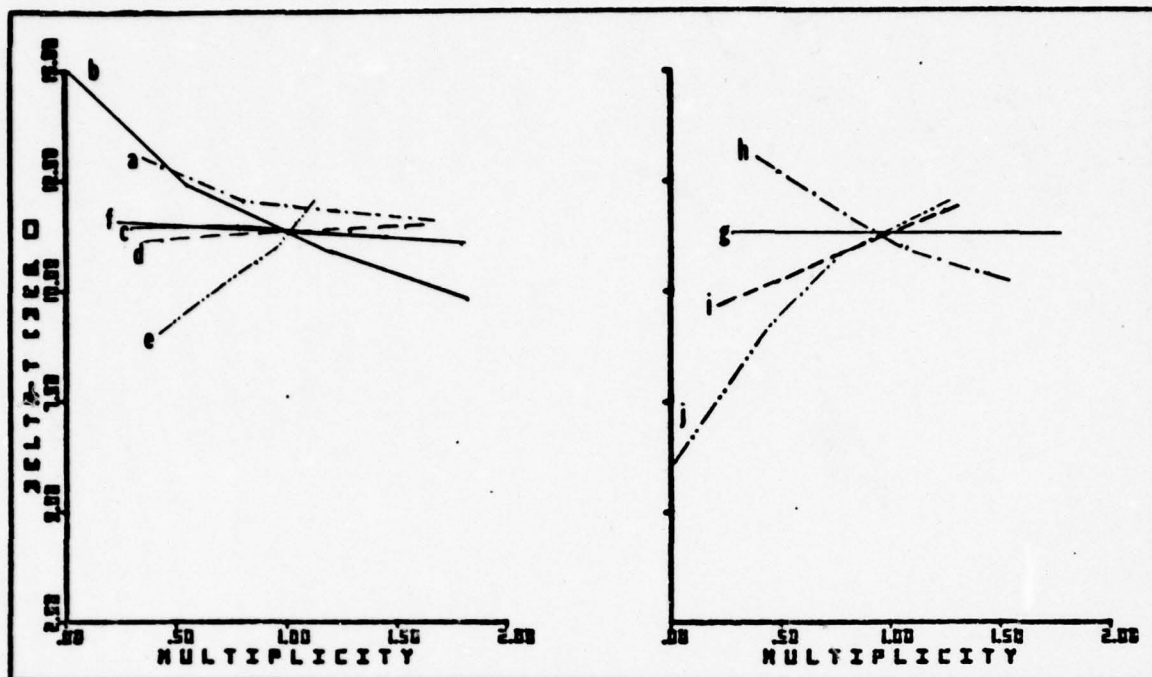


Fig. 19(f). Parameter Analysis; Nighttime  
Season: Winter; Latitude:  $32^{\circ}$ .

The external factors of diffusivity, sunshine, and reflectivity have become even more neutral compared to the winter simulation with snow. The effect of the absolute humidity appears to be stronger at this time, more like it was for the summer in the  $50^{\circ}$  graphs, this may be due to the increased amount of insolation at this latitude. There has been very little, if any, change in the internal parameter curves, with the internal convection being the most sensitive still (due mostly to the cold night temperatures).

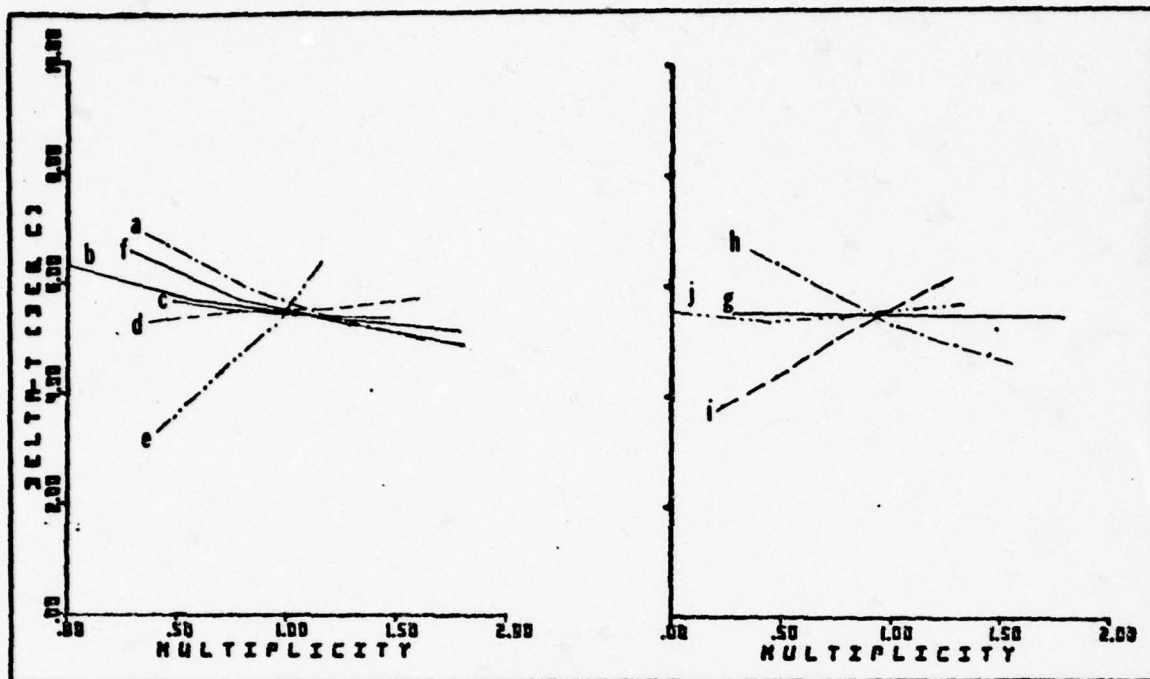


Fig. 19(g). Parameter Analysis; Nighttime  
Season: Spring; Latitude:  $32^{\circ}$ .

The major change in these curves is the loss of importance of the convection terms. This is most likely due to the warmer air temperatures, and a subsequent drop in the temperature difference between the tank and the air inside and outside the surface. The only other noticeable change is the increase in sensitivity of the diffusivity of the soil. This is probably caused by the higher insolation, and thus a higher heat-load at the surface of the ground.



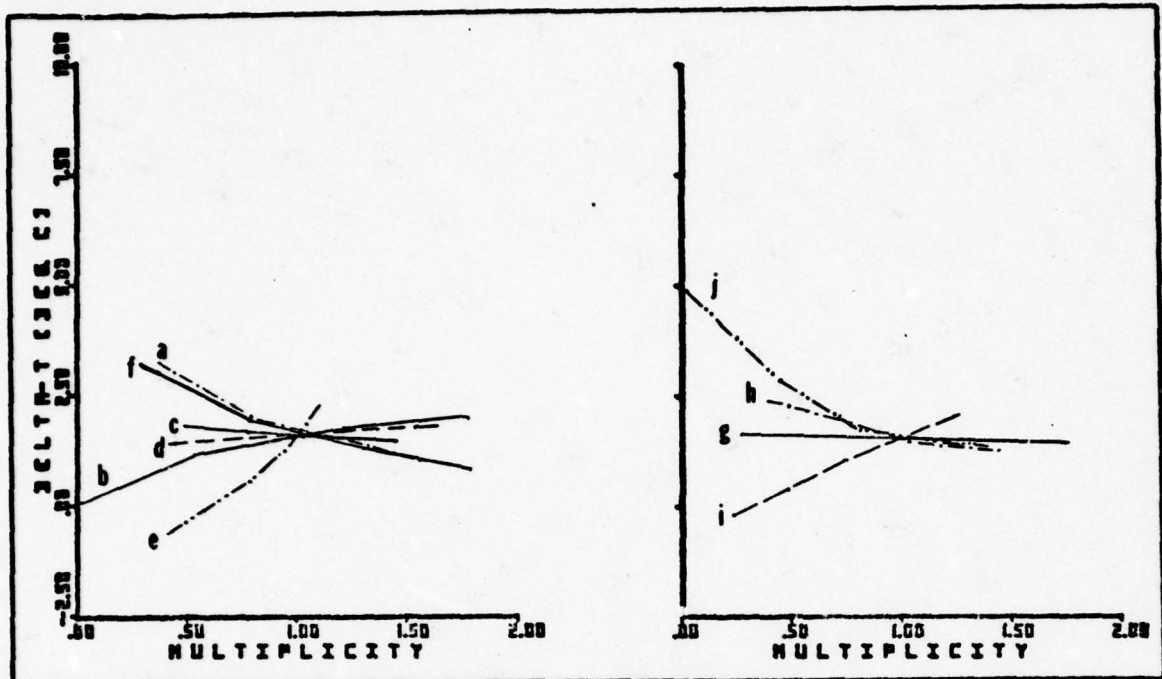


Fig. 19(h). Parameter Analysis: nighttime  
Season: Summer; Latitude:  $32^{\circ}$ .

With the warm summer evenings the slopes of the convection terms continue to change as the night air has a tendency to warm the tank and the air conditioning within cools it. The ground diffusivity parameter still becomes more effective as the daily insolation now reaches its peak so that the sun is up longer and more energy gets stored in the soil to radiate (and convect) away at night. The slopes of the emissivities of both the tank and the ground appear to be a little less steep. This is probably due to the warmer air temperatures causing more atmospheric thermal radiation so that the net cooling effect due to radiation is less.

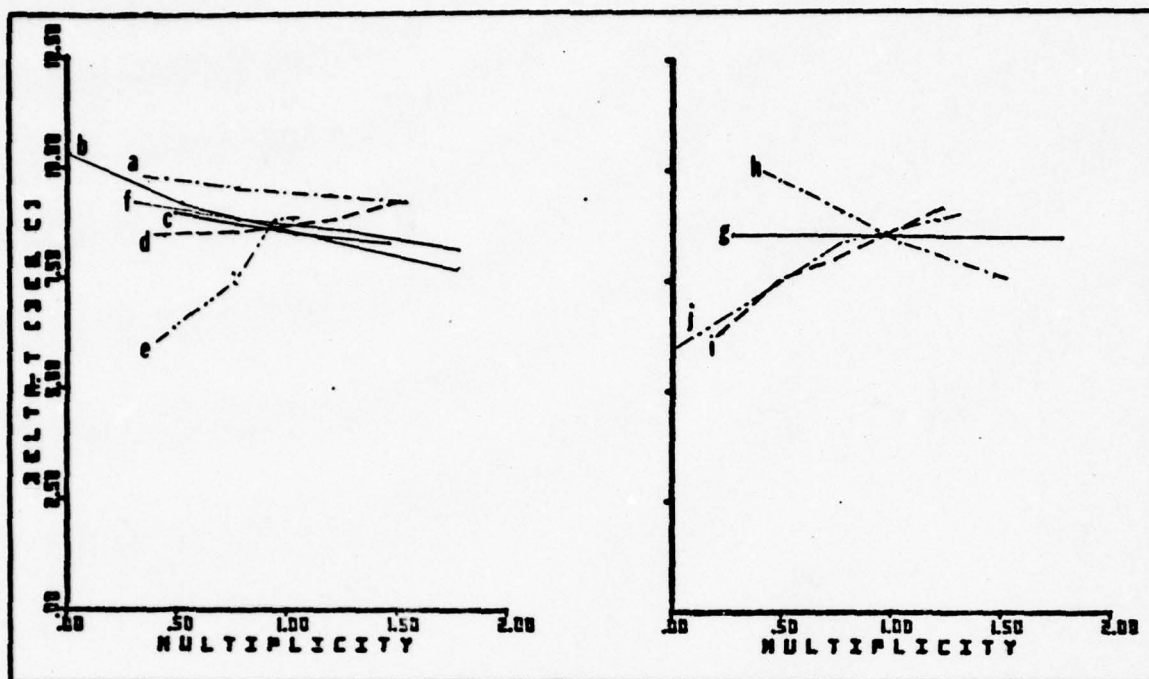


Fig. 19(i). Parameter Analysis: nighttime  
Season: Winter; Latitude:  $20^{\circ}$ .

The angles of the desert curves are fairly similar to those at  $32^{\circ}$  in the winter, except that they are shifted down somewhat (the air temperature is warmer) and that the convective heat terms are not nearly so dominant, again because of the warmer air temperature. There is a slightly more downward slope to both the sunshine (c) and the diffusivity (f) curves than there was in the previous latitude in the winter. This may be due to a higher amount of insolation during the day accentuating the effects of these terms during the nighttime. This may even affect the reflectivity curve of the ground as well. The target reflectivity still indicates an almost flat response.

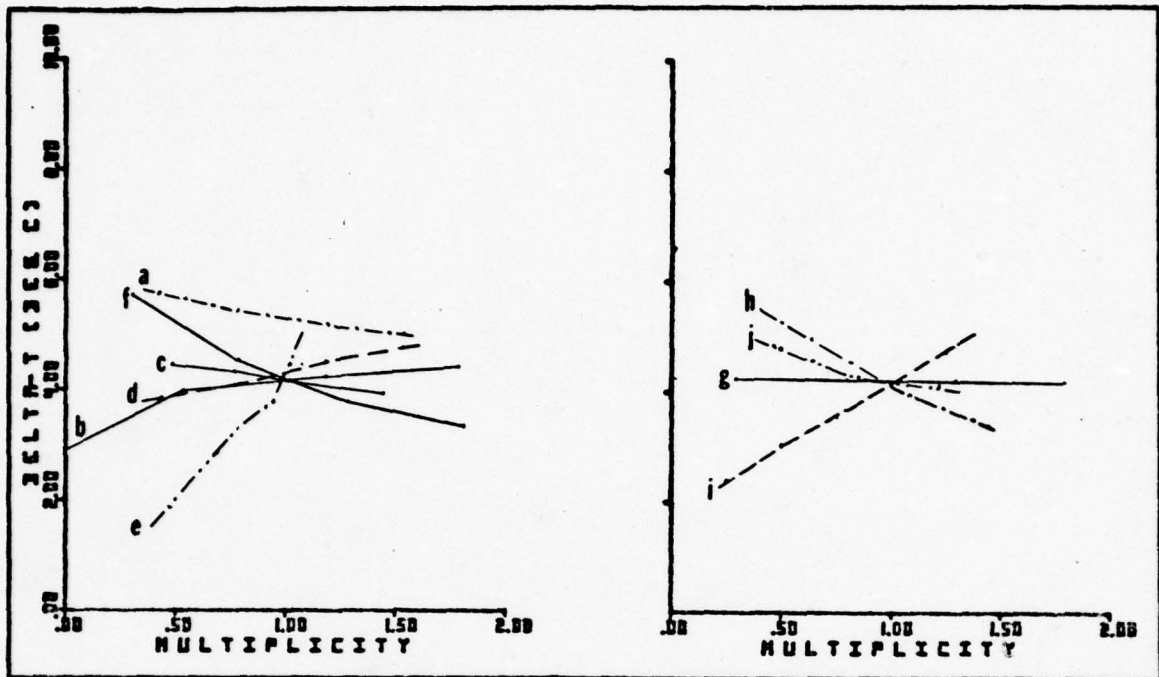


Fig. 19(j). Parameter Analysis: nighttime  
Season: Spring; Latitude:  $20^{\circ}$ .

Once again the convection terms begin to swing to different slopes as the air temperature warms up, and again, as before, the soil diffusivity slope increases negatively. There also appears to be a very slight change in the sensitivity of the ground reflectivity but not very much. Except for the convection term, the internal factors are almost totally unaltered in the change of season from winter to spring. The upward displacement of the absolute humidity terms is possibly due to a slight change in the computer program when that data set was run. There was insufficient time to go back and verify the data. At any rate the size of a vertical shift in the curve is rather arbitrary since the changes in slope are what is most important for this analysis.



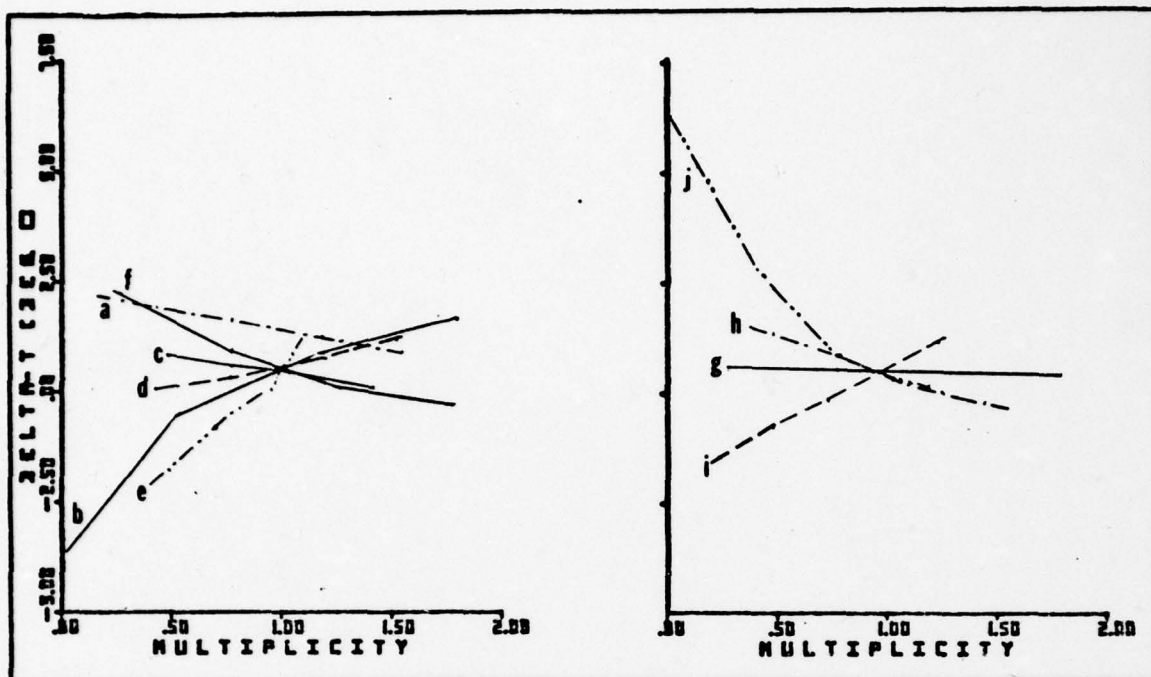


Fig. 19(k). Parameter Analysis: nighttime  
Season: Summer; Latitude:  $20^{\circ}$ .

Because of the large difference between the tank temperature and the air during a desert summer night the convective terms dominate as the most important factors. Were the basic temperature inside the tank changed, a subsequent change in the convective terms will show up as well. As was also seen in the set of curves for the summer at  $32^{\circ}$  latitude, the diffusivity of the soil, and the emissivities of the soil and tank have flattened out somewhat, possibly another result of the increased air temperature. No other significant changes seem to have occurred.

## VI. Conclusions and Recommendations

### Conclusions

Table IV is a summary of ranking the parameters using the curves in Figs 18(a) to 19(k). The letters refer to the parameters (see Fig. 17(a)), and are listed from high to low importance (left to right)

Table IV

Summary of Parameter Strengths for Eleven  
Hypothetical, Geographic and Climatic Conditions

Condition	Latitude	Day	Night
Winter (Snow)	50°N	j,b,f,e,d,h,i,a,g,c	j,b,e,h,i,f,a,d,c,g
	32°N	j,b,d,f,h,i,e,c,g,a	b,j,e,i,h,a,d,f,c,g
Winter (No Snow)	50°N	j,b,f,e,h,i,d,a,c,g	j,b,e,h,i,f,a,d,c,g
	32°N	j,b,e,f,h,i,g,d,c,a	j,b,e,h,i,a,f,d,c,g
	20°N	d,e,f,g,h,i,j,c,a,b	e,i,j,h,b,c,f,a,d,g
Spring	50°N	j,f,e,b,g,h,c,i,a,d	j,b,h,e,i,a,c,d,f,g
	32°N	f,e,d,g,a,c,h,i,b,j	e,i,a,h,f,b,c,d,j,g
	20°N	d,b,f,e,g,j,h,i,c,a	e,i,f,h,j,b,d,a,c,g
Summer	50°N	f,e,g,d,h,i,a,c,b,j	e,i,a,h,f,c,d,j,b,g
	32°N	f,d,b,e,j,g,i,h,a,c	j,e,a,f,i,b,h,g,d,c
	20°N	d,j,g,b,e,f,h,c,i,a	j,e,i,b,f,h,a,d,c,g

If values of 1 (most important) to 10 (least important) are assigned to the ranking of each scenario, and if these values are summed for each parameter, an overall parameter strength can be determined (the lowest sum representing the highest overall importance).

The day and night totals for the parameters are shown in Table V.

Although ground emissivity is the most important overall factor, its value changes very little for most natural objects in the 8 to 12 micron region (See Appendix E). On the other hand, the diffusivity varies greatly for different soils, and the wind velocity changes continually, so these parameters can be the sources of significant changes in Delta-T. The low insolation rating is surprising, but may actually

Table V

Overall Day and Night  
Parameter Strength Rating

Day			Night		
(I.D.)	Parameter Name	(Sum)	(I.D.)	Parameter Name	(Sum)
(f)	Ground Diffusivity	31	(e)	Ground Emissivity	24
(e)	Ground Emissivity	40	(j)	Internal A.C. Velocity	33
(d)	Ground Reflectivity	45	(i)	Target Thickness	40
(j)	Internal A.C. Velocity	45	(b)	Wind	45
(b)	Wind	49	(h)	Target Emissivity	49
(g)	Target Reflectivity	65	(a)	Absolute Humidity	64
(h)	Target Emissivity	66	(f)	Ground Diffusivity	65
(i)	Target Thickness	77	(d)	Ground Reflectivity	87
(c)	Solar Insolation	92	(c)	Solar Insolation	90
(a)	Absolute Humidity	95	(g)	Target Reflectivity	108

be caused by the small difference (.1) between the reflectivities of the standard target and background. The insensitivity of the absolute humidity may be due to the assumption of drier than normal standard climates. The data in Table V should be used cautiously, because many seasonal climate characteristics have been encompassed into one figure of merit.

#### Recommendations

To improve the reliability of the program, the basic weather models should be made more analytical to allow better adjustments for meteorological conditions. The test models (the ground, tank, and trees) should be checked to ensure that the heat transfer mechanisms are represented in the proper magnitude.

An attempt should be made to validate the computer model by running it with actual real-time data, such as temperature, wind, cloud-cover, and insolation. A time increment of 15 minutes is recommended for such a trial, since it seems to work well for the heat transfer models in this study. Longer increments would cause poorer resolution, and shorter increments lead to problems where time independence is assumed.



### Bibliography

1. Hudson, R.D. Jr. Infrared Systems Engineering. New York: John Wiley and Sons, Inc., 1969.
2. Rapp, James R. A Computer Model for Predicting Infrared Emission Signatures of an M60A1 Tank. Ballistic Research Labs BRL-1916, Aberdeen, Md: Aberdeen Proving Ground, August 1976. AD B013411L.
3. Kusada, T. Earth Temperatures Beneath Five Different Surfaces. NBS Report 10 373. Washington: National Bureau of Standards, February 1971. AD 733 944.
4. Bhumralkar, Chandrakant M. Numerical Experiments on the Computation of Ground Surface Temperature in an Atmospheric Circulation Model. The Rand Corporation Interim Report R-1511-ARPA. Los Angeles: Defense Advanced Research Projects Agency, May 1974. AD 783 922.
5. Gates, D.M., Energy Exchange in the Biosphere. New York: Harper and Row Publishers, Inc., 1962.
6. Johnson, F.S. "The Solar Constant." Journal of Meteorology, 11: 431-439 (1954).
7. Bell, E.E., et al. "Spectral Radiance of Sky and Terrain II." Journal of the Optical Society of America, 50: 1314-1320 (1960).
8. Boelter, L.M., et al. Heat Transfer Notes. Los Angeles: University of California Press, 1946.
9. United States Naval Observatory, Air Almanac; 1977 January-June. Washington, D.C., 1976.
10. Brooks, F.A. An Introduction to Physical Microclimatology. University of California, Davis, 1959.
11. Haurwitz, B. "Insolation in Relation to Cloud Type." Journal of Meteorology, 5: 110-113 (1948).
12. Angstrom, A. Smithsonian Miscellaneous Collection, 65, No. 3 (1915).
13. Geiger, R., The Climate Near the Ground. Cambridge, Massachusetts: Harvard University Press, 1957.
14. Lotman, M. and J. Ackerman. A Statistical Study of Target Temperature. Aero Service Corporation Report 5-232-5. Philadelphia, Pa: RADC, February 1966. AD 801 521.
15. Eckert, E.R.G., and R.M. Drake, Jr., Heat and Mass Transfer. New York: McGraw-Hill Book Company, Inc., 1959.

16. Kreith, F. Principles of Heat Transfer (Second Edition). Scranton, Pennsylvania: International Textbook Company, 1965.
17. Van Bavel, C.H.M., and J. Conaway, Remote Measurement of Surface Temperature and its Application to Energy Balance and Evaporation Studies of Bare Soil Surfaces. United States Water Conservation Laboratory Interim Report 392. Fort Huachuca, Arizona: U.S. Army Electronics Command Atmospheric Sciences Laboratory, Research Division, December 1966. AD 650 286.
18. Chemical Rubber Company, Handbook of Tables for Applied Engineering Science (Second Edition). Cleveland, Ohio: CRC Press, 1976.
19. Brunt, D. Physical and Dynamical Meteorology (second Edition). London: Cambridge University Press, 1944.
20. Byers, H.R., General Meteorology. New York: McGraw-Hill Book Company, 1959.
21. Carslaw, H.S. and J.C. Jaeger. Conduction of Heat in Solids (Second Edition). Oxford, England: Oxford University Press, 1959.
22. Case, C., Maj, USAF. Personal Communication, August 1977.
23. U.S. Air Force Environmental Technical Applications Center, Monthly Summary of Specified Hourly Weather Criteria: Grafenwoehr, W. Germany, February 1977.
24. Gates, D.M. "Heat Transfer in Plants." Scientific American, 213: 76-84 (1965).
25. Gates, D.M., R. Alderfer, and E. Taylor "Leaf Temperatures of Desert Plants." Science, 159: 994-995 (1968).
26. Pruitt, W.O., et al. Energy, Momentum and Mass Transfers Above Vegetative Surfaces. University of California. Davis, Ca: U.S. Army Electronics Command, May 1968. AD 670 051.
27. Earing, D. Data Compilation of Target and Background Characteristics (Second Volume). University of Michigan. Ann Arbor, Mi: U.S. Air Force Avionics Laboratory, 1967. AD 819 712.
28. Forsythe, W.E. Smithsonian Physical Tables (Ninth Edition). Washington: Smithsonian Institute Press, 1969.
29. McClatchey, R.A. Optical Properties of the Atmosphere (Third Edition). Air Force Cambridge Research Laboratories, Bedford, Ma: Report No. AFCRL 720497, August 1972.

## Appendix A

### Comparison of Ground Conduction Model to Analytical Solution Using Sinusoidal Input

Fig. 20 shows the analytical solution to ground temperature for a semi-infinite slab as computed from Carslaw and Jaeger (Ref 21:76). Fig. 21 shows the solution using Eq. (14) and a time increment of .25 and Fig. 22 shows the Eq. (14) solution with a time increment of .02. Additionally Fig. 23 gives an example of the TEMPS program plot with a .25 hour time increment and Fig. 24 gives an example of another TEMPS plot with a .15 hour time increment. The greatest difference between Fig. 23 and Fig. 24 is the maximum of the ground temperature; it is equal to 30.89 °C when  $DT=.25$  and it equals 31.07 when  $DT=.15$ .



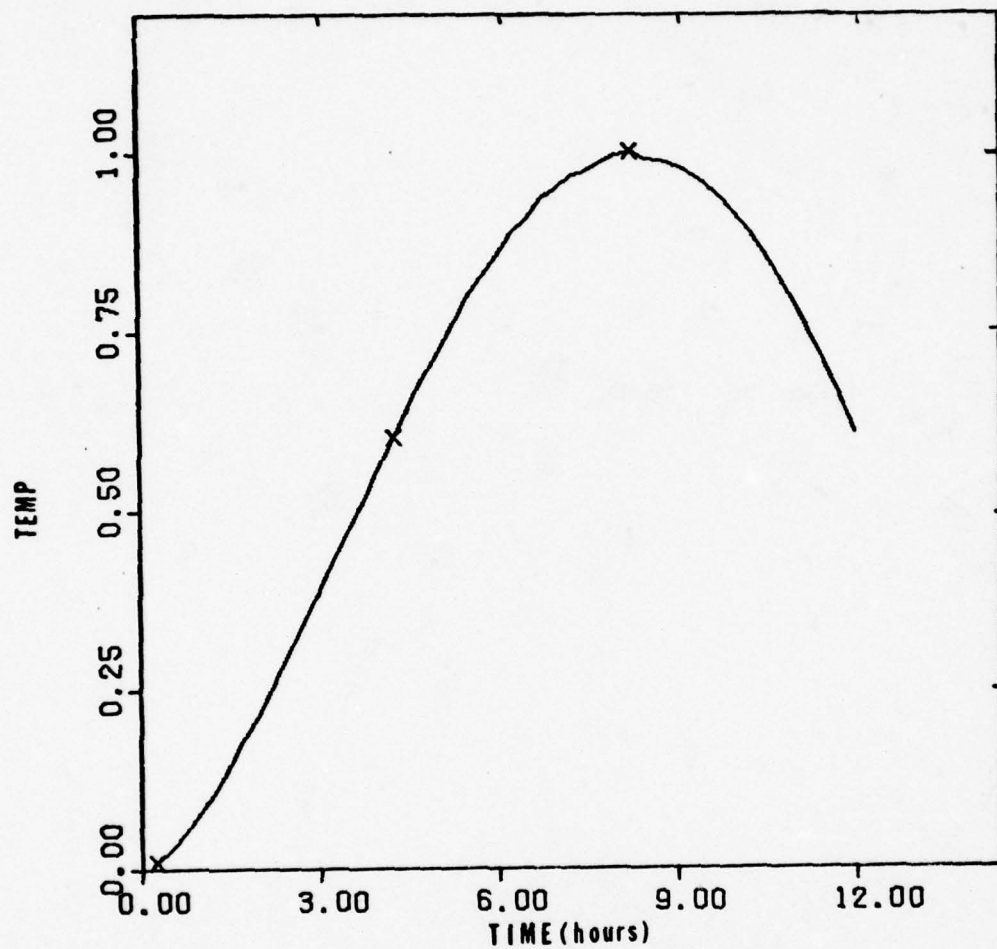


Fig. 20 Graph of analytical solution for semi-infinite slab heat conduction equation (Ref 21:76)

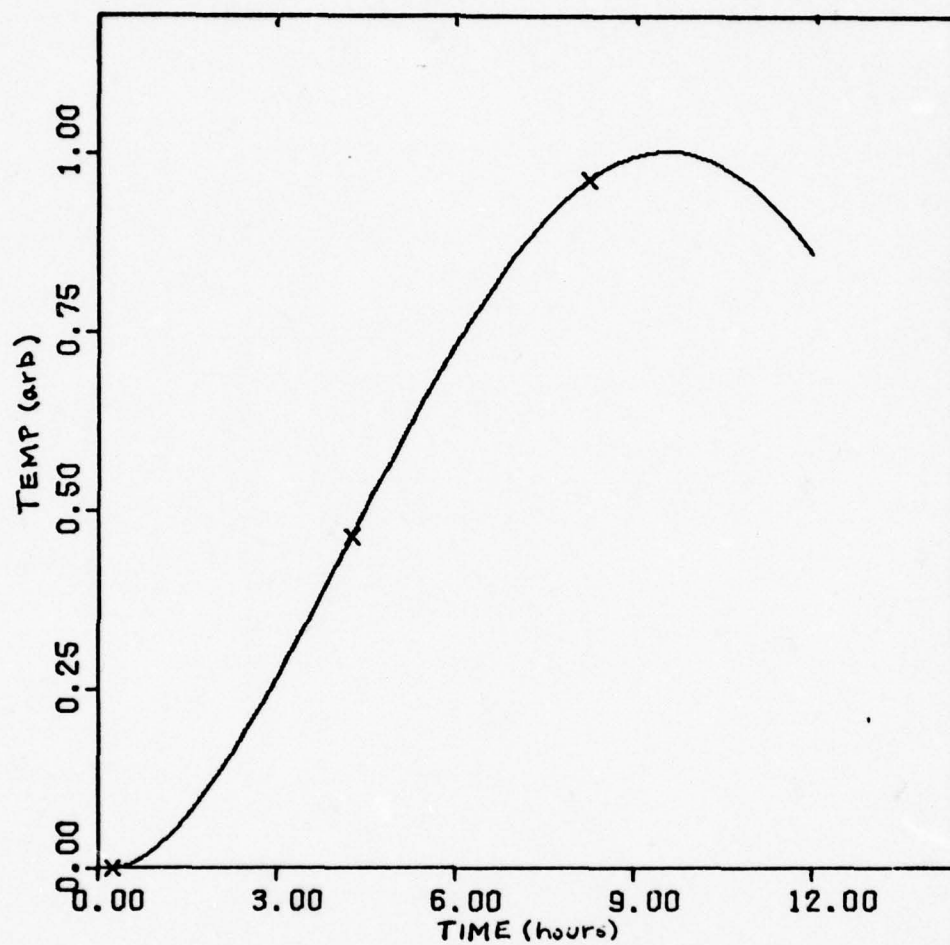


Fig. 21 Eq. (14) solution to semi-infinite slab problem, with  $DT=.25$ .

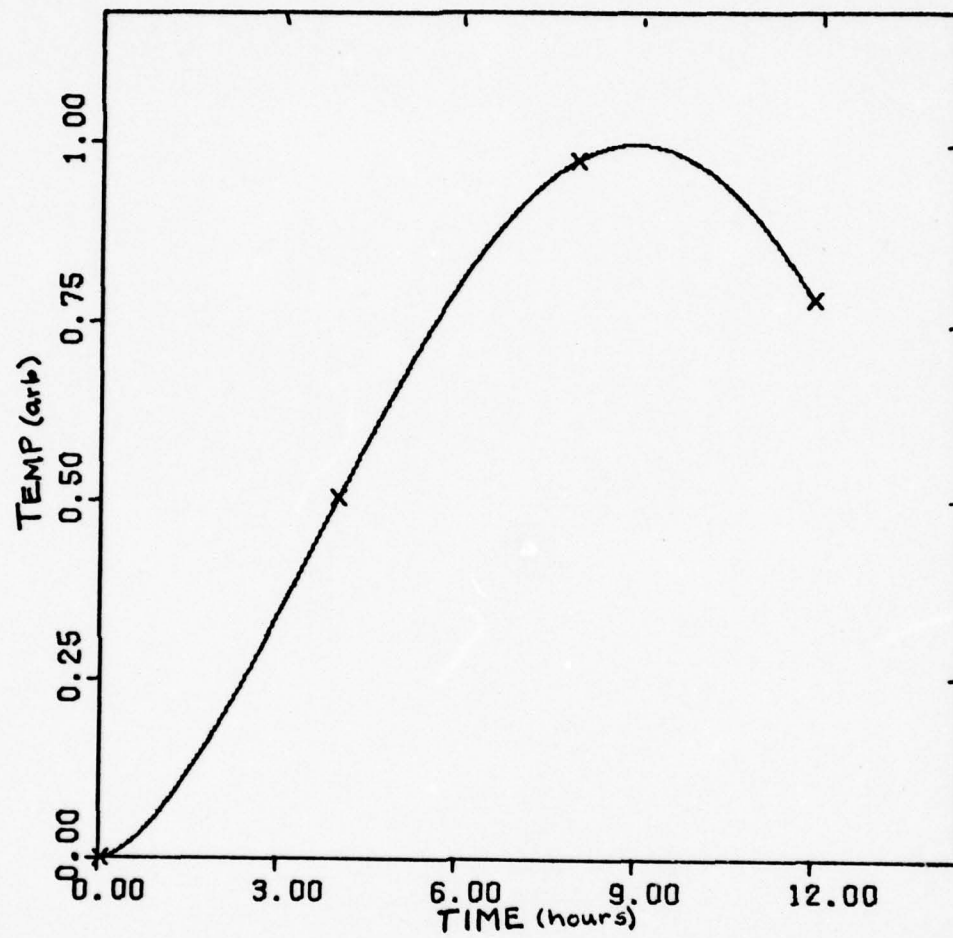


Fig. 22 Eq. (14) solution to semi-infinite slab problem, with  $DT=.02$ .



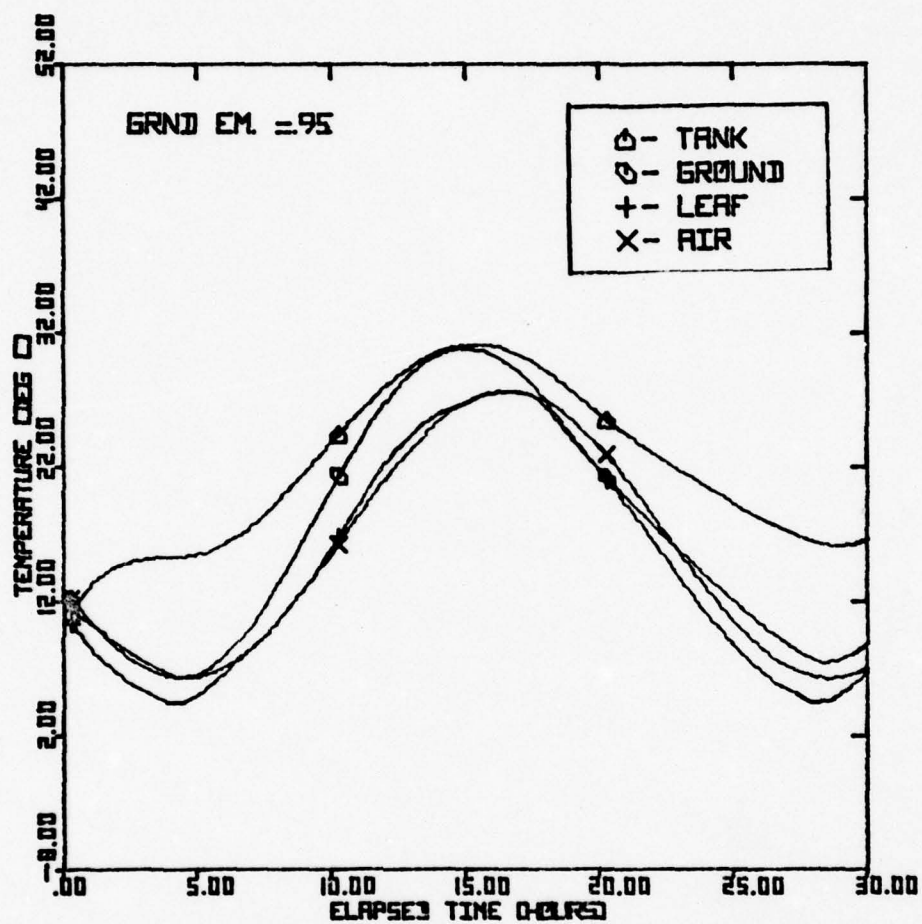


Fig. 23. TEMPS solution with DT=.25

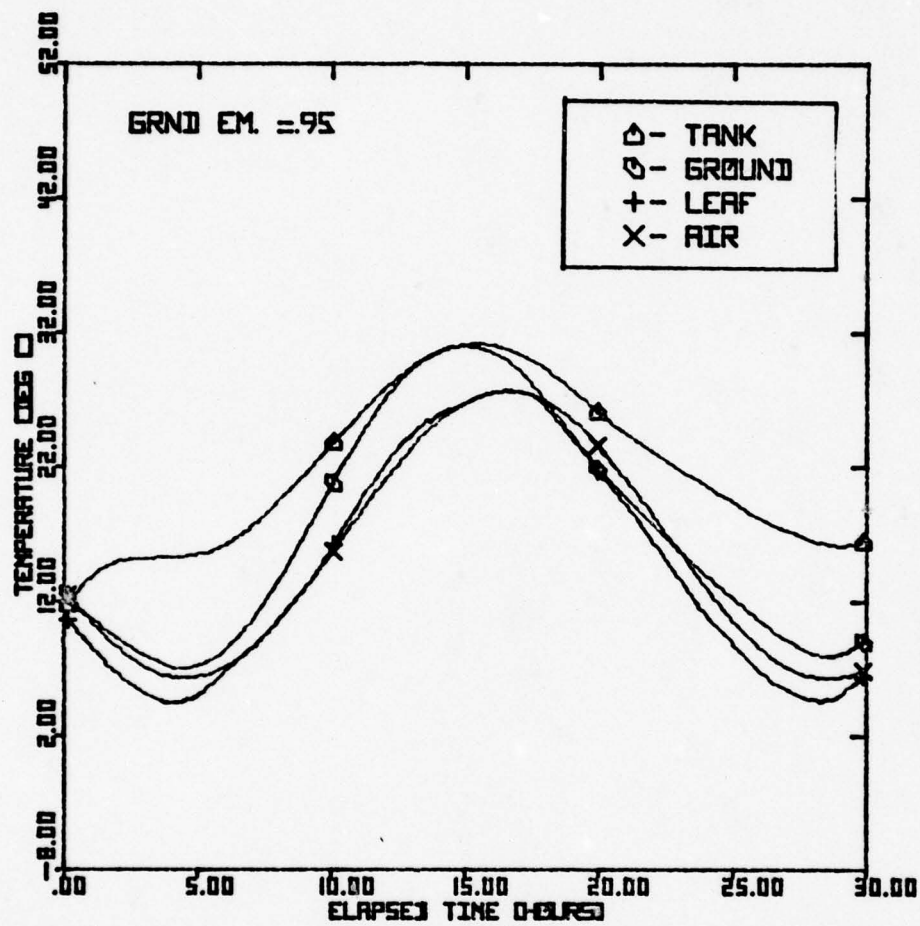


Fig. 24. TEMPS solution with DT=.15

## Appendix B

### Computer Programs TEMPS and DELTA

#### Input Data:

<u>Card</u>	<u>Symbol</u>	<u>Description</u>
1	NGRAPHS	Determines how many sets of plots are to be plotted.
	DMIN	Sets the minimum value for the graphs in program DELTA only. Is a dummy variable in program TEMPS.
	LL	An integer which determines whether the letter "S" is printed after some of the plotting information to indicate that the data is set for snow on the ground. (Data is read in by the operator though)
2	LAT	The latitude in degrees of the model location.
	DAY	The day of the run (Julian calendar).
	SPEED	Velocity of the wind in cm/sec
	CTEMP1	DC term in air temperature calculation °C
	NCLOUD	An integer that determines the type of clouds present it corresponds to the grouping listed in Table I and sets the appropriate values for the particular type of cloud.
	CLOUD	A real number from 0.0 to 1.0 to indicate what fraction of the insolation actually reaches the earth, a type of filter factor.
	WATER	Real number which indicates the total precipitable water vapor in a column one meter square reaching through the atmosphere.
	RH	Relative Humidity in a number from 0 to 100.



<u>Card</u>	<u>Symbol</u>	<u>Description</u>
2	PRESS	Atmospheric pressure in millibars.
	DUST	A measure of the particulate matter in the air in particles/cc.
3	DESOIL	The density of the soil in gm/cc.
	CPSOIL	Specific heat of the soil in Cal/gm-°C.
	DSOIL	Diffusivity of soil in cm <sup>2</sup> /min.
	ESOIL	Emmissivity of the soil.
	RSOIL	Reflectivity of the soil.
	KSOIL	Thermal conductivity of the soil in Cal/min-cm-°C.
	WET	The amount of moisture in the soil from 0.0 to 1.0.
4	DETANK	The density of the skin of the tank in gm/cc.
	CPTANK	Specific heat of the tank material in Cal/gm-°C.
	ETANK	Emmissivity of the tank.
	RTANK	Reflectivity of the tank.
	SPEEDGI	Velocity of air movement inside tank in cm/sec.
	TEMPGI	Internal temperature of the tank °C
	TTANK	Thickness of the tank in cm.
	DELEAF	The density of the leaf in gm/cc.
5	CPLEAF	Specific heat of the leaf in Cal/gm-°C.
	DIMEN	Dimension of leaf along the flow of air in cm.
	TRANS	The maximum rate of transpiration of the leaf in grams per min.
	ELEAF	Emmissivity of the leaf.
	ALEAF	Absorptivity of the leaf.
	TLEAF	Thickness of the leaf in cm.

<u>Card</u>	<u>Symbol</u>	<u>Description</u>
6	DT	Length of the time increment in hours.
	HRS	Length of desired plot in hours.
	PLOTNO	Integer used to identify the set of plots with a certain parameter that is varied (See Fig. 13)
7	DSOIL	Any parameter that is being varied (in this case it is the diffusivity of the soil). This can be any of the desired values that the operator chooses.
	XXX	The minimum value of the parameter to be varied. This value is printed in a block on the plot set that is produced by program TEMPS.
	YYY	The maximum value of the parameter to be varied.
8	DSOIL	Second value of parameter to be used in second time through the program.
9	DSOIL	Third value of parameter for third run.
10	DSOIL	Fourth value of parameter for fourth run.

Note: The sequence of cards 2 through 10 is repeated as many times as the number NGRAPHS has been set to.

The remainder of this appendix contains a listing of the Fortran program, TEMPS including all subroutines, then the Fortran program DELTA, excluding subroutines (they are identical to those used in TEMPS) and then a sample output listing from program DELTA.

```

PROGRAM TEMPS(INPUT,OUTPUT,PLOT)
REAL KSOIL,KTEMPG,KTEMPA,KTEMPT,LAT,A(8),R(8)
C,CTEMPA(122),CTEMPG(122),CTEMPT(122),CTEMPL(122)
C,TIME(122),SUN(122),SKYRAD(122),GRAD(122),7(122)
DATA (A=32.2,37.1,52.5,39.0,34.7,23.8,11.2,15.4)
DATA (R=.179,.148,.112,.063,.104,.139,-.167,.028)
READ*,NGRAPHS,OMIN,LL
DO 111 L3=1,NGRAPHS
  READ*,LAT,DAY,SPEED,CTEMP1,NCLOUD,CLOUD,WATER,RH,PRESS,DUST
  READ*,NCSOIL,CPSOIL,NSOIL,ESOIL,RSOIL,KSOIL,WET
  READ*,NETANK,CPTANK,ETANK,RTANK,SPEEDGI,TEMPGI,TANK
  READ*,OFLTAF,CPLEAF,DIMFN,TRANS,ELEAF,ALEAF,TLEAF
  READ*,O1,IPS,PLOTNO
  PT=3.141592654
  LAST=4PS/IT
  CALL PLOTS(30)
  DO 500 L=1,4
    PEAKA=PEAKG=PEAKT=PEAKL=0
    PTIMEA=PTIMEG=PTIMET=PTIMEL=0
    K=0
    L2=L-1
    IF(L.EQ.1) READ*,NSOIL,XXX,YYY
    IF(L.GT.1) READ*,OSOIL
    ITI=LAST+
    DO 15 L1=1,ITI
      CTEMPA(L1)=0
      CTEMPG(L1)=0
      CTEMPT(L1)=0
      CTEMPL(L1)=0
      TIME(L1)=1
      SUN(L1)=0
      SKYRAD(L1)=0
      GRAD(L1)=0
      7(L1)=0
    CONTINUE
    DO 1 I=1,LAST

```



```

FVAP=510
TIME(I)=T*OT
CTEMPA(I)=CTEMP1+10*SIN(1.05*PI+TIME(I)/12*PI)+2.5*SIN(1.5*PI
CATIME(I)/12*PI)
RHO=(295.77/(295.8*(CTEMPA(I)+273)))*.1
ETA=(17+(CTEMPA(I)+3)*.049)*1E-5/RHO
TEMP,GT,1)GO TO 5
CTEMPOT=CTEMPTI=CTEMPLI=CTEMPA(1)
CONTINUE
CALL TENVTH(DAY,LAT,TIME,Z,PI,I)
CALL INSOLA(R,NCLOUD,CLOUD,Z,TIME,PRESS,WATER,DUST,SUN,PI,I)
CALL E(CTEMPA,SKYRAD,RH,I)
CALL COND(CTEMPOT,CTEMPA,SPEED,SUN,SKYRAD,CTEMPOT,TIME,RHO,RH,
CGRAD,FSOIL,PSOIL,PI,I,OSOIL,DESOIL,CPSOIL,ETA,DT,KSOIL,WET,PRESS,
CFAD)
IF(CTEMPOT(I).LT.0.AND.LL.EQ.1)EVAP=530
RHO=(295.77/(295.8*(TEMPOT(I)+273)))*.1
ETAGT=(17+(TEMPOT(I)+3)*.049)*1E-5/RHOT
CALL TANK(SPEED,SPEEDGT,ETA,ETAGT,CTEMPOT,CTEMPA,RTANK
CTEMPOT,I,DT,DETANK,CTANK,SUN,SKYRAD,CTEMPOT,CTEMPTI
CTANK,TANK)
CALL LEAF(SPEED,NIMEN,ETA,SUN,RSOIL,CTEMPL,DT,CTEMPA
C,ELFAF,ALFAF,SKYRAD,GRAD,TRANS,FVAP,I)
J1=I-1
J2=I-2
IF(CTEMPA(J1).GT.CTEMPA(J2).AND.CTEMPA(J1).GT.CTEMPA(I))
CPEAKA=CTEMPA(J1)
IF(CTEMPA(J1).GT.CTEMPA(J2).AND.CTEMPA(J1).GT.CTEMPA(I))
CPTIMEA=TEMP(I)
IF(CTEMPOT(J1).GT.CTEMPOT(J2).AND.CTEMPOT(J1).GT.CTEMPOT(I))
CPEAKC=CTEMPOT(J1)
IF(CTEMPOT(J1).GT.CTEMPOT(J2).AND.CTEMPOT(J1).GT.CTEMPOT(I))
CPTIMEG=TIME(J1)
IF(CTEMPOT(J1).GT.CTEMPOT(J2).AND.CTEMPOT(J1).GT.CTEMPOT(I))
CPEAKT=CTEMPOT(J1)
IF(CTEMPOT(J1).GT.CTEMPOT(J2).AND.CTEMPOT(J1).GT.CTEMPOT(I))

```

```

000460
000470
000480
000490
000500
000510
000520
000530
000540
000550
000560
000570
000580
000590
000600
000610
000620
000630
000640
000650
000660
000670
000680
000690
000700
000710
000720
000730
000740
000750
000760
000770
000780
000790
000800
000810
000820

```

```

COTIME=TIME(J1)
IF(CTEMPL(J1).GT.CTEMPL(J2).AND.CTEMPL(J1).GT.CTEMPL(I))GO TO 19
GO TO 1
CONTINUE
IF(K.EQ.0)PEAKL=CTEMPL(J1)
IF(K.EQ.0)PTIME=TIME(J1)
K=K+1
IF(CTEMPL(J1).GT.PEAKL)PTIME=TIME(J1)
IF(CTEMPL(J1).GT.PEAKL)PEAKL=CTEMPL(J1)
CONTINUE
IF(L.EQ.1)PRINT*, " --PLOT SET--", PLOTNO, LAT, DAY
PRINT*, "PEAK TEMPS AND TIMES-ITERATION #", L
PRINT*, "*****"
PRINT*, "AIR ", PEAKL, " ", PTIME
PRINT*, "GROUND ", PEAKL, " ", PTIME
PRINT*, "TANK ", PEAKL, " ", PTIME
PRINT*, "LEAF ", PEAKL, " ", PTIME
PRINT*, "*****"
PRINT*
M1=LAST+1
M2=LAST+2
TIME(M1)=1
TIME(M2)=IPS/6
NLAST=LAST/3
CTEMPA(M1)=CTEMPG(M1)=CTEMPT(M1)=CTEMPL(M1)=CTEMP1-25
CTEMPA(M2)=CTEMPG(M2)=CTEMPT(M2)=CTEMPL(M2)=10
IF(L.EQ.1)CALL PLOT(1.,-11.,-3)
CALL FACTOR (.43)
IF(L.EQ.1)CALL PLOT(3.,12.,-3)
IF(L.EQ.2)CALL PLOT(7.,0.,-3)
IF(L.EQ.3)CALL PLOT(-7.,-7.5,-3)
CALL AXIS(0.,0.,20*ELAPSED TIME (HOURS),-20,6.,0.,TIME(M1),
CTIME(M2))
CALL PLOT(6.,0.,3)
DO 122 I1=1,6
X12=I12

```

```

000830
000840
000850
000860
000870
000880
000890
000900
000910
000919
000920
000930
000940
000950
000960
000970
000980
000990
001000
001010
001020
001030
001040
001050
001060
001070
001080
001090
001100
001110
001120
001130
001140
001150
001160

```

19

1

```

122 CALL PLCT(5.,X12,2)
CALL PLCT(5.9,X12,2)
CALL PLCT(6.,X12,3)
ON 123 112=1,6
X12=5.-11,
CALL PLCT(X12,6.,2)
CALL PLCT(X12,5.9,2)
CALL PLCT(X12,5.,3)
CALL PLCT(X12,6.,2)
CALL AXTC(0.,0.,19,TEMPERATURE (DEG C),19,6.,90.,CTEMPA(M1),
CTEMPA(M2))
IF(L.GT.1)GO TO 35
CALL SYM3L(9.,8.5.,14,2,0.,-1)
CALL SYM3L(99.,99.,14,7H - TANK,0.,7)
CALL SYM3L(9.,8.25.,14,1,0.,-1)
CALL SYM3L(99.,99.,14,9H - GROUND,0.,9)
CALL SYM3L(9.,8.,14,3,0.,-1)
CALL SYM3L(99.,99.,14,7H - LEAF,0.,7)
CALL SYM3L(9.,7.75.,14,4,0.,-1)
CALL SYM3L(99.,99.,14,6H - AIR,0.,6)
CALL SYM3L(2.,5.375.,2,9H PLOT SET,0.,9)
CALL NUMBER(99.,99.,2,1H/0.,-1)
CALL SYM3L(99.,99.,2,1H/0.,1)
CALL NUMBER(99.,99.,2,LAT,0.,-1)
CALL SYM3L(99.,99.,2,1H/0.,1)
CALL NUMBER(99.,99.,2,DAY,0.,-1)
IF(L.F.C.1)CALL SYM3L(99.,99.,2,1HS,0.,1)
CALL SYM3L(2.,8.,14,14HGRND DIFF RANGE,0.,19)
CALL NUMBER(2.,7.75.,14,XX,0.,2)
CALL SYM3L(99.,99.,14,4H TO,0.,4)
CALL NUMBER(99.,99.,14,YYY,0.,2)
CALL SYM3L(99.,99.,14,9H SQ CM/MIN,0.,9)
CALL PLCT(1.75,7.5,3)
CALL PLCT(1.75,8.75,2)
CALL PLCT(10.5,8.75,2)
CALL PLCT(10.5,7.5,2)
001170
001180
001190
001200
001210
001220
001230
001240
001250
001260
001270
001280
001290
001300
001310
001320
001330
001340
001350
001360
001370
001380
001390
001400
001410
001420
001430
001440
001450
001460
001470
001480
001490
001500
001510
001520

```



```

35      CALL PLOT(1.75,7.5,2)
        CONTINUE
        CALL SYMOL(.5,5.5,.14,10,GRND DIFF=0.,10)
        CALL NUMBER(999.,99.,.14,DSOIL,0.,2)
        CALL LINE(TIME,CTEMP0,LAST,1,NLAST,4)
        CALL LINE(TIME,CTEMP0,LAST,1,NLAST,1)
        CALL LINE(TIME,CTEMP1,LAST,1,NLAST,2)
        CALL LINE(TIME,CTEMP1,LAST,1,NLAST,3)
        CONTINUE
500      IF(L3.LT. IGRAPH5)CALL PLOT(11.,0.,-3)
        IF(L3.EQ. IGRAPH5)CALL PLOT6
        CONTINUE
111      STOP
        END
        SUBROUTINE ZENITH(DAY,LAT,TIME,Z,PI,I)
        REAL LAT,TIME(122),Z(122)
        DECL=((TA/183*52.88)-25.64)/180*PI
        IF(DAY.GT.183)Z=CL=(26.64-DAY/365*52.88)/180*PI
        ELZ=(LAT/180*PI)
        TIMEZ=(TIME(I)/12*PI)+PI
        IF(TIMEZ.GT.2*PI)TIMEZ=TIMEZ-2*PI
        A=COS(DECL)*COS(ELZ)*COS(TIMER)
        B=SIN(DECL)*SIN(ELZ)
        C=A+B
        Z(I)=ACOS(C)
        RETURN
        END
        SUBROUTINE INSOL(A,Z,N,CLOUD,Z,TIME,PRESS,WATER,DUST,SUN,PI,I)
C)
        REAL A(8),B(8),Z(122),TIME(122),SUN(122),M
        IF(Z(I).GT.PI/2)SUN(I)=0
        IF(Z(I).GT.PI/2)RETURN
        M=1/COS(Z(I))
        A1=-.085*(PRESS/1013**4)**.75
        A2=-.174*(WATER/20**4)**.6
        A3=-.087*(DUST**4)**.9

```

```

001530
001540
001550
001560
001570
001580
001590
001600
001610
001620
001630
001640
001650
001660
001670
001680
001690
001700
001710
001720
001730
001740
001750
001760
001770
001780
001790
001790
001800
001810
001820
001830
001840
001850
001860
001870
001880

```

```

001890      ARG1=A1+A2+A3
001900      QP=2.0*EXP(ARG1)
001910      QP=QP/M
001920      IF(NCLOUD.EQ.0)SUN(I)=0
001930      IF(NCLOUD.EQ.0)RETURN
001940      ARG2=-((1/NCLOUD)-.059)*M
001950      SUN1=0*(1/(NCLOUD)/3+.4)*EXP(ARG2)
001960      SUN(I)=SUN1*(.35+.61*NCLOUD)
001970      RETURN
001980      END
001990      SUBROUTINE F(CTEMPA,SKYRAD,RH,I)
002000      REAL CTEMPA(122),SKYRAD(122),KTEMPA
002010      EFAC=24/10*(6.1+(CTEMPA(I)/50)**2*117.3)
002020      FFAC1=EFAC*.052
002030      ALPHA=(.91-(.2411)*(1)*EFAC1)
002040      KTEMPA=CTEMPA(I)+273
002050      SKYRAD(I)=.793E-10*KTEMPA**4*ALPHA
002060      RETURN
002070      END
002080      SUBROUTINE GRAD(CTEMPG,CTEMPA,SPEED,SUN,SKYRAD,CTEMPGI,TIME,RHO,RH)
002090      C,GRAD,FSOIL,RSOIL,PI,I,DSOIL,DESOIL,CPSOIL,ETA,DT,KSOIL,WET,PRESS,CEVAP)
002100      REAL TIME(122),KTEMPG,CTEMPG(122),CTEMPA(122),CONVG(122),SUN(122)
002110      C,SKYRAD(122),GRAD(122),RG(122),ENERGY1(122),KSOIL,Y(122),KAPPA
002120      C,KTEMPA,L(122)
002130      I1=I-1
002140      KTEMPG=CTEMPG(I1)+273
002160      IF(I.EQ.1)KTEMPG=CTEMPA(I)+273
002170      KTEMPA=CTEMPA(I)+273
002210      FS=EXP((KTEMPG-273)/(KTEMPG*273)*5423)*6.1071
002220      FA=EXP((KTEMPA-273)/(KTEMPA*273)*5423)*.061071*RH
002230      LE(I)=.79122*EVAP*PSPEED*PHO*WET/PRESS*(ES-FA)
002240      IF(LE(I).LT.0)LE(I)=0
002250      DELTAT=CTEMPG(I1)-CTEMPA(I1)
002260      IF(I1.LT.2)DELTAT=0
002270      A1=1.8+((CPFEQ-152.4)/306.8*2.4)-((SPFEQ-152.4)/1771.6)**2*2.6
002280

```

```

CONV3(I)=11*8.136E-3*DEL TAT
ASOIL=1-OSOIL
GPAN(I)=.793E-10*ESOIL*KTEMPG**4
OG(I)=SUM(I)*(ASOIL)+SKYPAD(I)*ESOIL-GRAD(I)-CONV3(I)-LE(I)
IF(I.LT.2)CTFMPG(I)=CTEMPDI
IF(I.LT.2)RETURN
ENERGY=0
T=0
X=0
DO 1 K=1,
M=K-1
NTIME1=(TIME(I)-TIME(K))*60
N7=SQRT(OSOIL*NTIME1)
KAPPA=- SQRT(PI/(720*OSOIL))
ALPHA=EXP(N7*KAPPA)
Y(K)=((CTFMPG(K)-12.75)*EXP(N7*KAPPA))
IF(Y(K).GT.X)T=TIME(K)
IF(Y(K).GT.X)X=Y(K)
ENERGY=OG(K)*DT*60/SQRT((T-M)*OSOIL*DT*60)+ENERGY
DELTATG=ENERGY/(OSOIL*OSOIL)
CTFMPG(I)=CTEMPDI+DELTATG
X1=X+12.75
IF(X1.LE.CTEMPG(I))RETURN
X2=X1-CTEMPDI
NTIME=TIME(I)-T
N7=SQRT(OSOIL*NTIME*60)
OADO=X2*OSOIL*OSOIL/77
OG(I)=OG(I)+OADO/(DT*60)
ENERGY=ENERGY+OADO
DELTATG=ENERGY/(OSOIL*OSOIL)
CTEMPDI(I)=CTEMPDI+DELTATG
RETURN
END
SUBROUTINE TANK(SPEED,SPEEOGI,ETA,ETAGI,CTEMPT,CTFMPA,RTANK
C,TEMPGI,I,DT,DETANK,CPTANK,SUN,SKYRAD,CTEMPTI
C,ETANK,TTANK)

```



```

002550      REAL CTEMP2(122),CTEMPA(122),CONVT1(122),CONVT2(122)
002560      C,TRAD(122),SUN(122),SKYRAD(122)
002570      A1=1.8+((SPEED-152.4)/374.8*2.4)-((SPEED-152.4)/1371.6)**2*2.6
002580      A2=1.8+((SPEED-152.4)/374.8*2.4)-((SPEED-152.4)/1371.6)**2*2.6
002590      I1=I-1
002700      DELTAT=CTEMPT(I1)-CTEMPA(I1)
002710      DELTGI=CTEMPT(I1)-TEMPGI
002720      IF(I.LT.2)DELTAT=0
002730      IF(I.LT.2)DELTGI=TEMPGI-CTEMPA(I)
002740      CONVT1(I)=A1*.135E-3*DELTAT
002750      CONVT2(I)=A2*.135E-3*DELTGI
002760      KTEMPT=CTEMPT(I1)+273
002770      IF(I.EQ.1)KTEMPT=CTEMPTI+273
002780      KTEMPGI=TEMPGI+273
002790      ATANK=1-ATANK
002800      TRAD(I)=.793E-10*KTEMPT**4*ETANK
002810      ONETT=(SUN(I)*(1-RTANK)+SKYRAD(I))*ETANK
002820      C=CONVT1(I)-CONVT2(I)-TRAD(I))*DT*60
002830      DELTATT=ONETT/(OFTANK*OBTANK*TTANK)
002840      IF(I.LT.2)CTEMPT(I)=CTEMPTI+DELTATT
002850      IF(I.LT.2)RETURN
002860      CTEMPT(I)=CTEMPT(I1)+DELTATT
002870      RETURN
002880      END
002890      SUBROUTINE LEAF(SPEED,DTMEN,ETA,SUN,PSOIL,CTEMPL,DT,CTE
002900      MPA,ELFAF,ALEAF,SKYRAD,GRAD,TRANS,EVAP,I)
002910      REAL SUN(122),CTEMP_(122),GRAD(122),CTEMPA(122),SKYRAD(122),LE,
002920      CLEMAX,LEAF
002930      DP=.71
002940      GO=2.04*((2.03-(CTEMPA(T)*.007))/(.145+(CTEMPA(I)*.0003))**2)
002950      S=SUM(I)*ALEAF*(1+RSOIL)
002960      P=(SKYRAD(I)+GRAD(I))*ELFAF
002970      A2=.564**5E-3*(PO)**.373*SQRT(SPEED/(DIMFN*ETA))
002980      LEMAX=TRANS*EVAP*2
002990      DELTAT= (
003000      N=0

```

003010  
003020  
003030  
003040  
003050  
003060  
003070  
003080  
003090  
003100  
003110  
003120  
003130  
003140  
003150  
003160  
003170  
003180  
003190  
003200  
003210  
003220  
003230  
003240  
003250  
003260

```

M=0
LF=0
1  R1=.71*.35-3*SQR(SQRT(GR*PR*ABS(DELTA T)/OIMFN))
   IF(R1.GT.12)R=R1
   IF(R2.GE.11)R=R2
   Z=2*R*DELTA T
   LPAO=2*.713E-10*(CTEMPA(I)+273+DELTA T)**4
   F=S+R-LF-Z-LRAD
   M=M+1
   IF(M.GT.1100)GO TO 3
   IF(F.LT.0.AND.N.EQ.0)N=1
   IF(F.LT.0.AND.N.EQ.2)GO TO 3
   IF(F.LT.0)GO TO 2
   IF(F.GT.0.AND.N.EQ.0)N=2
   IF(F.GT.0.AND.N.EQ.1)GO TO 3
   IF(LF.GE.LEMAX)GO TO 4
   LF=LF+.001*M
   GO TO 1
4  DELTA T=DELTA T+.01*M
   GO TO 1
2  DELTA T=DELTA T-.01*M
   GO TO 1
3  CTEMP(I)=CTEMPA(I)+DELTA T
   IF(M.GT.1100)PRINT*, "TOO MANY LEAF ITERATIONS AT I=",I
   RETURN
   END

```

```

PROGRAM DELTA(INPUT, OUTPUT, PLOT)
REAL KSOIL, KTEMPG, KTEMPA, KTEMPT, LAT, A(8), R(8)
C, CTEMPA(12), CTEMPG(122), CTEMPT(122), CTEMPPL(122)
C, TIME(122), SUM(122), SKYDAD(122), GRA(122), Z(122)
C, TIME2(122), X1(122), XL1(122)
DATA (A=82.2, 87.1, 52.5, 39.0, 34.7, 23.8, 11.2, 15.4)
DATA (R=.179, .148, .112, .063, .104, .139, -.167, .028)
PRINT*, "READ IN NUMBER OF GRAPHS, MIN DELTA-T, AND SNOW (1)"
READ*, NGRAPHS, OMIN, LL
DO 111 L3=1, NGRAPHS
PRINT*, "READ IN ENVIRONMENTAL FACTORS"
PRINT*, "LAT, JULIAN DAY, WIND, MEANTEMP, CLOUDTYPE, PERCENT SUN"
PRINT*, "WATER VAPOR, HUMIDITY, PRESSURE, DUST"
PRINT*
READ*, LAT, DAY, SPEED, CTEMP1, NCLOUD, CLOUD, WATER, RH, PRESS, DUST
PRINT*
PRINT*, "READ IN GROUND PARAMETERS"
PRINT*, "DENSITY, SPECIFIC HEAT, DIFFUSIVITY, EMISSIVITY, REFLECTIVITY,
THERMAL CONDUCTIVITY, MOISTURE"
PRINT*
READ*, DSOIL, CPSOIL, DSOIL, ESOIL, RSOIL, KSOIL, WET
PRINT*
PRINT*, "READ IN TANK PARAMETERS"
PRINT*, "DENSITY, SPECIFIC HEAT, EMISSIVITY, REFLECTIVITY, A.C.VEL"
PRINT*, "INTERNAL TEMP, THICKNESS"
PRINT*
READ*, DETANK, CPTANK, ETANK, RTANK, SPEEDGI, TEMPGI, TTANK
PRINT*
PRINT*, "READ IN LEAF PARAMETERS"
PRINT*, "DENSITY, SPECIFIC GRAVITY, SIZE, TRANSPIRATION RATE"
PRINT*, "EMISSIVITY, ABSORPTION, THICKNESS"
PRINT*
READ*, CLEAF, CPLEAF, DIMEN, TRANS, ELEAF, ALEAF, TLEAF
PRINT*
PRINT*, "READ IN CONTROL FACTORS"
PRINT*, "TIME INCREMENT, #HRS. PRINT #"

```

```

000100
000110
000120
000130
000140
000150
000160
000170
000180
000190
000200
000210
000220
000230
000240
000250
000260
000270
000280
000290
000300
000310
000320
000330
000340
000350
000360
000370
000380
000390
000400
000410
000420
000430
000440
000450

```





```

PRINT*, "REFLECTIVITY=", PTANK
PRINT*, "AIR CONDITIONING VELOCITY=", SPEEDGI
PRINT*, "INTERNAL TEMPERATURE=", TEMPGI
PRINT*, "THICKNESS=", TTANK
PRINT*
PRINT*, "LEAF PARAMETERS"
PRINT*, "-----"
PRINT*, "DENSITY=", DELFAF
PRINT*, "SPECIFIC HEAT=", CPLEAF
PRINT*, "SIZE=", DIMEN
PRINT*, "TRANSPARATION RATE=", TRANS
PRINT*, "EMISSIVITY=", ELFAF
PRINT*, "ABSORPTION=", ALFAF
PRINT*, "THICKNESS=", TLEAF
PRINT*, "*****"
PRINT*
PRINT*
PRINT*
IF (L3.L5.1) CALL PLOT(1., -11., -3)
CALL FACTOR (.43)
IF (L3.G7.1) GO TO 8
CALL PLOT(30)
CALL PLOT(3.5, 12., -3)
CALL SYMOL(.5, 9.35, .2, 234DELTA-T (TARGET-GROUND), 0., 23)
CALL SYMOL(.4, 8.02, .14, 10HPARAMETER-, 0., 10)
CALL SYMOL(399., 999., .14, 9HGRND DIFF, 0., 9)
CALL SYMOL(3.55, 9.02, .14, 11JULIAN DAY-, 0., 11)
CALL NIMVER(999., 999., .14, DAY, 0., -1)
IF (L3.L5.1) CALL SYMOL(999., 999., .14, 1HS, 0., 1)
CALL PLOT(5.8, 8.8, 3)
CALL PLOT(5.8, 9.75, 2)
CALL PLOT(.15, 9.75, 2)
CALL PLOT(.15, 3.8, 2)
CALL PLOT(5.8, 9.8, 2)
CONTINUE
CALL SYMOL(.1, 5.65, .12, 9HPLOT SET, 0., 9)
CALL PLOT(0., 5.5, 3)

```

001190  
001200  
001210  
001220  
001230  
001240  
001250  
001260  
001270  
001280  
001290  
001300  
001310  
001320  
001330  
001340  
001350  
001360  
001370  
001380  
001390  
001400  
001410  
001420  
001430  
001440  
001450  
001460  
001470  
001480  
001490  
001500  
001510  
001520  
001530  
001540

CALL PLCT(2.15,5.5,2)  
CALL PLCT(2.15,5.95,2)  
CALL PLCT(3.9,5.95,3)  
CALL PLCT(3.9,5.15,2)  
CALL PLCT(6.125,5.15,2)  
CALL NUNMER(999.,.12,FLOTNO,0.,-1)  
CALL SYMNL(999.,.12,1H/,0.,1)  
CALL NUNMER(999.,.12,LAT,0.,-1)  
CALL SYMNL(999.,.12,1H/,0.,1)  
CALL NUNMER(999.,.12,DAY,0.,-1)  
CALL PLCT(0.,5.95,3)  
DO 122 I1=1,6  
X12=I12\*1.  
CALL PLCT(X12,5.95,2)  
CALL PLCT(X12,5.85,2)  
CALL PLCT(X12,5.95,3)  
CALL PLCT(6.125,5.95,2)  
CALL PLCT(6.125,5.,2)  
CALL PLCT(6.025,5.,2)  
CALL PLCT(6.125,5.,3)  
DO 123 I1=1,5  
Y12=5-I12  
CALL PLCT(6.125,Y12,2)  
CALL PLCT(6.025,Y12,2)  
CALL PLCT(6.125,Y12,3)  
DO 100 I1=1,4  
PEAKA=PEAKG=PEAKT=PEAKL=0  
PTIME=A=PTIMEG=PTIMET=PTIMEL=0  
K=0  
IF(L.EQ.1)INC=3  
SUNNY=0  
EVAP=6.0  
L2=L-1  
IF(L.EQ.1)PEAO\*,DSOIL,XX,YYY  
IF(L.GT.1)RFAD\*,DSOIL  
ITL=LAST+2

122

123



```

DO 15 L1=1,III
CTEMPA(L1)=0
CTEMPG(L1)=0
CTEMPT(L1)=0
CTEMPL(L1)=0
TIME(L1)=1
SUN(L1)=0
SKYRAD(L1)=0
GRAD(L1)=1
Z(L1)=0
XL1(L1)=0
X1(L1)=0
TIME2(L1)=0
DO 1 I=1, LAST
TIME(I)=I*DT
CTEMPA(I)=CTEMP1+10*SIN(1.05*PI+TIME(I)/12*PI)+2.5*SIN(1.5*PI
C+TIME(I)/12*PI)
RH0=(PRESS/(285.8*(CTEMPA(I)+273)))*.1
FTA=(17+(CTEMPA(I)+3)*.049)*1E-5/RH0
IF(I.GT.1)GO TO 5
CTEMPGI=CTEMPOTI=CTEMPLI=CTEMPA(1)
CONTINUE
CALL ZENITH(DAY,LAT,TIME,7,PI,I)
CALL INSOL(A,3,NCLOUD,CLOUD,Z,TIME,PRESS,WATER,DUST,SUN,PI,I)
IF(LT.2)SUNNY=SUNNY+SUN(I)*DT*60
CALL F(CTEMPA,SKYRAD,RH,I)
CALL GRN(CTEMPG,CTEMPA,SPEED,SUN,SKYRAD,CTEMPGI,TIME,RH0,RH
C,GRAD,ESOL,RSOIL,PI,I,CSOIL,DESOIL,CPSOIL,ETA,DT,KSOIL,WET,PRESS,
CEVAP)
IF(CTEMPG(I).LE.0)EVAP=R0
IF(CTEMPG(I).GT.0)EVAP=R00
RHOT=(PRESS/(285.8*(CTEMPGI+273)))*.1
ETAGI=(17+(CTEMPGI+3)*.049)*1E-5/RHOT
CALL TANK(SPEED,SPEEDGI,FTA,ETAGI,CTEMPT,CTEMPA,RTANK
C,TFMGI,I,DT,DETANK,CPTANK,SUN,SKYRAD,CTEMPTI
C,ETANK,TTANK)

```

```

001550
001560
001570
001580
001590
001600
001610
001620
001630
001640
001650
001660
001670
001680
001690
001700
001710
001720
001730
001740
001750
001760
001770
001780
001790
001800
001810
001820
001830
001840
001850
001860
001870
001880
001890
001900

```

16  
15

5

```

CALL LEF(SPEED, DIMEN, FTA, SUN, RSOIL, CTEMP, OT, CTEMPA
C, ELEAF, ALTA, SKYRAD, GRAD, TRANS, EVAP, I)
J1=I-1
J2=I-2
IF(CTEMPA(J1).GT.CTEMPA(J2).AND.CTEMPA(J1).GT.CTEMPA(I))
CPEAKA=CTEMPA(J1)
IF(CTEMPA(J1).GT.CTEMPA(J2).AND.CTEMPA(J1).GT.CTEMPA(I))
CPTIMEA=TIME(J1)
IF(CTEMPG(J1).GT.CTEMPG(J2).AND.CTEMPG(J1).GT.CTEMPG(I))
CPEAKG=CTEMPG(J1)
IF(CTEMPG(J1).GT.CTEMPG(J2).AND.CTEMPG(J1).GT.CTEMPG(I))
CPTIMEG=TIME(J1)
IF(CTEMPT(J1).GT.CTEMPT(J2).AND.CTEMPT(J1).GT.CTEMPT(I))
CPEAKT=CTEMPT(J1)
IF(CTEMPT(J1).GT.CTEMPT(J2).AND.CTEMPT(J1).GT.CTEMPT(I))
CPTIME=TIME(J1)
IF(CTEMPL(J1).GT.CTEMPL(J2).AND.CTEMPL(J1).GT.CTEMPL(I))GO TO 19
GO TO 9
IF(K.LE.0)PEAKL=CTEMPL(J1)
IF(K.LE.0)PTIME=TIME(J1)
K=K+1
IF(CTEMPL(J1).GT.PEAKL)PTIME=TIME(J1)
IF(CTEMPL(J1).GT.PEAKL)PEAKL=CTEMPL(J1)
CONTINUE
IF(I.LT.3)GO TO 7
OT1=CTEMPG(I)-CTEMPT(I)
OT2=CTEMPG(J1)-CTEMPT(J1)
OT3=CTEMPG(I)-CTEMPL(I)
OT4=CTEMPG(J1)-CTEMPL(J1)
OT5=CTEMPT(I)-CTEMPL(I)
OT6=CTEMPT(J1)-CTEMPL(J1)
IF(TIME(I).LT.6)GO TO 200
I3=I-(6/OT)+1
TIME2(I3)=6+I3*OT
X1(I3)=-OT
IF(I3.EQ.1)YMAX=X1(I3)

```

19

9

AD-A055 642

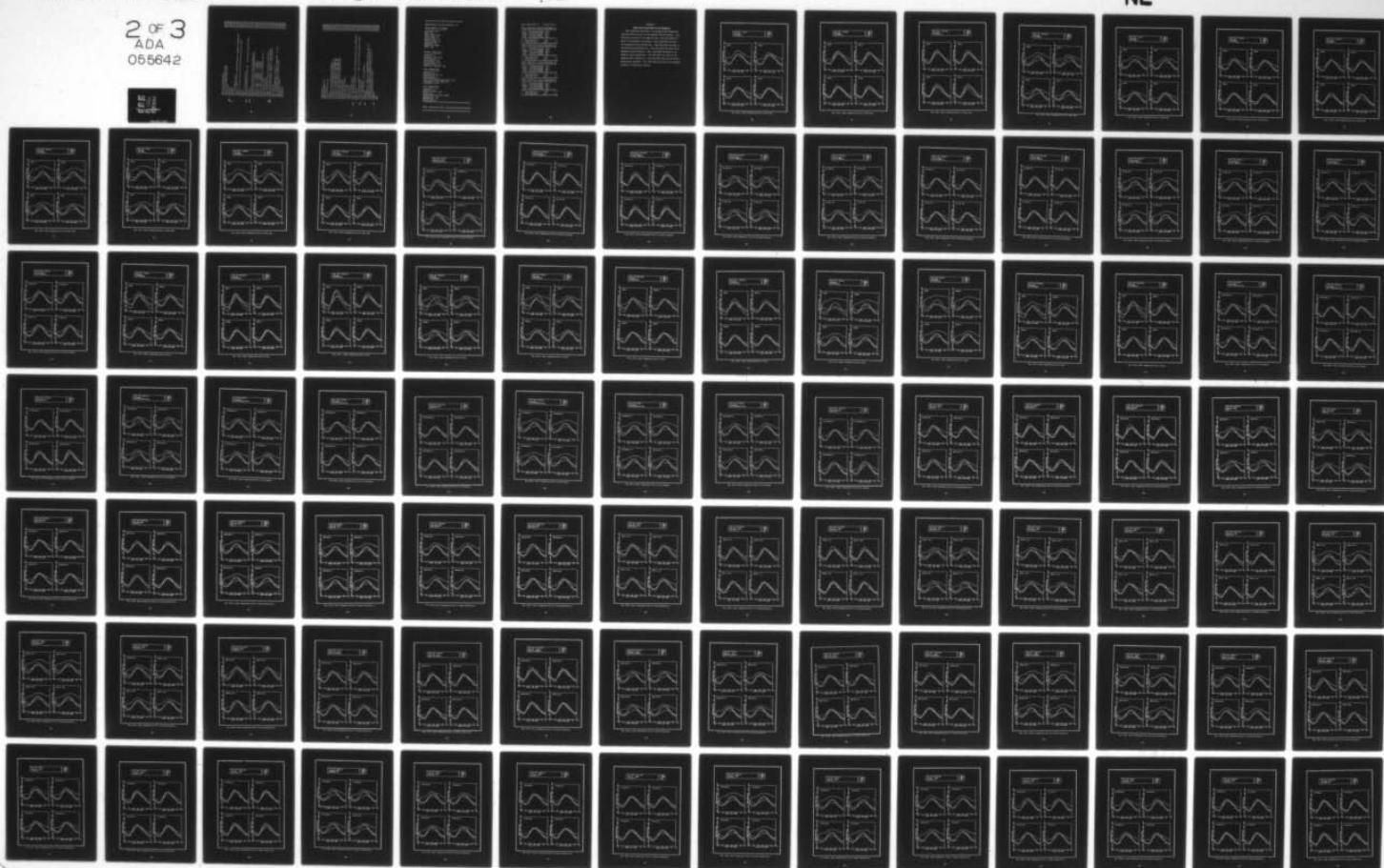
AIR FORCE INST OF TECH WRIGHT-PATTERSON AFB OHIO SCH--ETC F/G 17/5  
A THEORETICAL ANALYSIS OF CHANGES IN THERMAL SIGNATURES CAUSED --ETC(U)  
DEC 77 J T SMALL

UNCLASSIFIED

AFIT/GEP/PH/77-12

NL

2 OF 3  
ADA  
055642





```

1200 IF(I3.EQ.1)YMIN=X1(I3)
1201 IF(X1(I3).LT.YMIN)YMIN=X1(I3)
1202 IF(X1(I3).GT.YMAX)YMAX=X1(I3)
1203 XL(I3)=.075
1204 CONTINUE
1205 CONTINUE
1206 CONTINUE
1207 IF(L.GT.1)GO TO 128
1208 IF(L.LT.2)PRINT,"TOTAL INSOLATION WAS: ",SUNNY," CAL/SQ.CM."
1209 PRINT*,"*****"
1210 PRINT*,"*****"
1211 PRINT*,"*****"
1212 PRINT*,"*****"
1213 PRINT*,"*****"
1214 PRINT*,"*****"
1215 PRINT 127,PLOTNO,LAT,DAY
1216 FORMAT(1X,20HDATA FOR PLOT SET ,F3.0,1H/,F3.0,1H/,F4.0)
1217 PRINT*
1218 CONTINUE
1219 PRINT*,"PEAK TEMPS AND TIMES-ITERATION #",L
1220 PRINT*,"*****"
1221 PRINT*,"AIR ",PEAKA," ",PTIMEA
1222 PRINT*,"GROUND ",PEAKG," ",PTIMEG
1223 PRINT*,"TANK ",PEAKT," ",PTIMET
1224 PRINT*,"LEAF ",PEAKL," ",PTIMEL
1225 PRINT*,"*****"
1226 PRINT 125,X1(8/NT)
1227 PRINT 125,X1(18/NT)
1228 PRINT*,"*****"
1229 FORMAT(1X,1H*,2X,14H2400 DELTA-T: ,F8.2,8X,1H*)
1230 FORMAT(1X,1H*,2X,14H1400 DELTA-T: ,F8.2,8X,1H*)
1231 Y1=5.9-.14*L
1232 CALL SYBOL(4.1,Y1,.1,L,0.,-1)
1233 CALL SYBOL(999.,999.,.1,14H - GRND DIFF= ,0.,14)
1234 CALL NUMBER(999.,999.,.1,0SOIL,0.,2)
1235 LAST1=LAST-(6/NT)+1
1236 M1=LAST+1
1237 M2=LAST+2

```

```

002630
002640
002650
002660
002670
002680
002690
002700
002710
002720
002730
002740
002750
002760
002770
002780
002790
002800
002810
002820
002830
002840
002850
002860
002870
002880
002890
002900
002910
002920
002930
002940
002950

TIME2(M1)=6.
TIME2(M2)=(HRS-6)/6
NLAST=LAST1/3
IF(._GT.4)GO TO 130
IMIN=0
IF(YMIN.LE.0.AND.YMIN.GT.-5)IMIN=-5
IF(YMIN.LE.-5.AND.YMIN.GT.-10)IMIN=-10
IF(YMIN.LE.-10.AND.YMIN.GT.-15)IMIN=-15
IF(YMIN.LE.-15.AND.YMIN.GT.-20)IMIN=-20
IF(YMIN.LE.-20.AND.YMIN.GT.-25)IMIN=-25
IF((YMAX-IMIN).GT.25)INC=(YMAX-IMIN)/5+1
X1(M1)=X1(M1)=IMIN
XL1(M2)=X1(M2)=INC
XYZ=ABS(X1(M1)/X1(M2))
DO 129 IX=1,15
Y004=6.2-.4*IX
Y0041=Y004-.2
CALL PLOT(Y004,XYZ,3)
CALL PLOT(Y0041,XYZ,2)
129 CALL AXYS(0.,0.,20HSLAPED TIME (HOURS),-20,6.125,0.,TIME2(M1),
CTIME2(M2))
CALL AXYS(0.,0.,15HDELTA T (DEG C),15,5.95,90.,X1(M1),X1(M2))
130 X1(M1)=XL1(M1)=IMIN
X1(M2)=XL1(M2)=INC
CALL LTYPE(TIME2,X1,-AST1,1,NLAST,L)
100 CONTINUE
IF(NGRAPH5.EQ.2.AND.L3.LT.NGRAPHS)CALL PLOT(0.,-3.,-3)
IF(NGRAPH5.GT.2.AND.L3.EQ.1)CALL PLOT(-3.5,-8.,-3)
IF(NGRAPH5.GT.2.AND.L3.EQ.2)CALL PLOT(7.5,0.,-3)
111 IF(L3.EQ.NGRAPHS)CALL PLOT
CONTINUE
STOP
END

```

\*\*\*\*\*

INFORMATION FOR PLOT NUMBER - 2.

ENVIRONMENTAL FACTORS:

-----

LATITUDE= 20.  
DAY= 90.  
WIND SPEED= 223.  
MEAN TEMP= 24.  
CLOUD TYPE= 1  
PERCENT SUN= .7  
WATER VAPOR= .6  
HUMIDITY= 30.  
PRESSURE= 1000.  
DUST= .25

GROUND PARAMETERS

-----

DENSITY= 2.  
SPECIFIC HEAT= .44  
DIFFUSIVITY= .3  
EMISSIVITY= .95  
REFLECTIVITY= .3  
CONDUCTIVITY= .21  
MOISTURE CONTENT= .15

TANK PARAMETERS

-----

DENSITY= 8.  
SPECIFIC HEAT= .11  
EMISSIVITY= .7  
REFLECTIVITY= .3  
AIR CONDITIONING VELOCITY= 447.  
INTERNAL TEMPERATURE= 25.  
THICKNESS= 7.62

LEAF PARAMETERS

-----

DENSITY= .5  
SPECIFIC HEAT= .88  
SIZE= 2.54  
TRANSPIRATION RATE= .0003  
EMISSIVITY= .95  
ABSORPTION= .7  
THICKNESS= .1

\*\*\*\*\*

TOTAL INSOLATION WAS: 473.2978654092 CAL/SQ.CM.

\*\*\*\*\*



DATA FOR PLOT SET 2./20./ 90.

PEAK TEMPS AND TIMES-ITERATION #1

\*\*\*\*\*

AIR 34.68040778449 16.5  
GROUND 33.87070521637 14.  
TANK 34.9191131613 14.5  
LEAF 34.58530426596 16.

\*\*\*\*\*

\* 1400 DELTA-T: .84 \*  
\* 2400 DELTA-T: 5.10 \*

\*\*\*\*\*

PEAK TEMPS AND TIMES-ITERATION #2

\*\*\*\*\*

AIR 34.68040778449 16.5  
GROUND 33.76678520909 14.  
TANK 34.84214163599 14.5  
LEAF 34.58510426596 16.

\*\*\*\*\*

\* 1400 DELTA-T: .87 \*  
\* 2400 DELTA-T: 6.10 \*

\*\*\*\*\*

PEAK TEMPS AND TIMES-ITERATION #3

\*\*\*\*\*

AIR 34.68040778449 16.5  
GROUND 33.68454322091 14.  
TANK 34.77985380326 14.5  
LEAF 34.58580426596 16.

\*\*\*\*\*

\* 1400 DELTA-T: .89 \*  
\* 2400 DELTA-T: 5.11 \*

\*\*\*\*\*

PEAK TEMPS AND TIMES-ITERATION #4

\*\*\*\*\*

AIR 34.68040778449 16.5  
GROUND 33.61412570207 14.  
TANK 34.72114313484 14.5  
LEAF 34.58580426596 16.

\*\*\*\*\*

\* 1400 DELTA-T: .90 \*  
\* 2400 DELTA-T: 6.11 \*

\*\*\*\*\*

## Appendix C

### Plots from Program TEMPS for all Parameters

Figs. 25(a)-25(k) are plots of the parameter Mean Temperature. Figs 26(a)-26(k) are plots of the parameter Absolute Humidity. Figs. 27(a)-27(k) are plots of the parameter Wind. Figs 28(a)-28(k) are plots of the parameter Sun Strength. Figs. 29(a)-29(k) are plots of the parameter Ground Reflectivity. Figs 30(a)-30(k) are plots of the parameter Ground Emmissivity. Figs 31(a)-31(k) are plots of the parameter Ground Diffusivity. Figs. 32(a)-32(k) are plots of the parameter Target Reflectivity. Figs 33(a)-33(k) are plots of the parameter Target Emmissivity. Figs 34(a)-34(k) are plots of the parameter Target Thickness. Figs. 35(a)-35(k) are plots of the parameter Internal Air Conditioning Velocity.

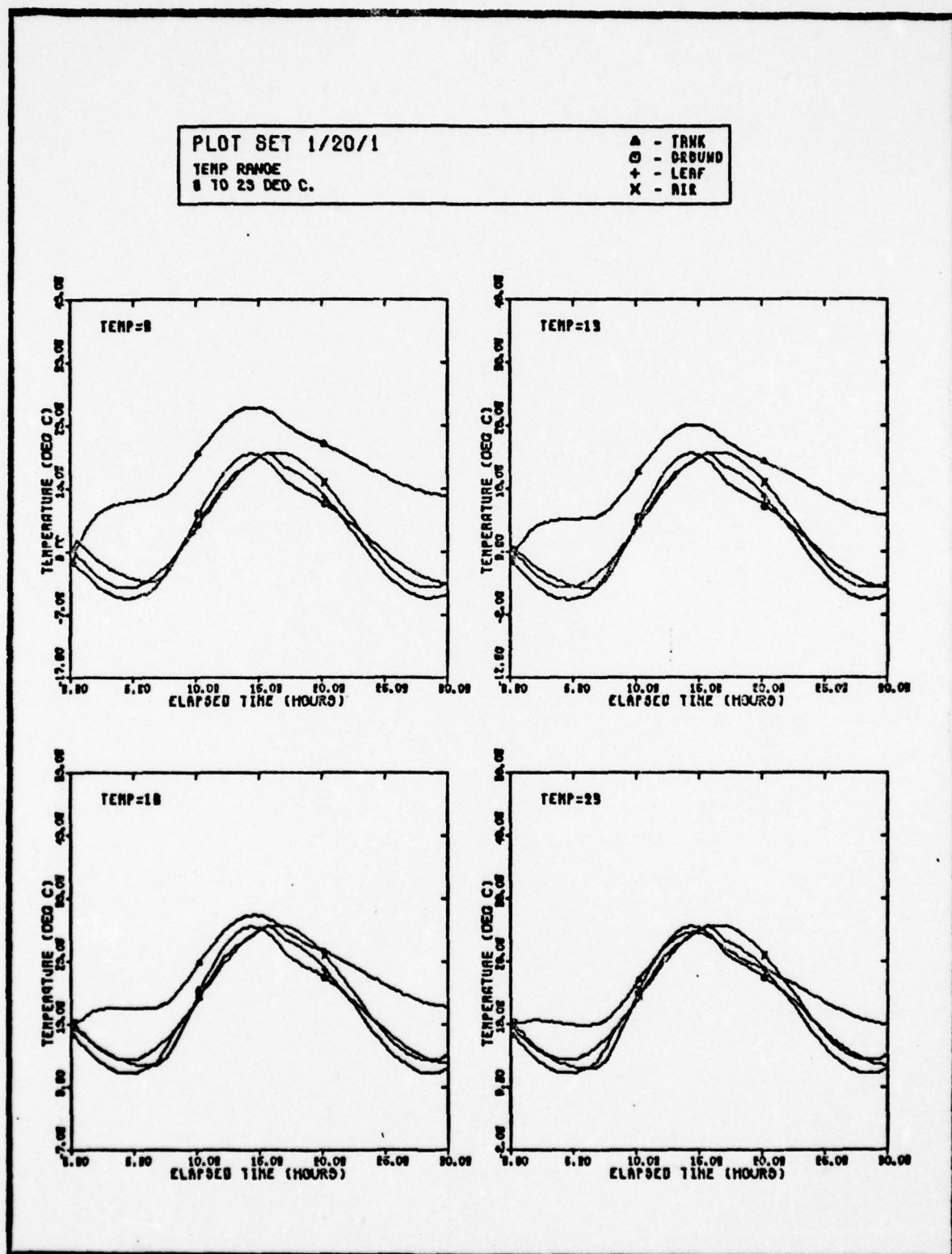


Fig. 25(a). Basic Temperature Plots of Mean Temp



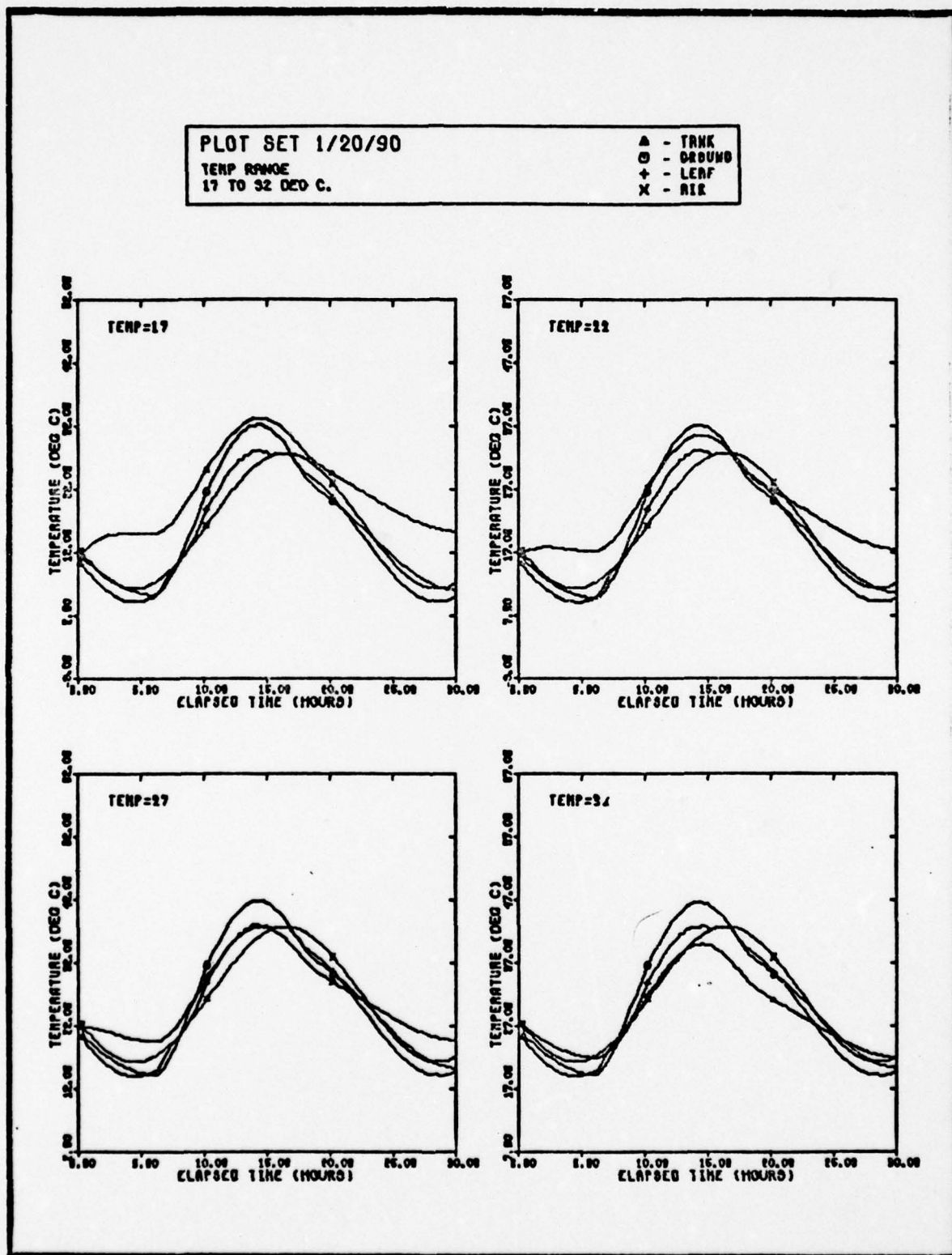


Fig. 25(b). Basic Temperature Plots of Mean Temp

PLOT SET 1/20/180

TEMP RANGE  
25 TO 40 DEG C.

△ - TRNK  
○ - GROUND  
+ - LEAF  
x - AIR

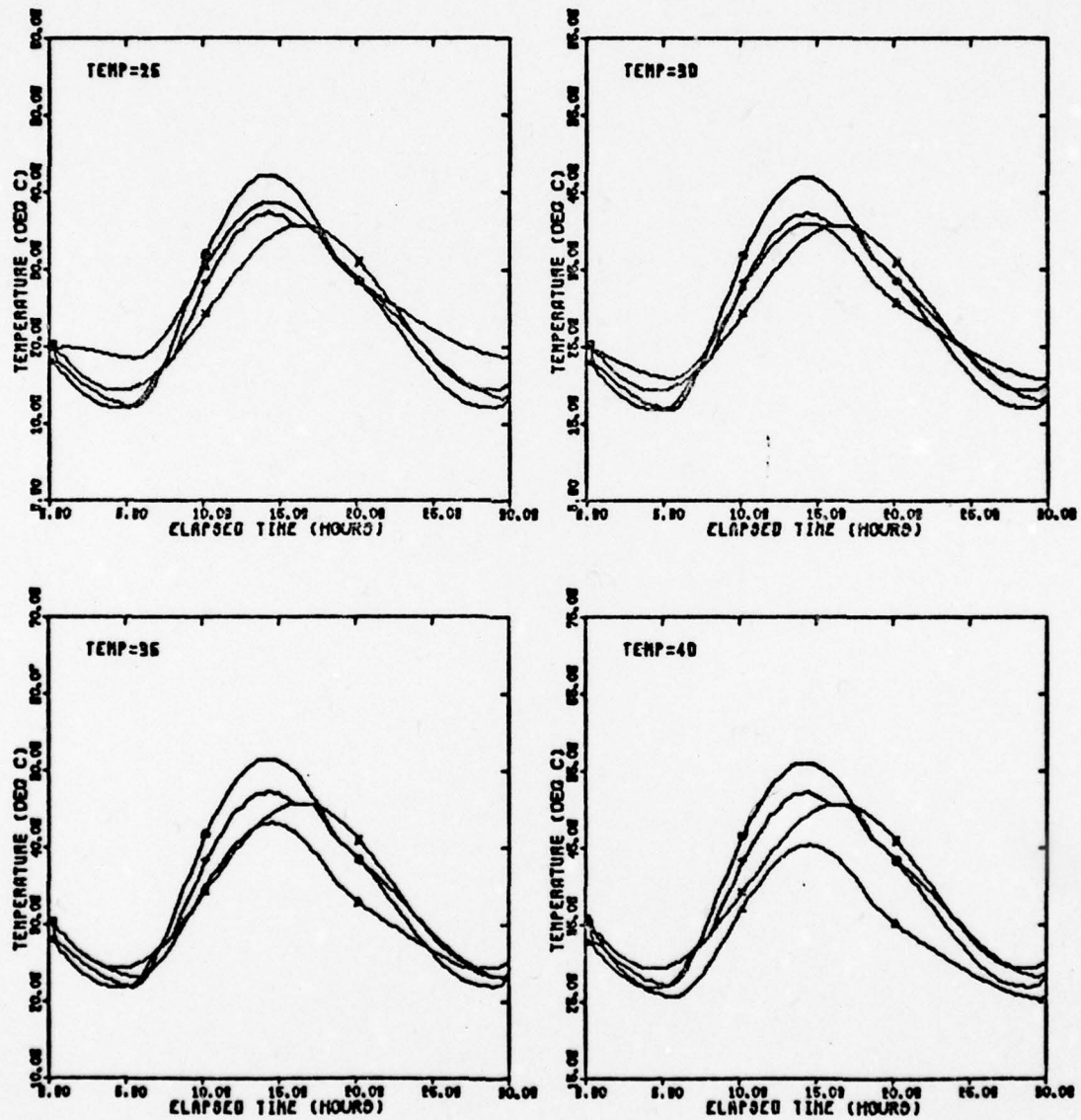


Fig. 25(c). Basic Temperature Plots of Mean Temp

PLOT SET 1/32/18

TEMP RANGE  
2 TO 17 DEG C.

▲ TANK  
○ - GROUND  
+ - LEAF  
X - AIR

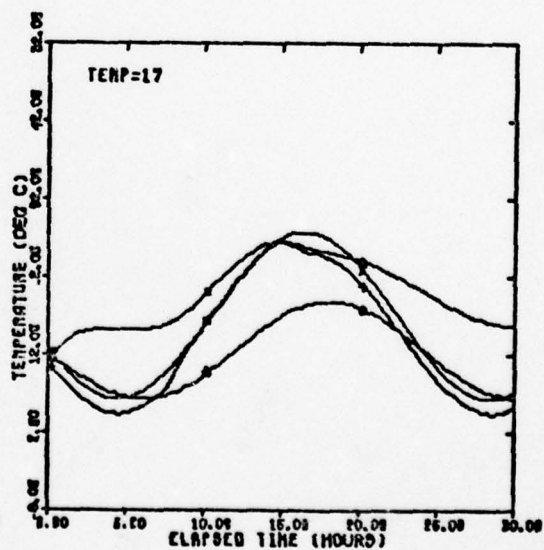
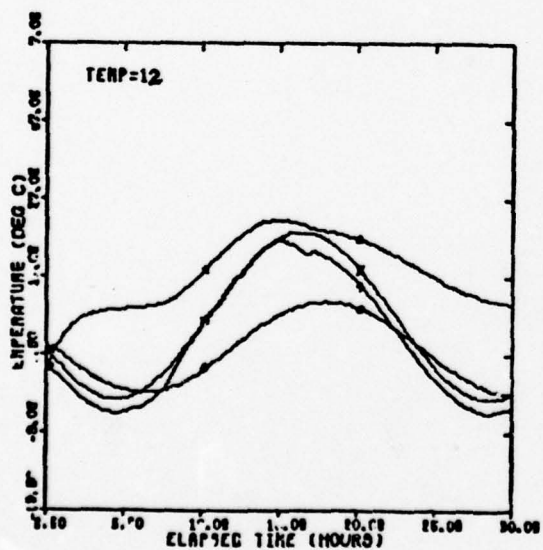
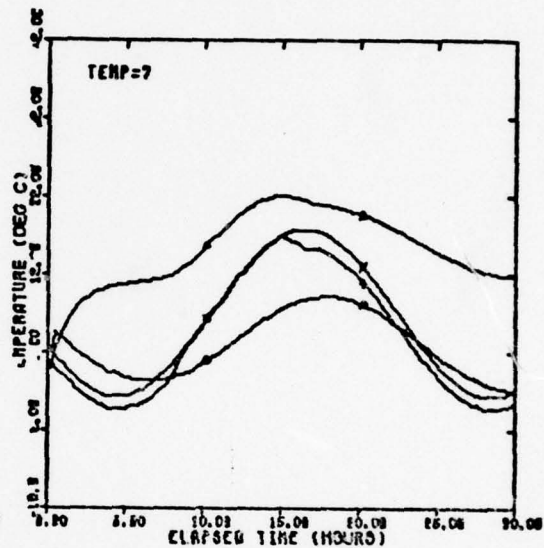
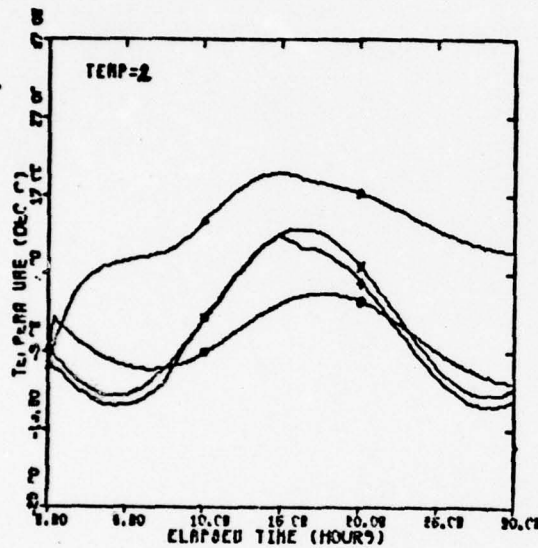


Fig. 25(d). Basic Temperature Plots of Mean temp



PLOT SET 1/32/1

TEMP RANGE  
2 TO 17 DEG C.

▲ - TRNK  
○ - GROUND  
+ - LEAF  
X - AIR

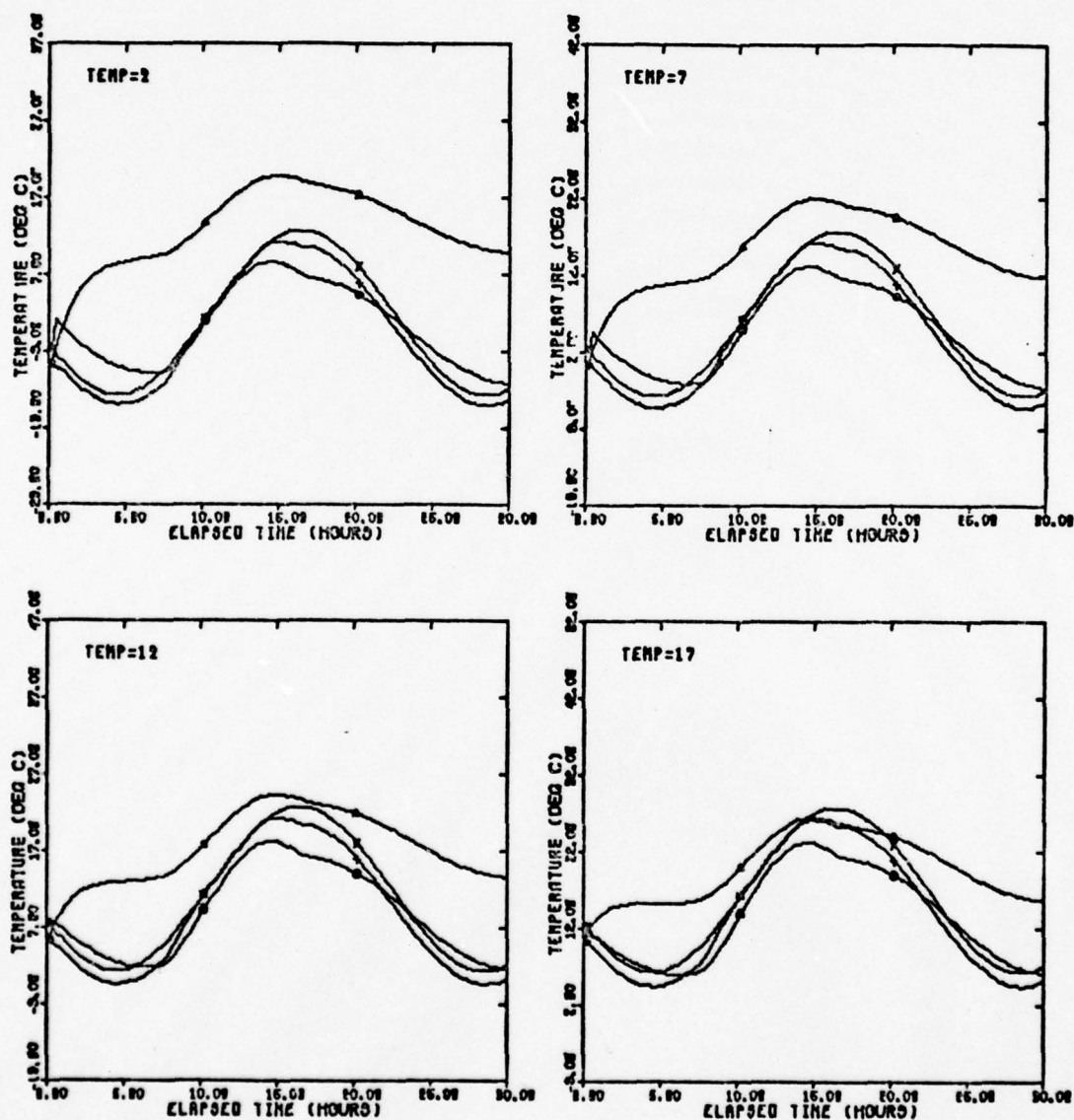


Fig. 25(e). Basic Temperature Plots of Mean Temp

PLOT SET 1/32/90

TEMP RANGE  
13 TO 28 DEG C.

Δ - TRNK  
○ - GROUND  
+ - LEAF  
X - AIR

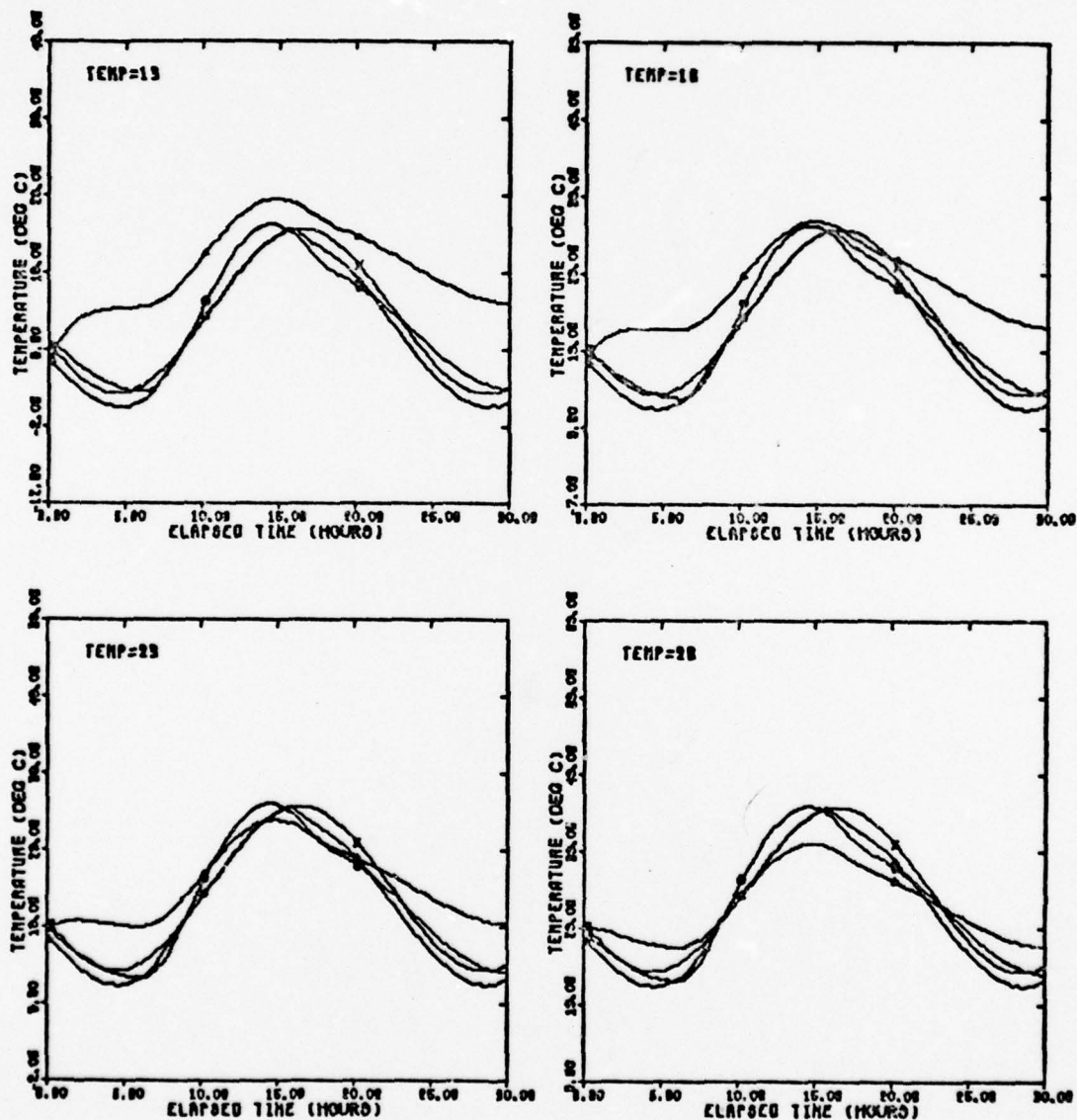


Fig. 25(f). Basic Temperature Plots of Mean Temp

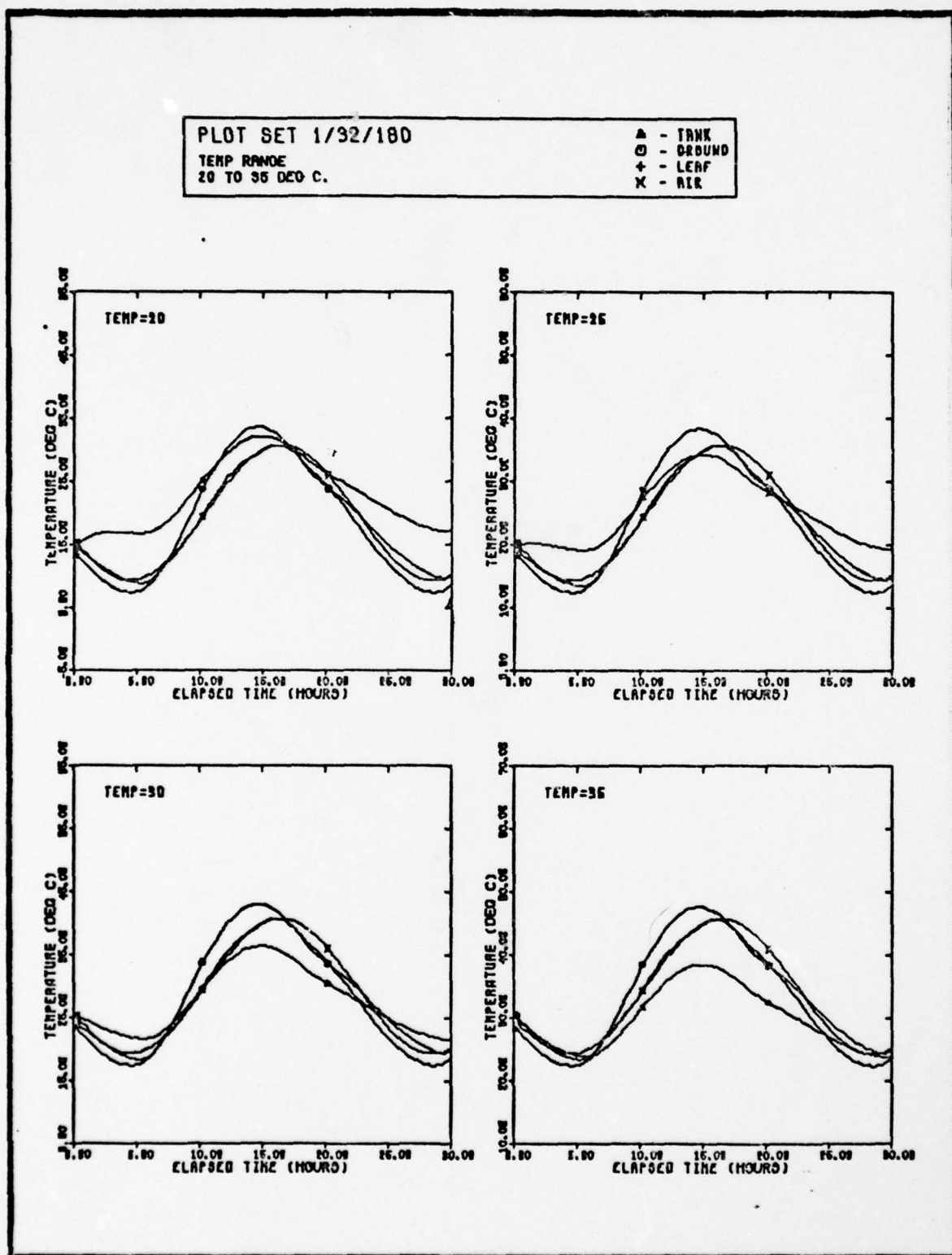


Fig. 25(g). Basic Temperature Plots of Mean Temp



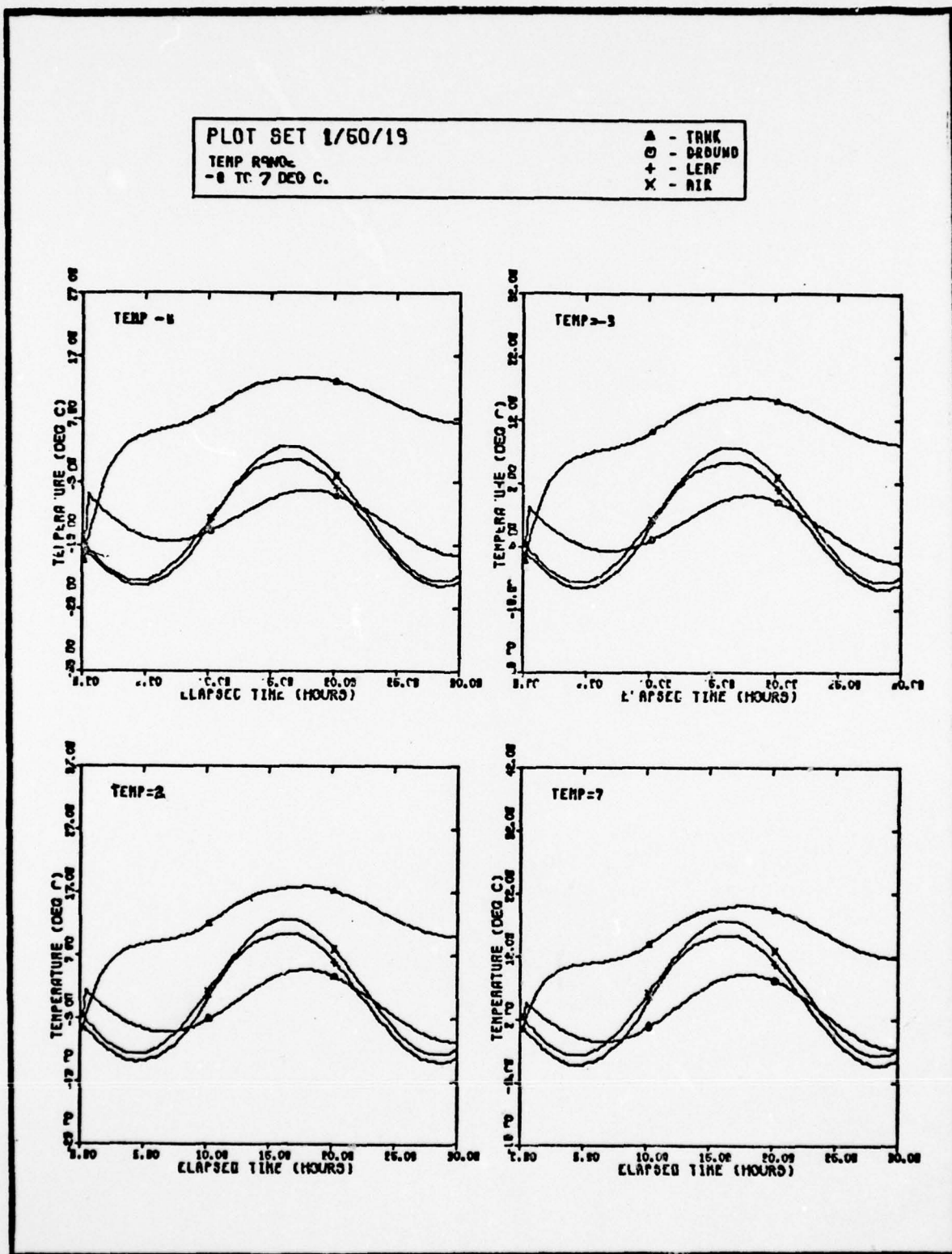


Fig. 25(h). Basic Temperature Plots of Mean Temp.

PLOT SET 1/60/1

TEMP RANGE  
-8 TO 7 DEG C.

▲ - TANK  
○ - DRUM  
+ - EAF  
X - AIR

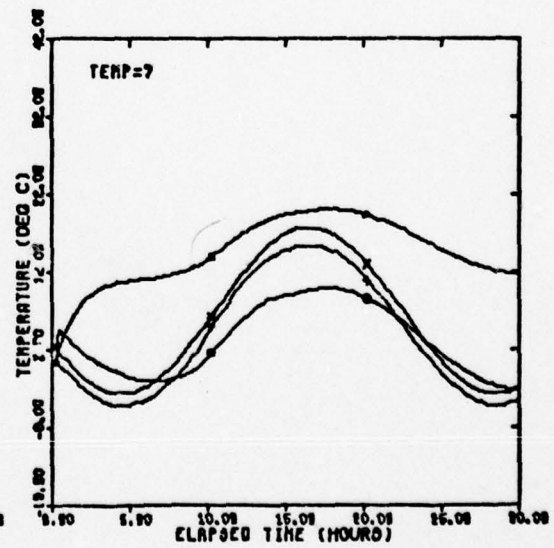
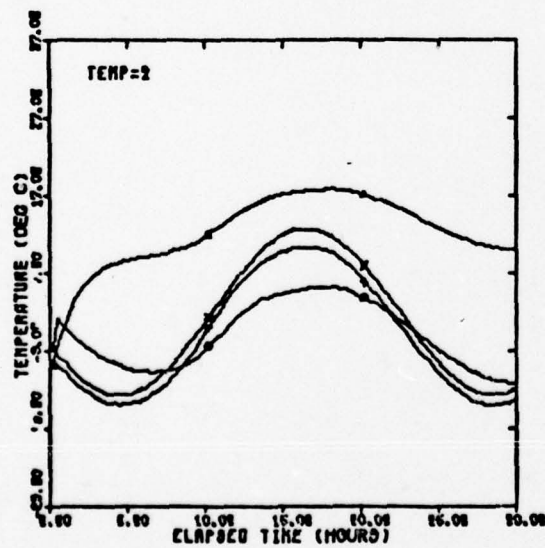
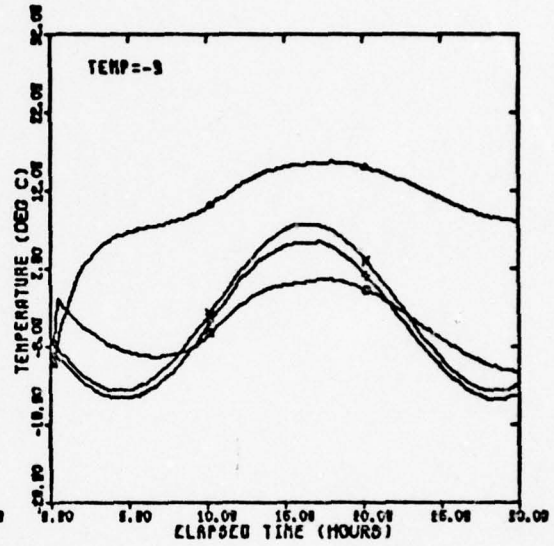
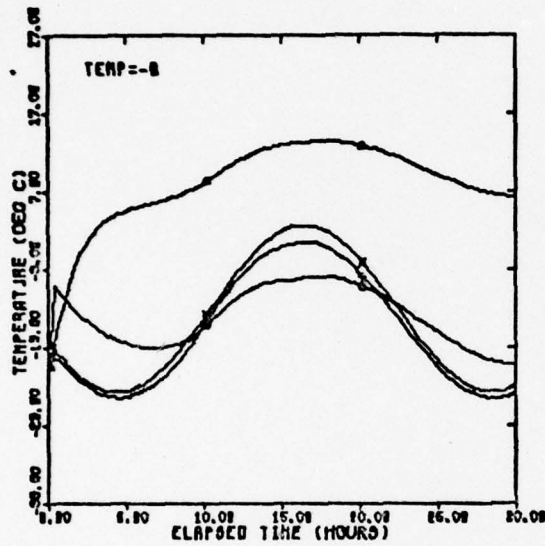


Fig. 25(1). Basic Temperature Plots of Mean Temp

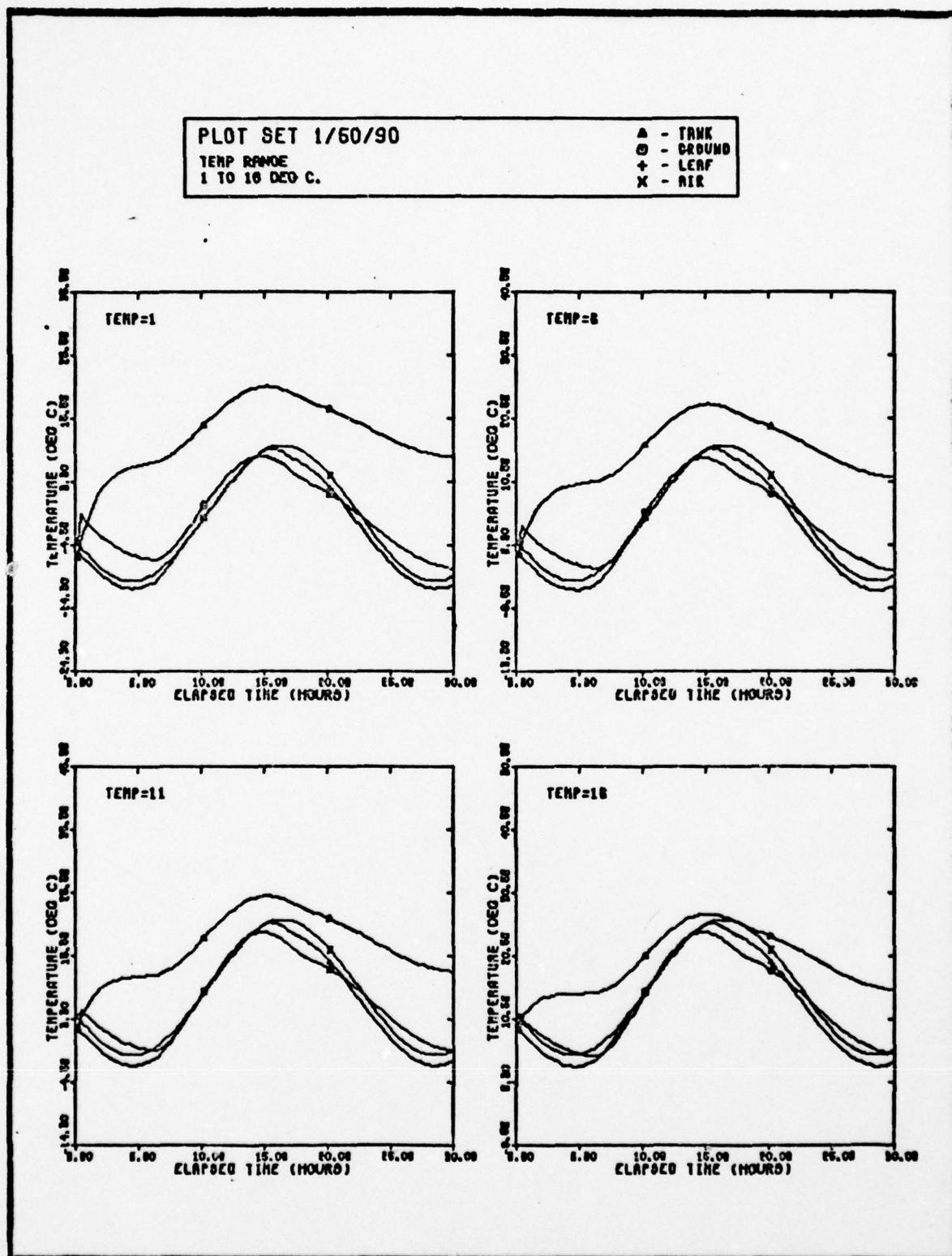


Fig. 25(j). Basic Temperature Plots of Mean Temp



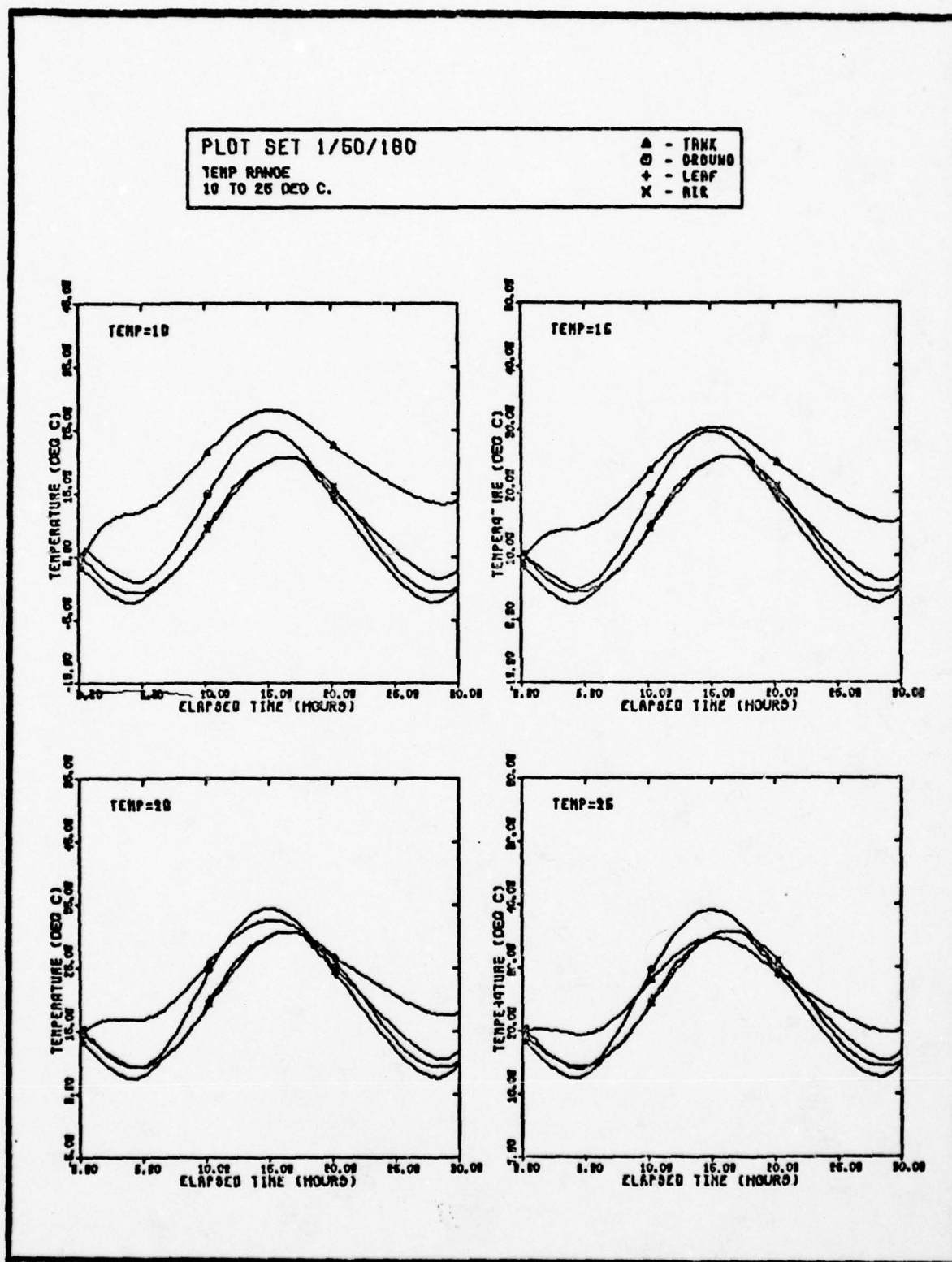


Fig. 25(k). Basic Temperature Plots of Mean Temp

PLOT SET 2/20/1

ABS. HUMID. RANGE  
0.10 TO 0.640M/CU. M.

Δ - TANK  
○ - DRUM  
+ - LEAF  
X - AIR

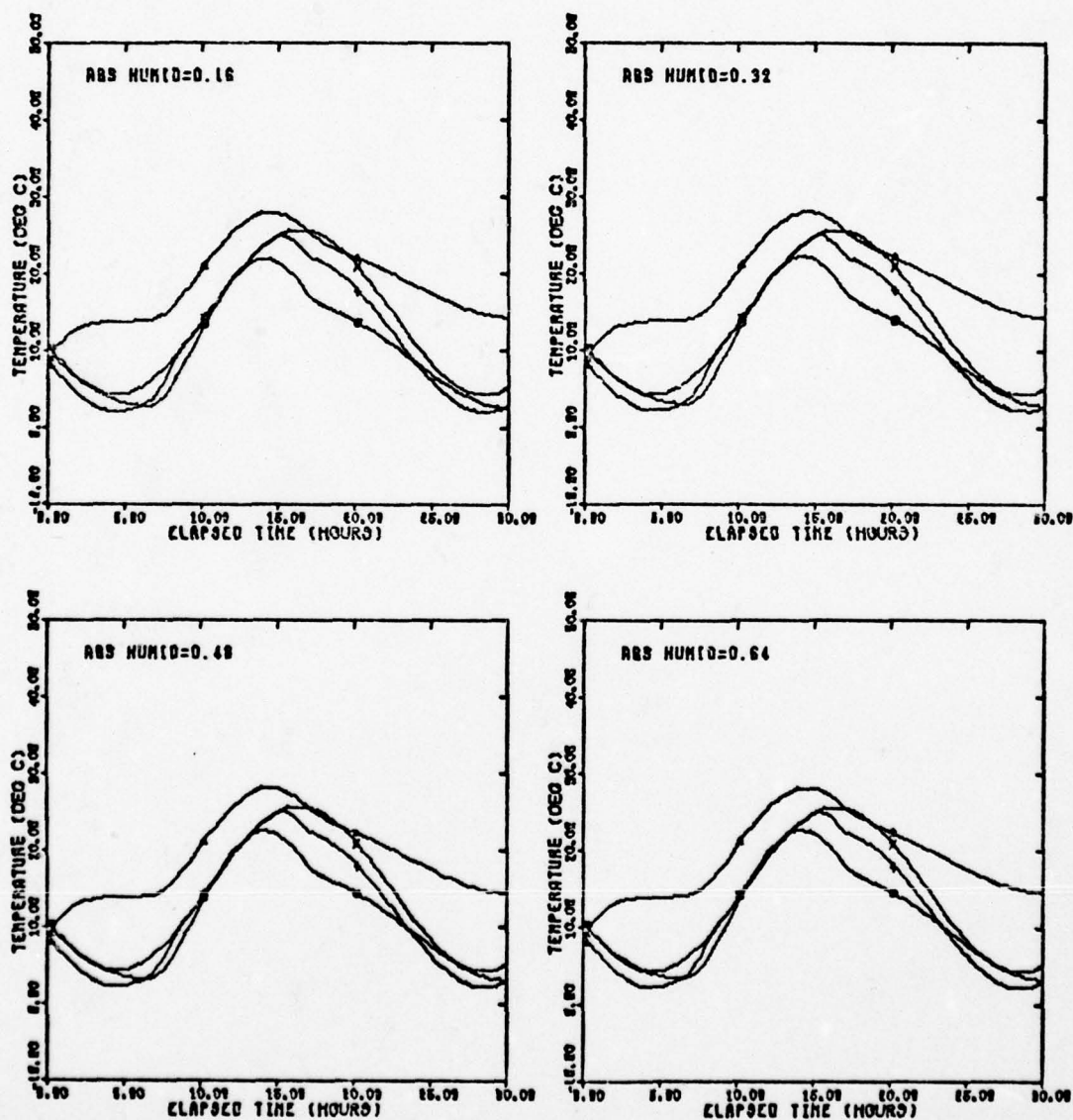


Fig. 26(a). Basic Temperature Plots of Absolute Humidity

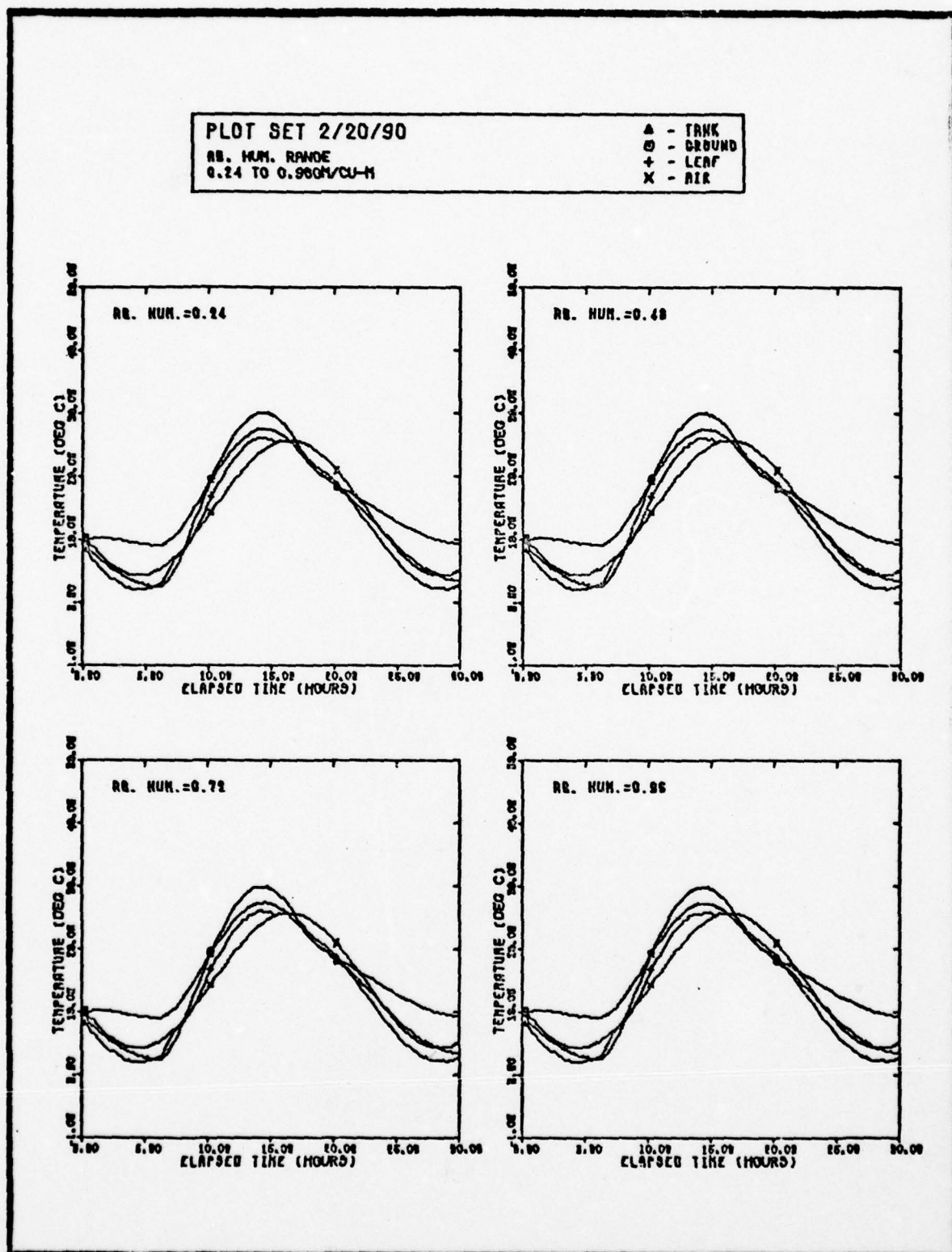


Fig. 26(b). Basic Temperature Plots of Absolute Humidity



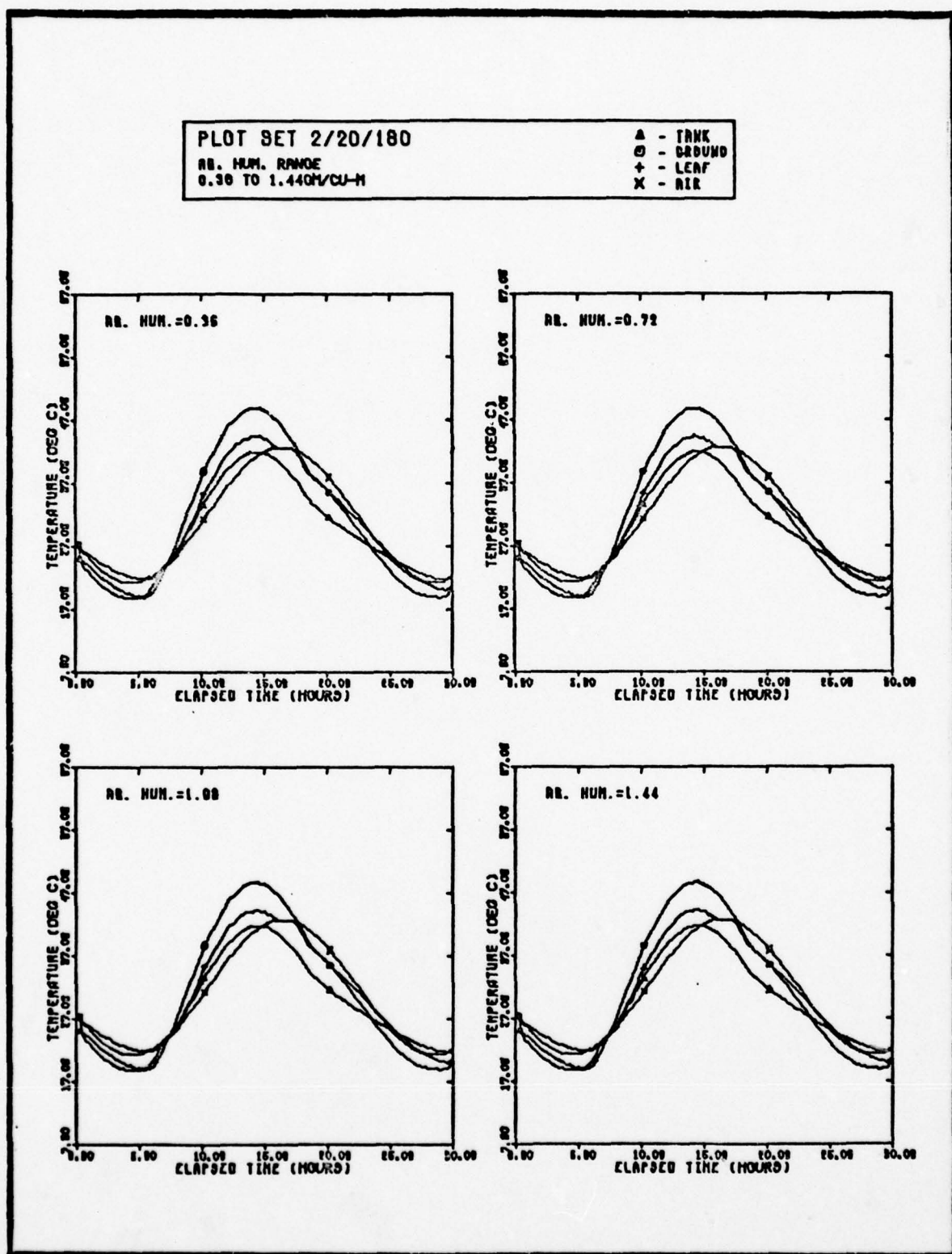


Fig. 26(c). Basic Temperature Plots of Absolute Humidity

PLOT SET 2/32/19

AB. HUM. RANGE  
0.40 TO 1.600M/CU-M

▲ - TANK  
○ - DROUND  
+ - LEAF  
X - AIR

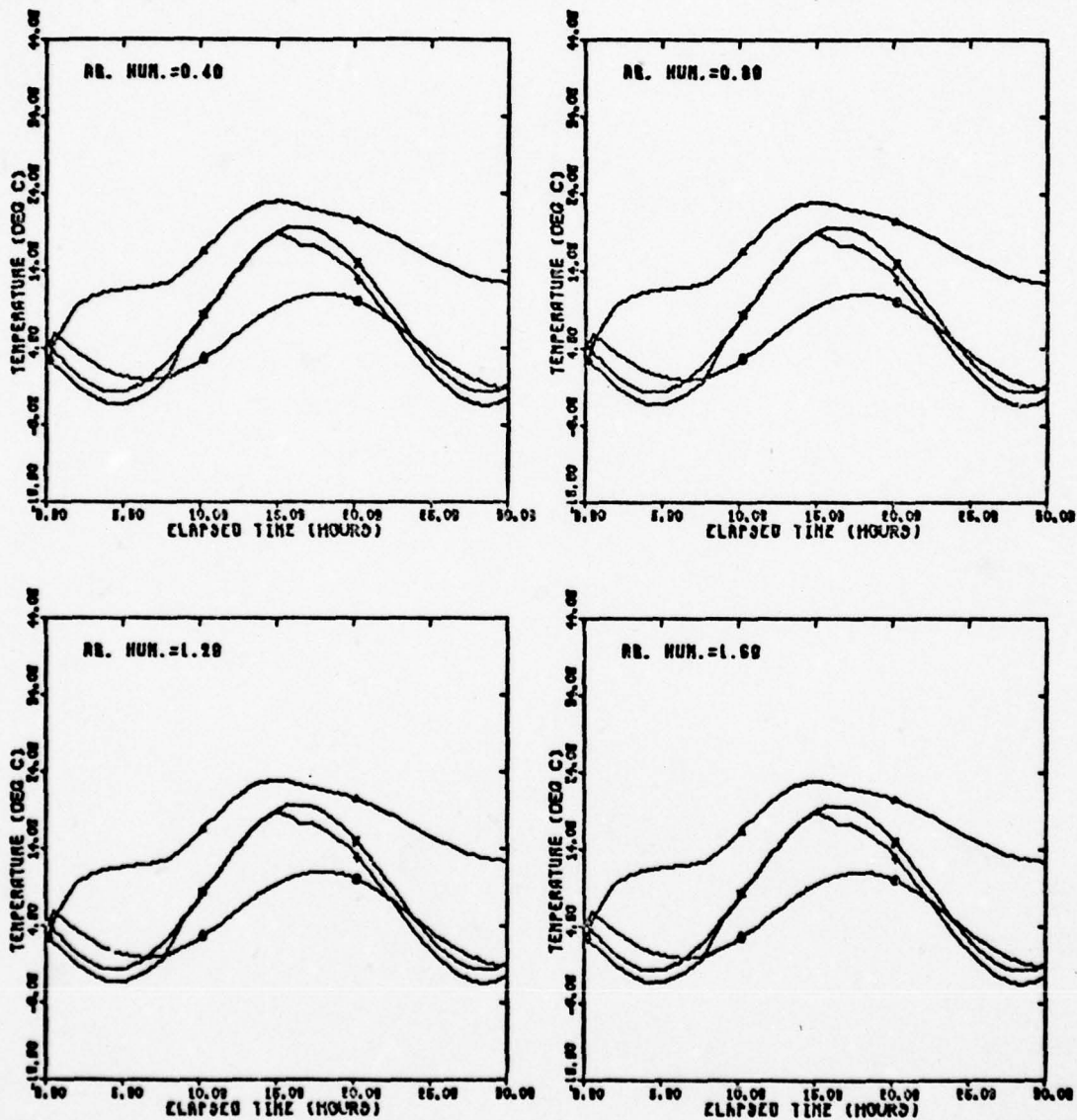


Fig. 26(d). Basic Temperature Plots of Absolute Humidity

PLOT SET 2/32/1

AB. HUM. RANGE  
0.40 TO 1.00H/CU-M

Δ - TRNK  
○ - GROUND  
+ - LEAF  
X - AIR

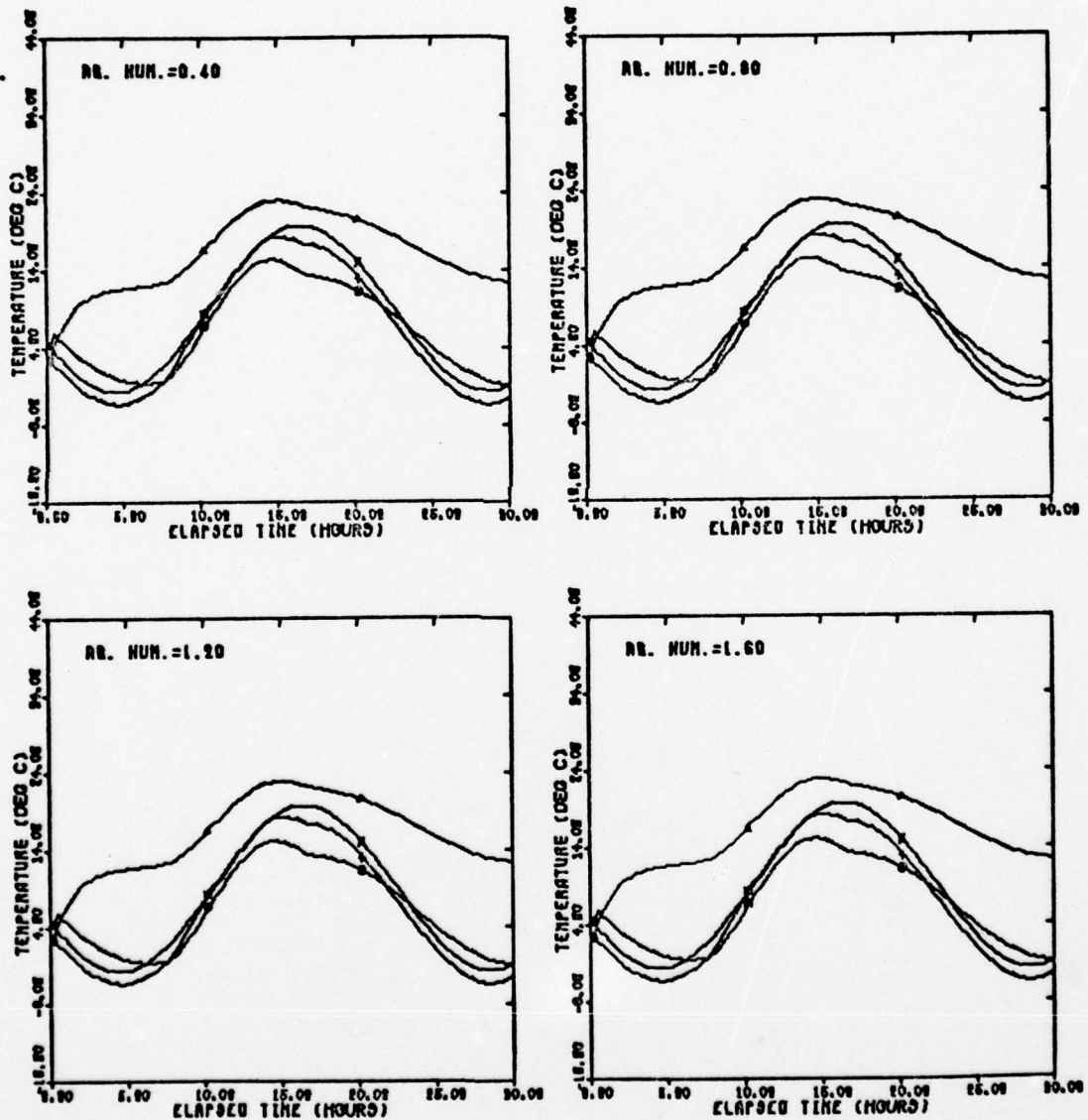


Fig. 26(e). Basic Temperature Plots of Absolute Humidity



PLOT SET 2/32/90

AB. HUM. RANGE  
1.20 TO 4.800M/CU-M

▲ - TANK  
○ - GROUND  
+ - LEAF  
X - AIR

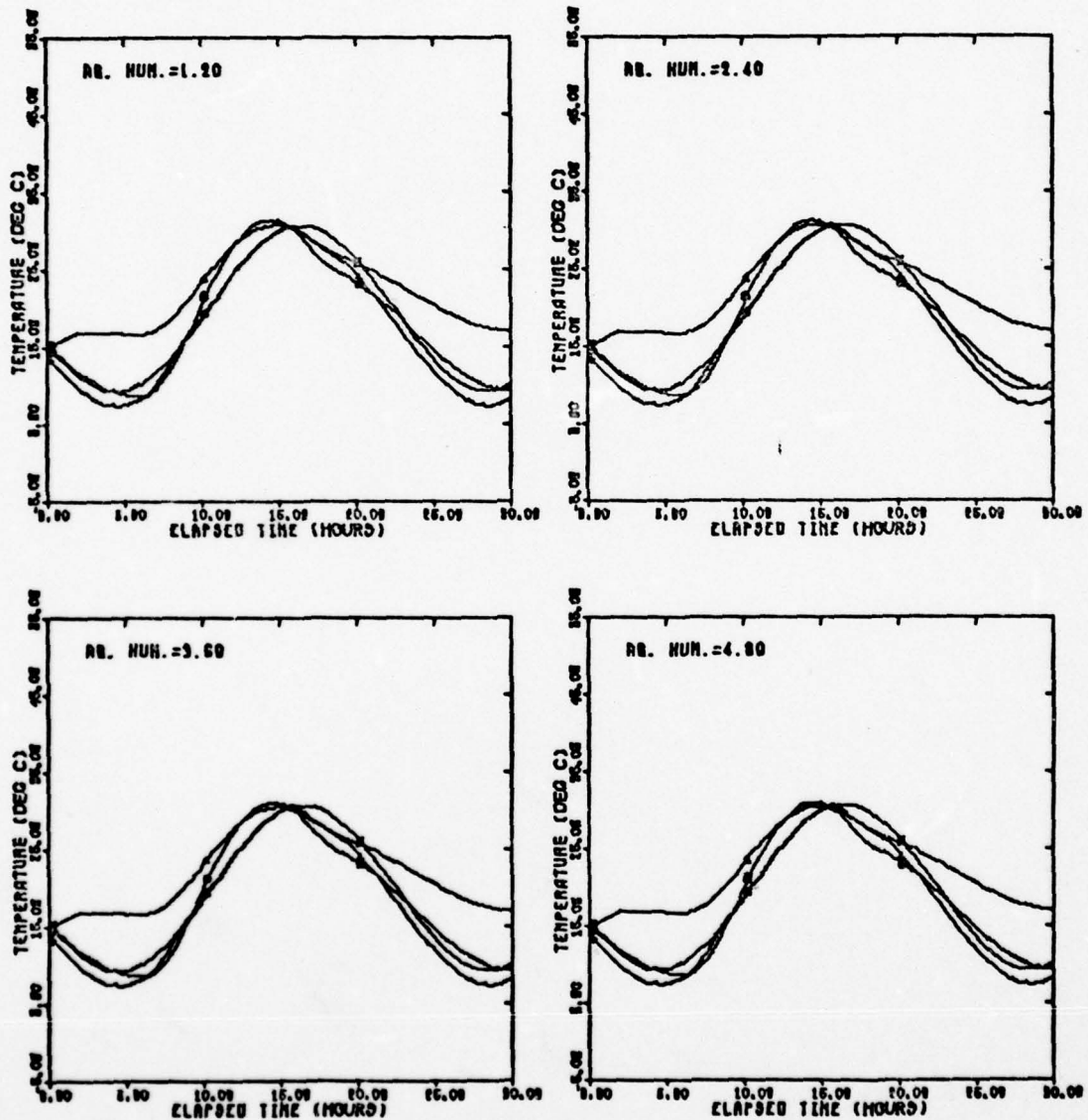


Fig. 26(f). Basic Temperature Plots of Absolute Humidity

PLOT SET 2/92/180

AB. HUM. RANGE  
1.00 TO 7.200M/CU-M

▲ - TANK  
○ - CASINO  
+ - LEAF  
X - AIR

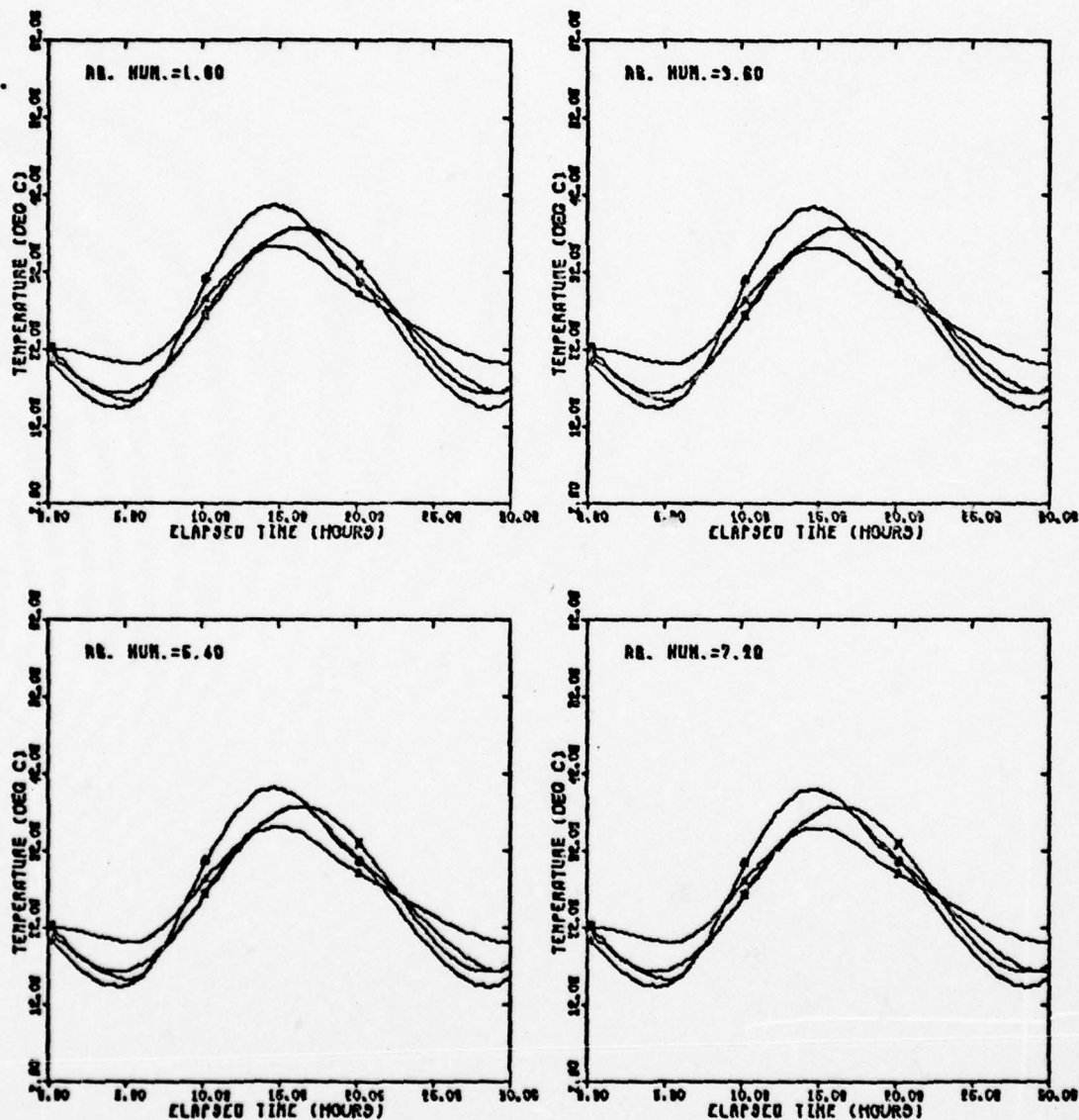


Fig. 26(g). Basic Temperature Plots of Absolute Humidity

PLOT SET 2/50/18

AB. HUM. RANGE  
0.80 TO 3.200H/CU-M

A - TANK  
O - GROUND  
+ - LEAF  
X - AIR

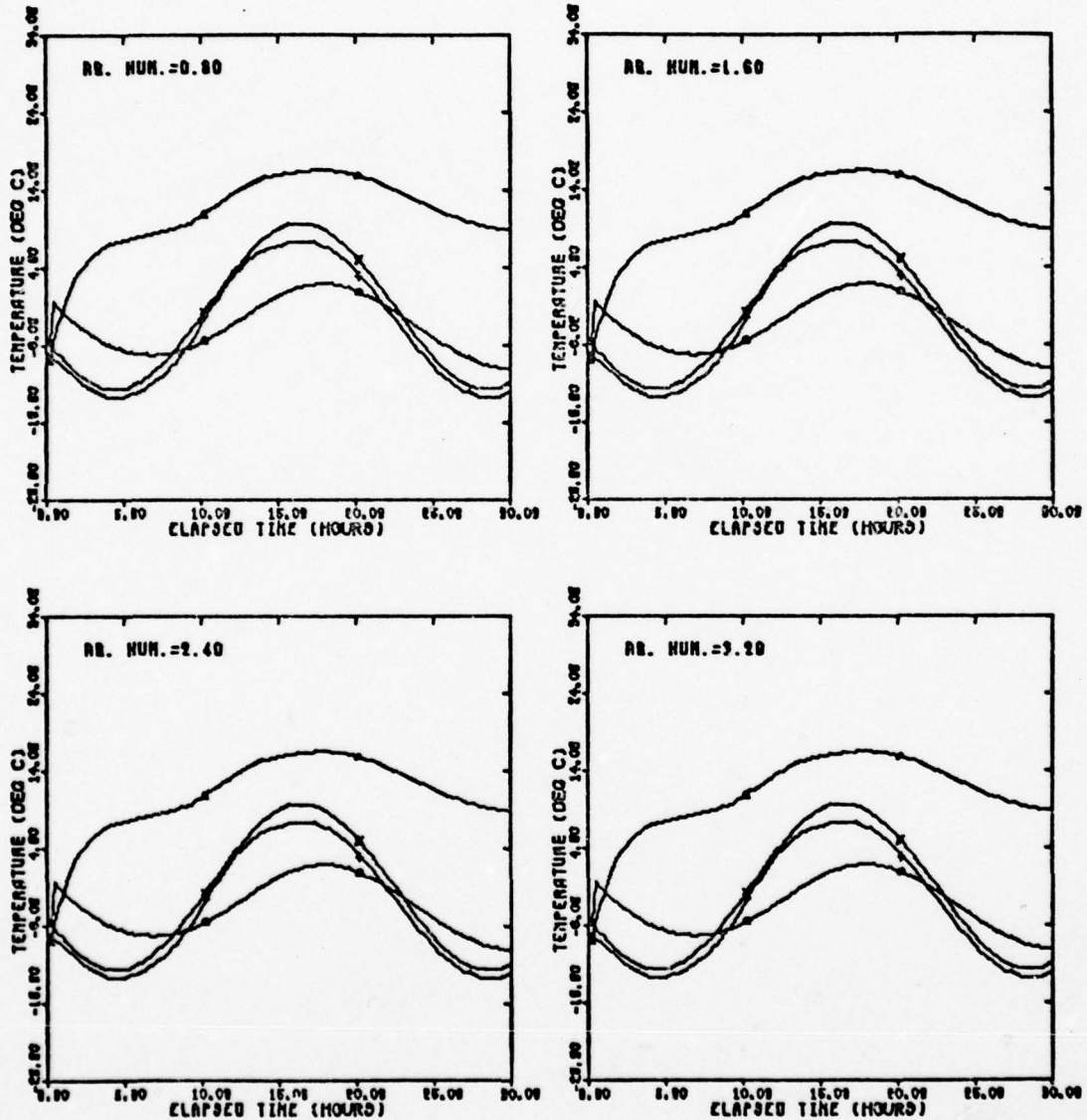


Fig. 26(h). Basic Temperature Plots of Absolute Humidity



PLOT SET 2/60/1

AB. HUM. RANGE  
0.60 TO 3.200H/CU-M

A - TRUNK  
O - DEBUNK  
+ - LEAF  
X - AIR

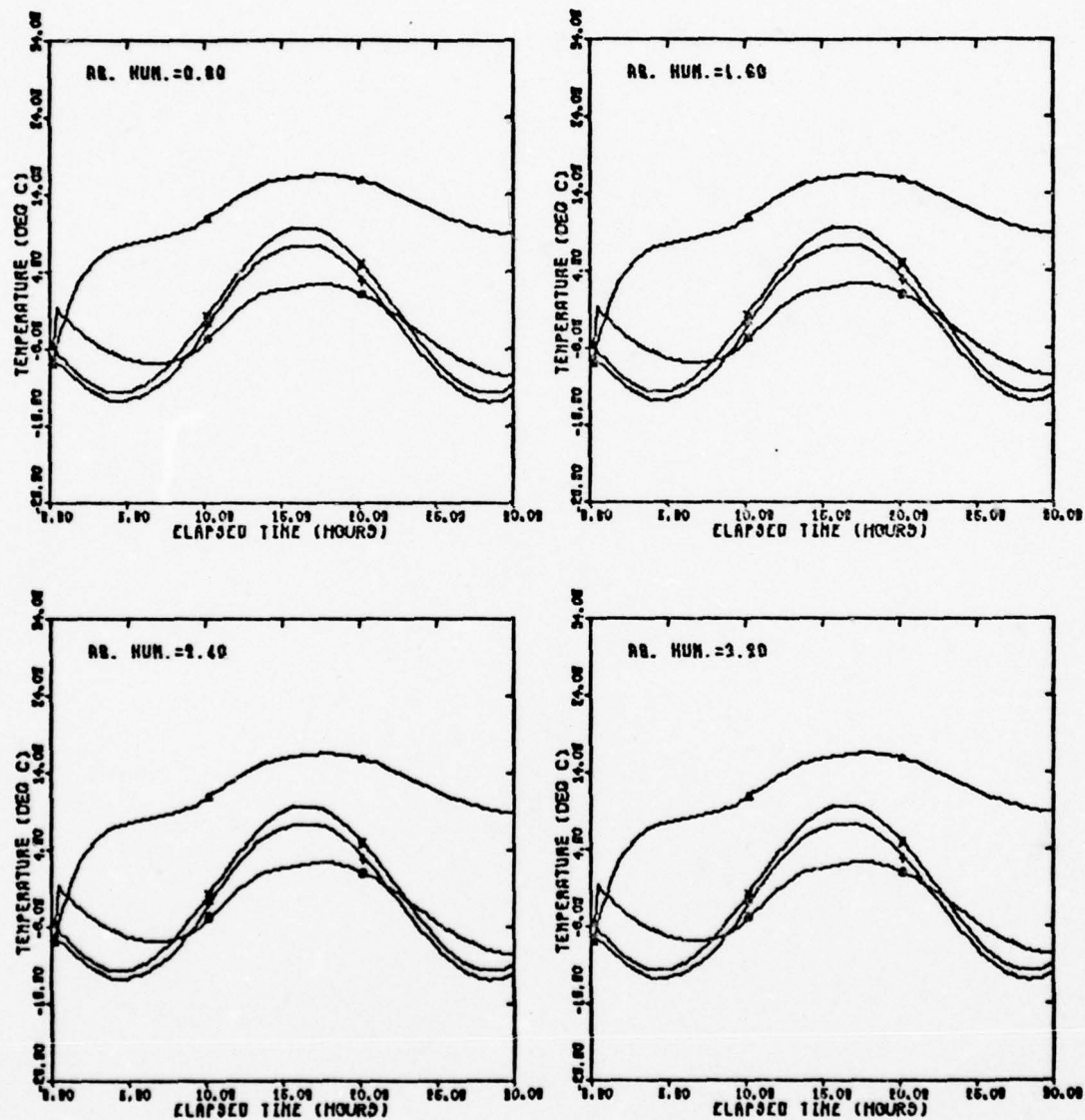


Fig. 26(1). Basic Temperature Plots of Absolute Humidity

PLOT SET 2/60/90

AB. HUM. RANGE  
1.20 TO 4.800M/CU-M

▲ - TANK  
○ - GROUND  
+ - LEAF  
X - AIR

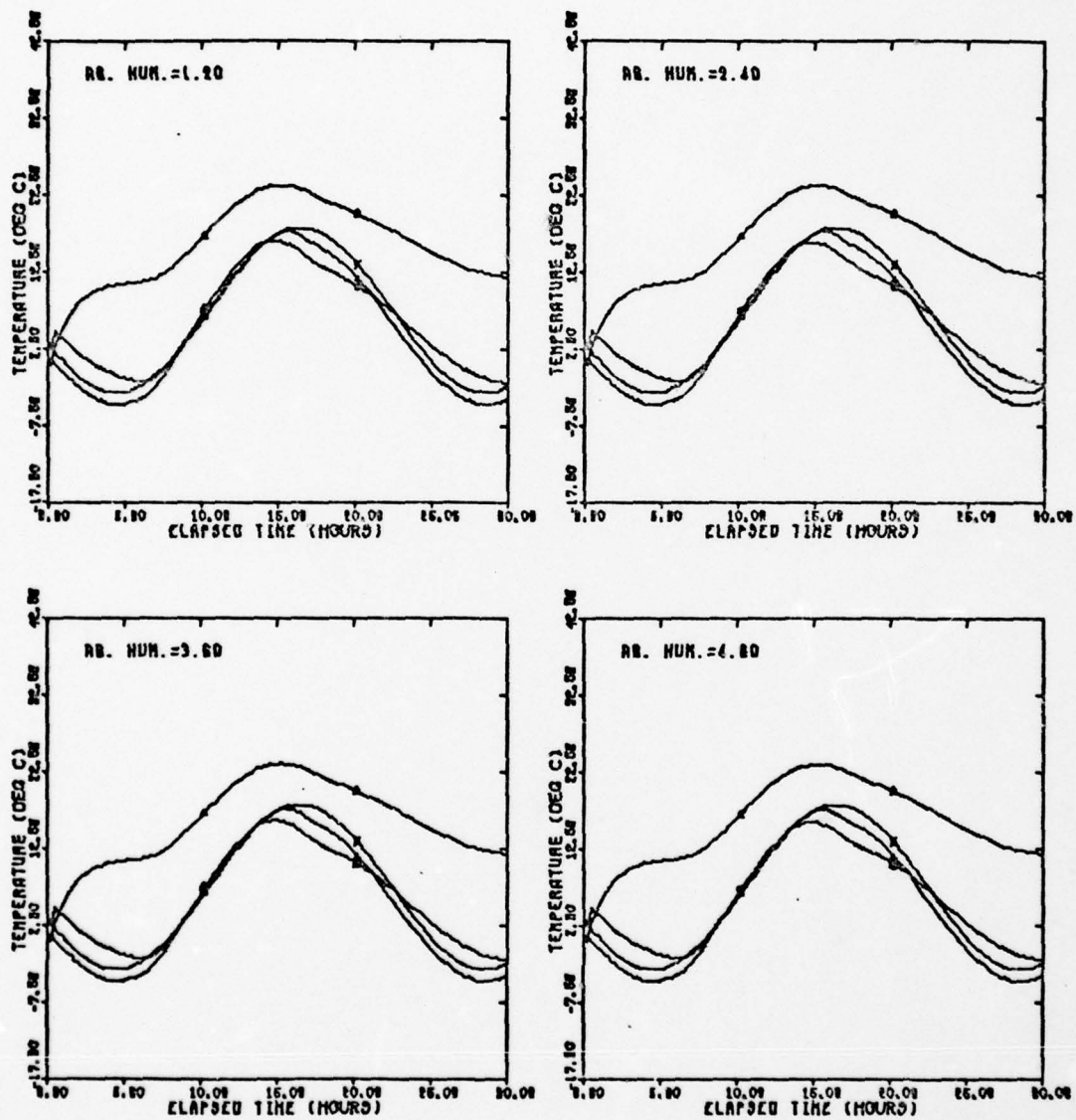


Fig. 26(j). Basic Temperature Plots of Absolute Humidity

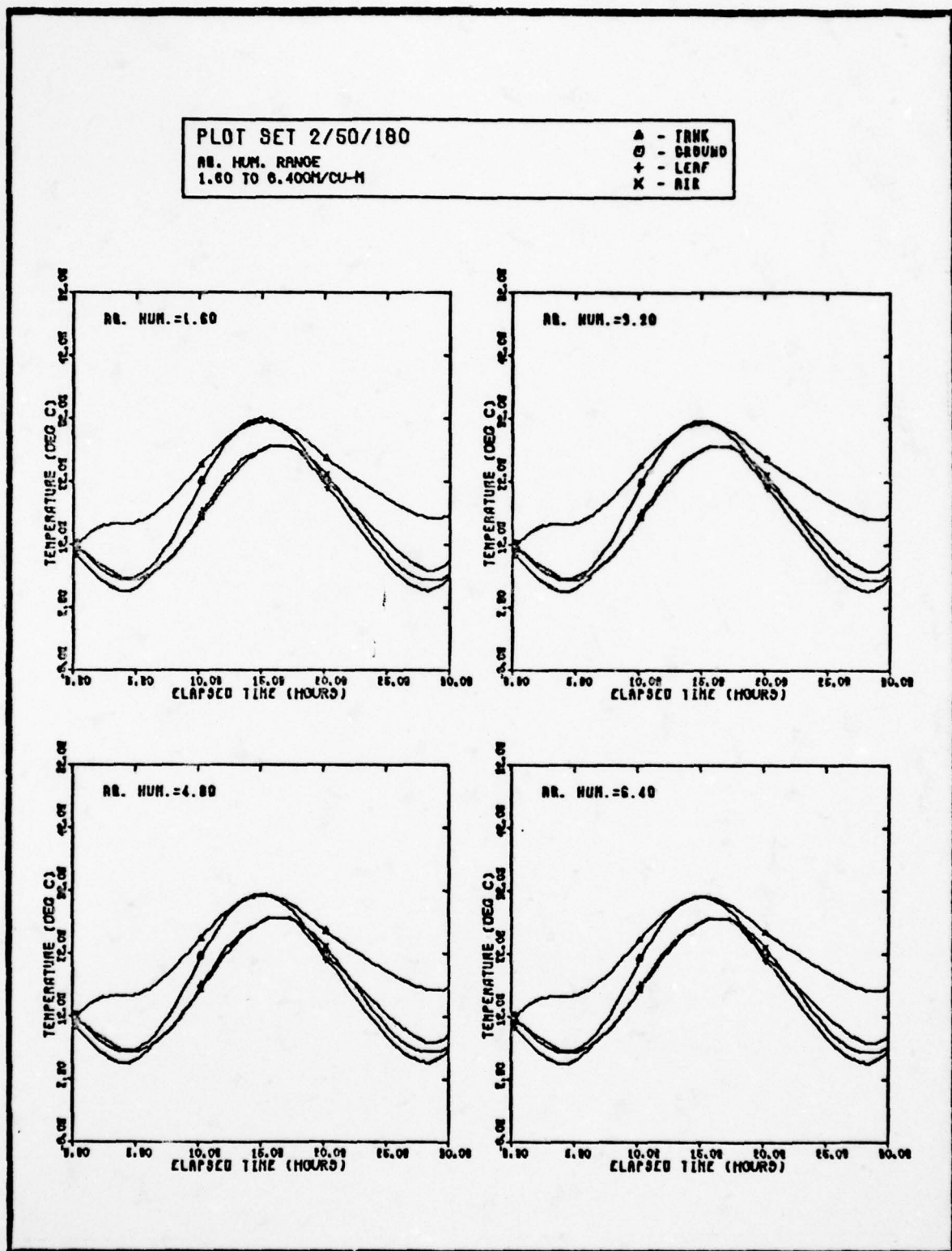


Fig. 26(k). Basic Temperature Plots of Absolute Humidity



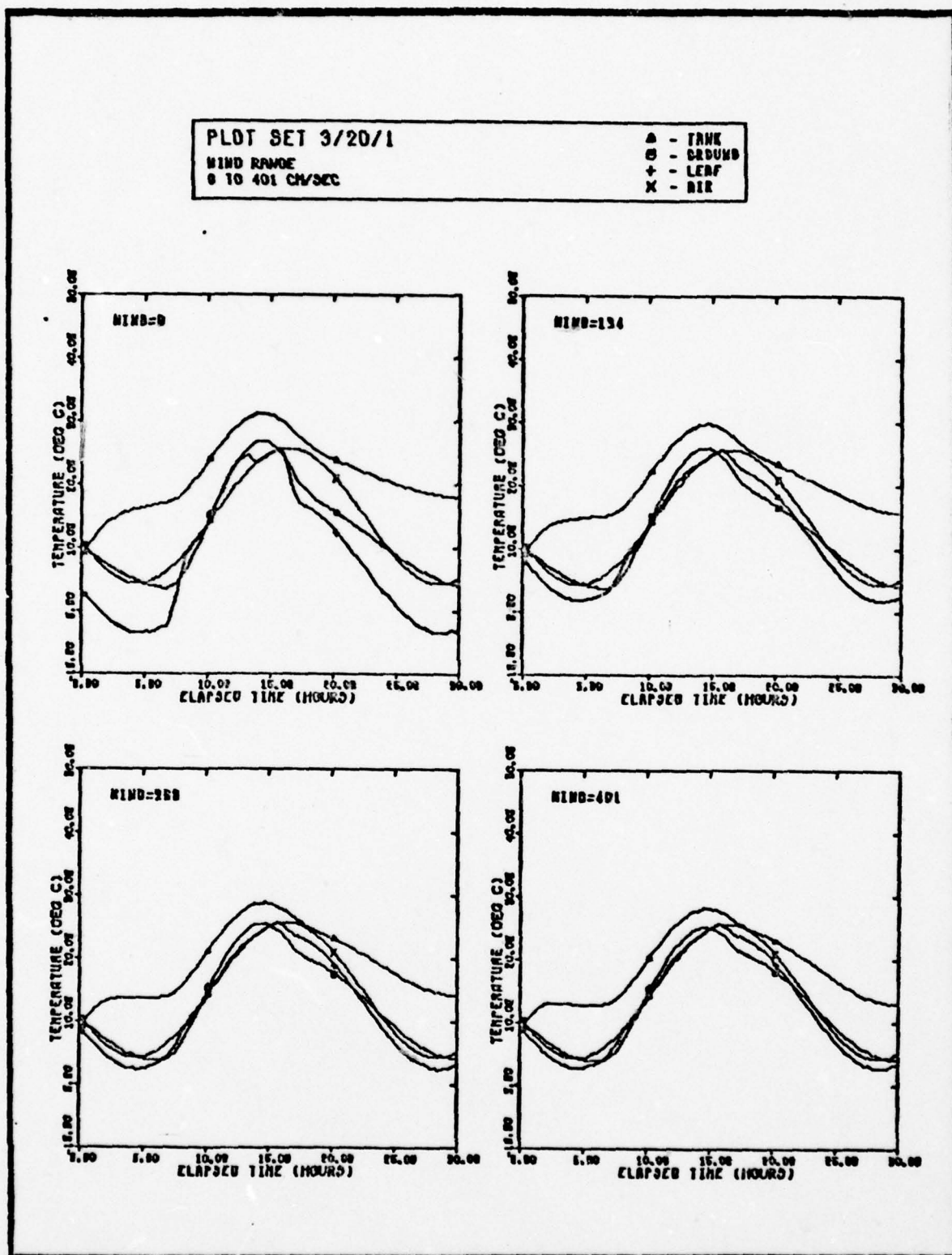


Fig. 27(a). Basic Temperature Plots of Wind

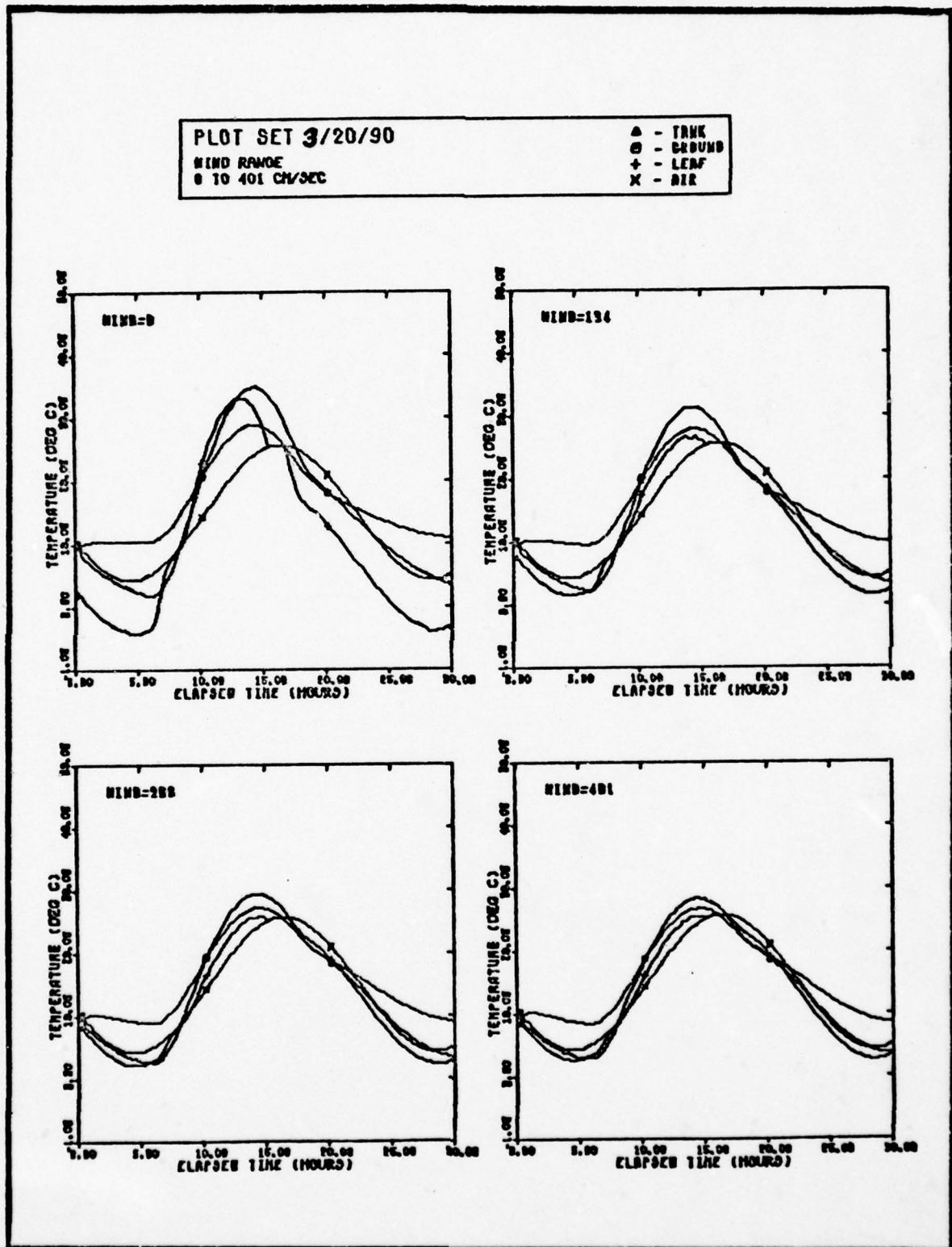


Fig. 27(b). Basic Temperature Plots of Wind

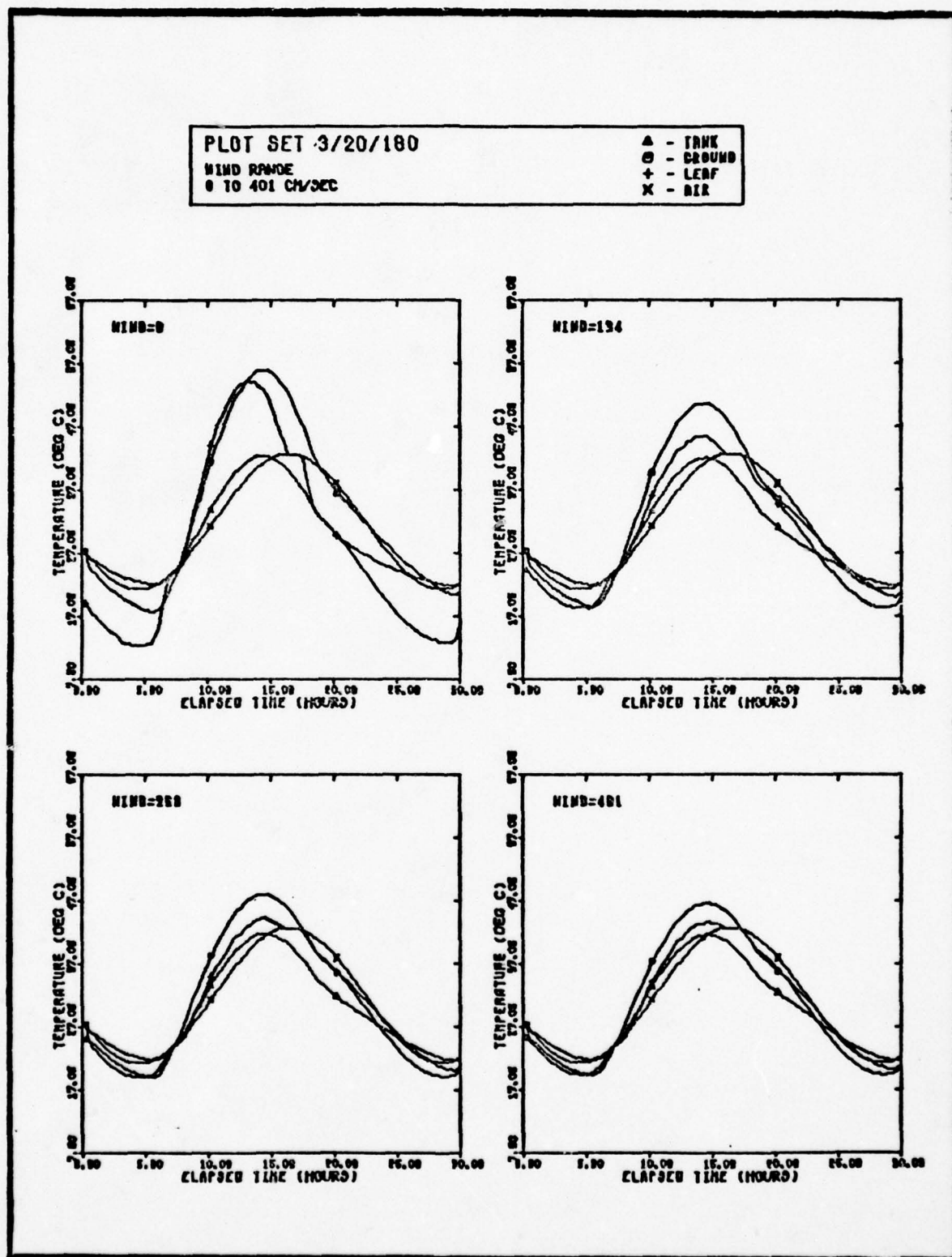


Fig. 27(c). Basic Temperature Plots of Wind



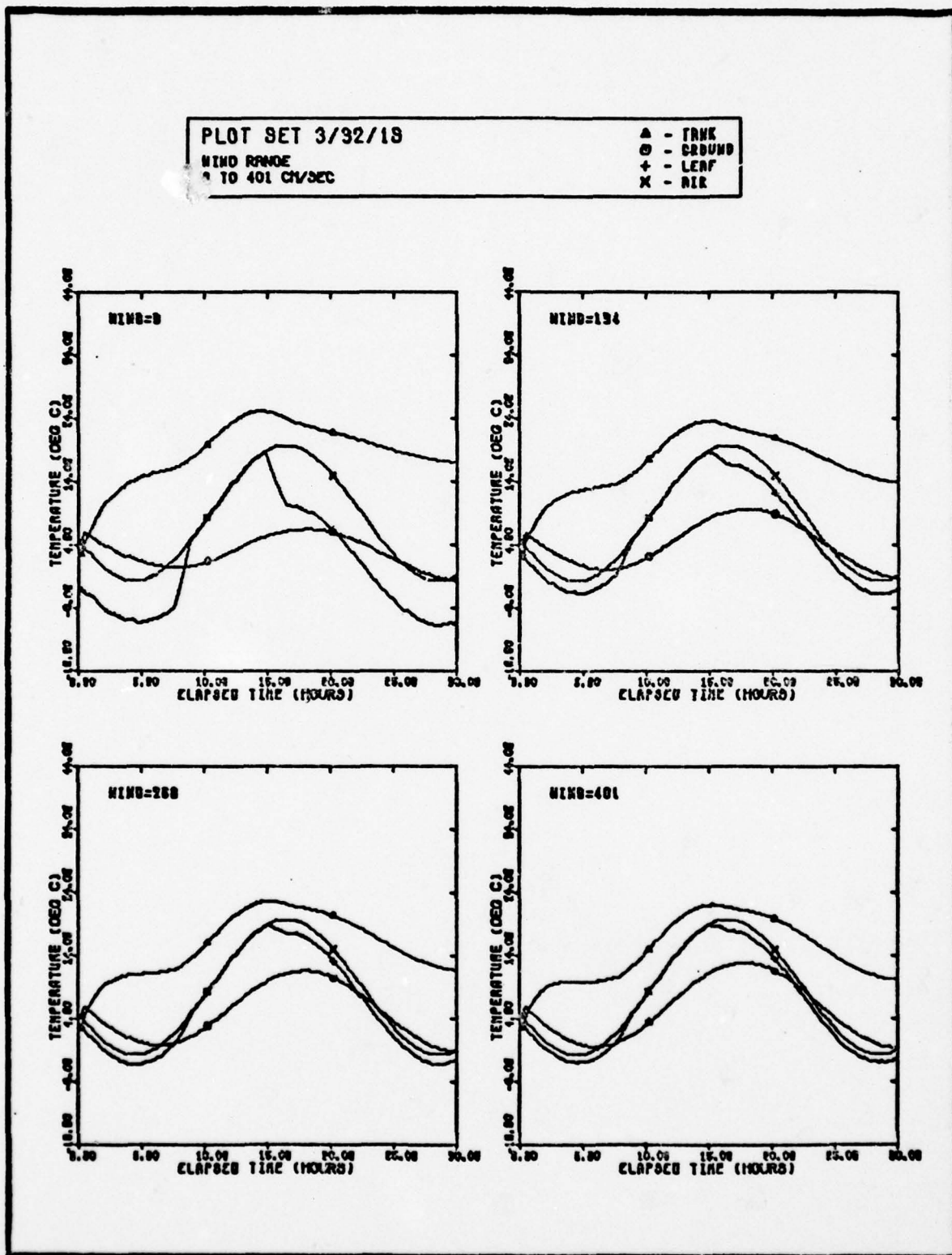


Fig. 27(d). Basic Temperature Plots of Wind

PLOT SET 3/32/1

WIND RANGE  
0 TO 401 CM/SEC

▲ - TANK  
○ - GROUND  
+ - LEAF  
X - AIR

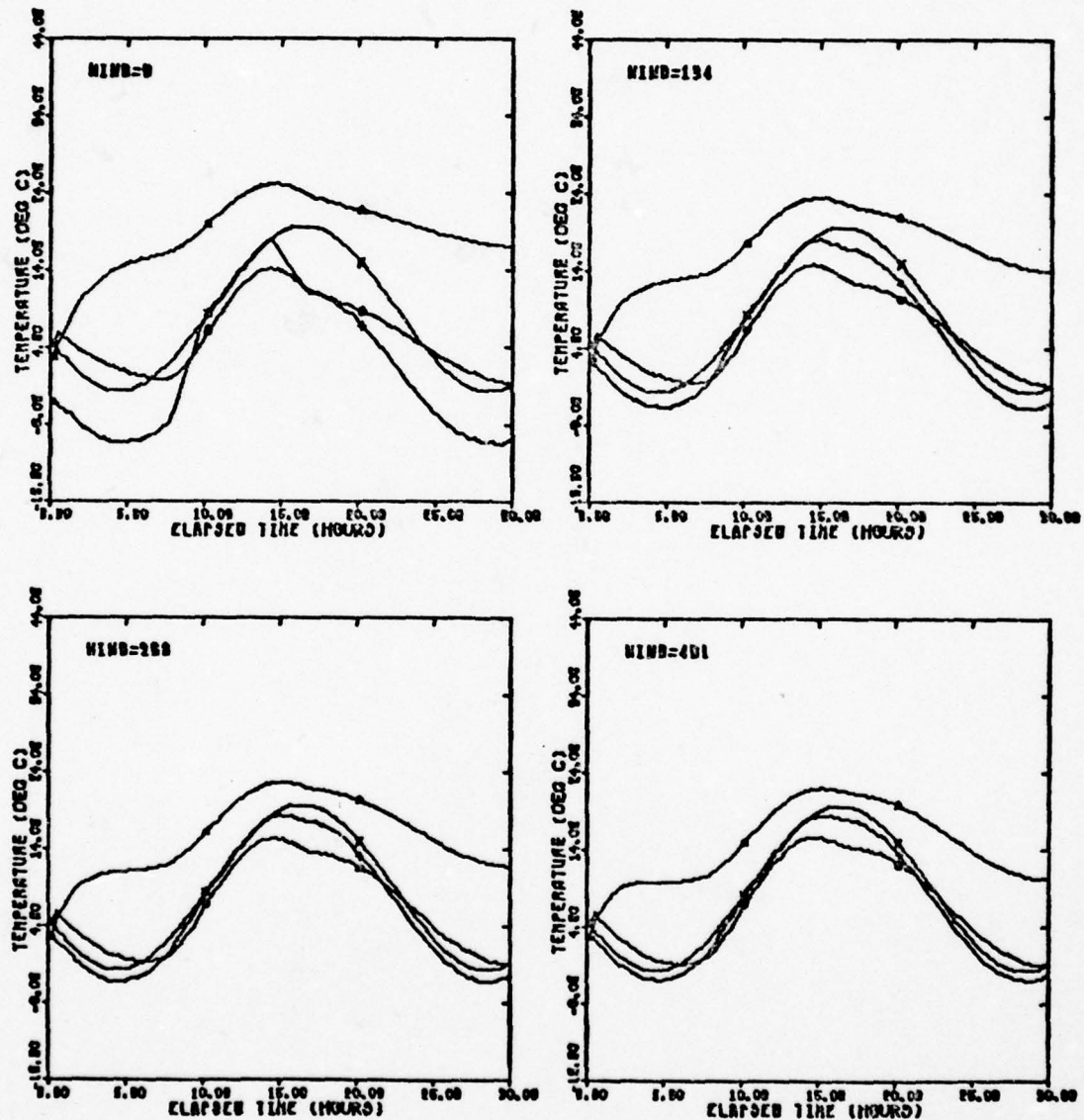


Fig. 27(e). Basic Temperature Plots of Wind

PLOT SET 3/32/90

WIND RANGE  
0 TO 401 CM/SEC

Δ - TANK  
○ - GROUND  
+ - LEAF  
x - AIR

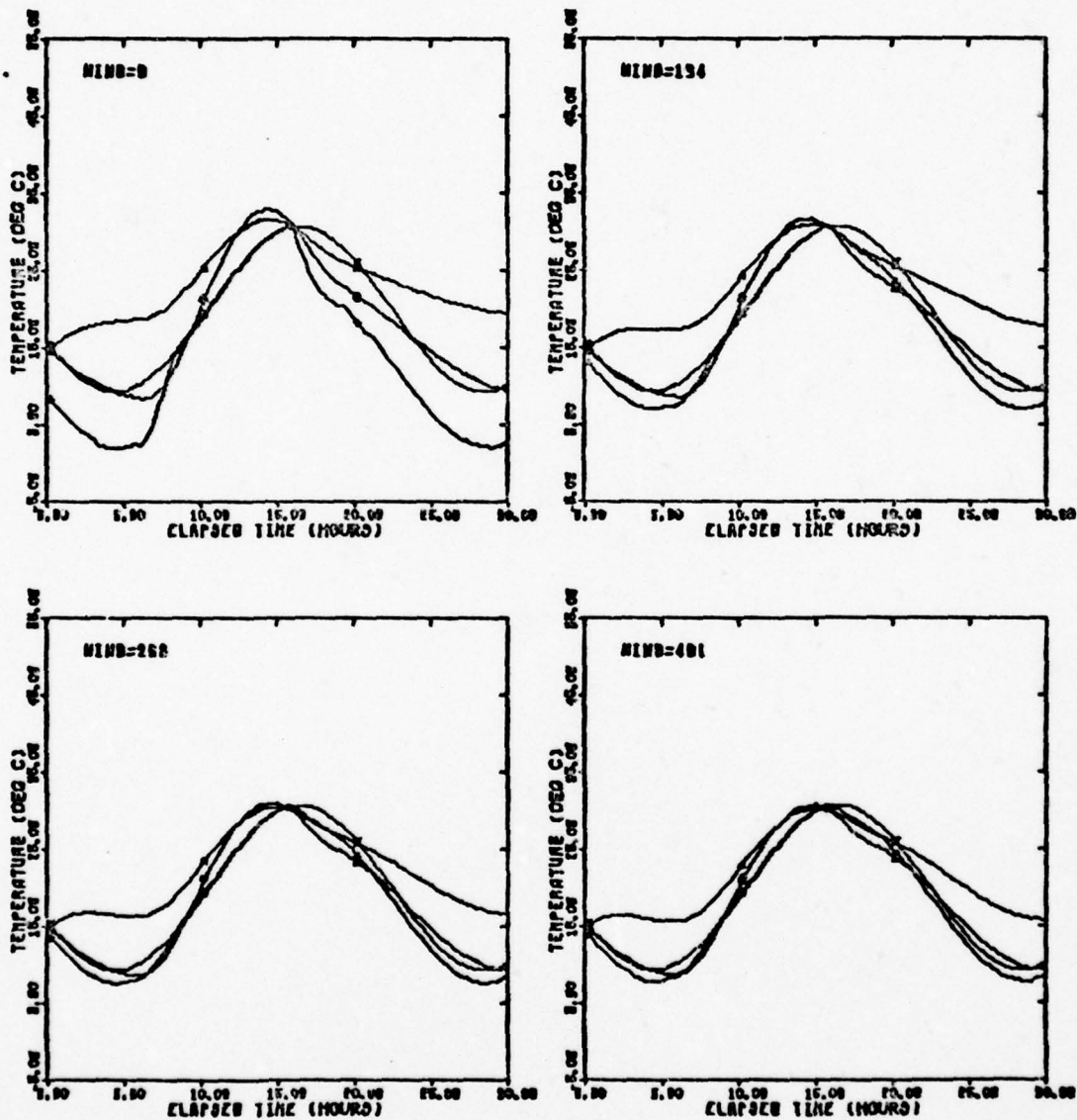


Fig. 27(f). Basic Temperature Plots of Wind

PLOT SET 3/32/180

WIND RANGE  
0 TO 401 CM/SEC

Δ - TRNK  
○ - DRUM  
+ - LEAF  
X - AIR

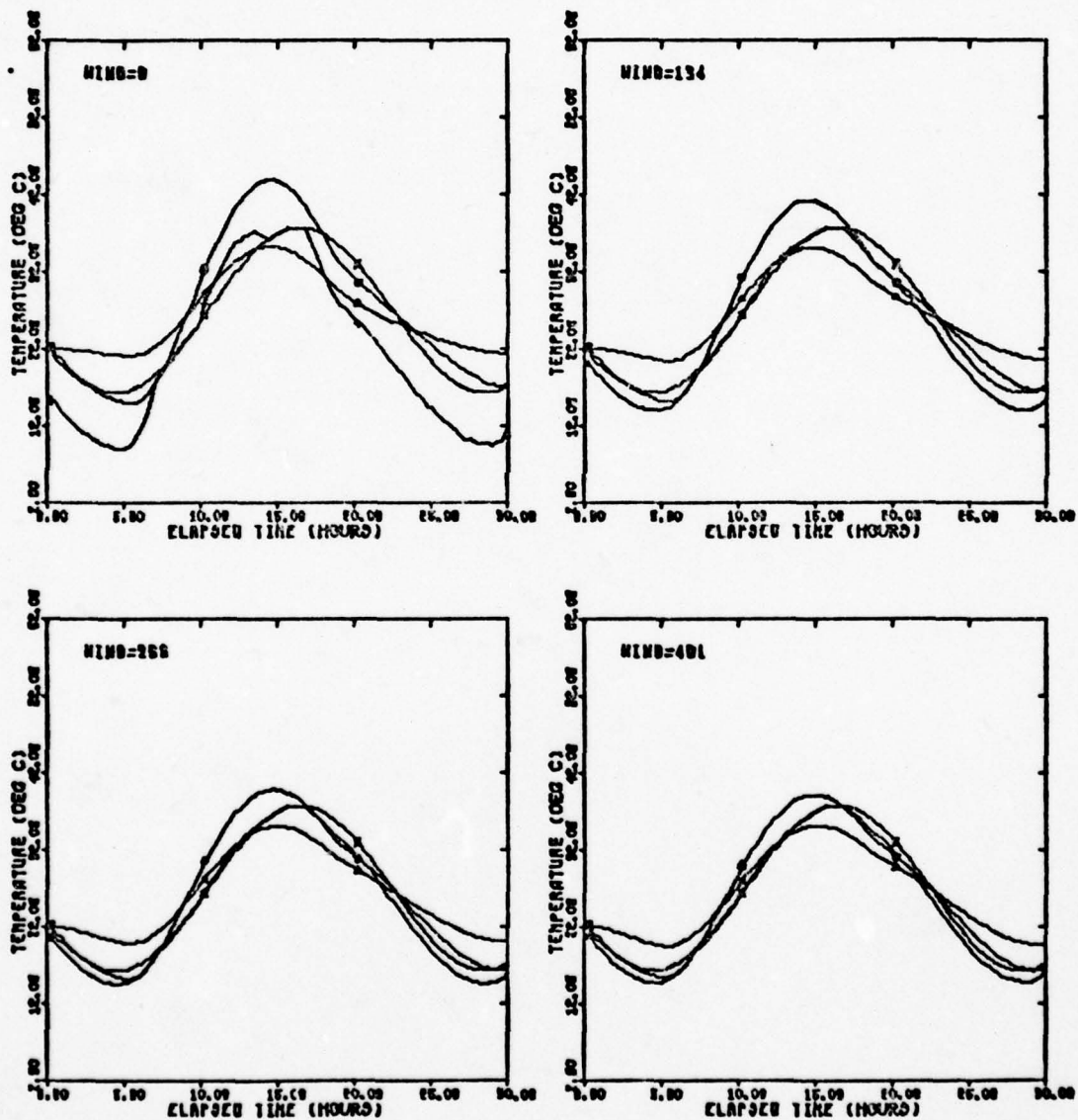


Fig. 27(g). Basic Temperature Plots of Wind



PLOT SET 3/50/18

WIND RANGE  
0 TO 401 CM/SEC

Δ - TRNK  
⊙ - GRND  
+ - LEAF  
x - AIR

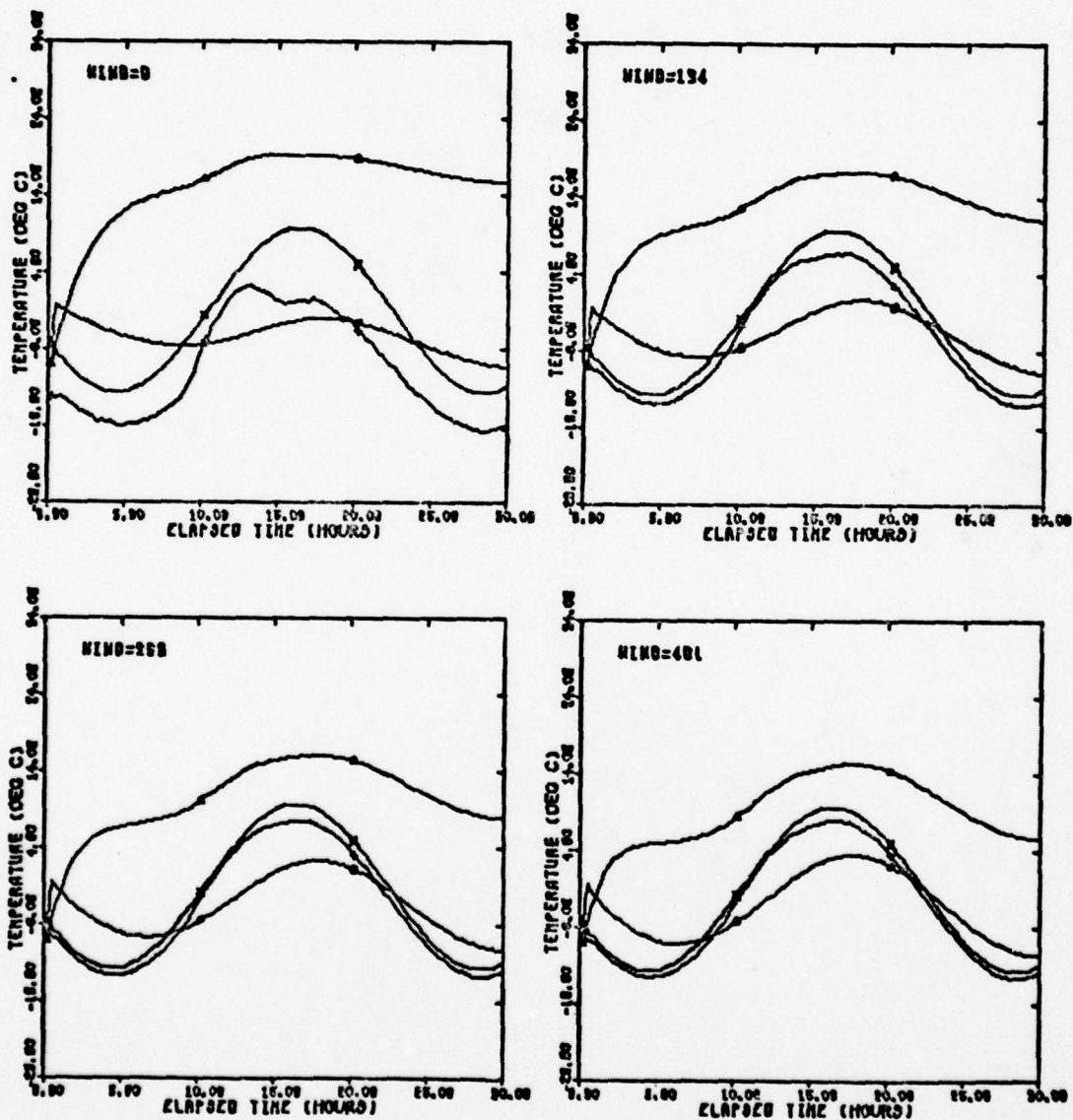


Fig. 27(h). Basic Temperature Plots of Wind

PLOT SET 3/60/1

WIND RANGE  
0 TO 401 CM/SEC

Δ - TRNK  
○ - GROUND  
+ - LEAF  
x - AIR

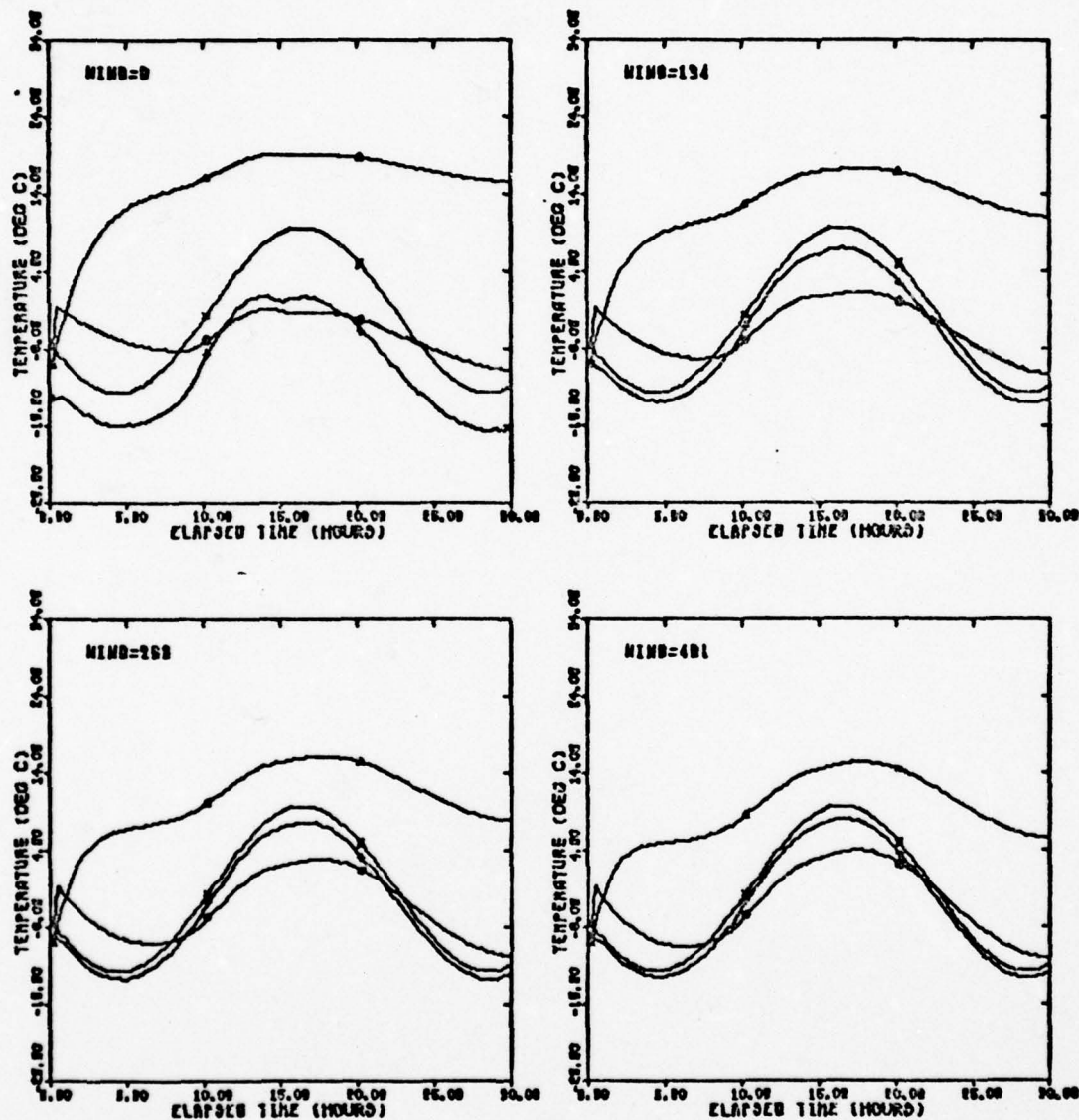


Fig. 27(1). Basic Temperature Plots of Wind

PLOT SET 3/60/90

WIND RANGE  
0 TO 401 CM/SEC

A - TRNK  
O - GROUND  
+ - LEAF  
X - AIR

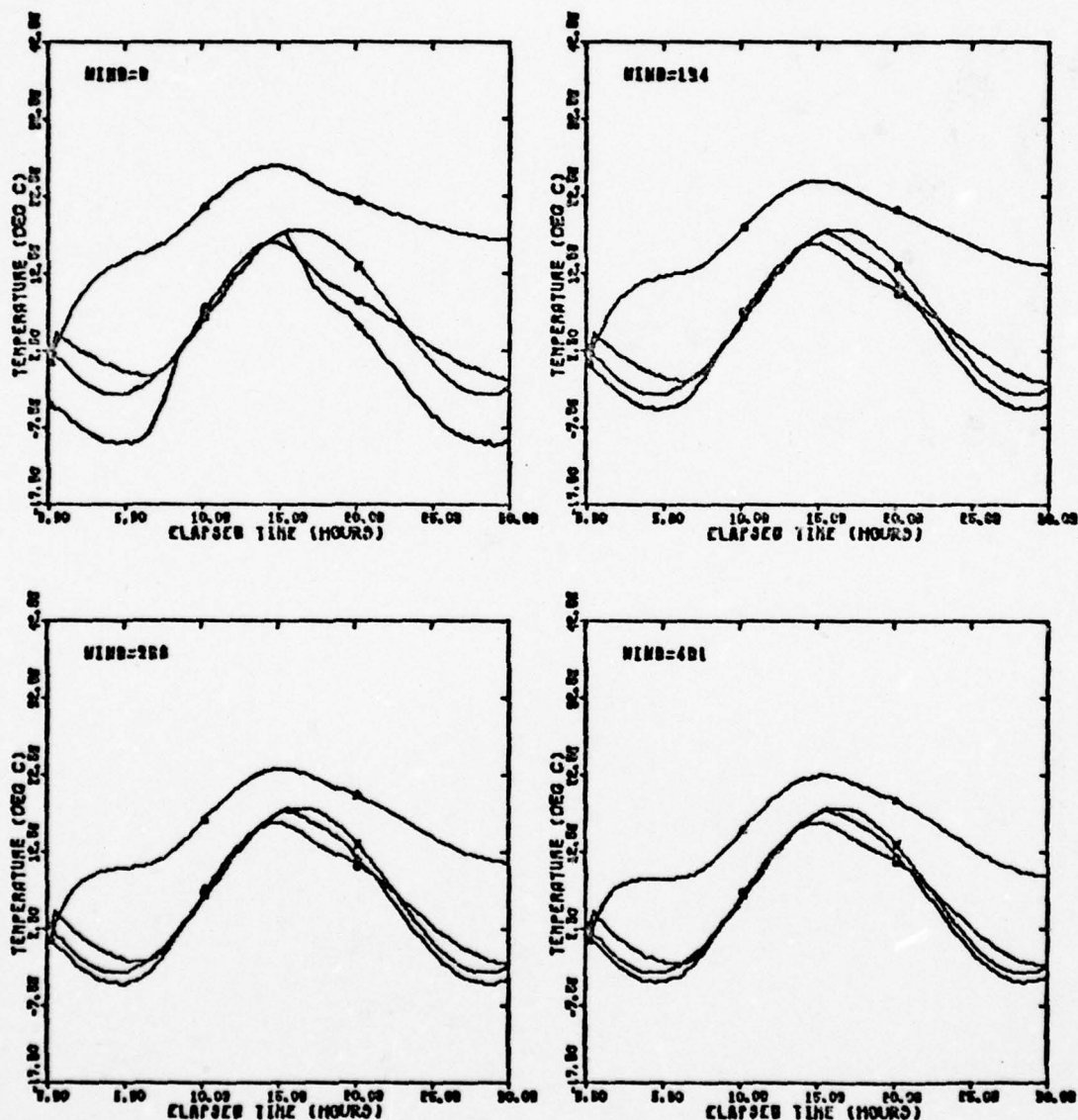


Fig. 27(j). Basic Temperature Plots of Wind

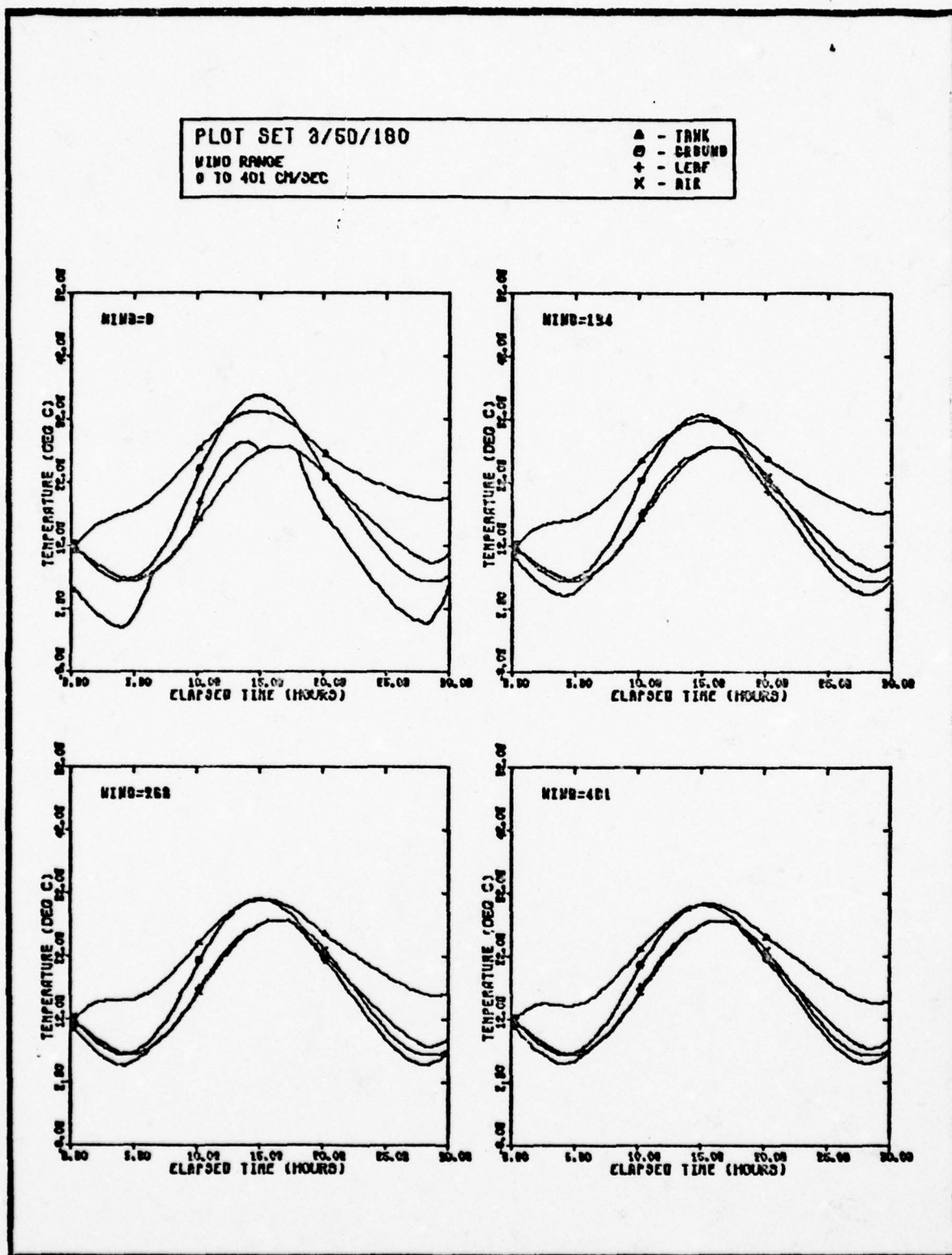


Fig. 27(k). Basic Temperature Plots of Wind



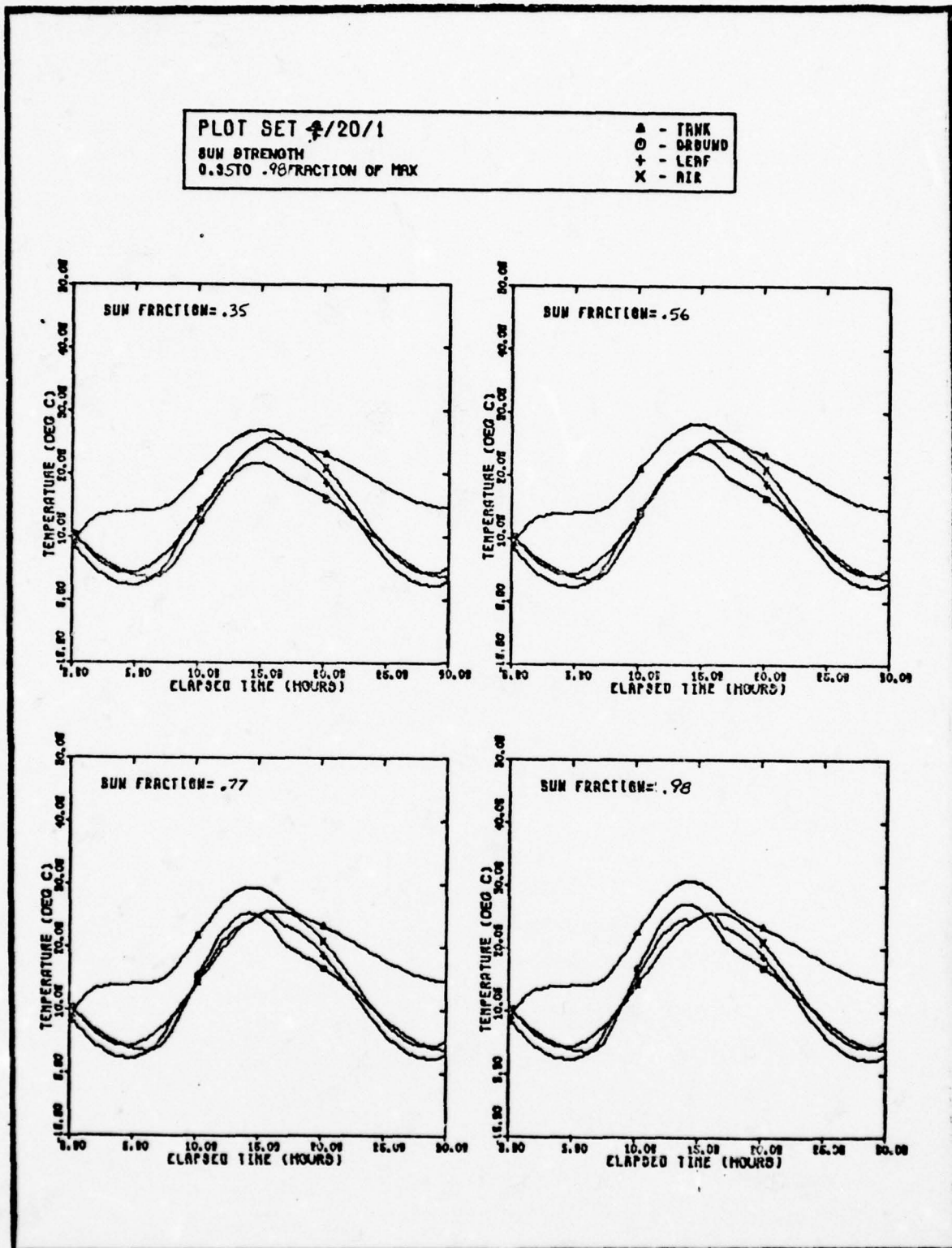


Fig. 28(a). Basic Temperature Plots of Sun Strength

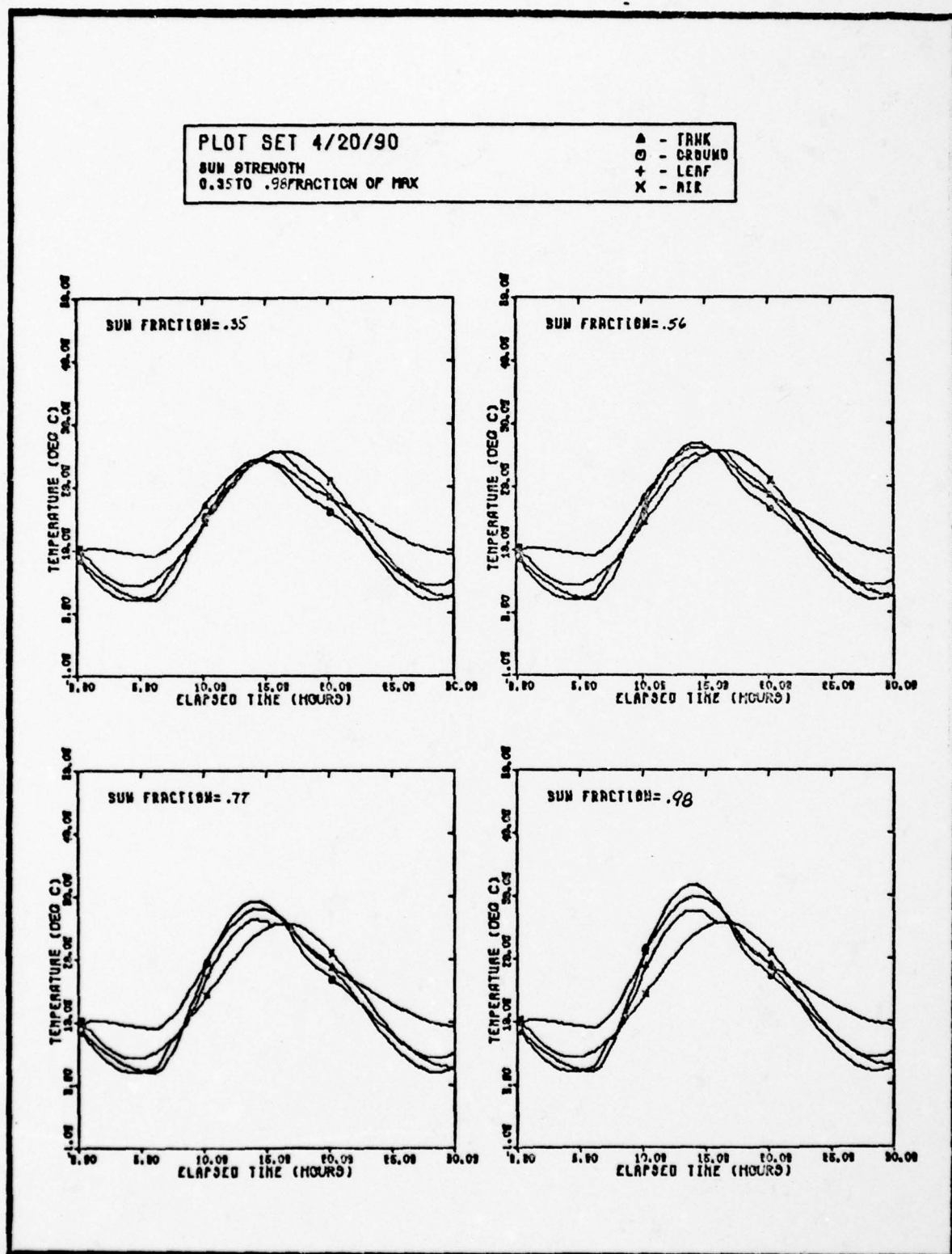


Fig. 28(b). Basic Temperature Plots of Sun Strength

PLOT SET 4/20/180

SUN STRENGTH RANGE  
0.43 TO 1.19

▲ - TRNK  
○ - GROUND  
+ - LEAF  
x - AIR

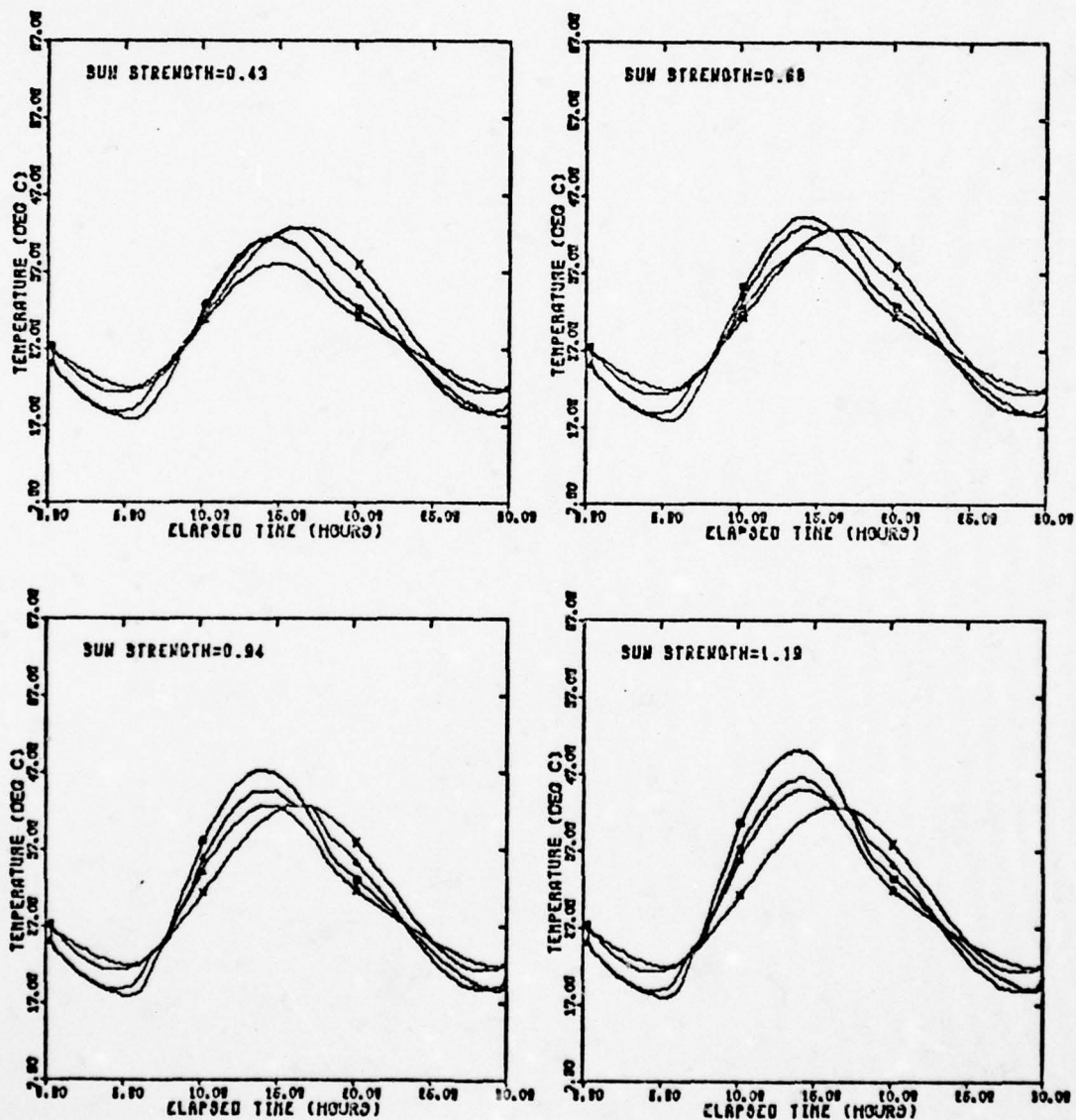


Fig. 28(c). Basic Temperature Plots of Sun Strength

PLOT SET 4/32/18  
 SUN STRENGTH  
 0.25 TO 0.7 FRACTION OF MAX

▲ - TANK  
 ○ - DRUM  
 + - LEAF  
 X - AIR

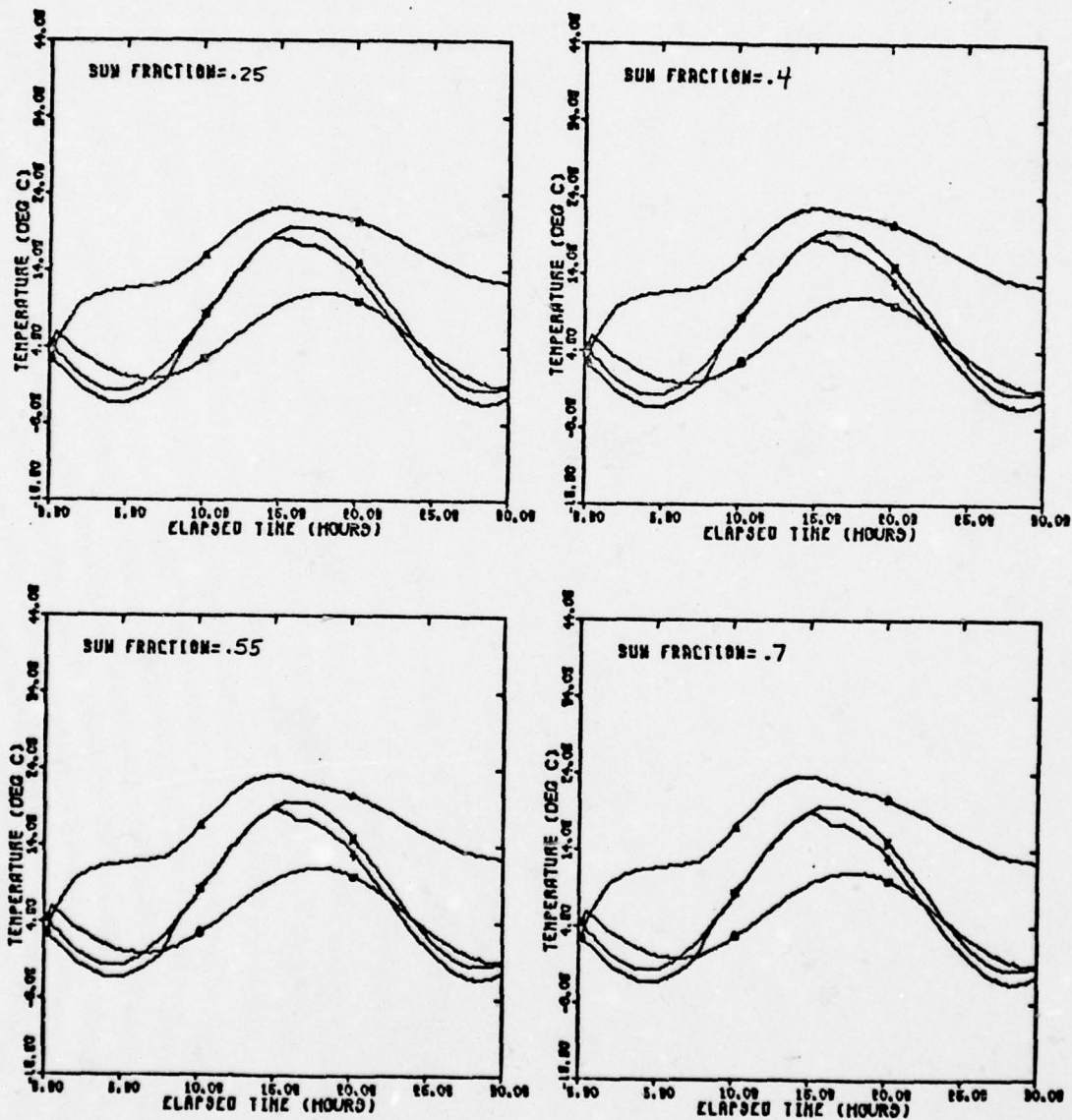


Fig. 28(d). Basic Temperature Plots of Sun Strength



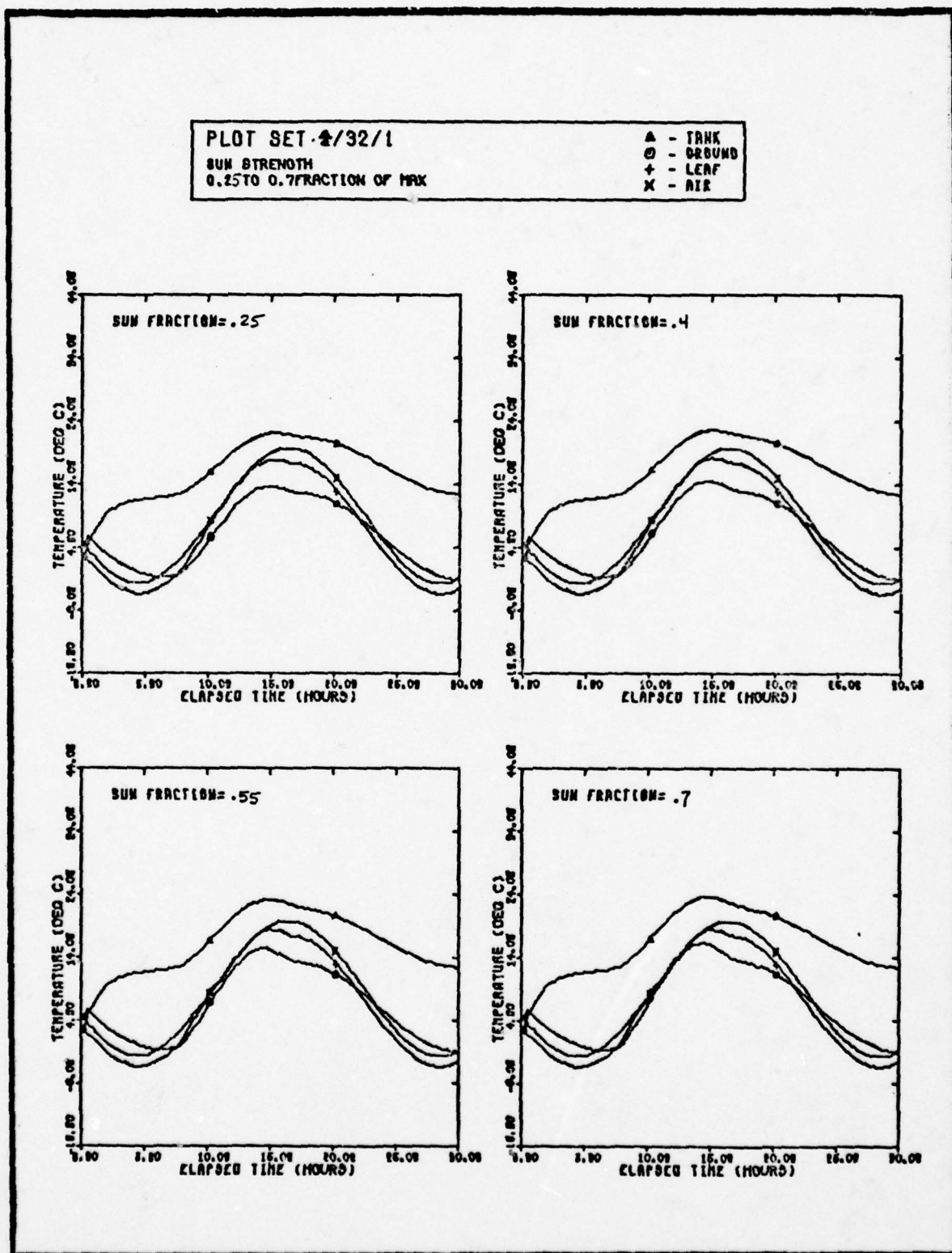


Fig. 28(e). Basic Temperature Plots of Sun Strength

PLOT SET 4/32/90  
 SUN STRENGTH  
 0.25 TO 0.7 FRACTION OF MAX

Δ - TRNK  
 ○ - CRDND  
 + - LEAF  
 x - AIR

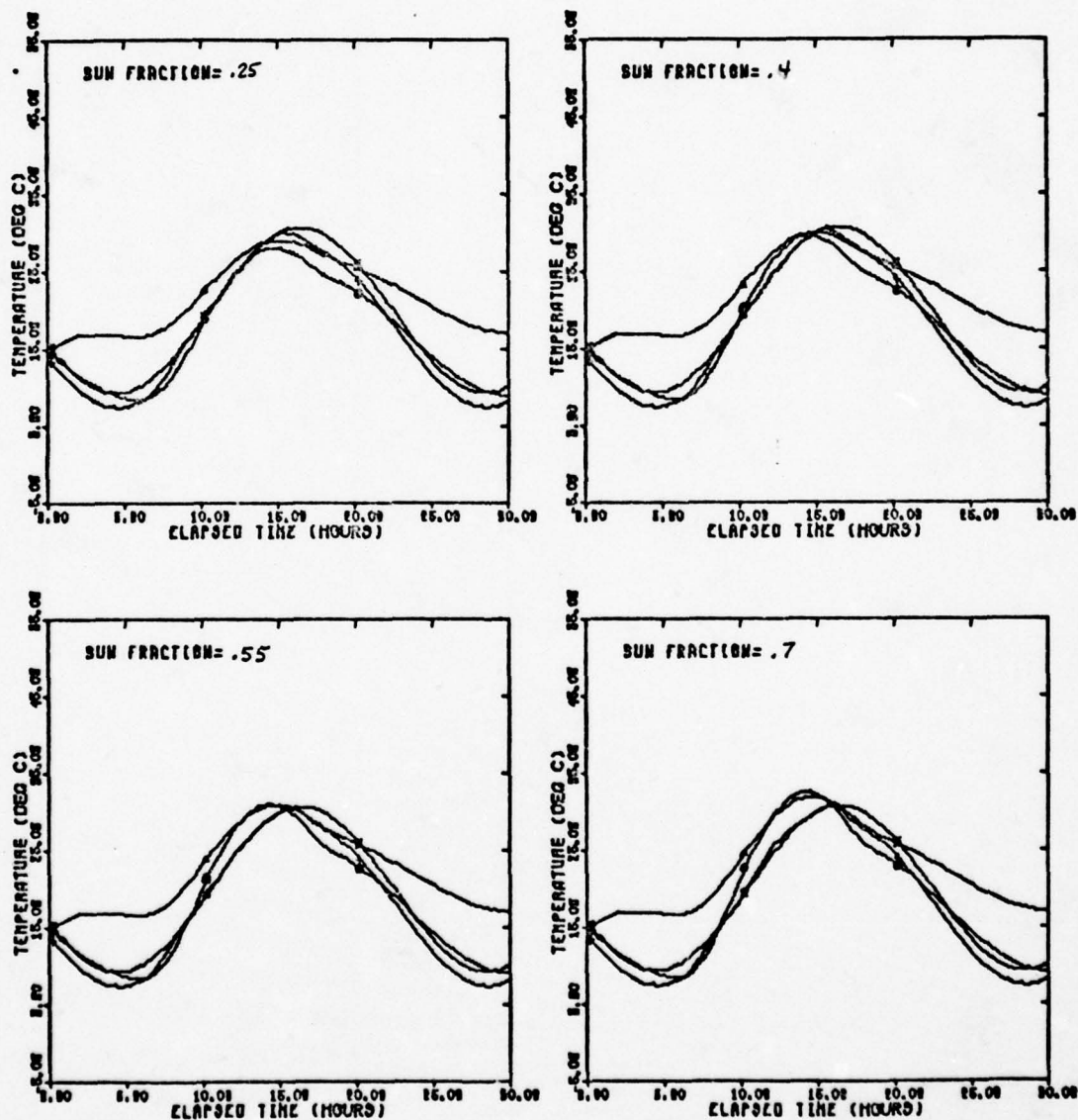


Fig. 28(f). Basic Temperature Plots of Sun Strength

PLOT SET 4/32/180

SUN STRENGTH RANGE  
0.25 TO 0.70

▲ - TRNK  
○ - GROUND  
+ - LEAF  
x - AIR

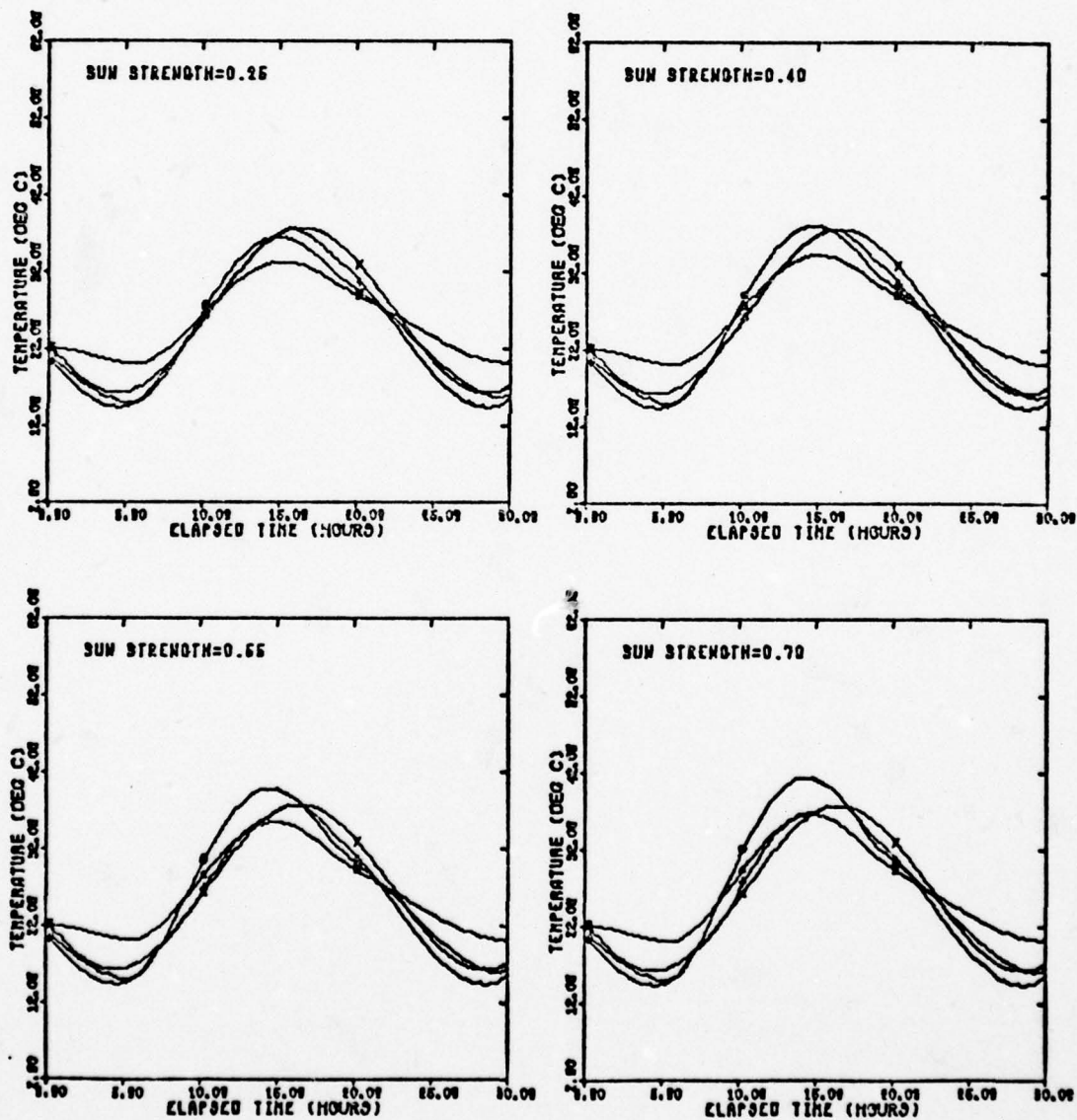


Fig. 28(g). Basic Temperature Plots of Sun Strength



PLOT SET 4/60/18  
 SUN STRENGTH  
 0.25 TO 0.7 FRACTION OF MAX

Δ - TANK  
 ○ - GROUND  
 + - LEAF  
 x - AIR

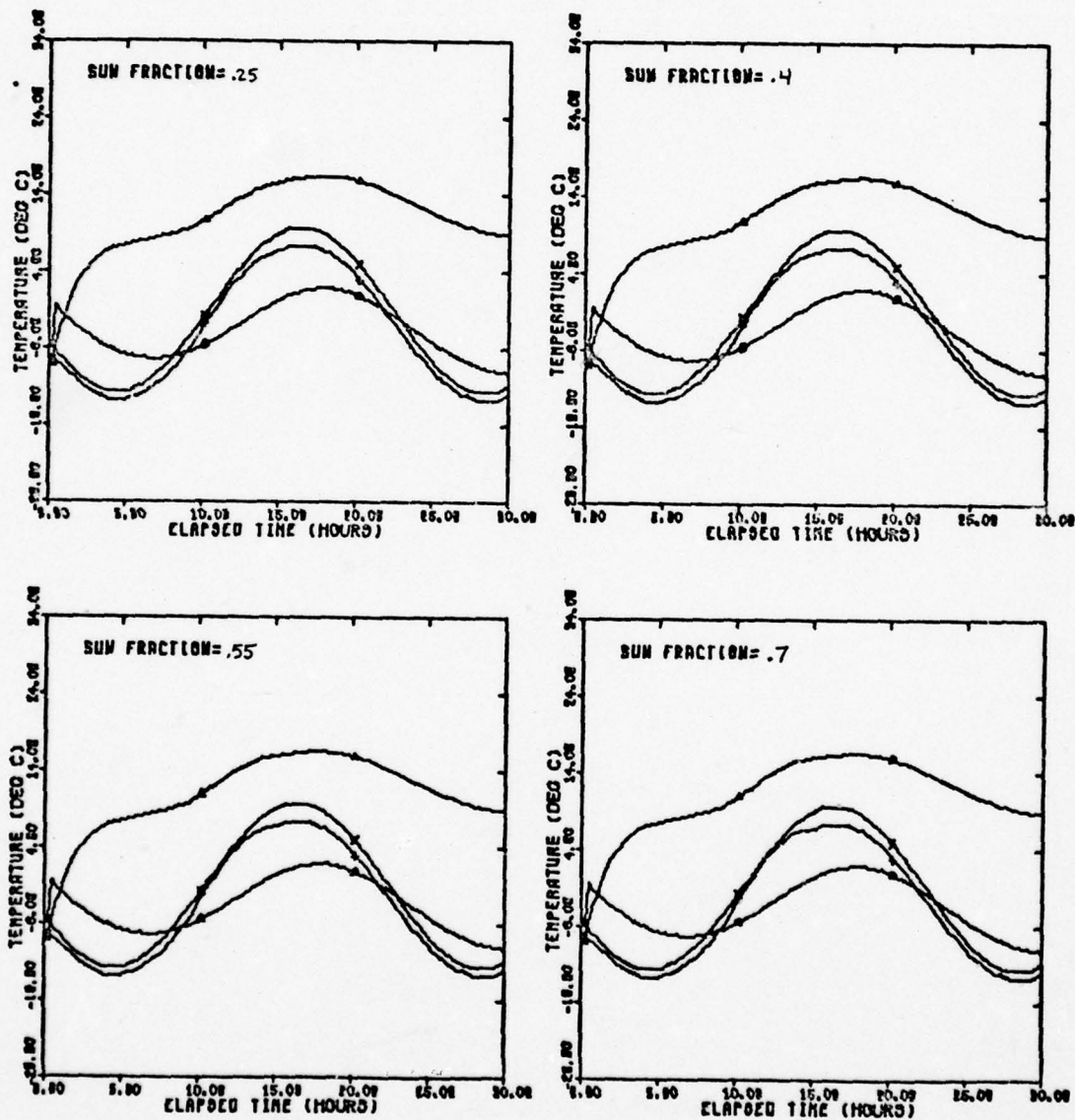


Fig. 28(h). Basic Temperature Plots of Sun Strength



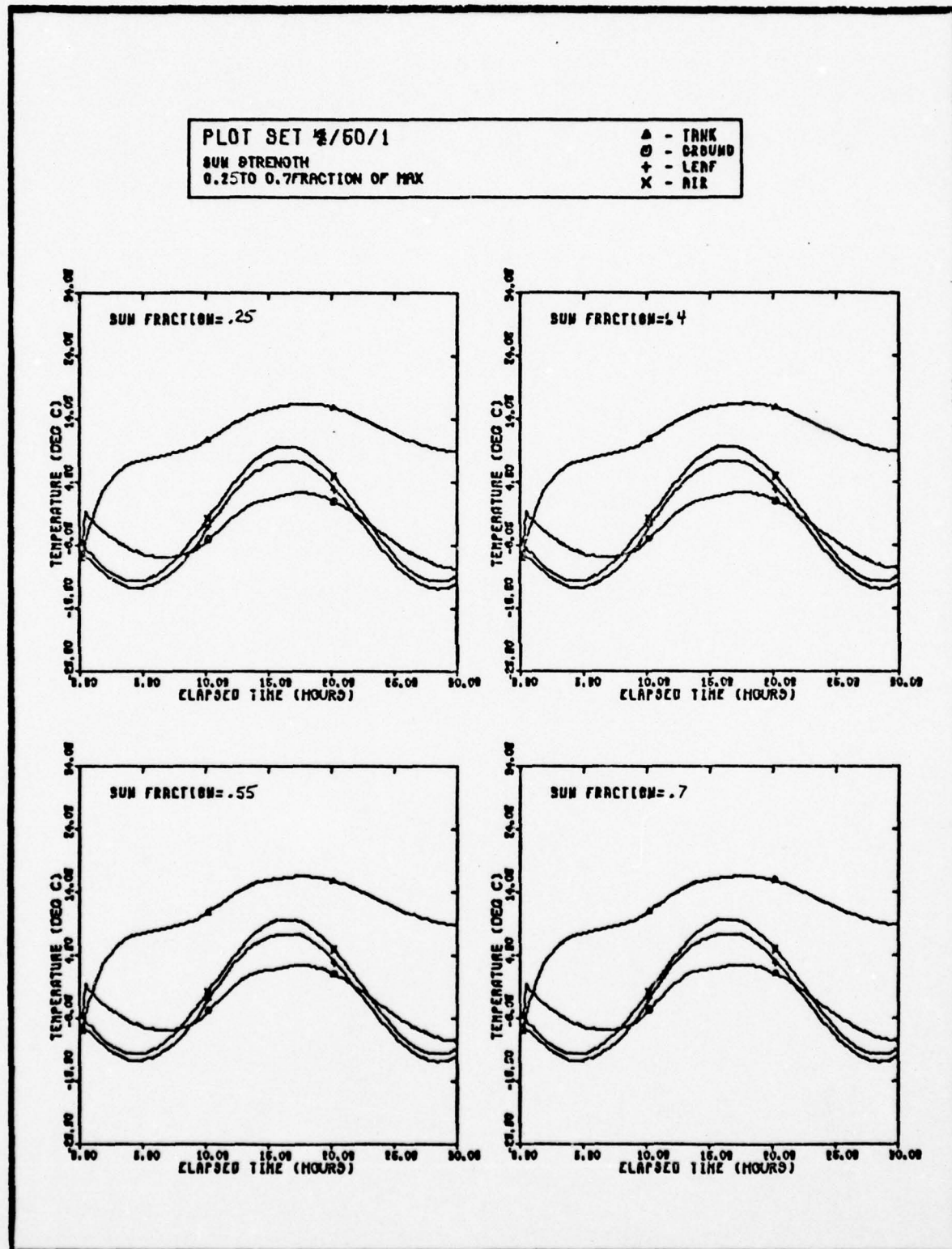


Fig. 28(1). Basic Temperature Plots of Sun Strength

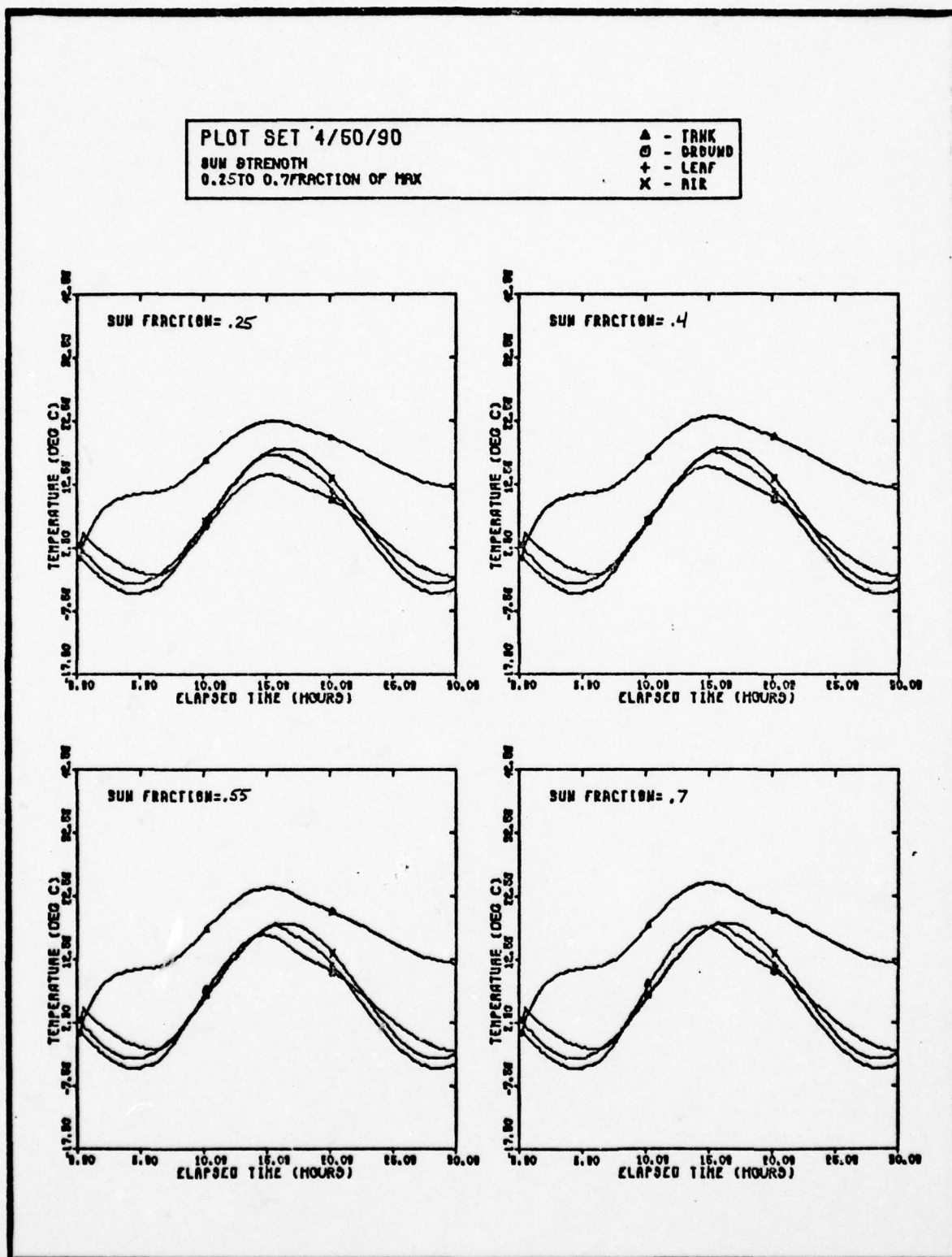


Fig. 28(j). Basic Temperature Plots of Sun Strength

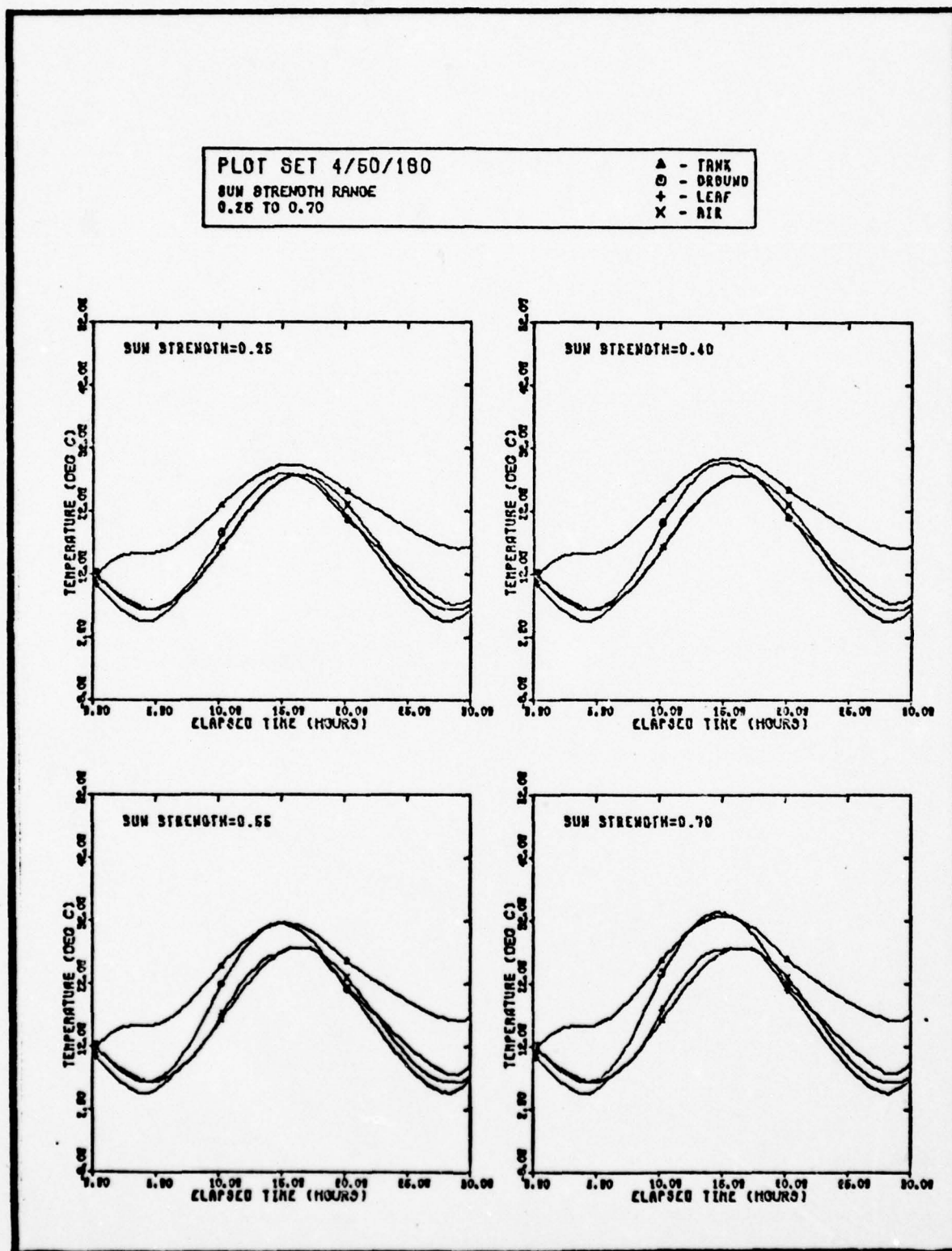


Fig. 28(k). Basic Temperature Plot of Sun Strength



PLOT SET 6/20/1  
GRND. REFL. RANGE  
.12 TO .64

▲ - TRNK  
○ - GROUND  
+ - LEAF  
x - AIR

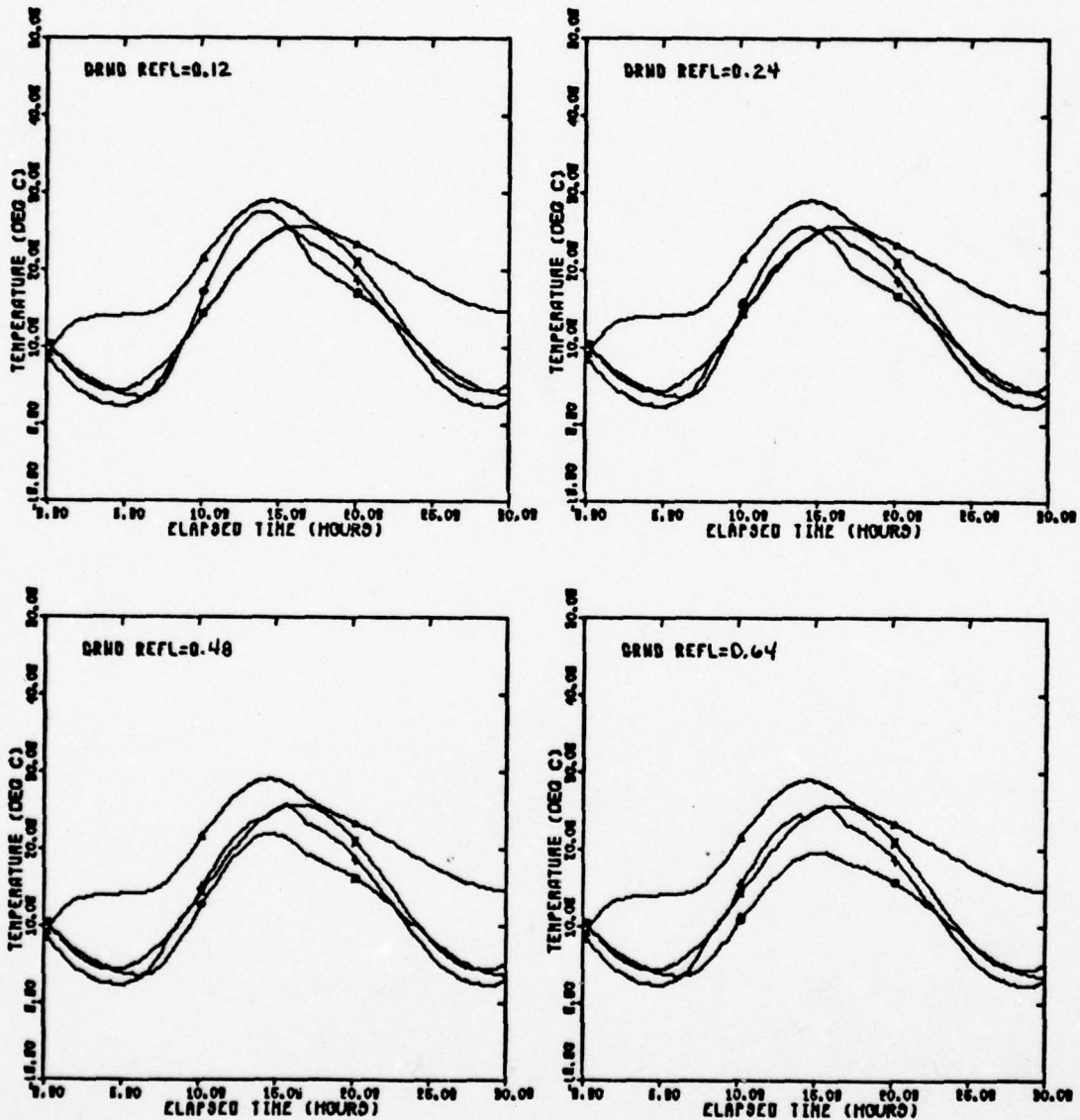


Fig. 29(a). Basic Temperature Plots of Ground Reflectivity



PLOT SET 5/20/90

GRND. REFL. RANGE  
0.12 TO 0.64

▲ - TRNK  
● - GROUND  
+ - LEAF  
X - AIR

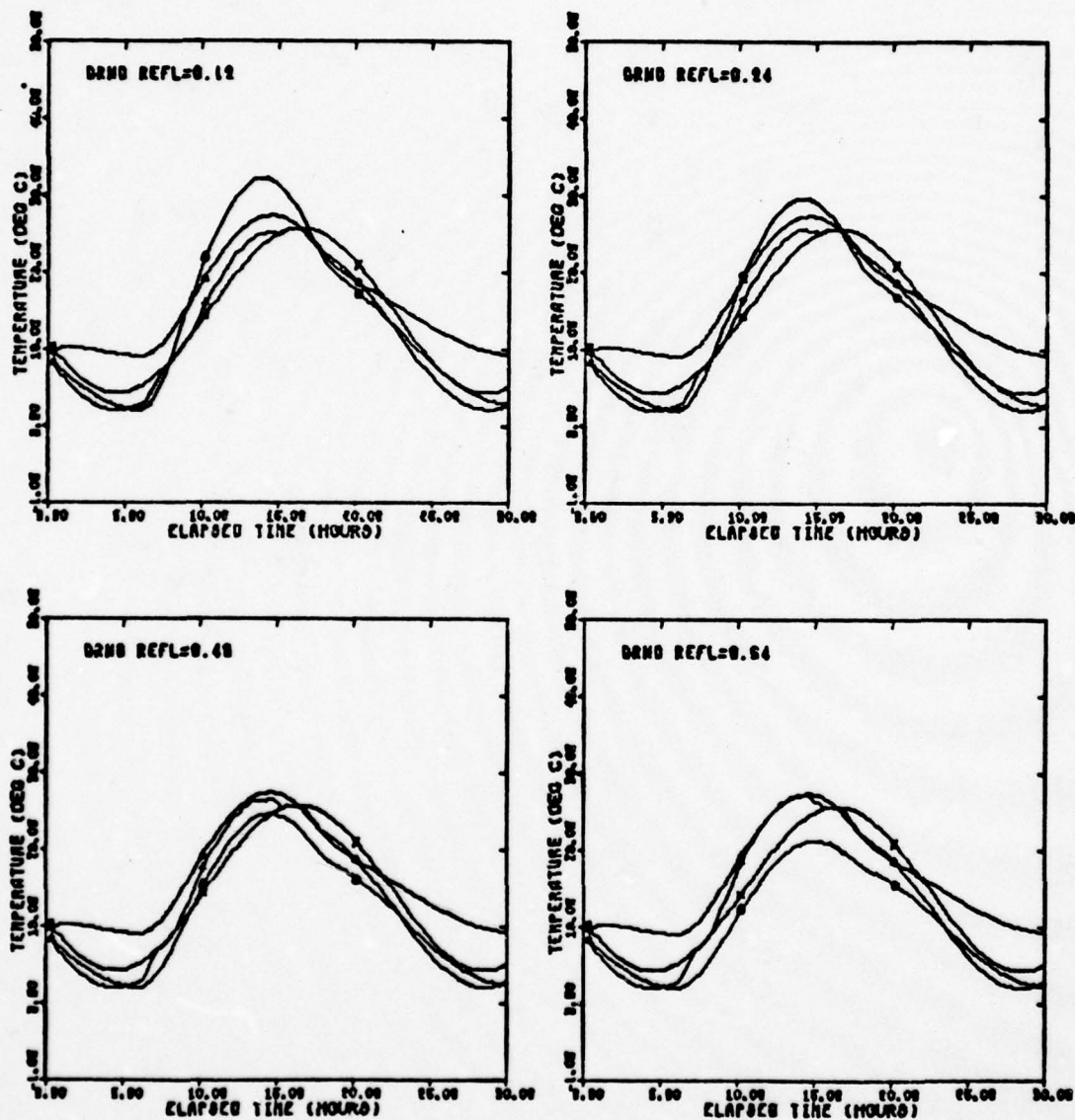


Fig. 29(b). Basic Temperature Plots of Ground Reflectivity

PLOT SET 6/20/180

GRND. REFL. RANGE  
0.12 TO 0.64

△ - TRNK  
⊙ - DRBUND  
+ - LEAF  
X - AIR

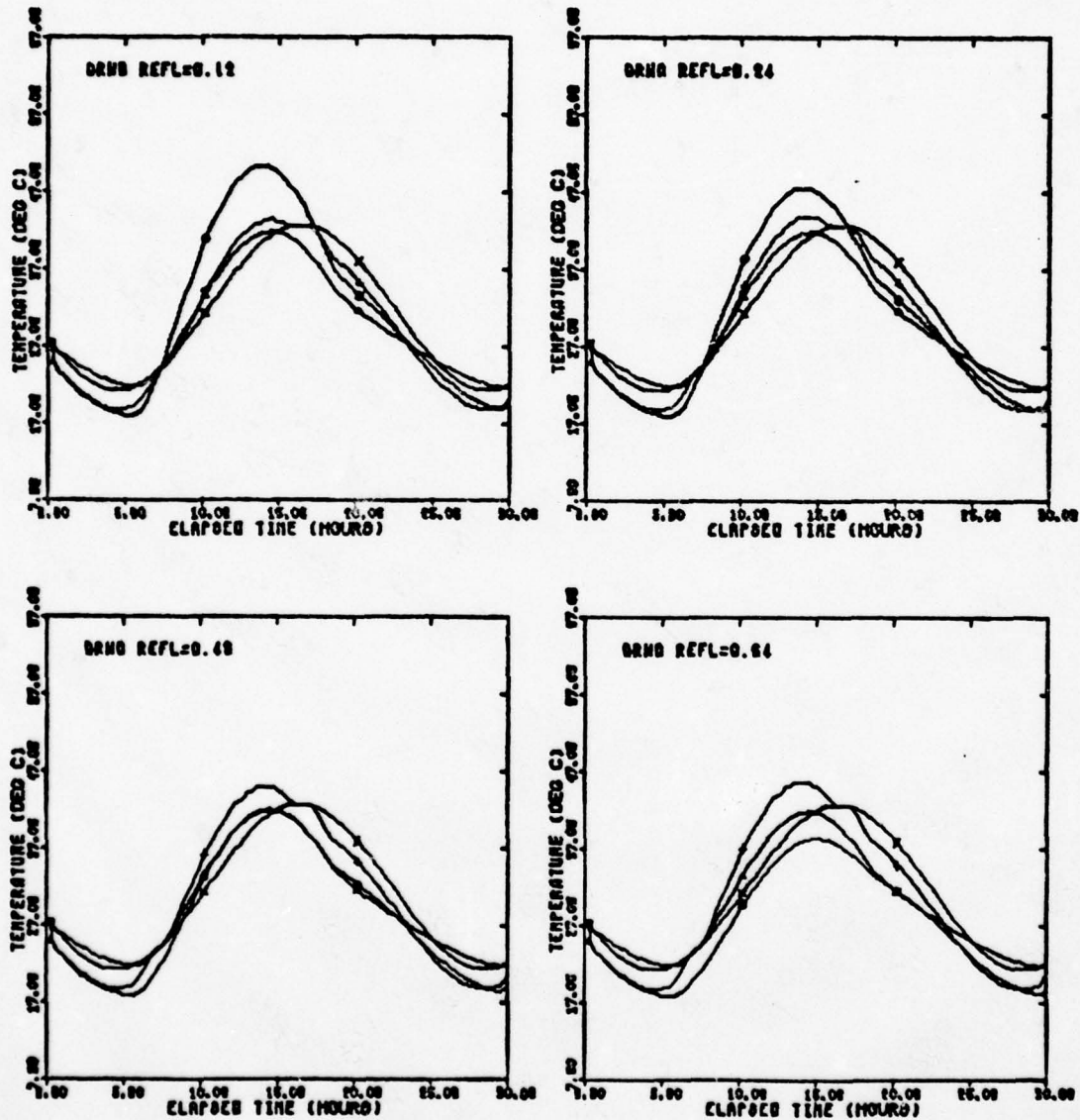


Fig. 29(c). Basic Temperature Plots of Ground Reflectivity

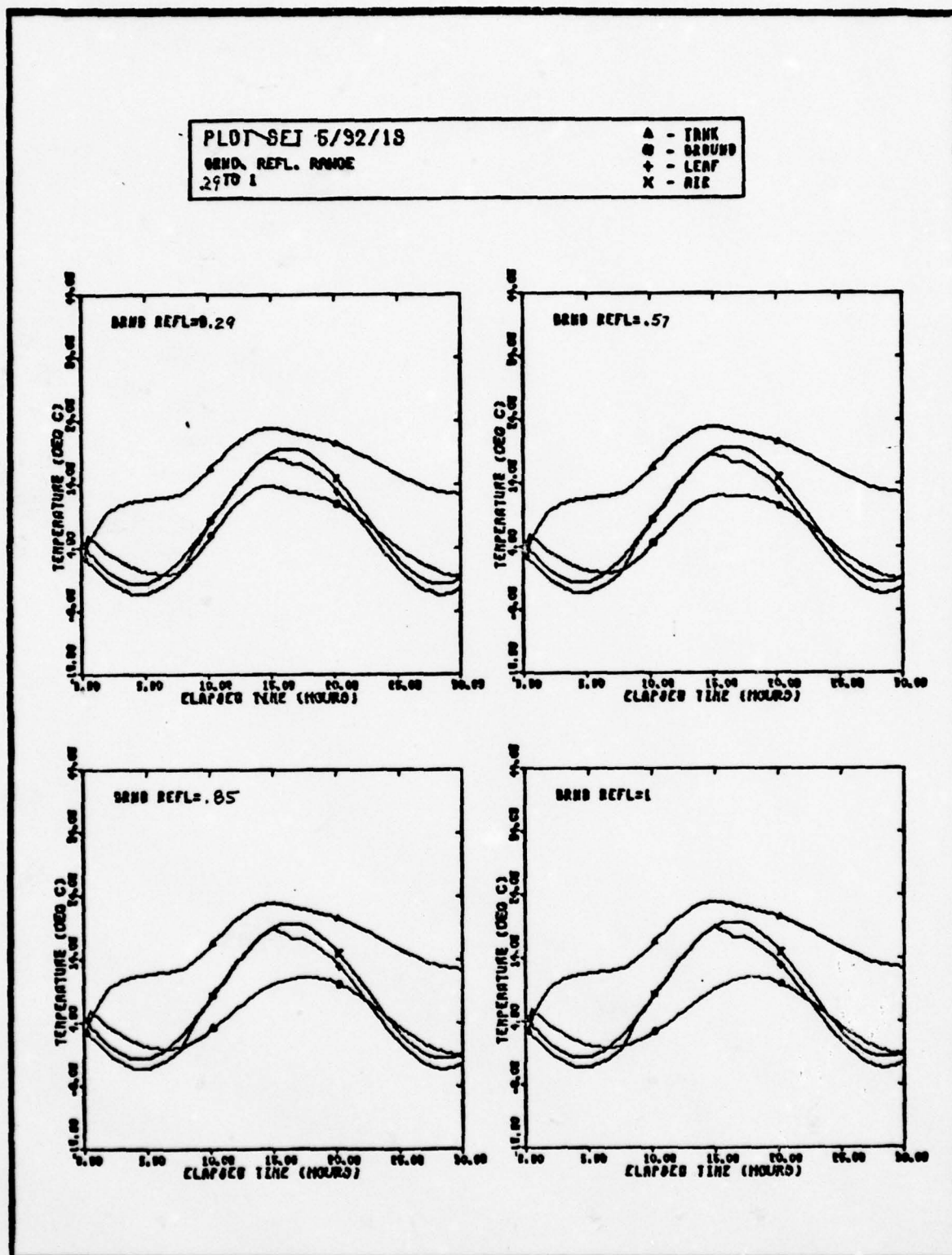


Fig. 29(d). Basic Temperature Plots of Ground Reflectivity



PLOT SET 6/32/1

GRND. REFL. RANGE  
.08 TO 0.32

▲ - TRNK  
○ - DRUND  
+ - LEAF  
X - AIR

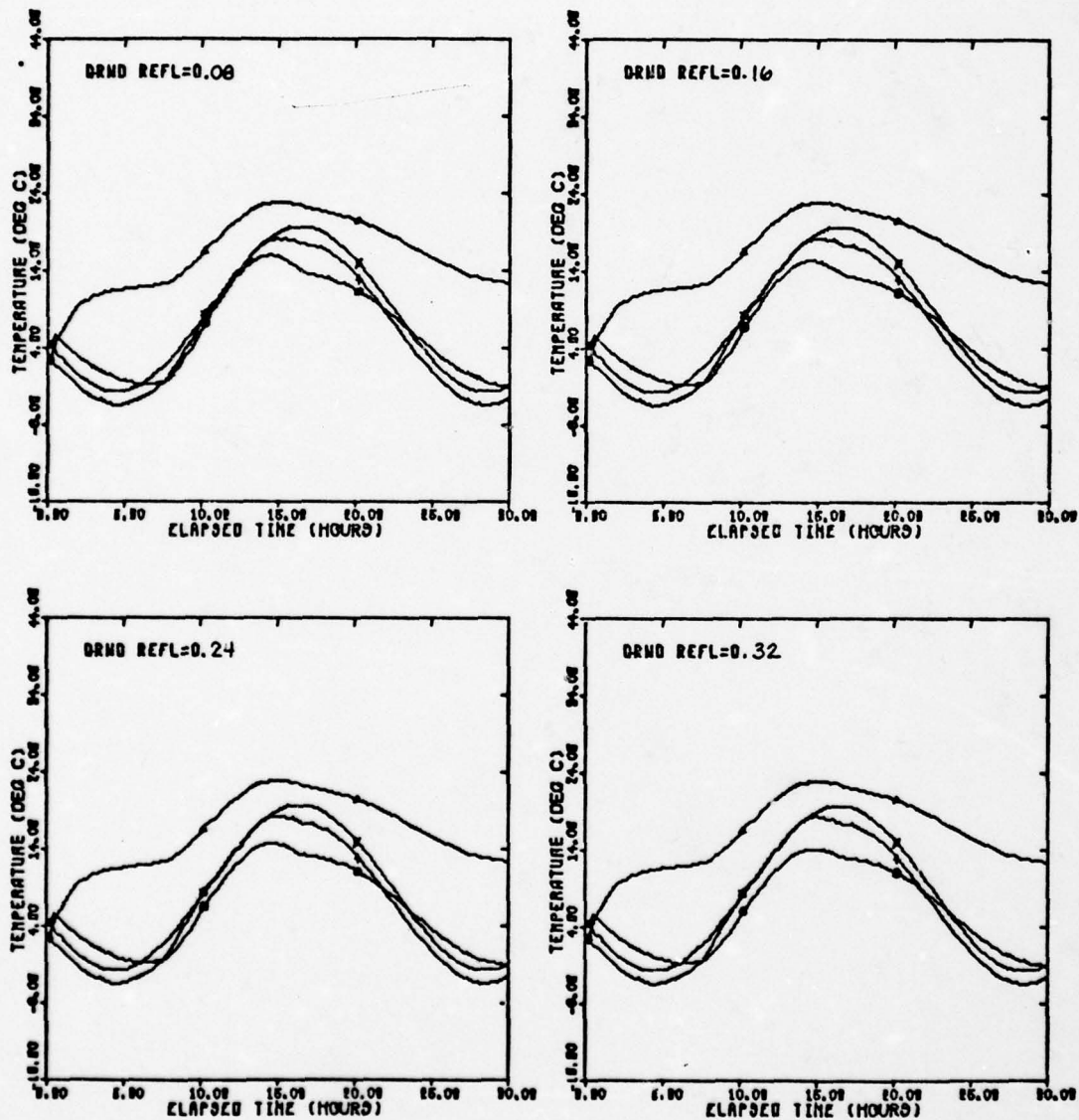


Fig. 29(e). Basic Temperature Plots of Ground Reflectivity



PLOT SET 5/32/90

GAND. REFL. RANGE  
0.00 TO 0.32

Δ - TRNK  
○ - GROUND  
+ - LEAF  
X - AIR

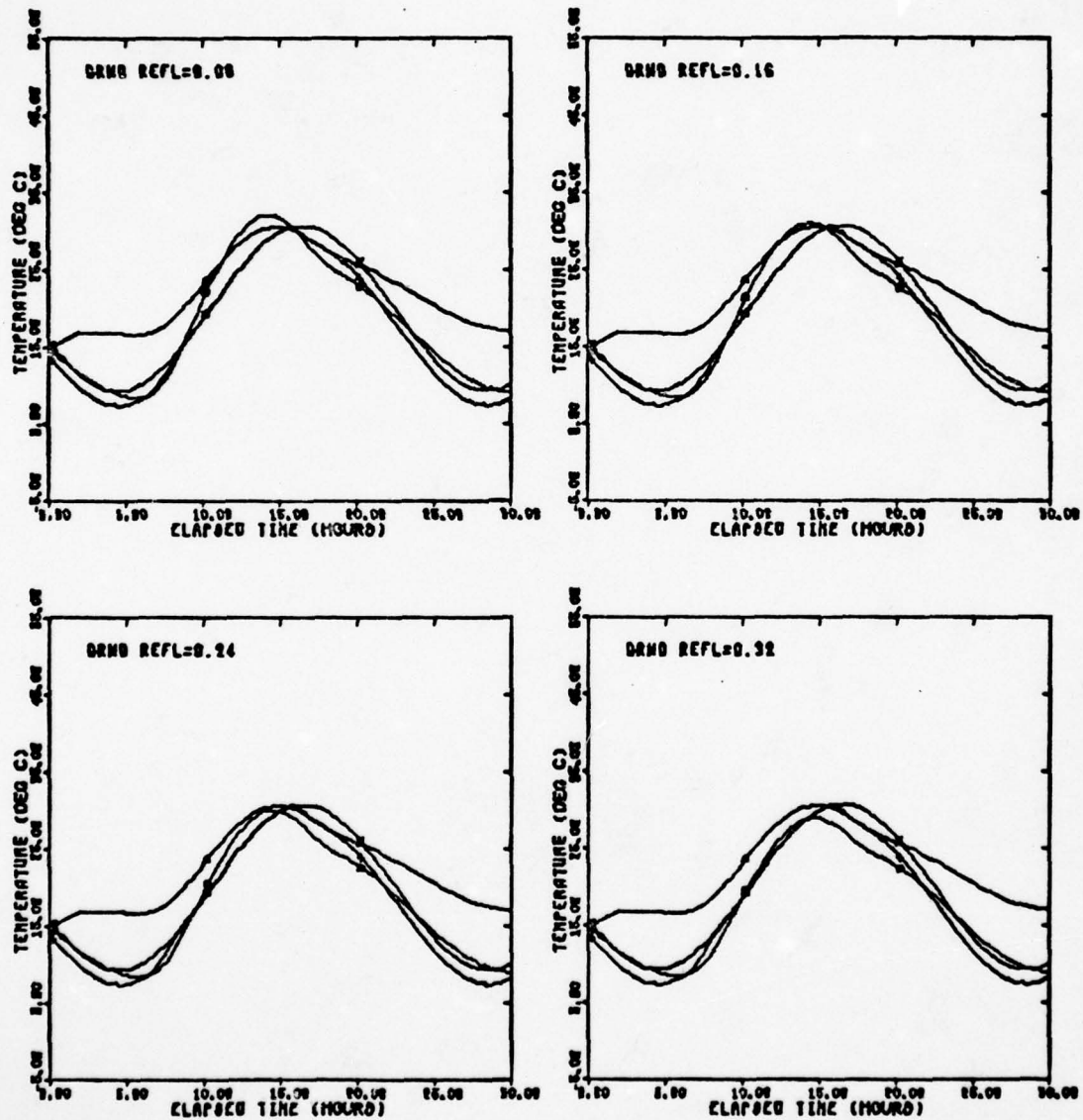


Fig. 29(f). Basic Temperature Plots of Ground Reflectivity

PLOT SET 5/32/180

GRND. REFL. RANGE  
0.00 TO 0.32

△ - TRNK  
○ - GROUND  
+ - LEAF  
x - AIR

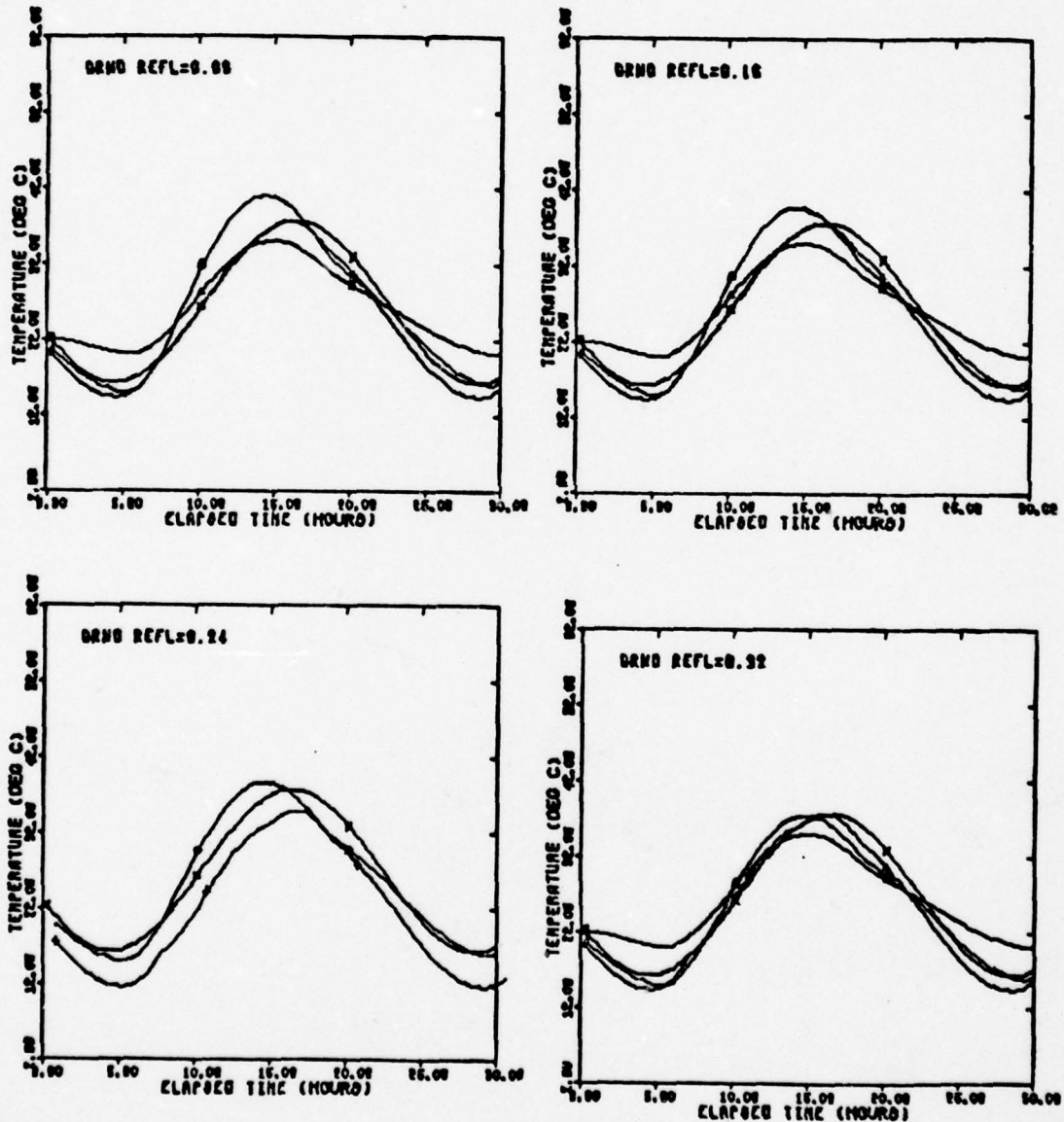


Fig. 29(g). Basic Temperature Plots of Ground Reflectivity

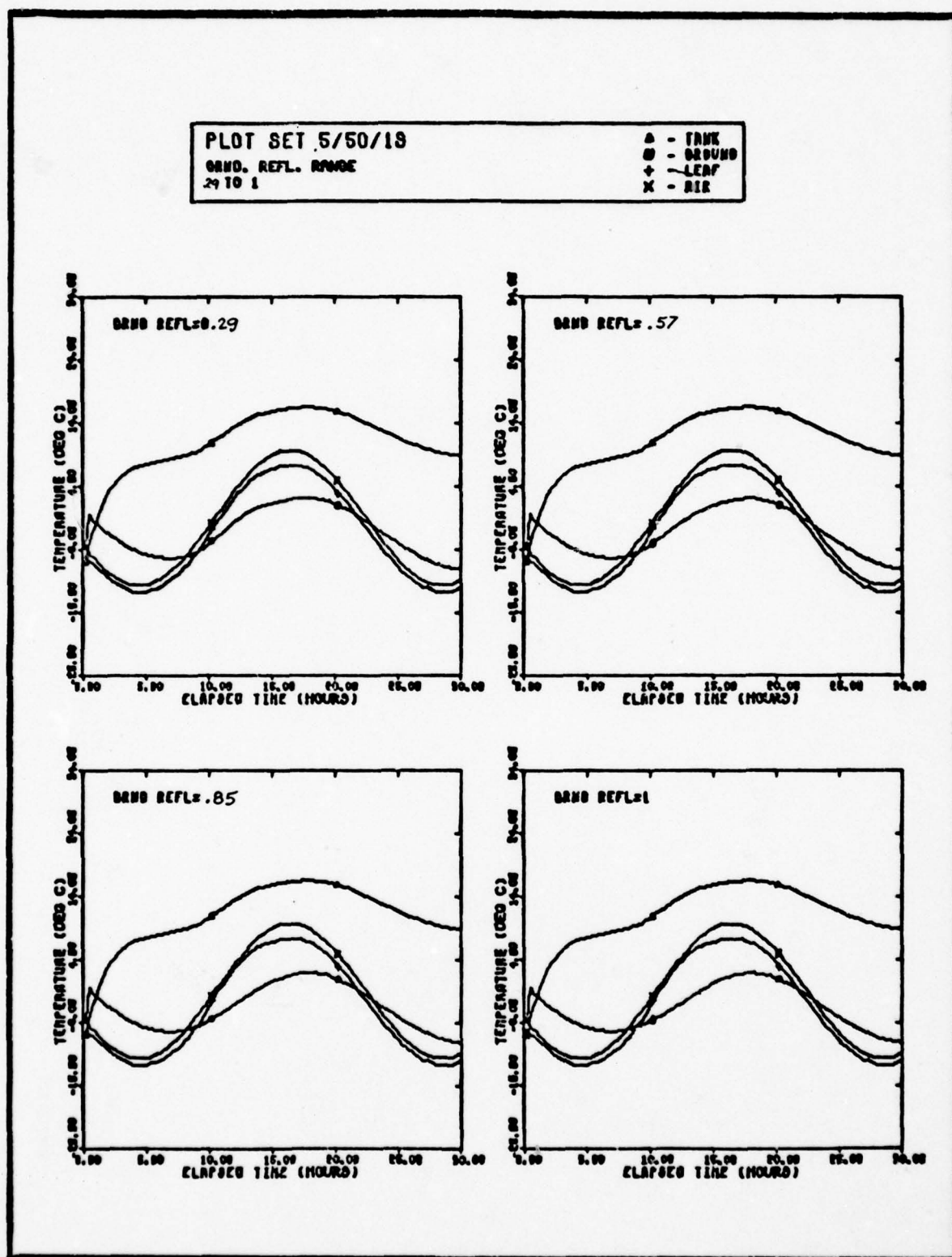


Fig. 29(h). Basic Temperature Plots of Ground Reflectivity

PLOT SET 5/50/1

COND. REFL. RANGE  
.08 TO 0.32

Δ - TANK  
● - GROUND  
+ - LEAF  
x - AIR

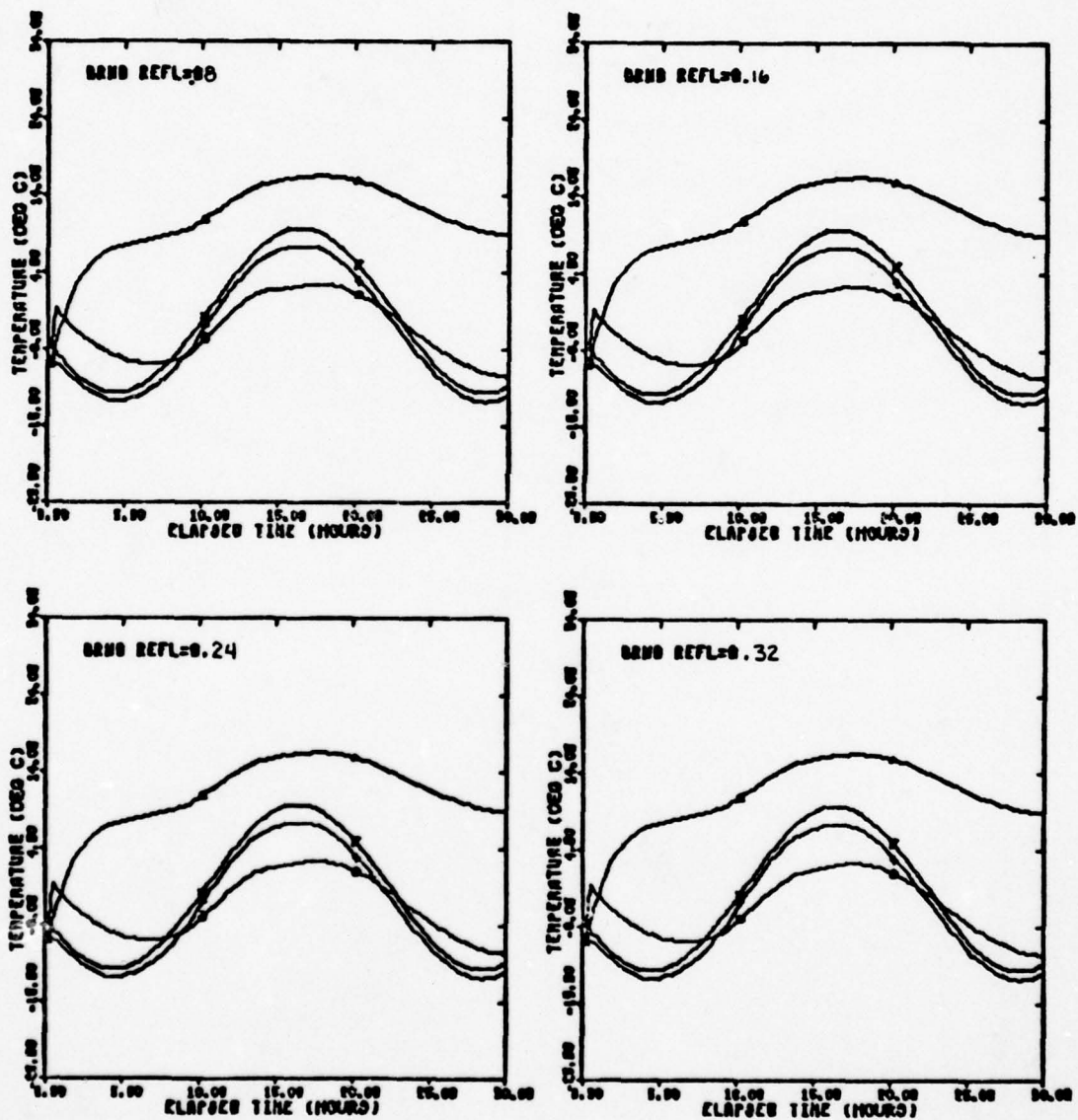


Fig. 29(1). Basic Temperature Plots of Ground Reflectivity



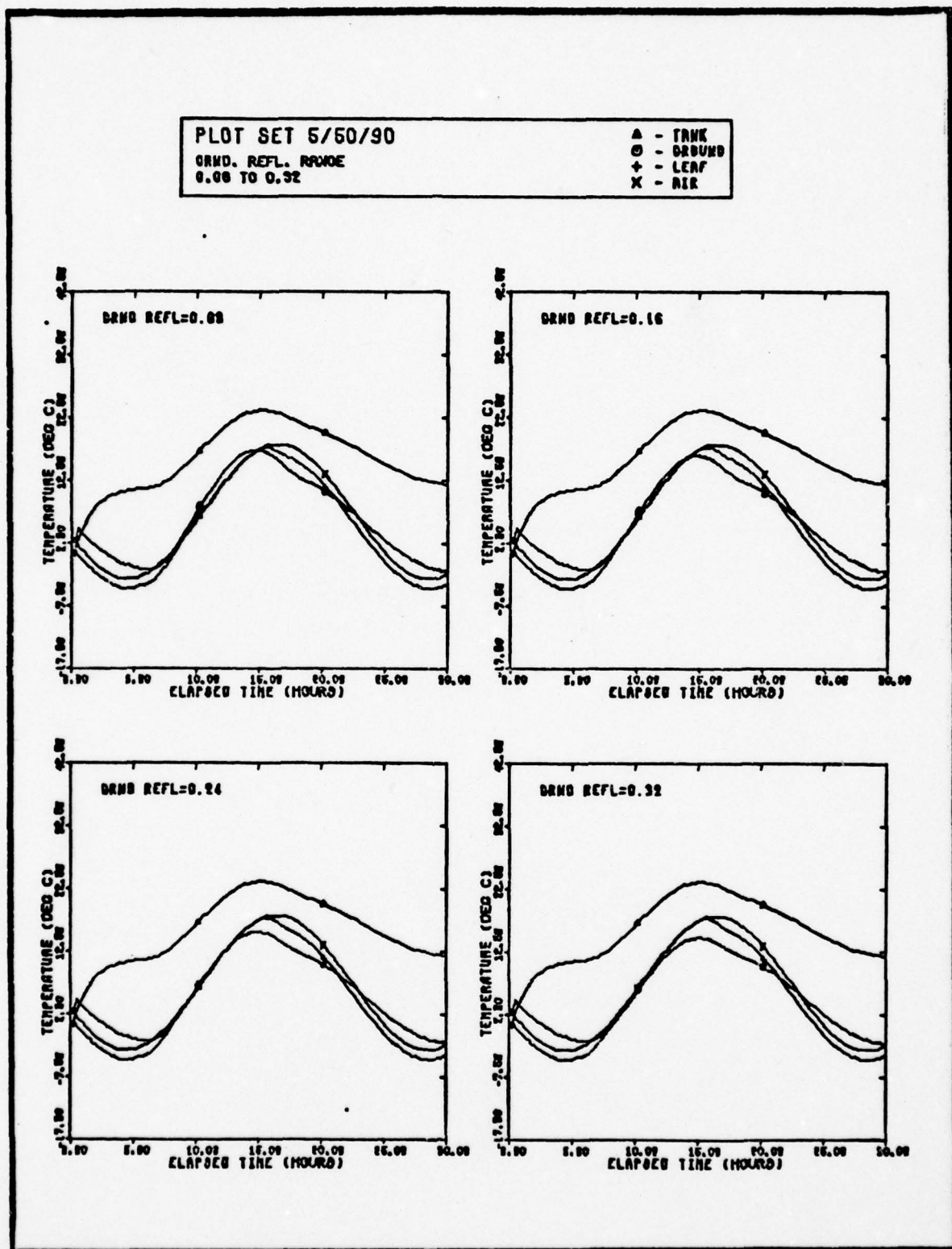


Fig. 29(j). Basic Temperature Plots of Ground Reflectivity

PLOT SET 5/60/180

GRND. REFL. RANGE  
0.00 TO 0.32

Δ - TANK  
○ - GROUND  
+ - LEAF  
X - AIR

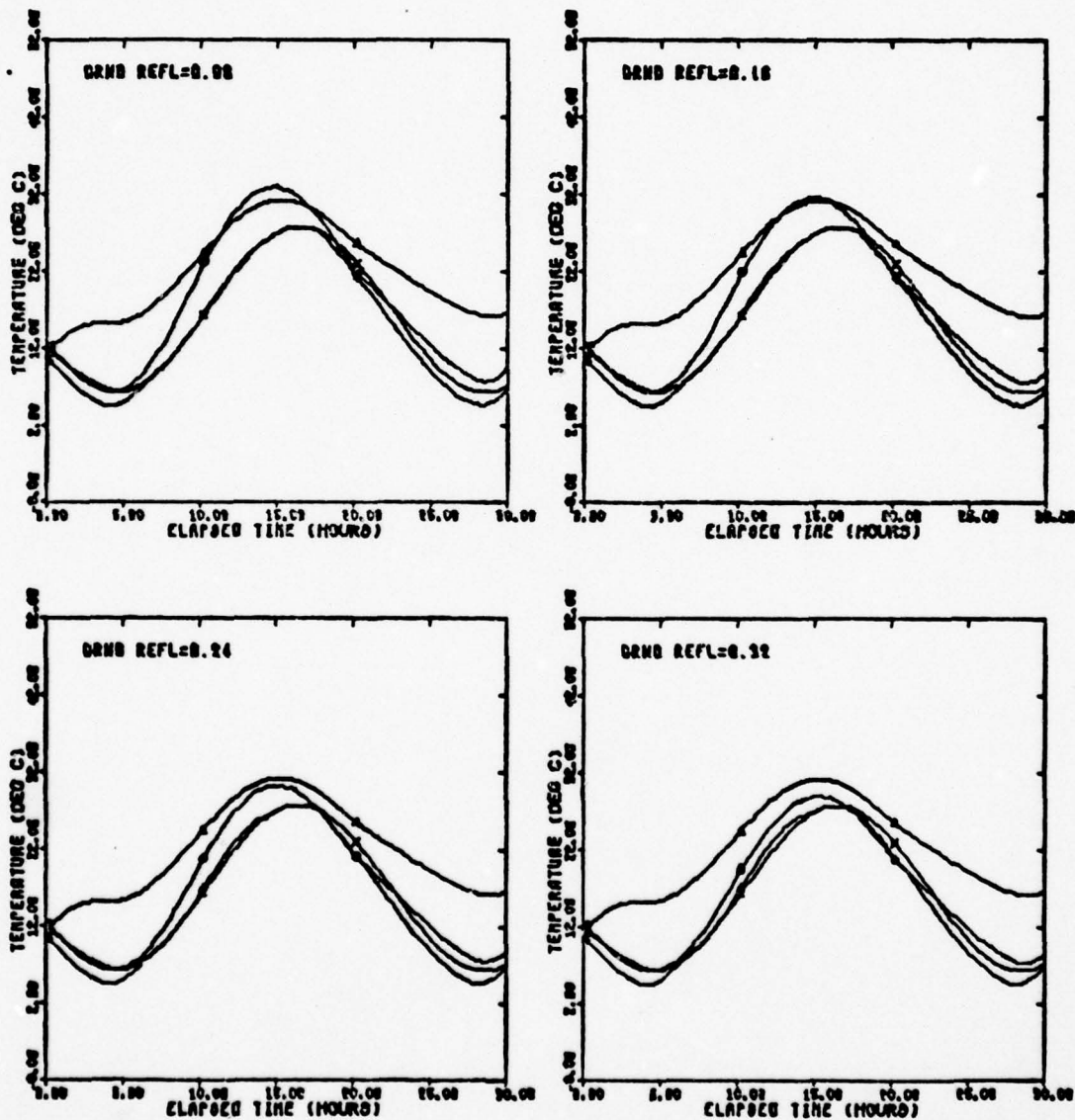


Fig. 29(k). Basic Temperature Plots of Ground Reflectivity

PLOT SET 6/20/1

GRND EMISS. RANGE  
0.47 TO 1.00

▲ - TANK  
○ - GROUND  
+ - LEAF  
X - AIR

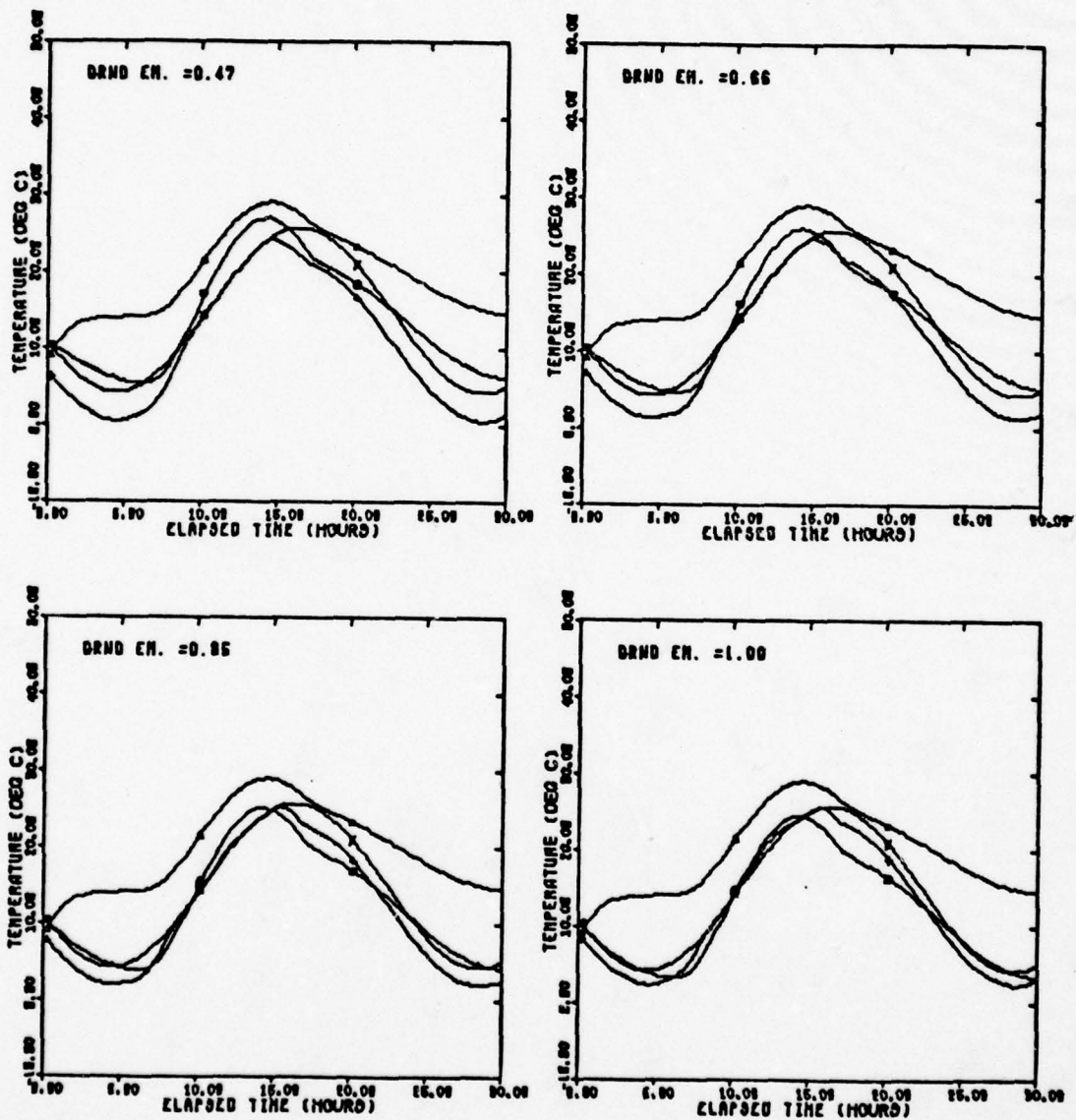


Fig. 30(a). Basic Temperature Plots of Ground Emmissivity



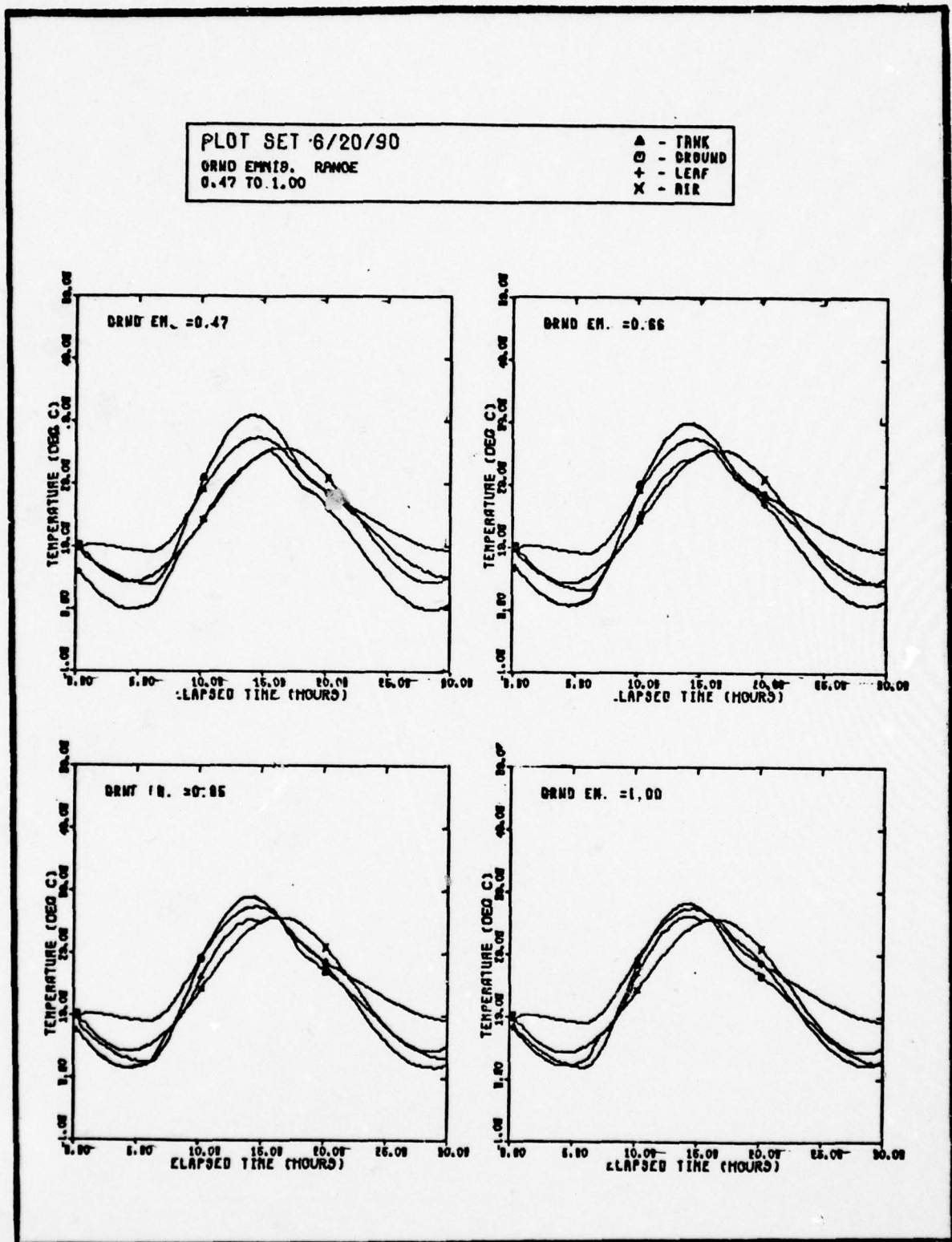


Fig. 30(b). Basic Temperature Plots of Ground Emmissivity



PLOT SET 6/20/180

GRND EMISS. RANGE  
0.47 TO 1.00

Δ - TANK  
○ - GROUND  
+ - LEAF  
X - AIR

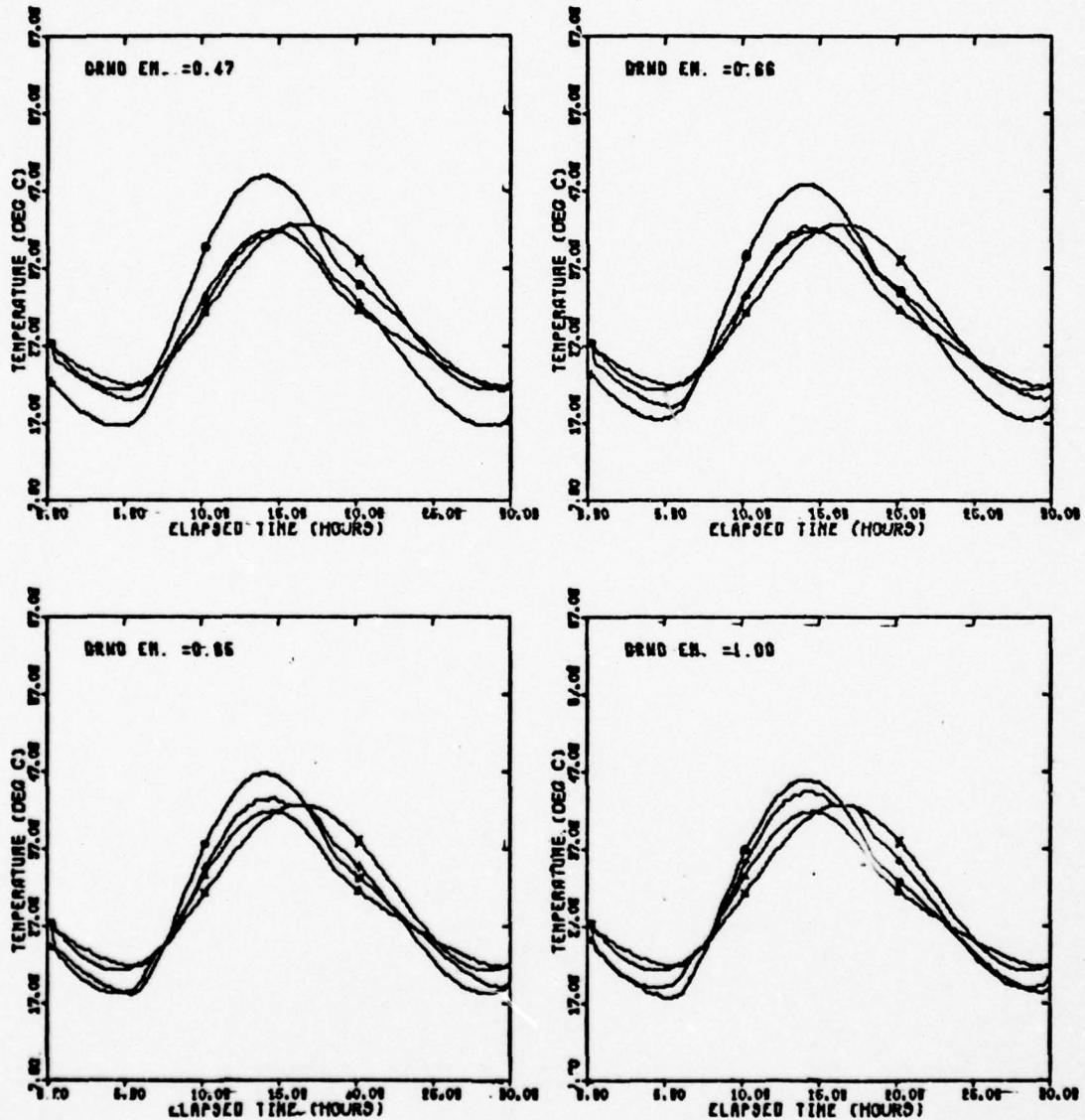


Fig. 30(c). Basic Temperature Plots of Ground Emmissivity

PLOT SET 6/32/18

GRND EMISS. RANGE  
0.47 TO 1.00

Δ - TRNK  
○ - GRND  
+ - LEAF  
X - AIR

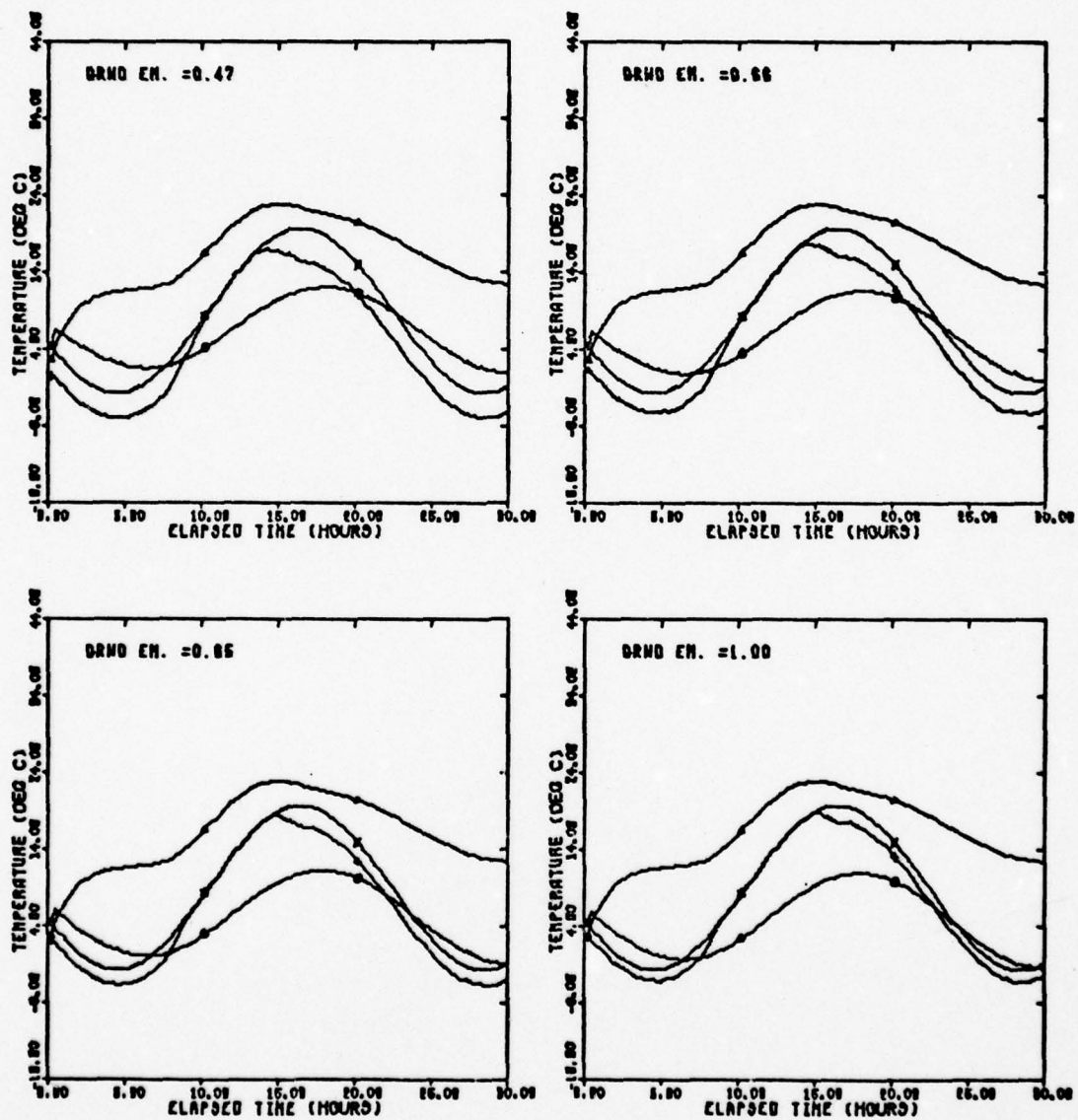


Fig. 30 (d). Basic Temperature Plots of Ground Emmissivity

PLOT SET 6/92/1

GRND EMISS. RANGE  
0.47 TO 1.00

Δ - TANK  
○ - GROUND  
+ - LEAF  
X - AIR

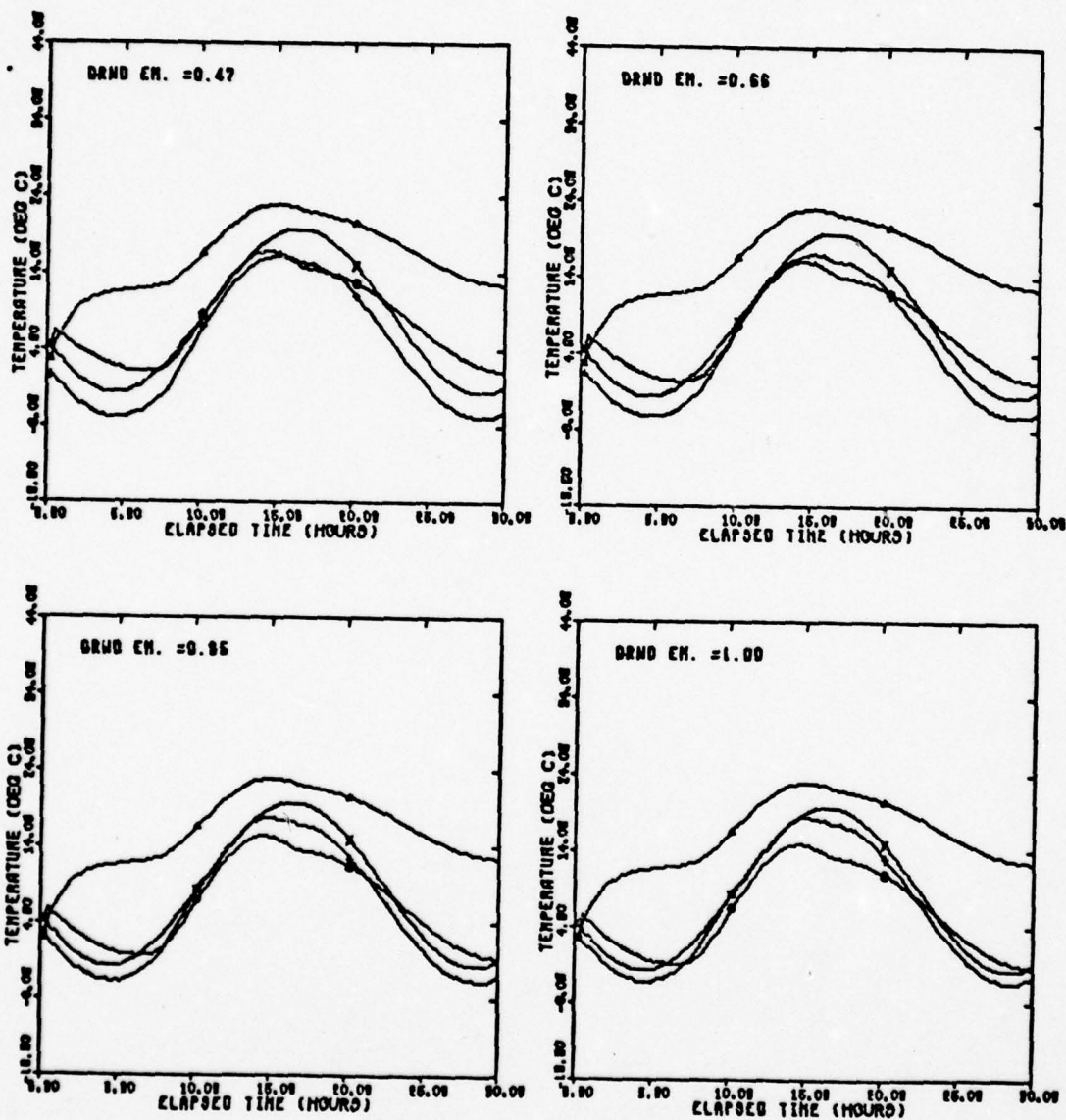


Fig. 30(e). Basic Temperature Plots of Ground Emmissivity



PLOT SET 6/32790

GRND EMISS. RANGE  
0.47 TO 1.00

▲ - TRNK  
○ - GROUND  
+ - LEAF  
X - AIR

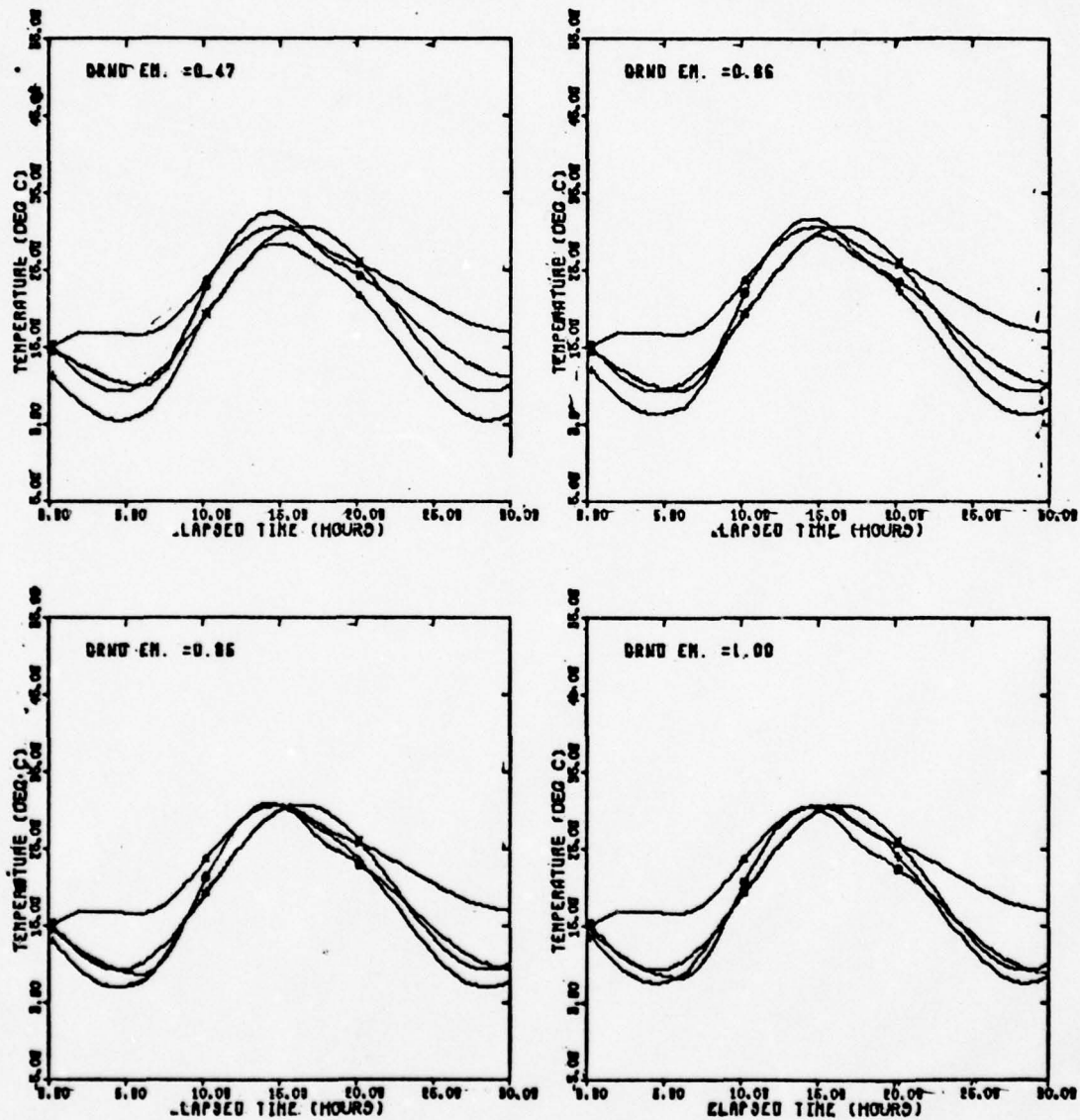


Fig. 30(f). Basic Temperature Plots of Ground Emmissivity



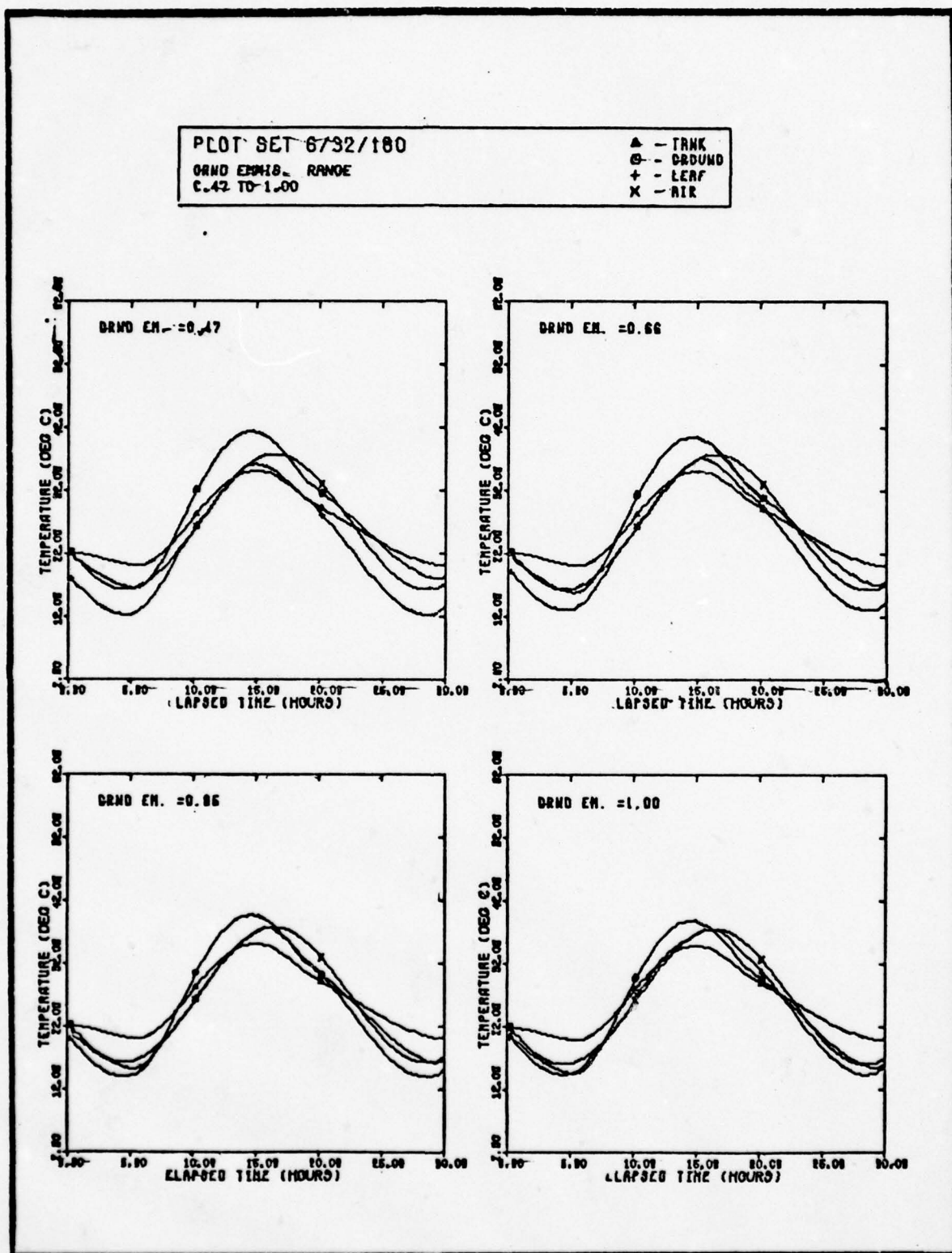


Fig. 30(g). Basic Temperature Plots of Ground Emmissivity

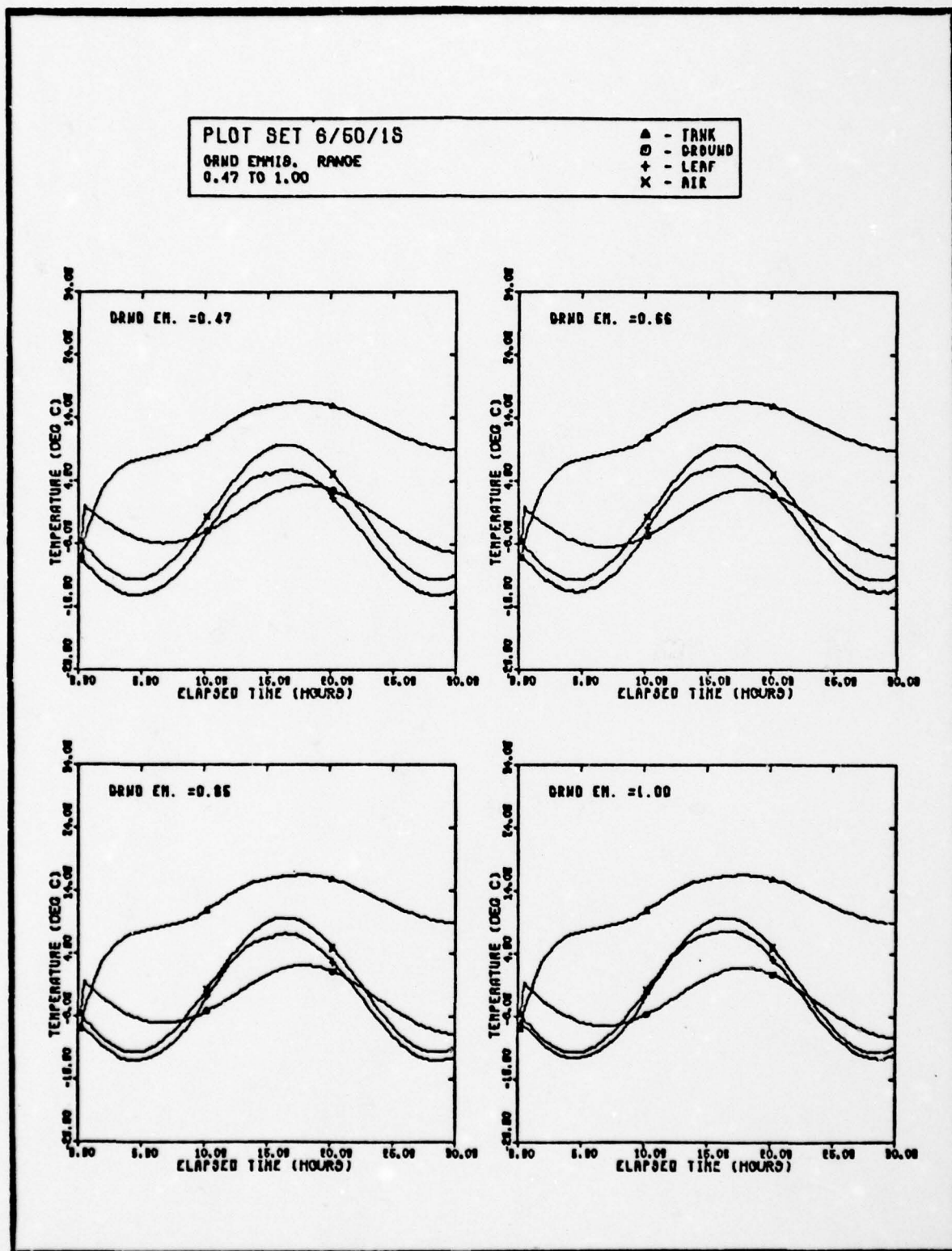


Fig. 30(h). Basic Temperature Plots of Ground Emmissivity

PLOT SET 6/50/1

GRND EMISS. RANGE  
0.47 TO 1.00

▲ - TANK  
○ - GROUND  
+ - LEAF  
X - AIR

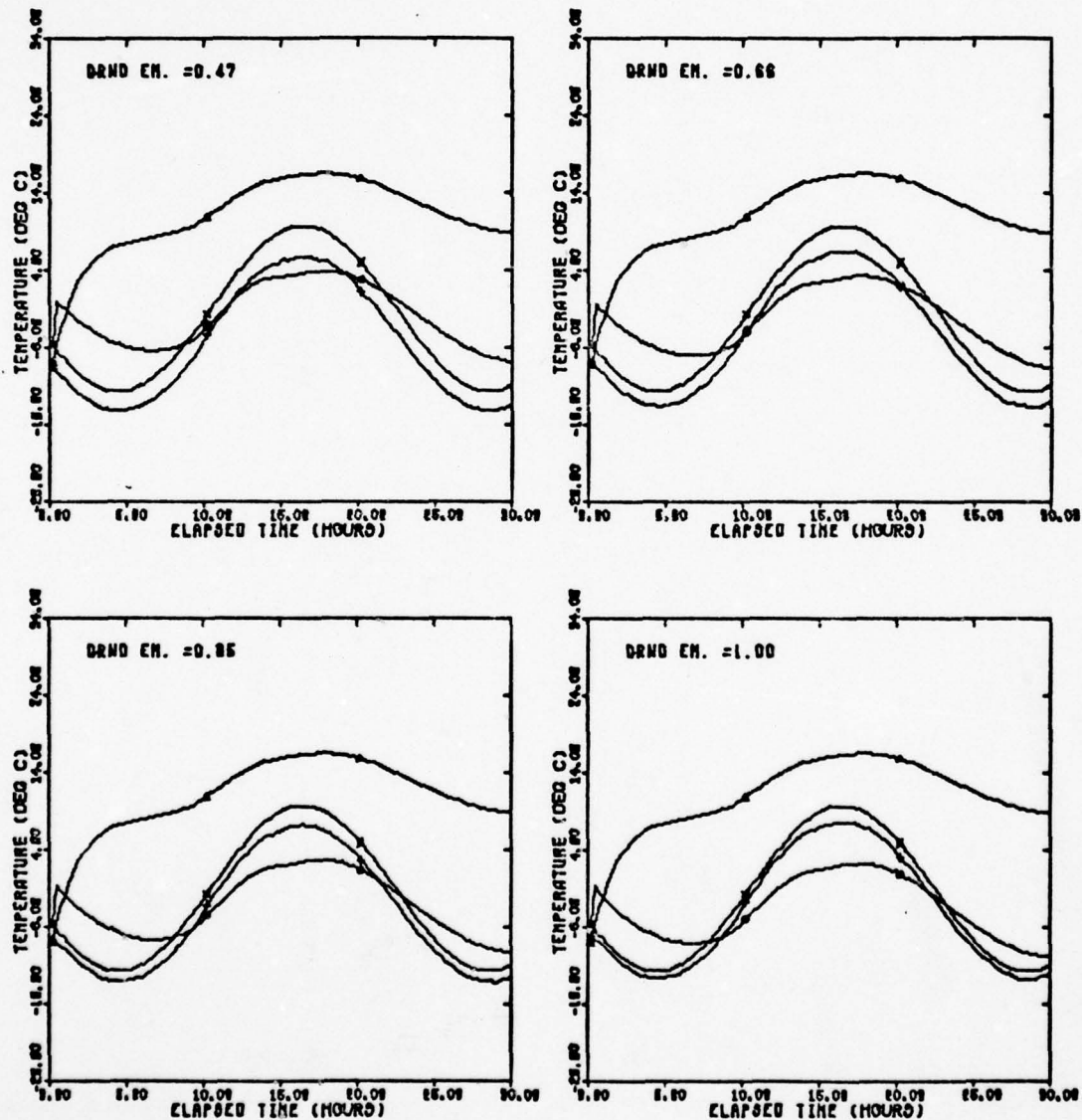


Fig. 30(1). Basic Temperature Plots of Ground Emmissivity

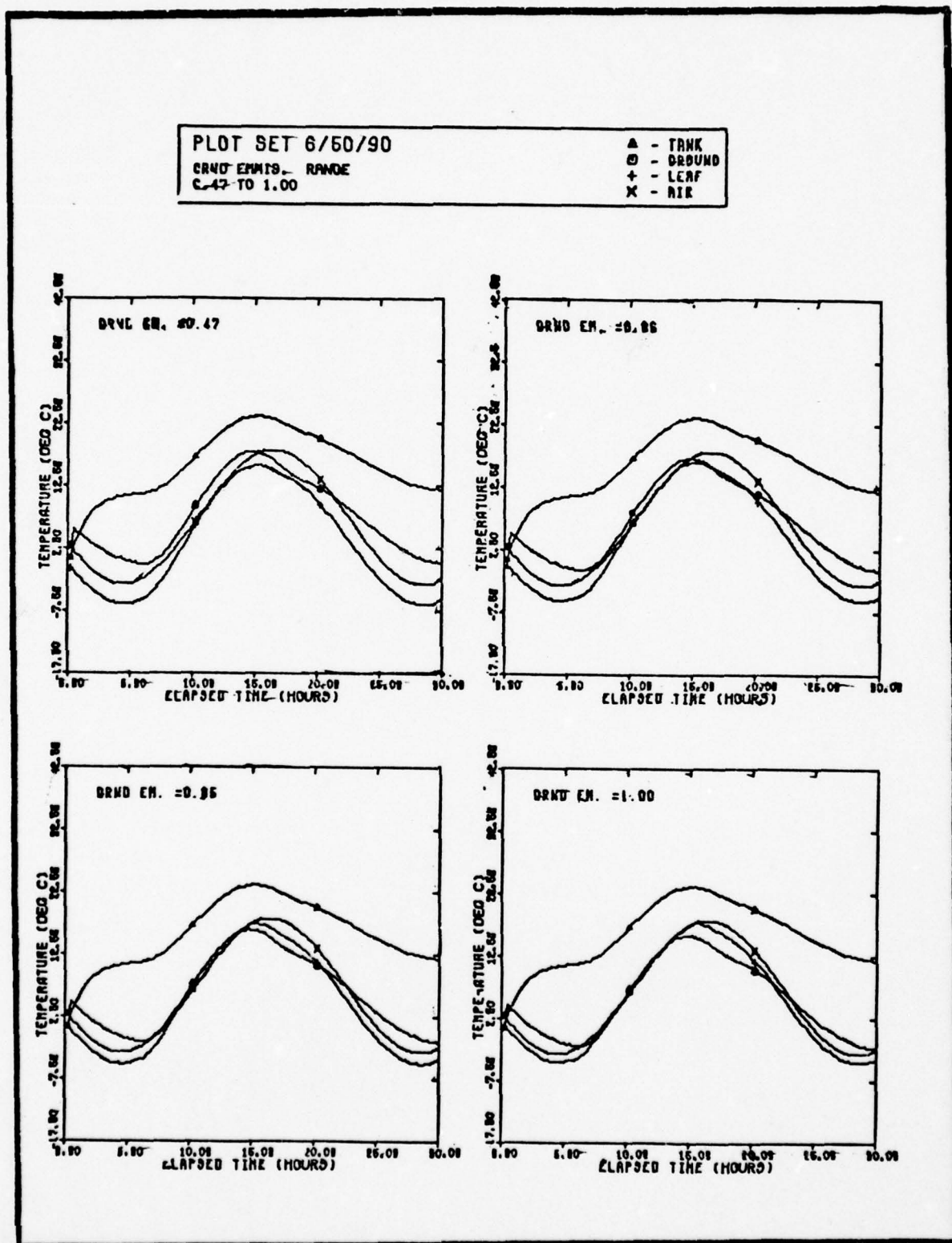


Fig. 30(j). Basic Temperature Plots of Ground Emmissivity



PLOT SET 6/50/180

GRND EMISS RANGE  
0.47 TO 1.00

▲ TANK  
● GROUND  
+ LEAF  
x AIR

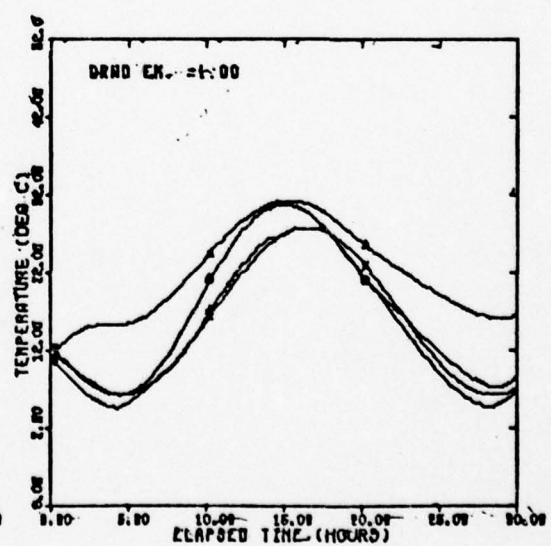
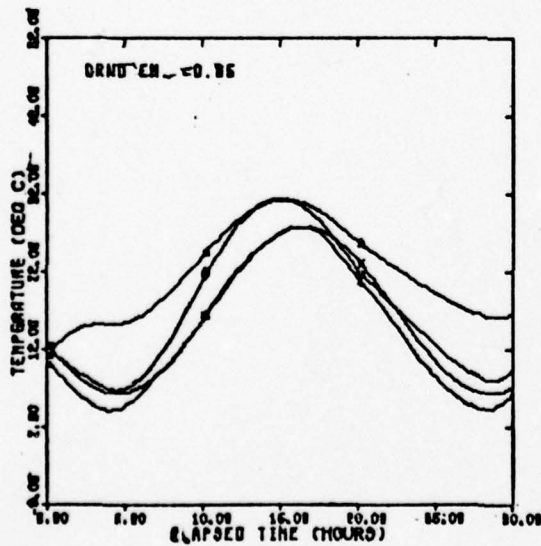
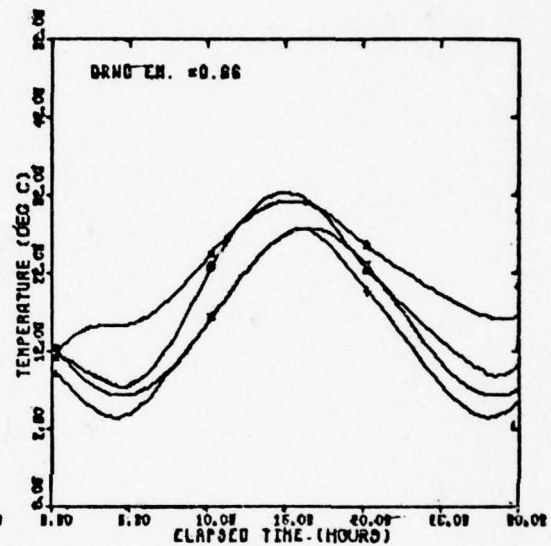
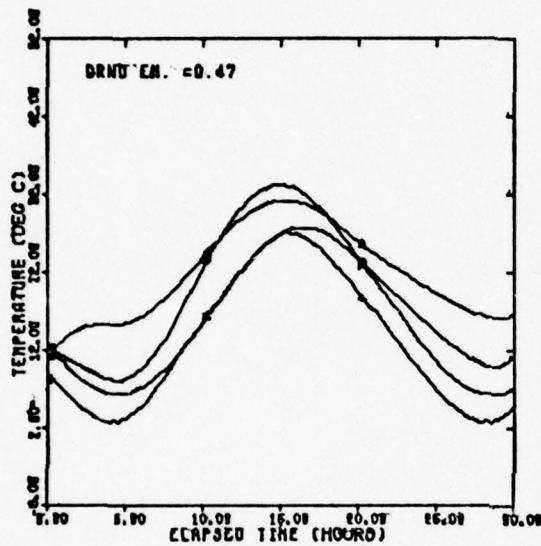


Fig. 30(k). Basic Temperature Plots of Ground Emmissivity

PLOT SET 7/20/1

GRND DIFF. RANGE  
0.09 TO 0.5499 CM/SEC

▲ - TANK  
● - GROUND  
+ - LEAF  
X - AIR

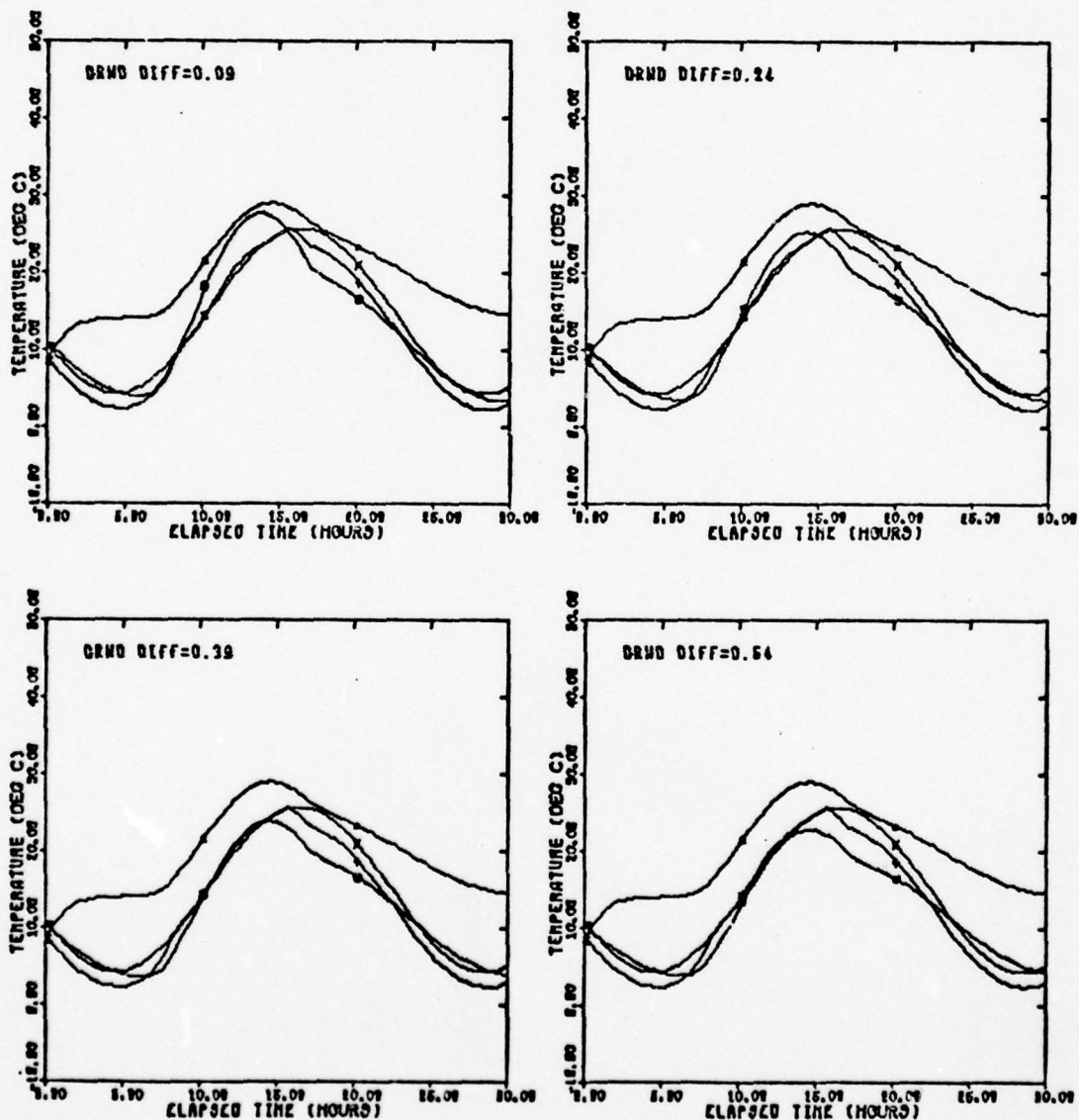


Fig. 31(a). Basic Temperature Plots of Ground Diffusivity

PLOT SET 7/20/90

GRND DIFF. RANGE  
0.09 TO 0.6439 CM/SEC

▲ - TANK  
○ - GROUND  
+ - LEAF  
X - AIR

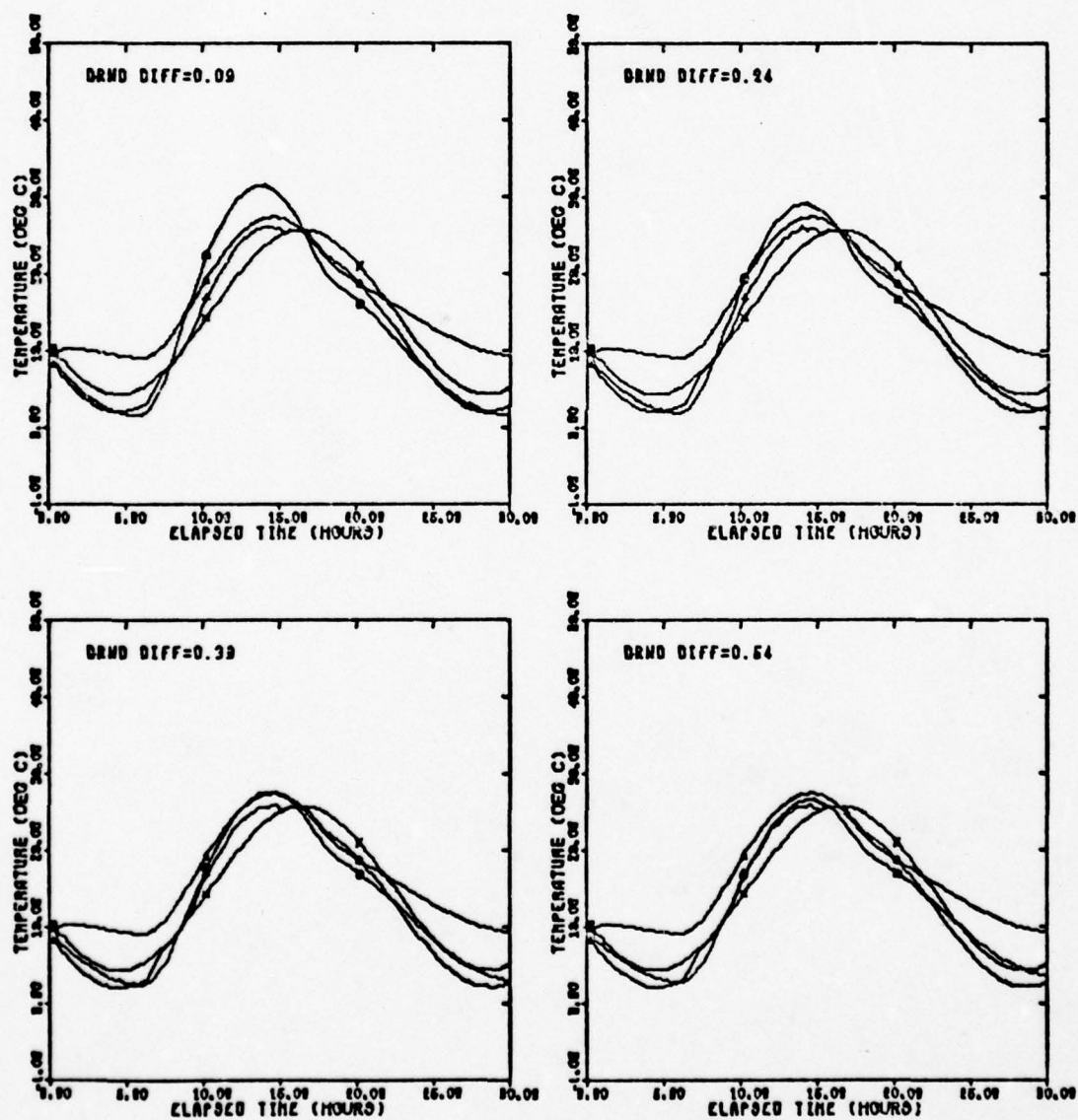


Fig. 31(b). Basic Temperature Plots of Ground Diffusivity

PLOT SET 7/20/180

GRND DIFF RANGE  
0.09 TO 0.6439 CM/MIN

▲ - TANK  
● - GROUND  
+ - LEAF  
X - AIR

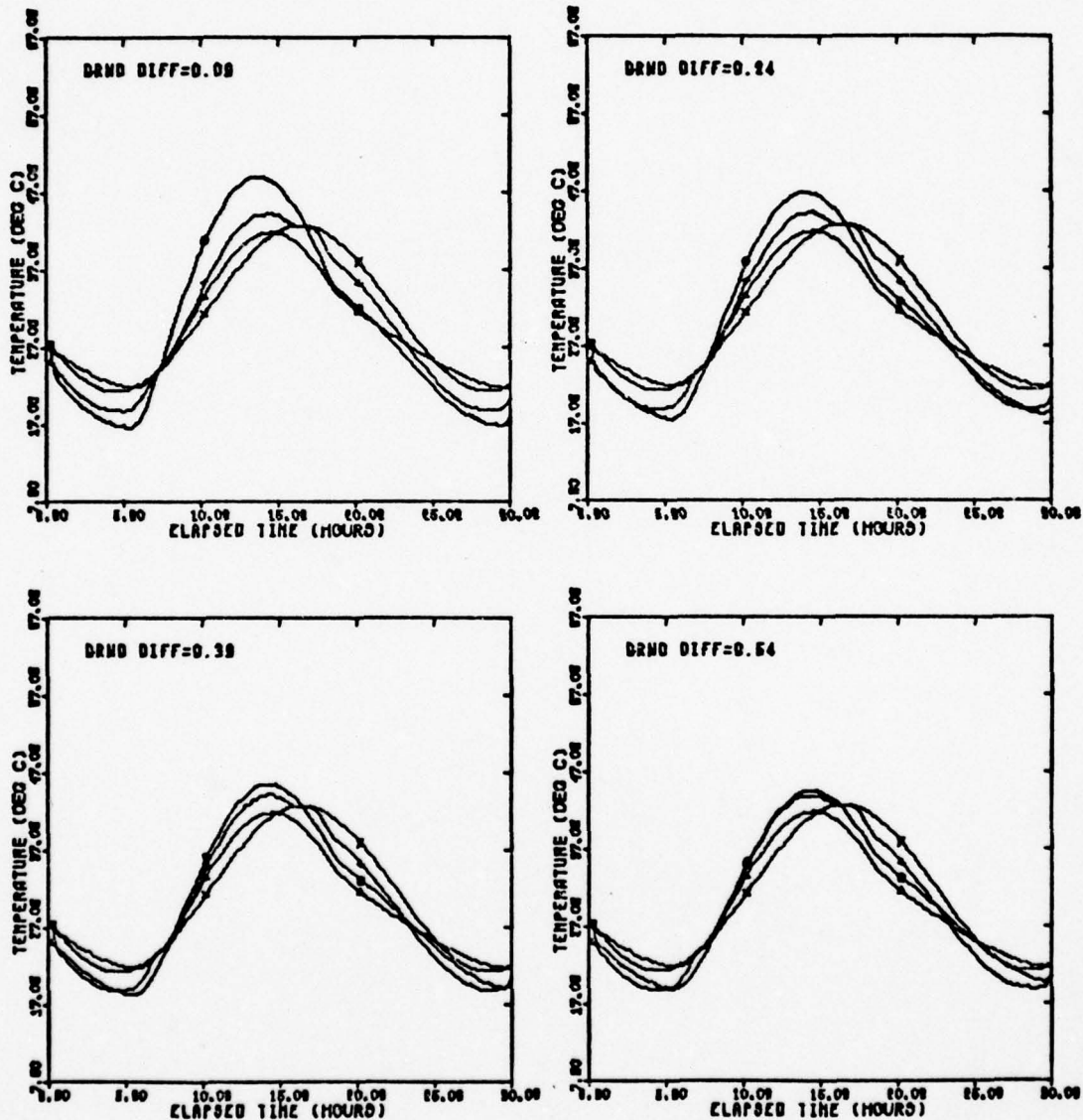


Fig. 31(c). Basic Temperature Plots of Ground Diffusivity



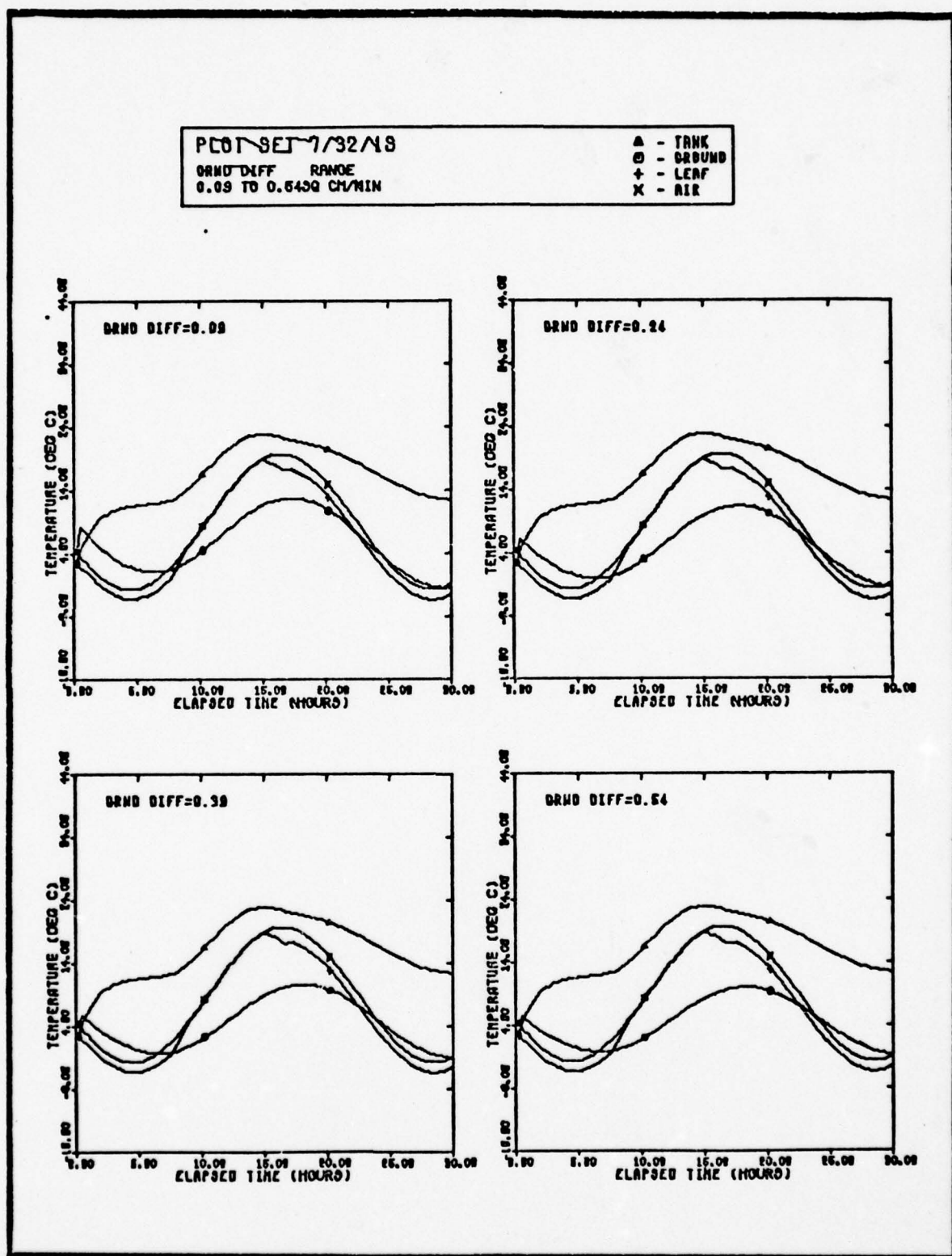


Fig. 31(d). Basic Temperature Plots of Ground Diffusivity

PLOT SET 7/32/1

GRND DIFF RANGE  
0.09 TO 0.5439 CM/MIN

▲ - TRNK  
● - GRBUND  
+ - LEAF  
X - AIR

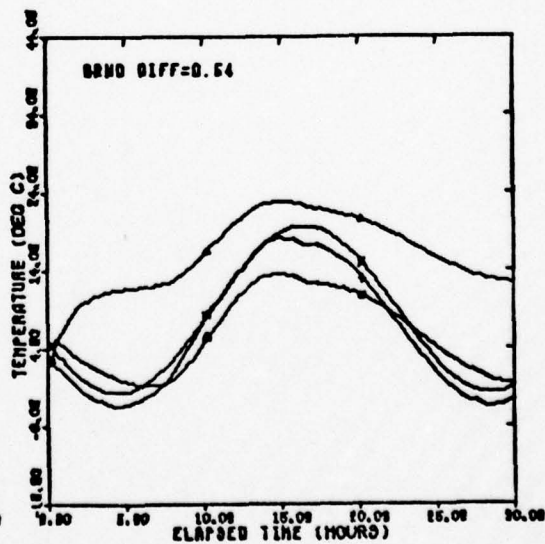
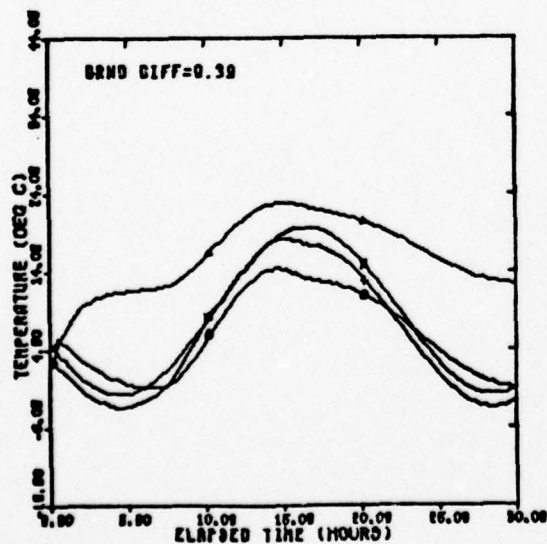
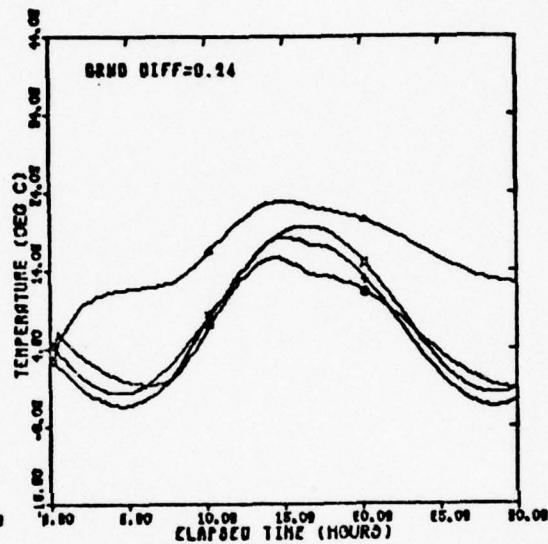
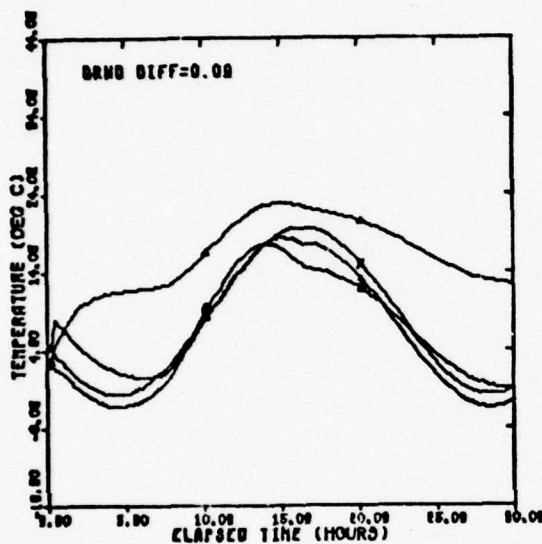


Fig. 31(e). Basic Temperature Plots of Ground Diffusivity

PLOT SET 7/32/90

GRND DIFF. RANGE  
0.09 TO 0.6499 CM/SEC

▲ - TRNK  
○ - GRUND  
+ - LEAF  
X - AIR

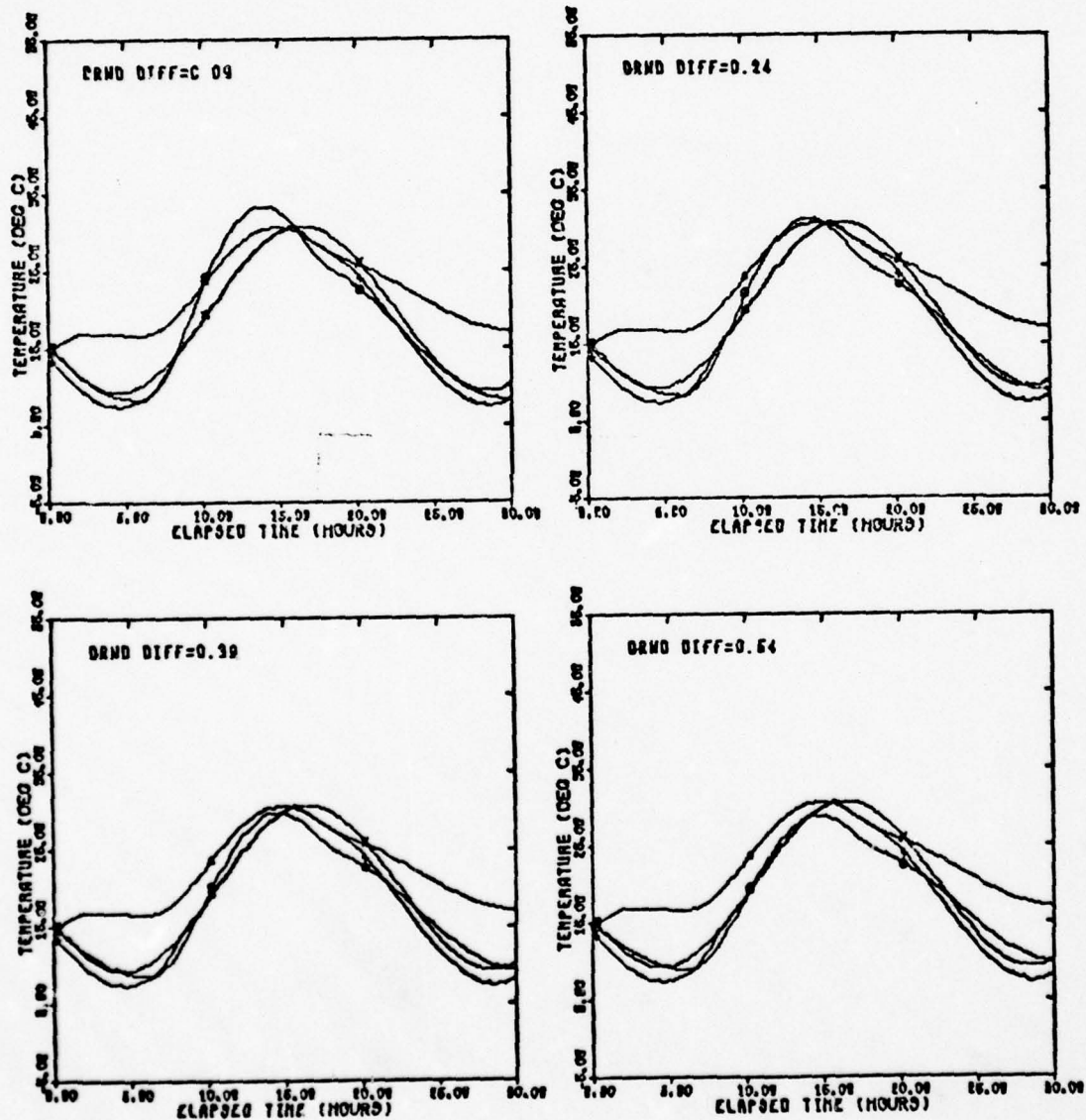


Fig. 31(f). Basic Temperature Plots of Ground Diffusivity

PLOT SET 7/92/180

GRND DIFF RANGE  
0.09 TO 0.6409 CM/HM

▲ - TANK  
○ - GROUND  
+ - LEAF  
x - AIR

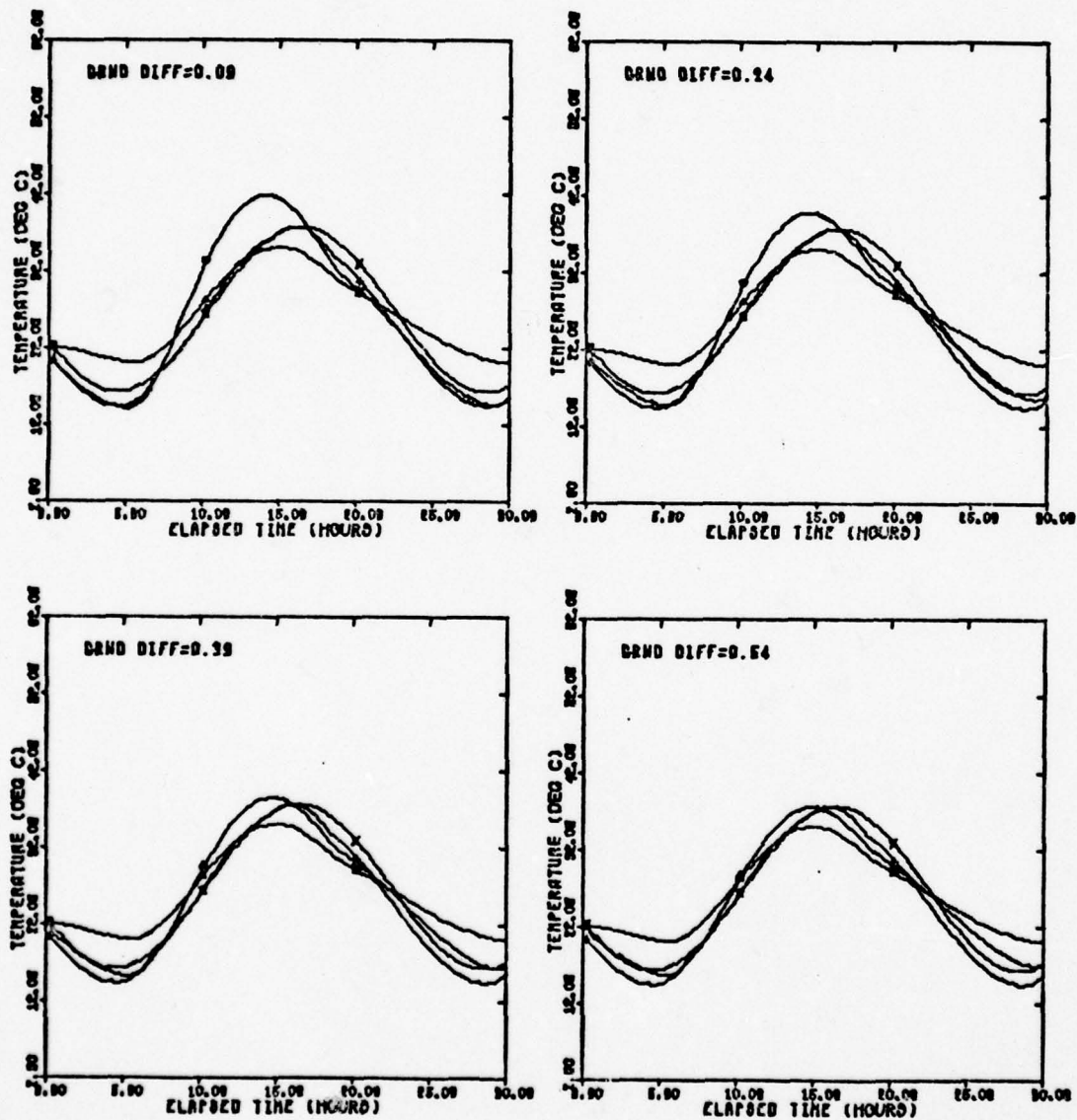


Fig. 31(g). Basic Temperature Plots of Ground Diffusivity



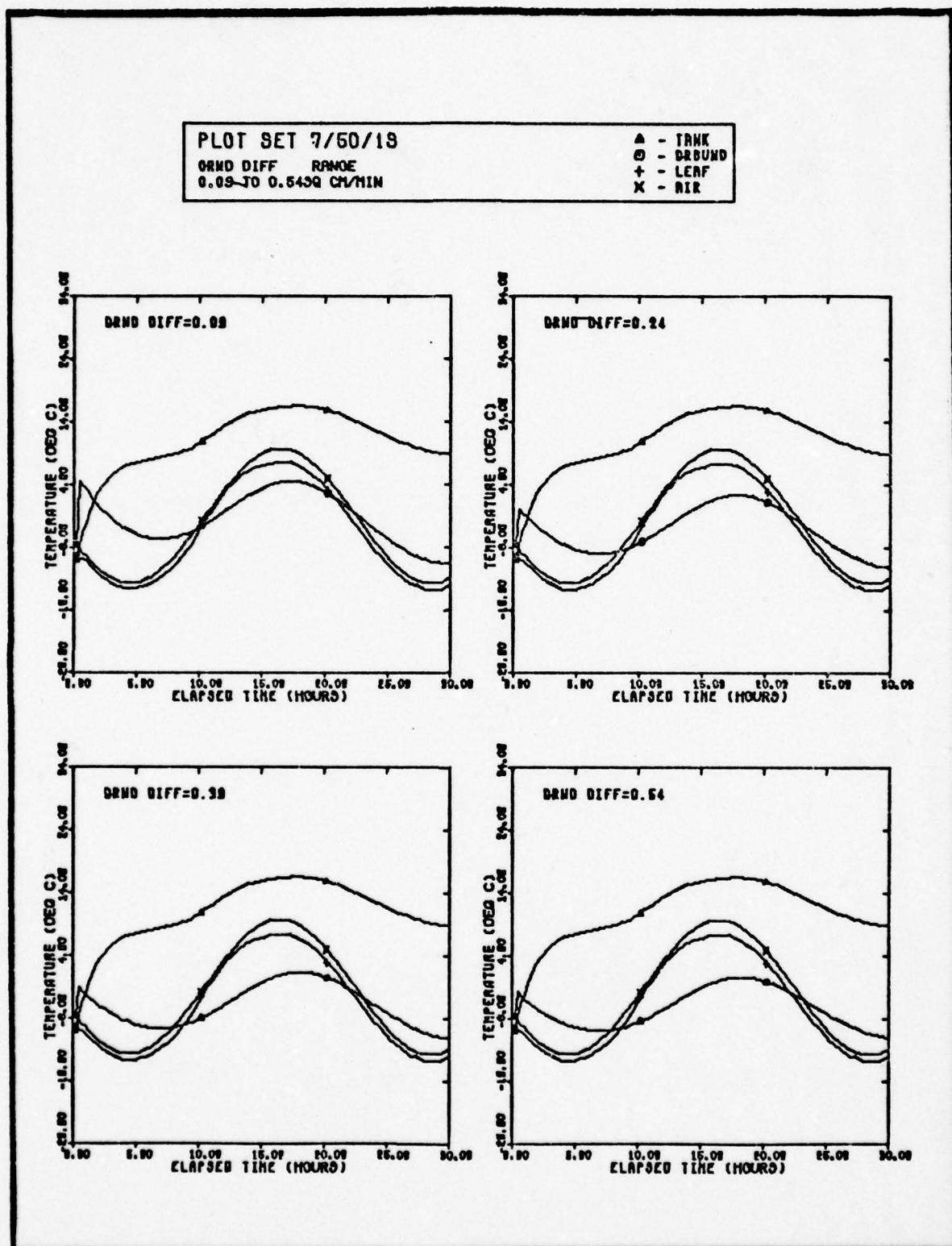


Fig. 31(h). Basic Temperature Plots of Ground Diffusivity

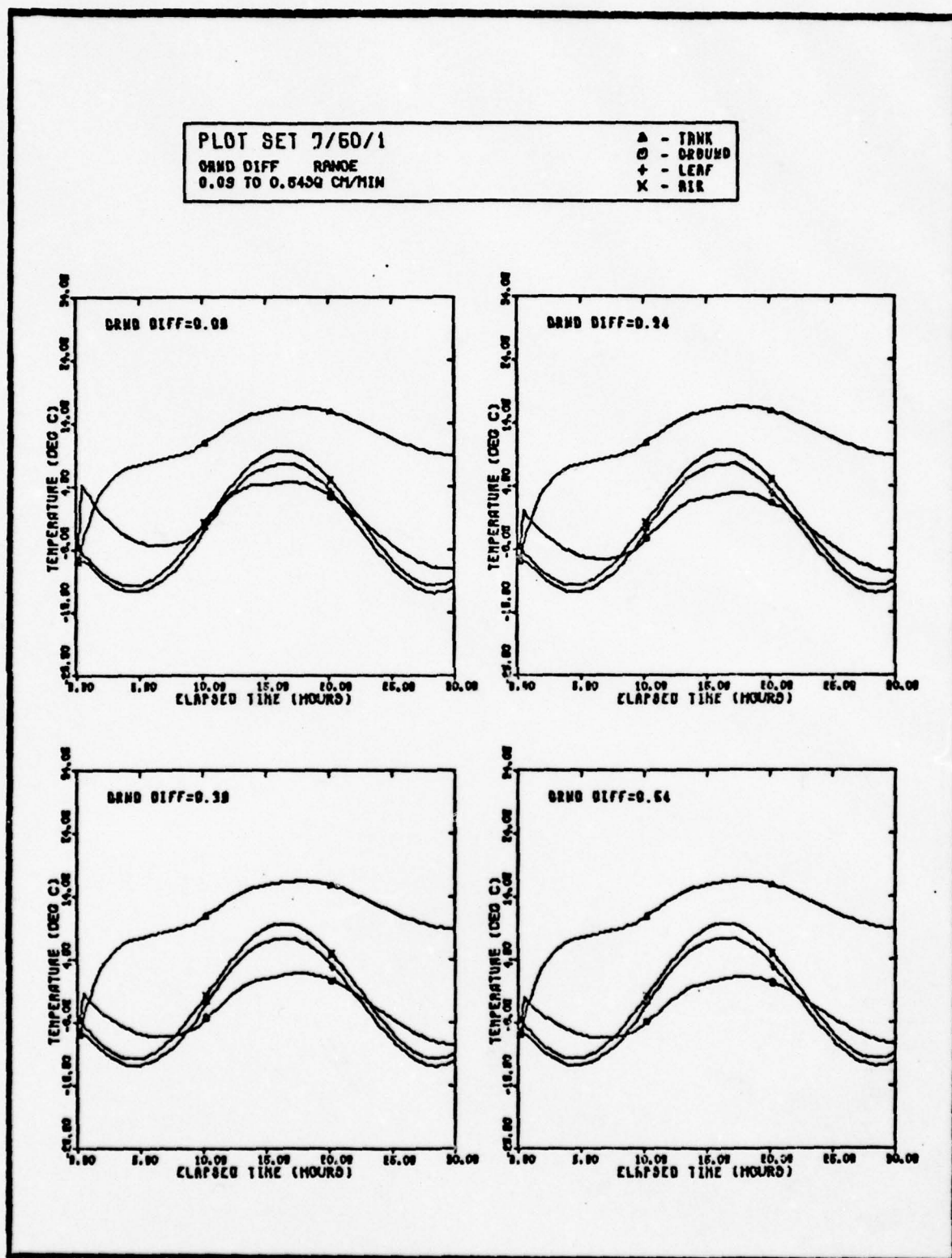


Fig. 31(1). Basic Temperature Plots of Ground Diffusivity

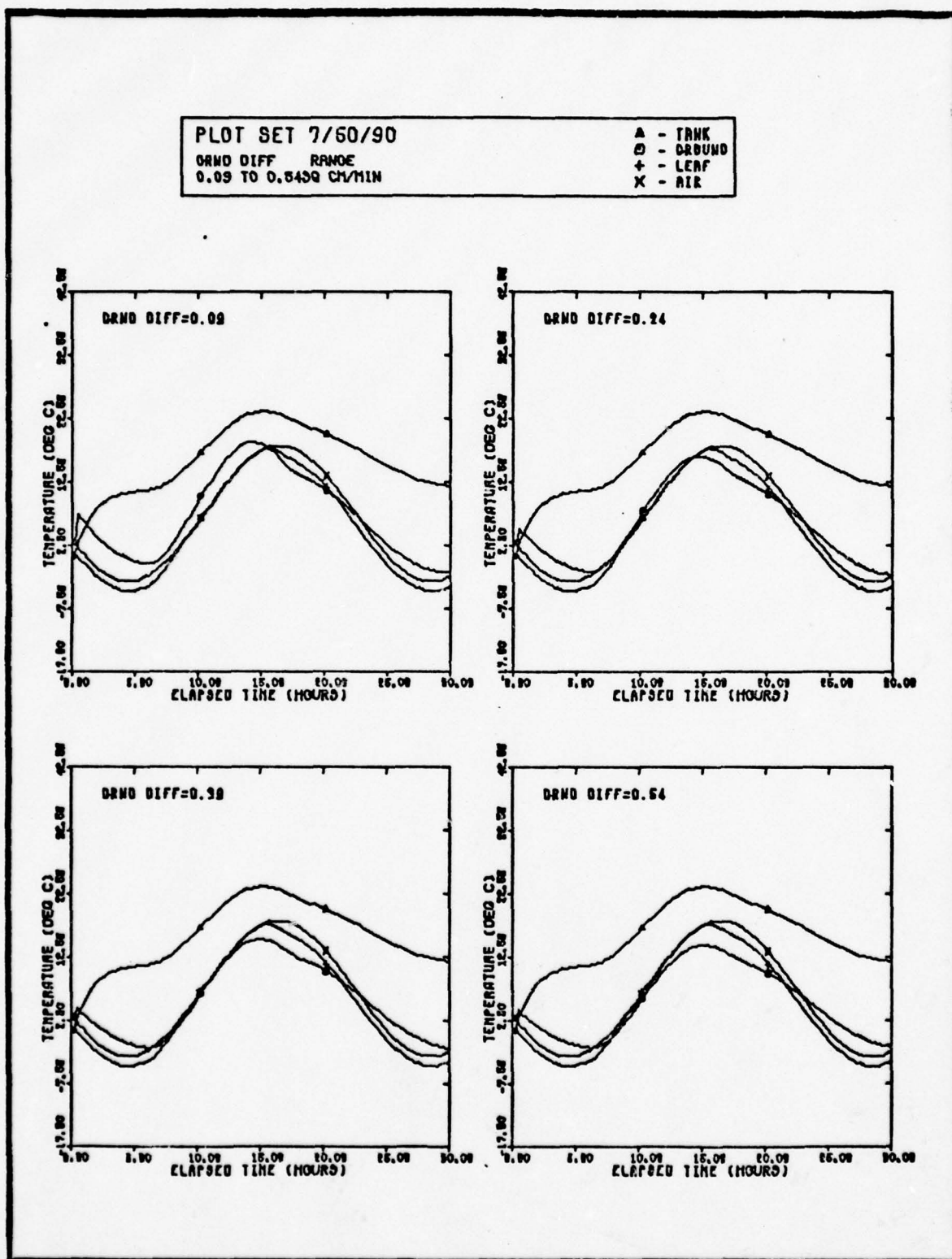


Fig. 31(j). Basic Temperature Plots of Ground Diffusivity

PLOT SET 7/60/180

GRND DIFF RANGE  
0.09 TO 0.5499 CM/MIN

▲ - TRNK  
○ - GROUND  
+ - LEAF  
X - AIR

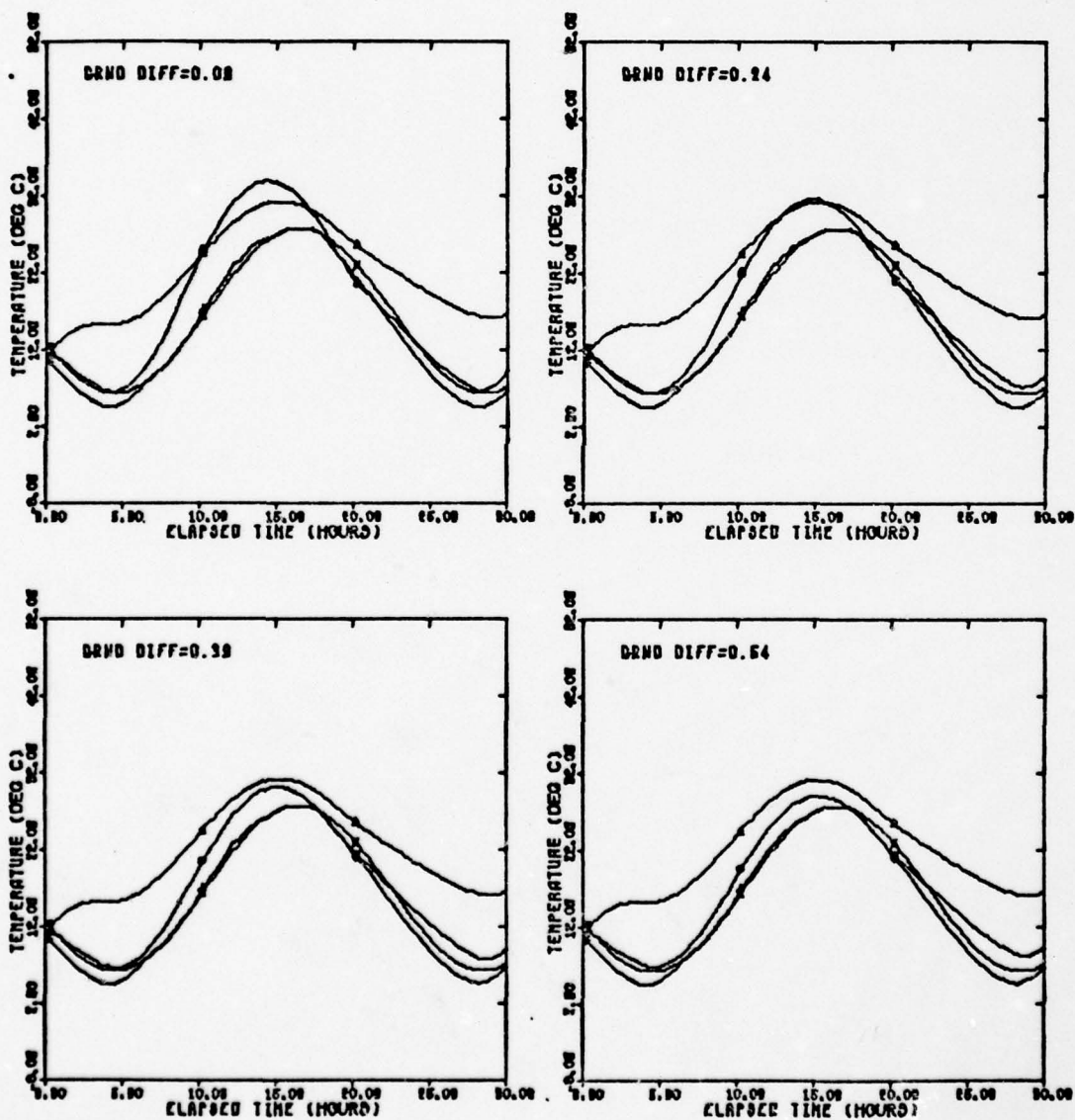


Fig. 31(k). Basic Temperature Plots of Ground Diffusivity



PLOT SET 8/20/1

TOT REFL RANGE  
0.09 TO 0.64

▲ - TANK  
⊙ - DRUM  
+ - LEAF  
X - AIR

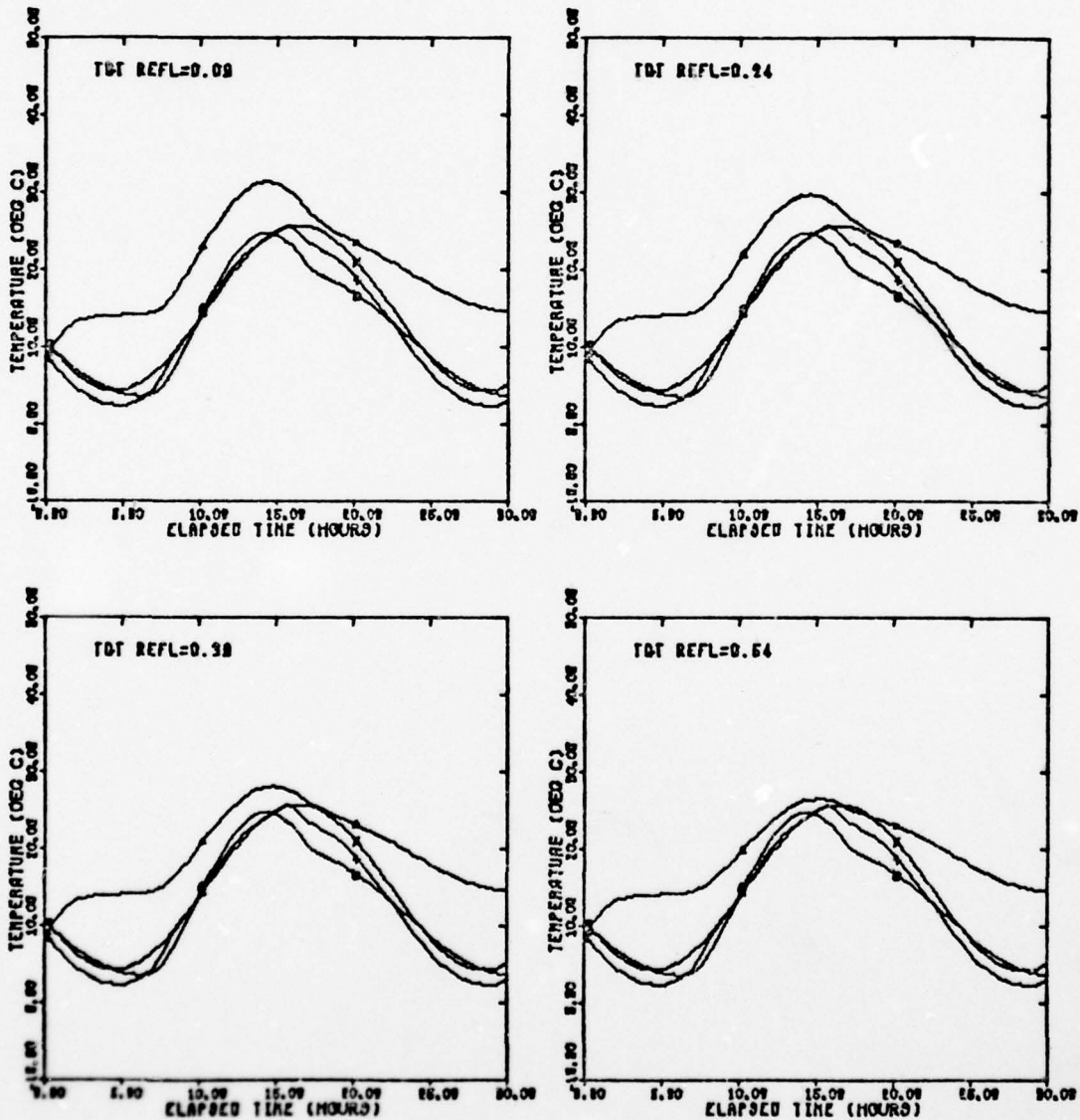


Fig. 32(a). Basic Temperature Plots of Target Reflectivity

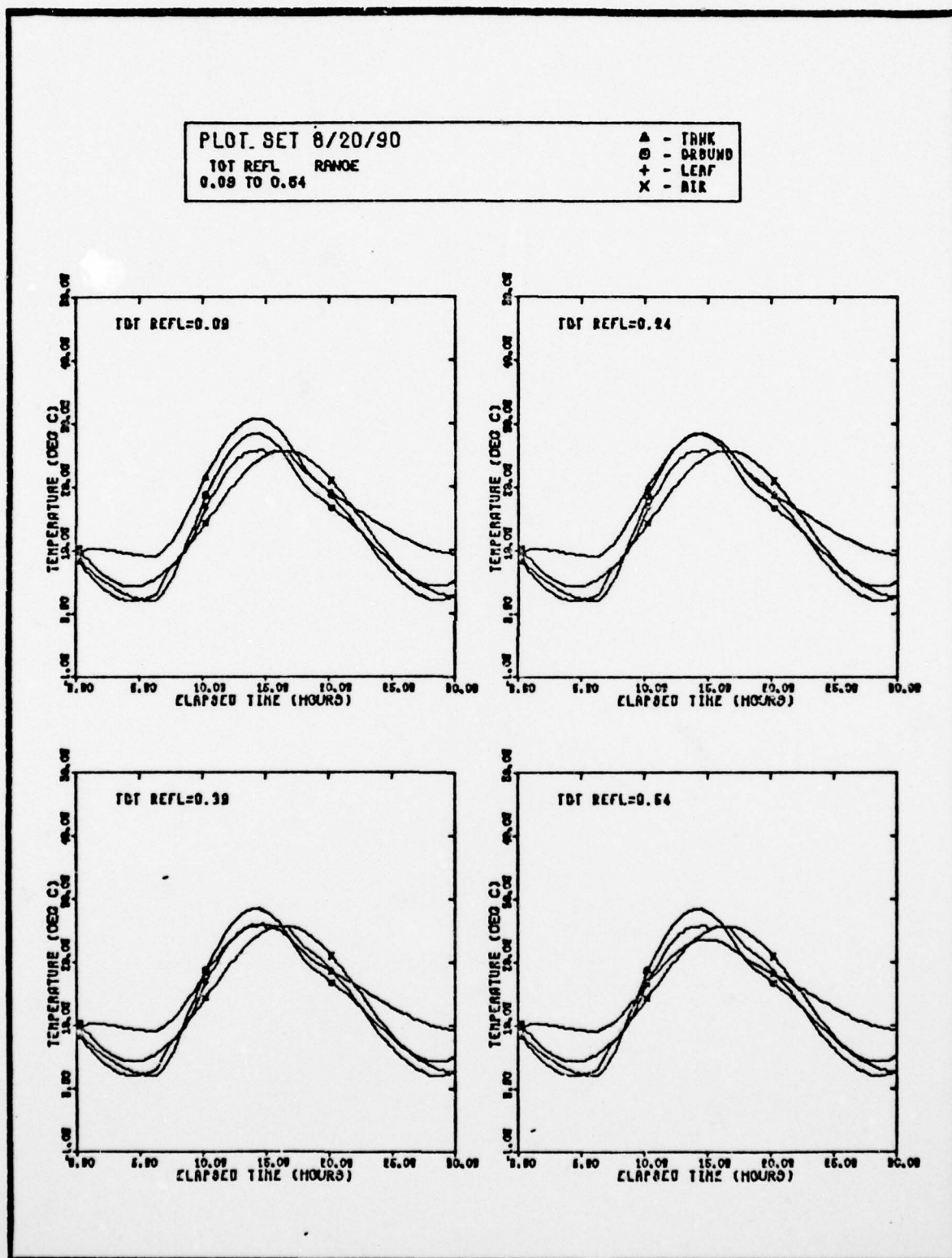


Fig. 32(b). Basic Temperature Plots of Target Reflectivity

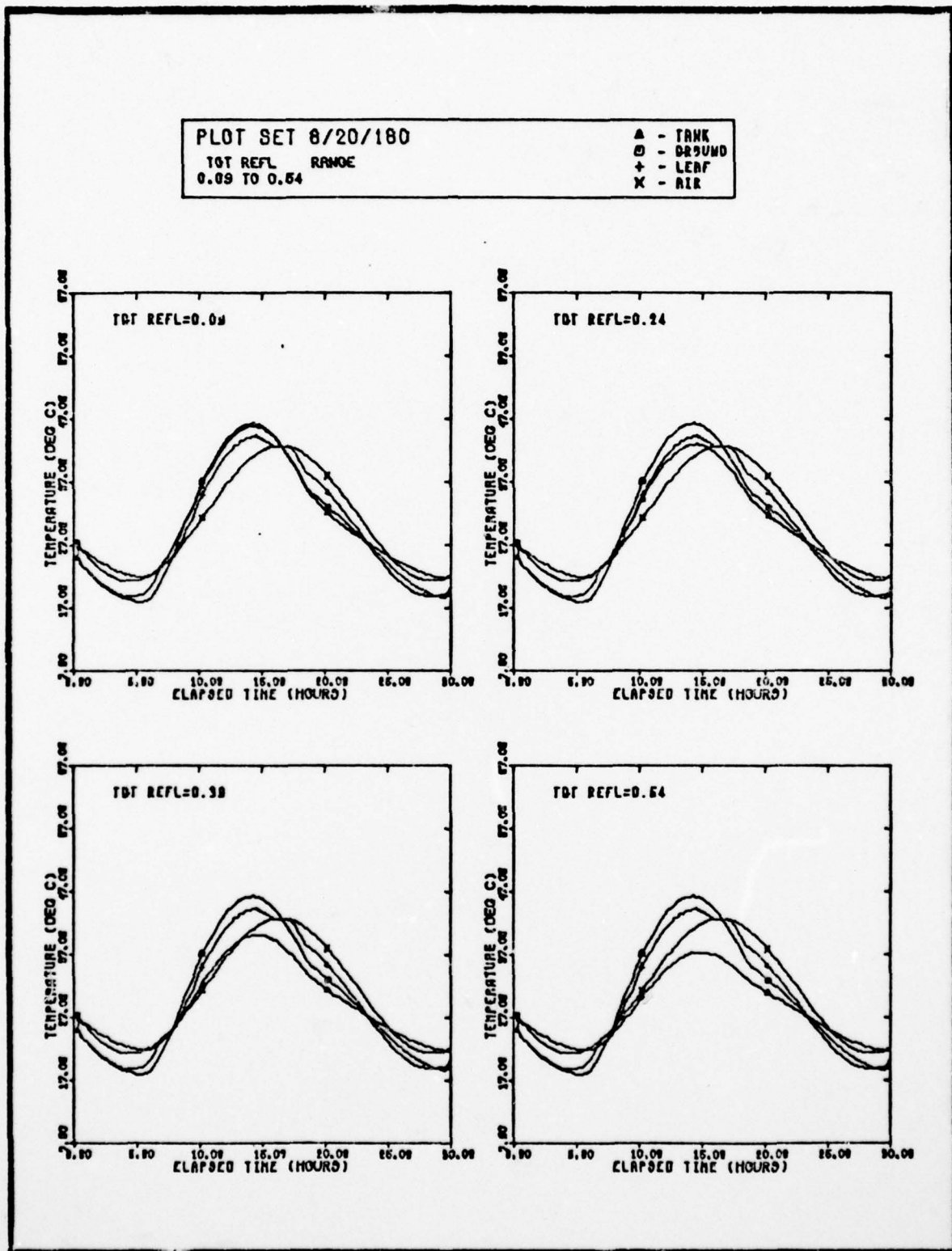


Fig. 32(c). Basic Temperature Plots of Target Reflectivity

PLOT SET 8/32/19

TGT REFL RANGE  
0.09-0.64

△ - TRNK  
○ - DRUMD  
+ - CERF  
X - AIR

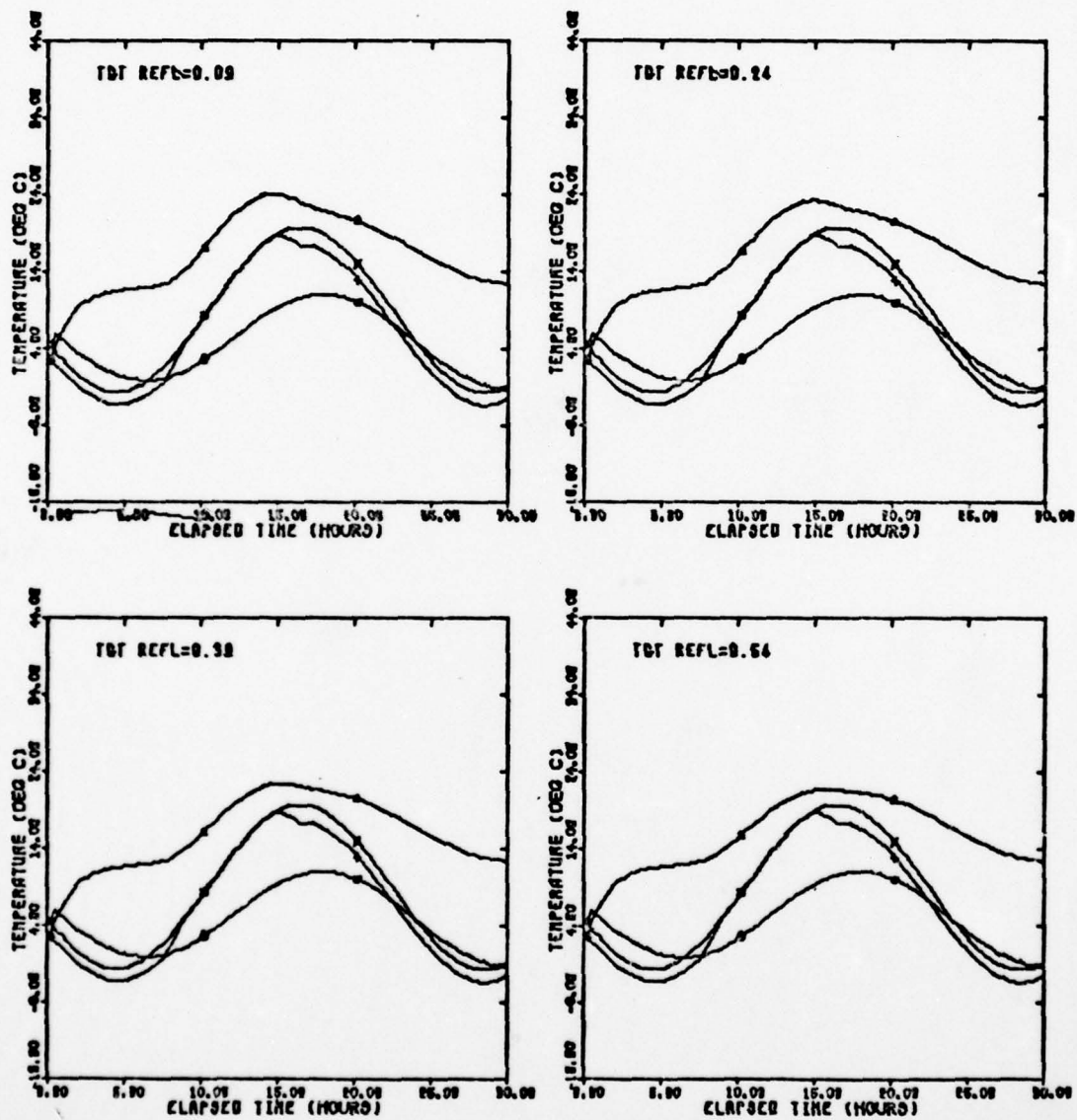


Fig. 32(d). Basic Temperature Plots of Target Reflectivity



PLOT SET 8/32/1

TGT REFL RANGE  
0.09 TO 0.64

▲ - TRNK  
⊙ - GROUND  
+ - LEAF  
x - AIR

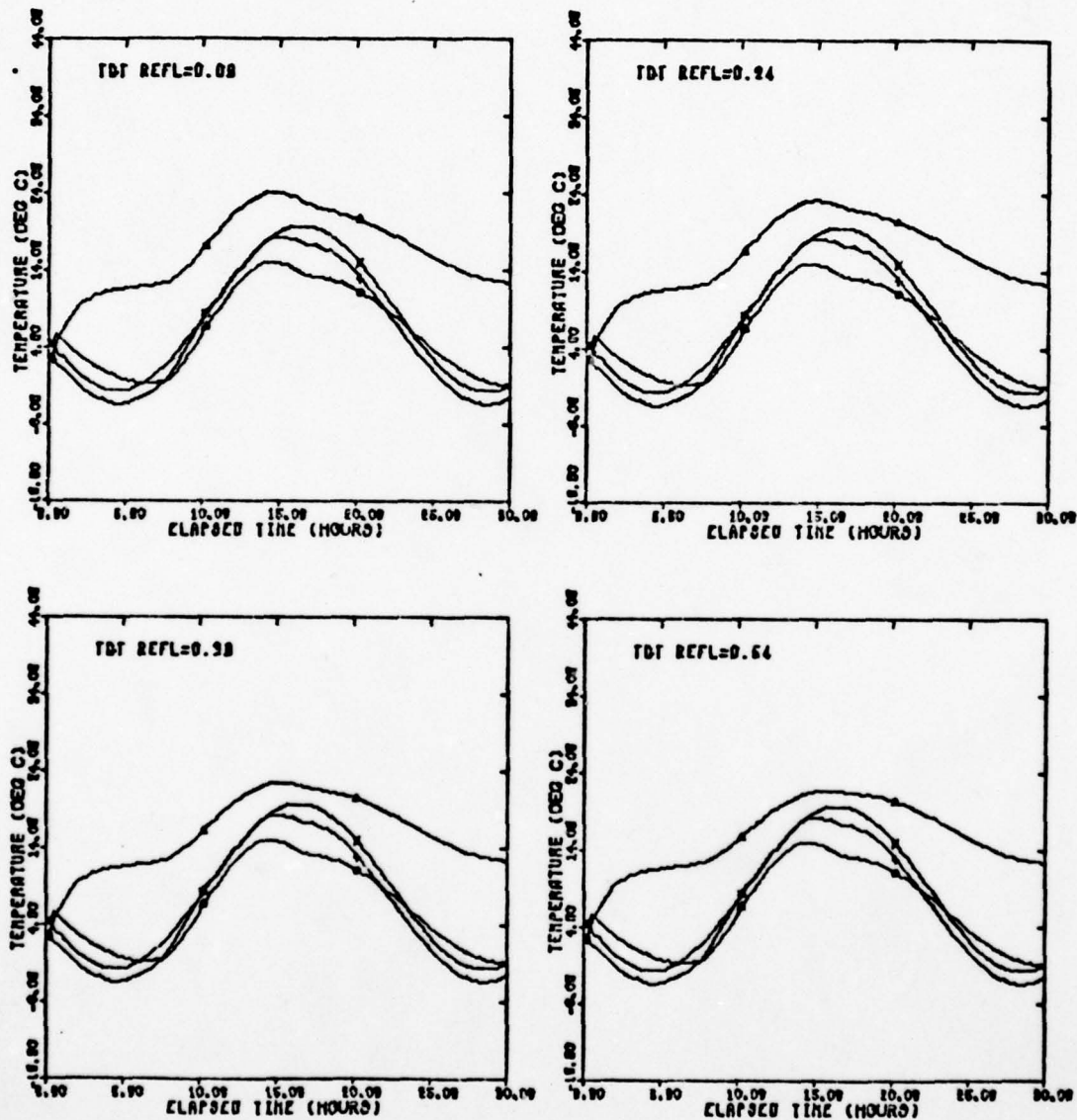


Fig. 32(e). Basic Temperature Plots of Target Reflectivity

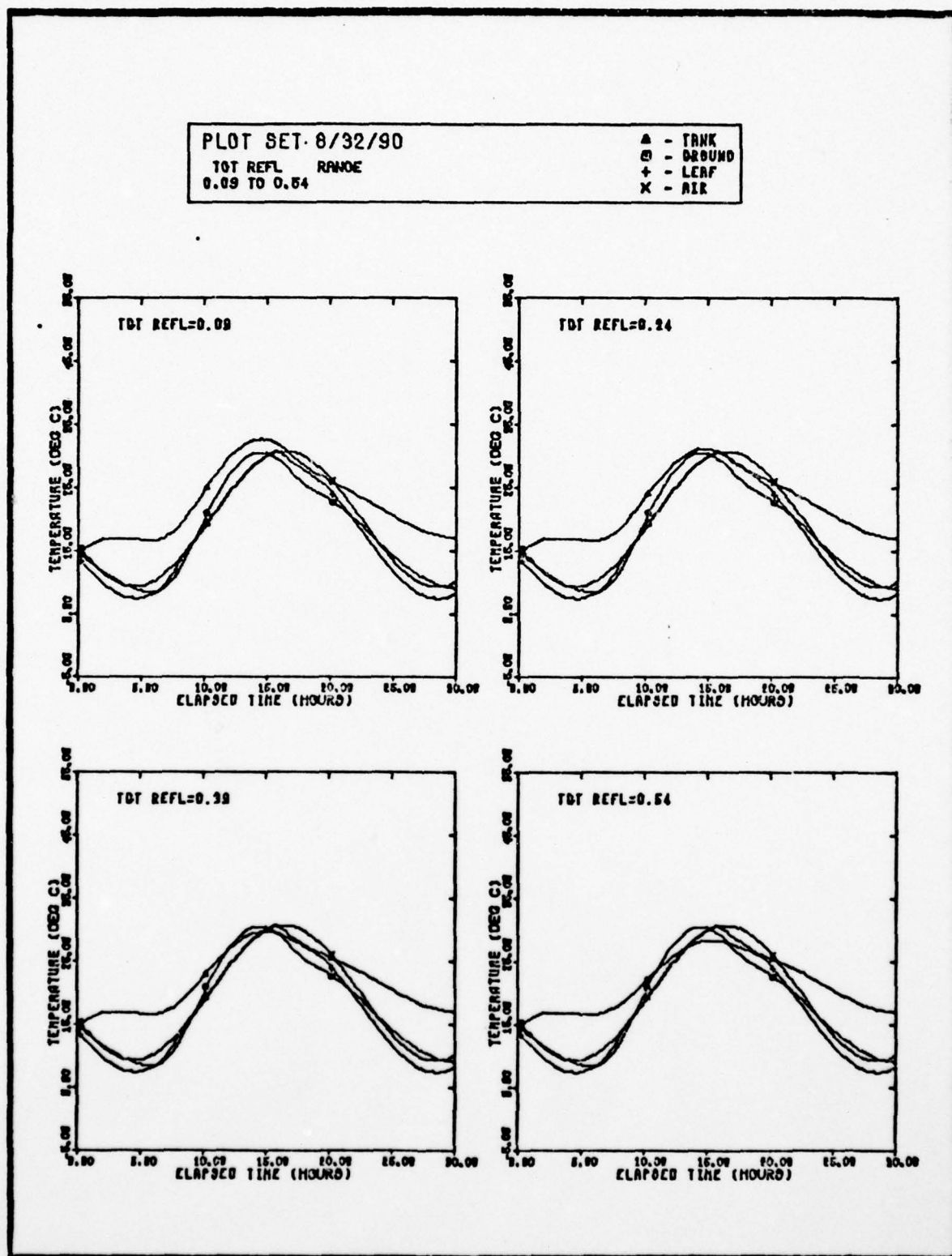


Fig. 32(f). Basic Temperature Plots of Target Reflectivity

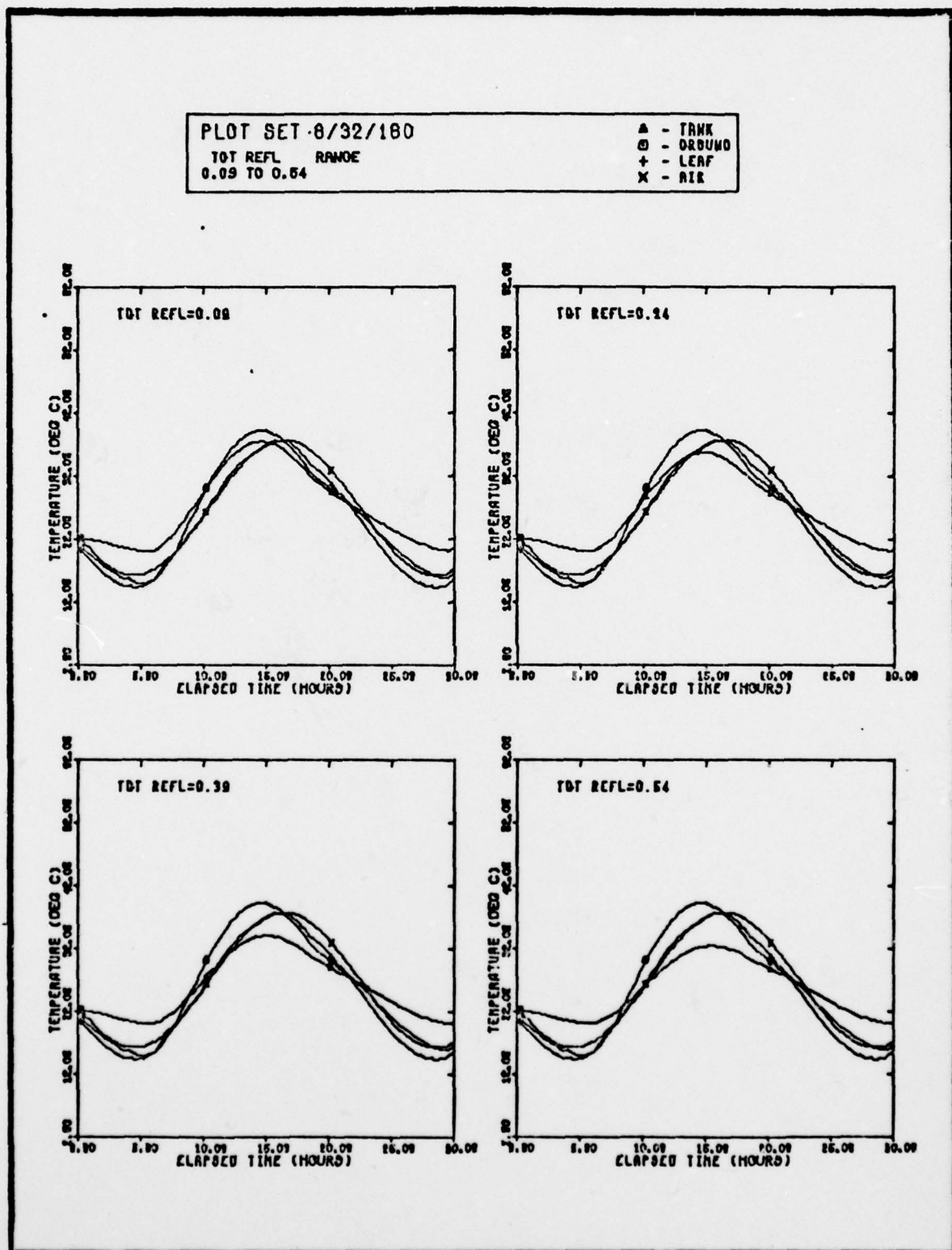


Fig. 32(g). Basic Temperature Plots of Target Reflectivity

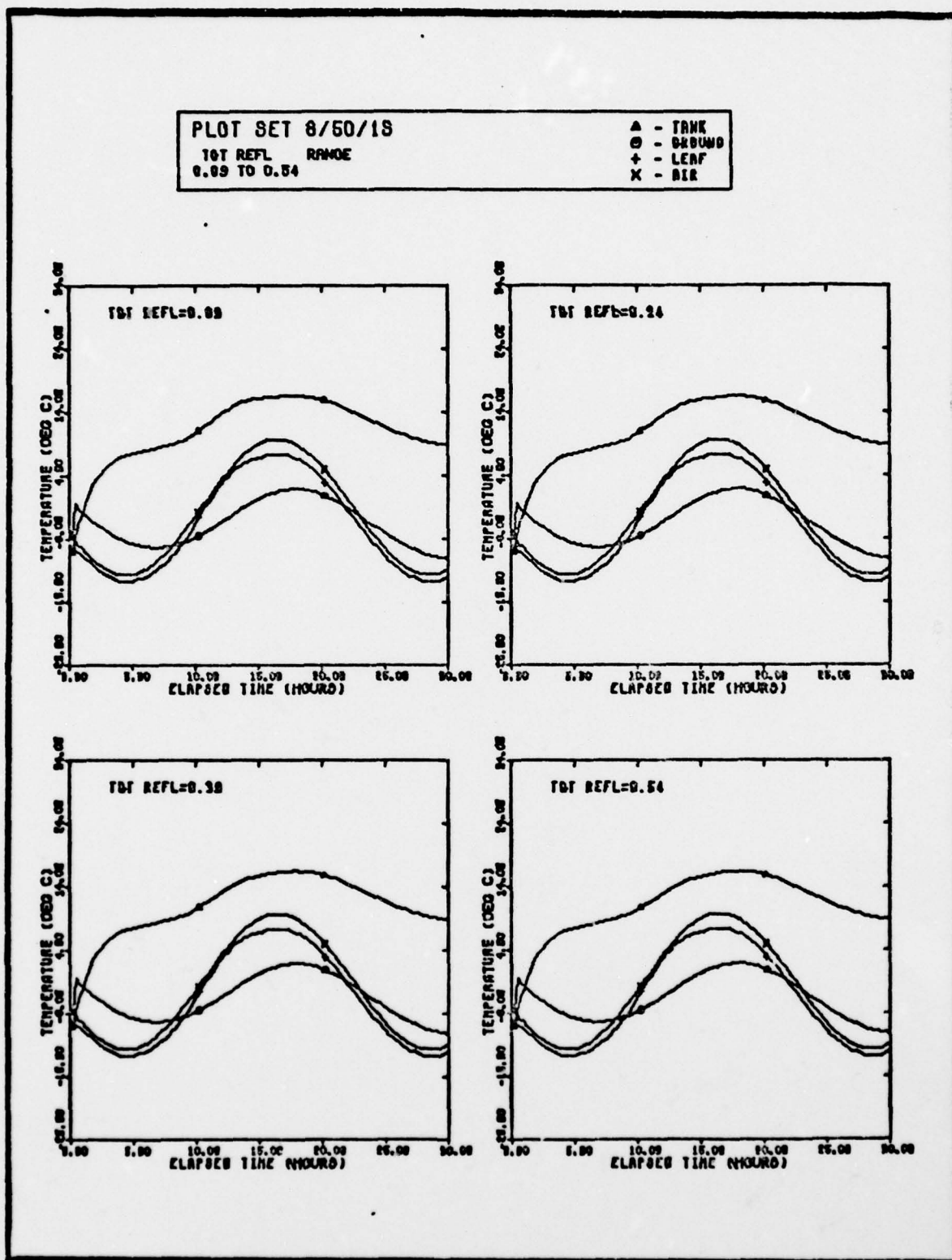


Fig. 32(h). Basic Temperature Plots of Target Reflectivity



PLOT SET 8/60/1

TOT REFL RANGE  
0.09 TO 0.64

Δ - TRUNK  
⊙ - GROUND  
+ - LEAF  
x - AIR

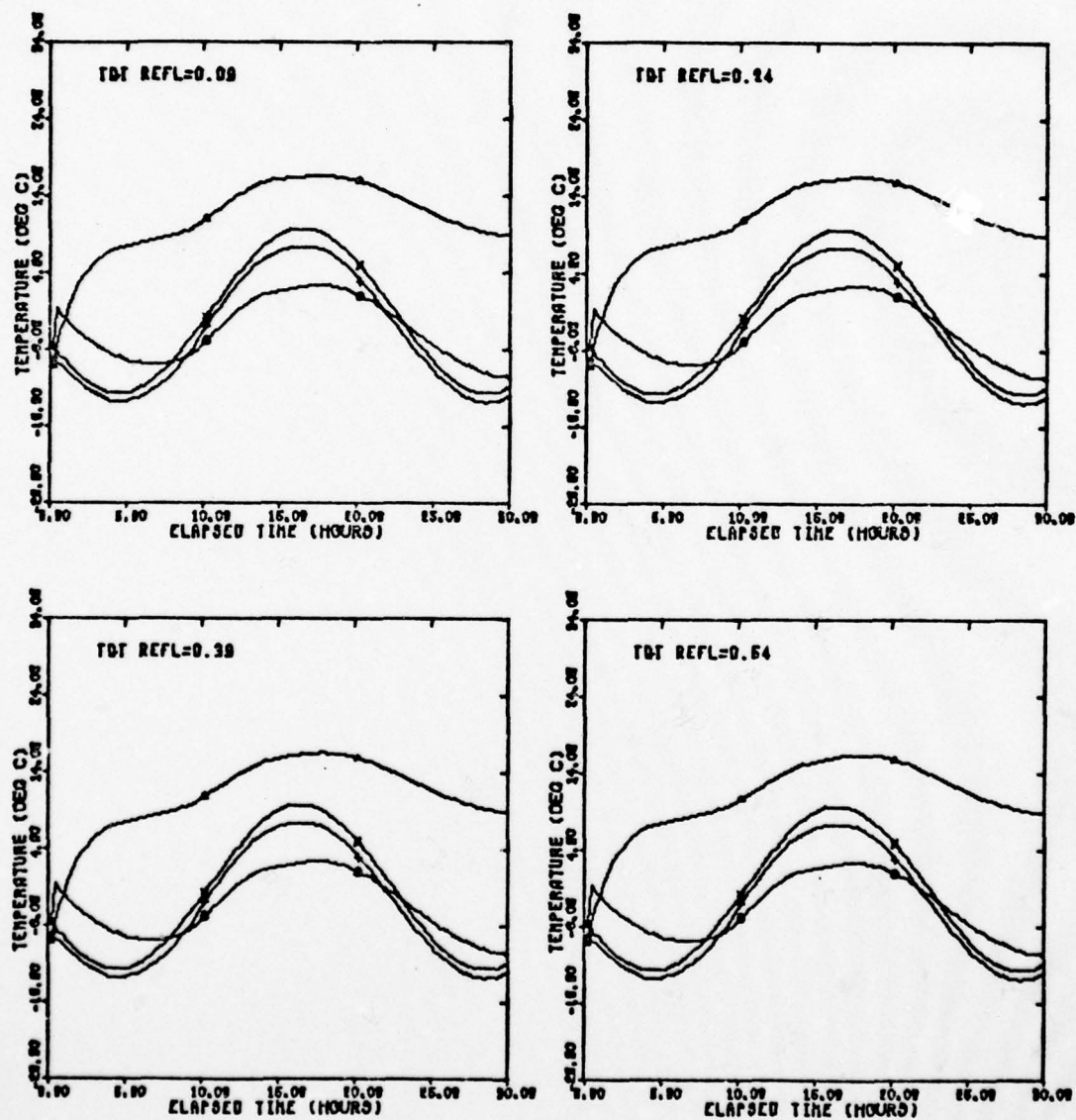


Fig. 32(1). Basic Temperature Plots of Target Reflectivity

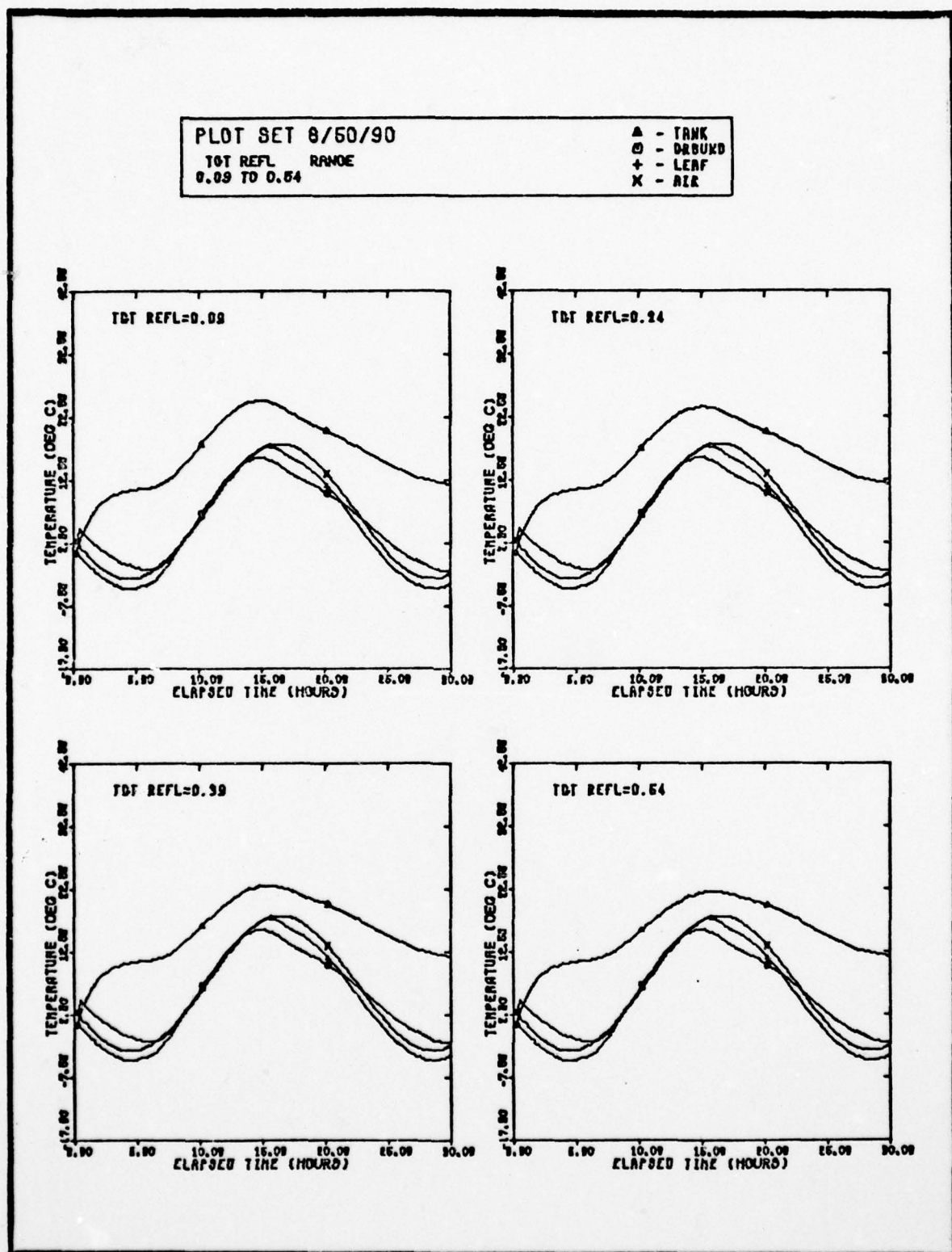


Fig. 32(j). Basic Temperature Plots of Target Reflectivity

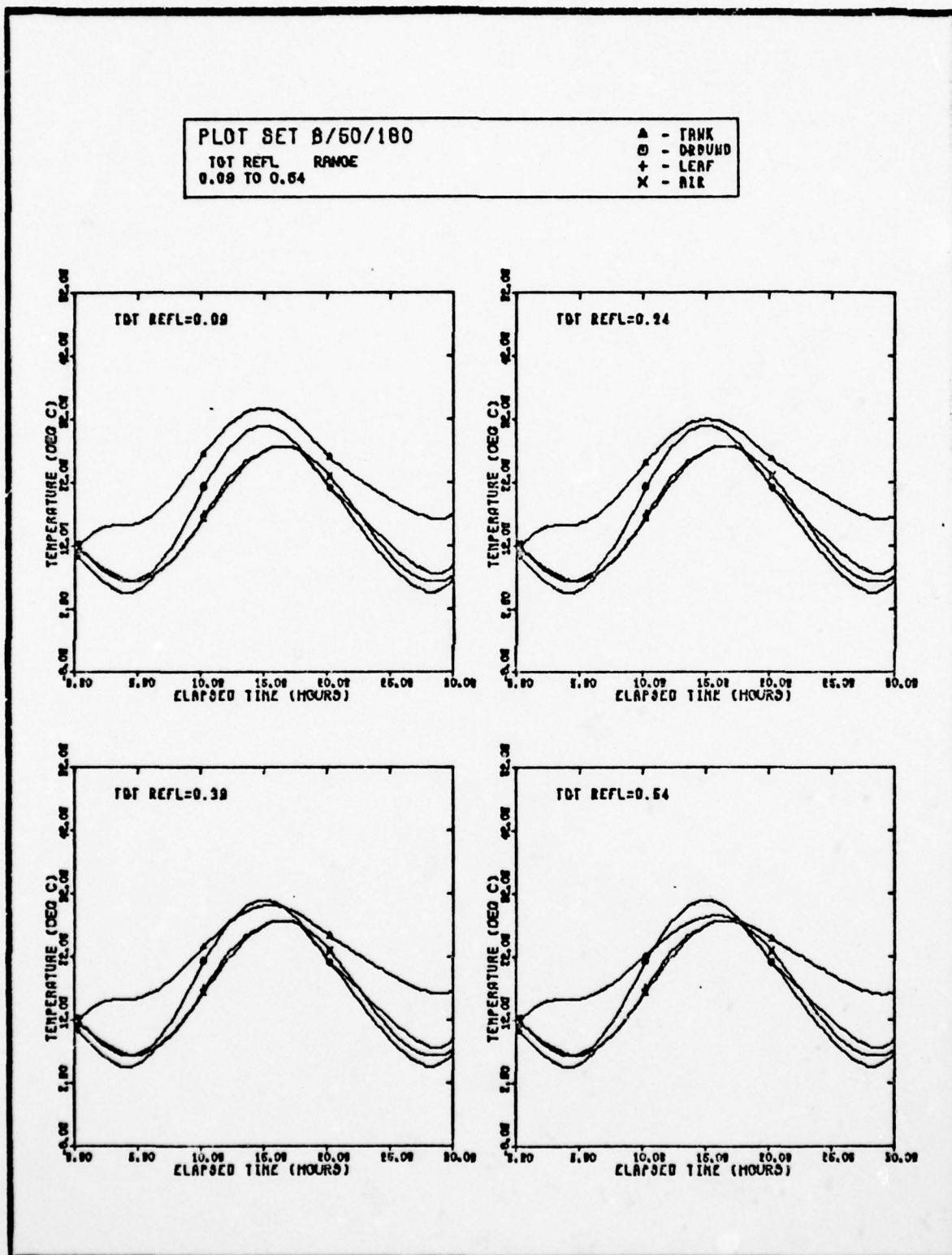


Fig. 32(k). Basic Temperature Plots of Target Reflectivity



PLOT SET 9/20/1

TOT EMISS RANGE  
0.35 TO 0.90

▲ - TANK  
● - GROUND  
+ - LEAF  
X - AIR

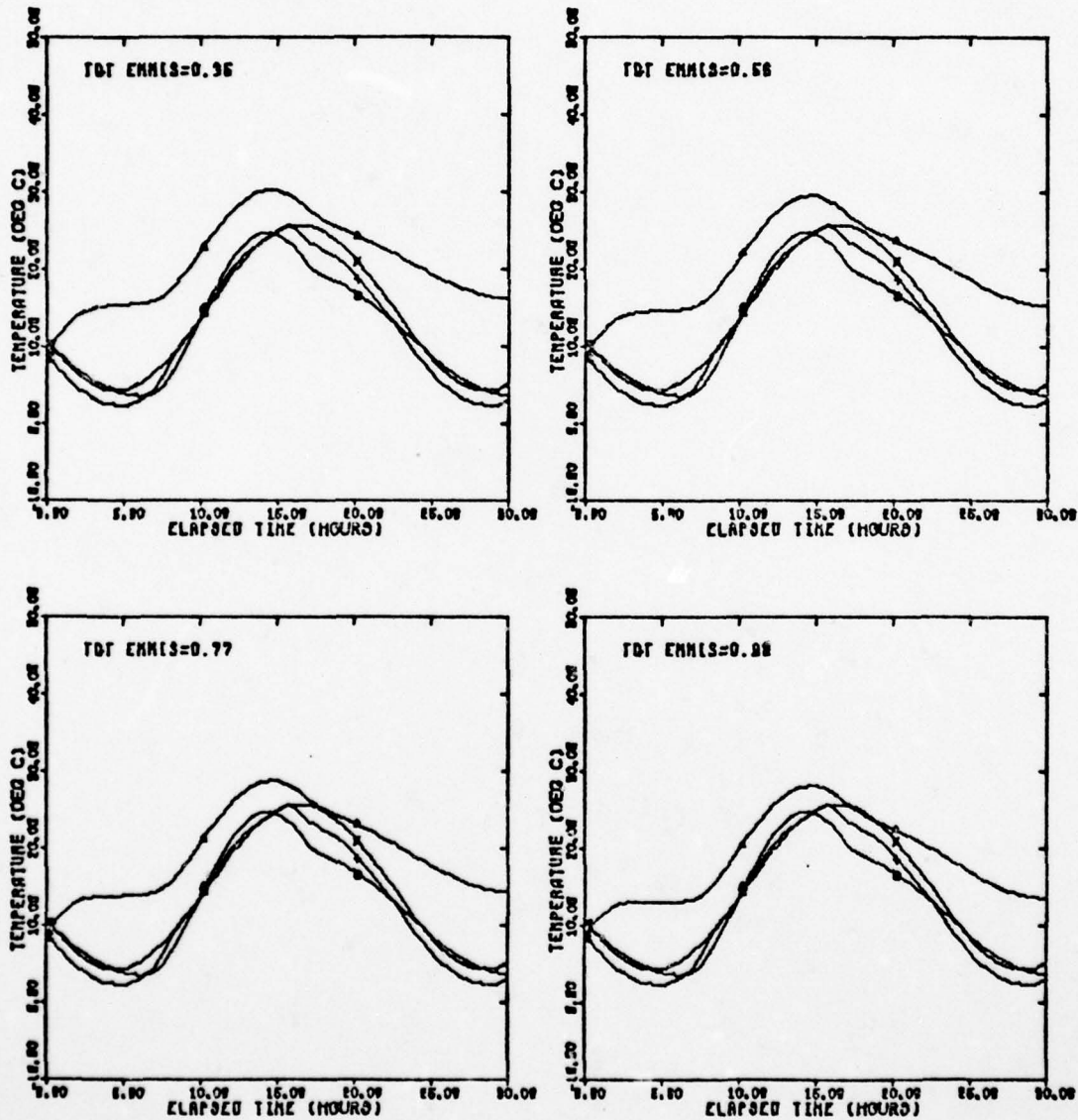


Fig. 33(a). Basic Temperature Plots of Target Emmissivity



PLOT SET 9/20/90

TOT EMISS RANGE  
0.95 TO 0.99

▲ - TANK  
○ - DRUM  
+ - LEAF  
x - AIR

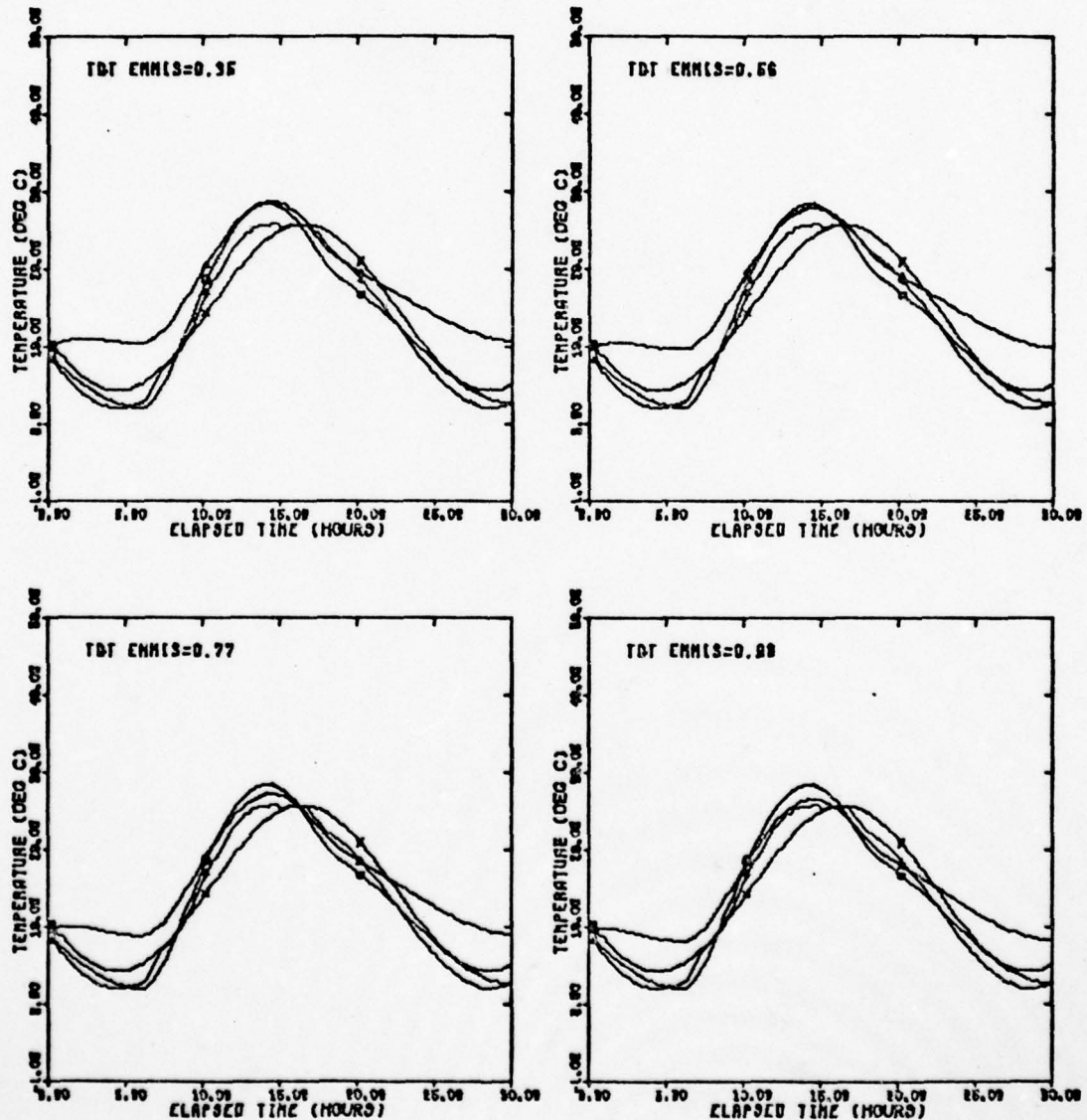


Fig. 33(b). Basic Temperature Plots of Target Emmissivity

PLOT SET 9/20/180

TOT EMHIS RANGE  
0.35 TO 0.90

▲ - TANK  
○ - GROUND  
+ - LEAF  
X - AIR

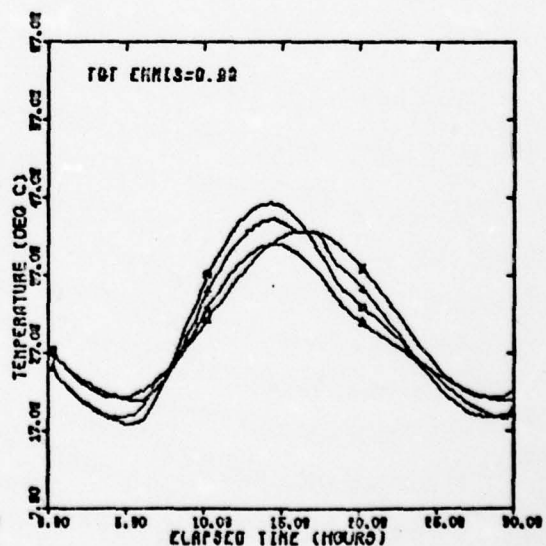
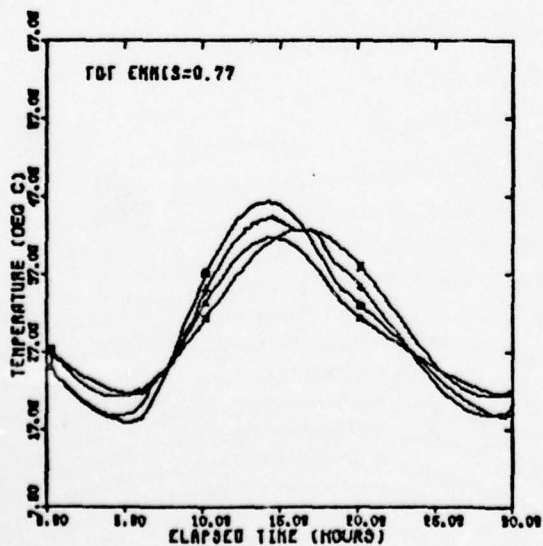
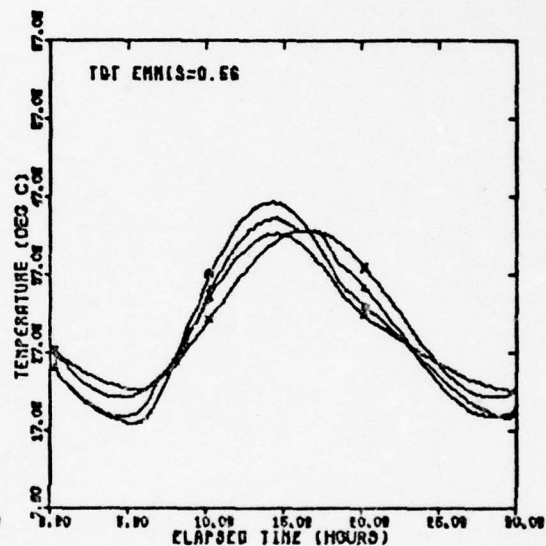
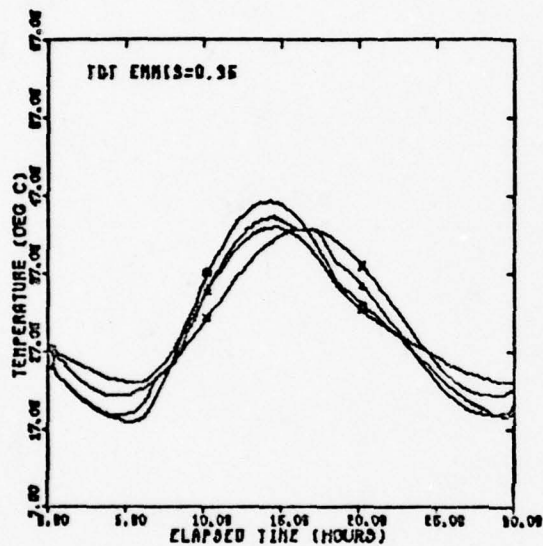


Fig. 33(c). Basic Temperature Plots of Target Emmissivity

AD-A055 642 AIR FORCE INST OF TECH WRIGHT-PATTERSON AFB OHIO SCH--ETC F/G 17/5  
A THEORETICAL ANALYSIS OF CHANGES IN THERMAL SIGNATURES CAUSED --ETC(U).  
DEC 77 J T SMALL

AIR FORCE INST OF TECH WRIGHT-PATTERSON AFB OHIO SCH--ETC F/G 17/5  
A THEORETICAL ANALYSIS OF CHANGES IN THERMAL SIGNATURES CAUSED --ETC(U)  
DEC 77 J T SMALL

AFIT/GEP/PH/77-12

NL

3 OF 3  
ADA  
055642

ADA  
055642

055642

END  
DATE  
FILMED  
8-78  
DDC

PLOT SET 9/92/19

TOT EMISS RANGE  
0.35 TO 0.95

▲ - TANK  
○ - GROUND  
+ - LEAF  
X - AIR

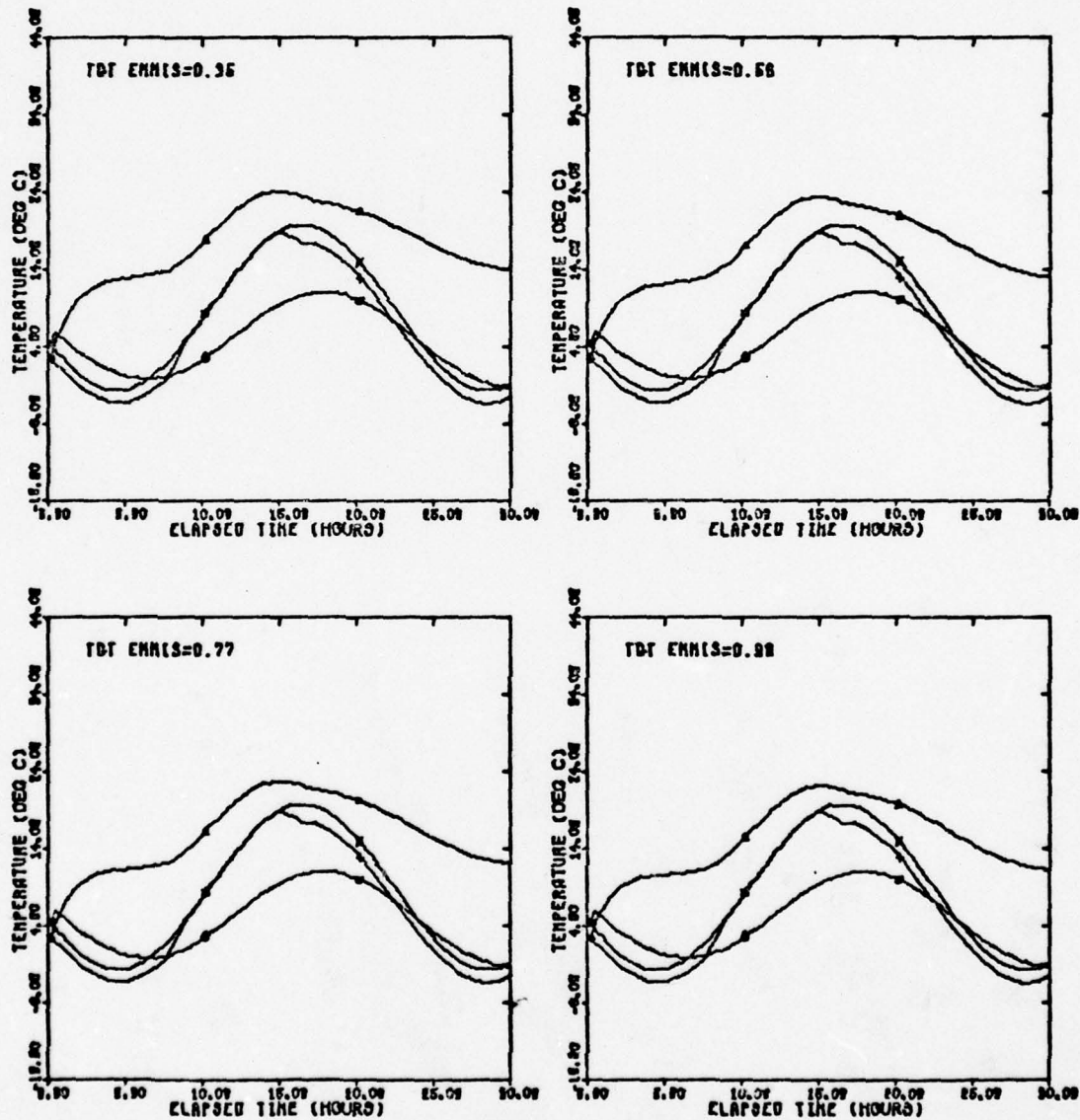


Fig. 33(d). Basic Temperature Plots of Target Emmissivity



PLOT SET 9/32/1

TGT EMIS RANGE  
0.35 TO 0.95

▲ - TRNK  
● - GROUND  
+ - LEAF  
x - AIR

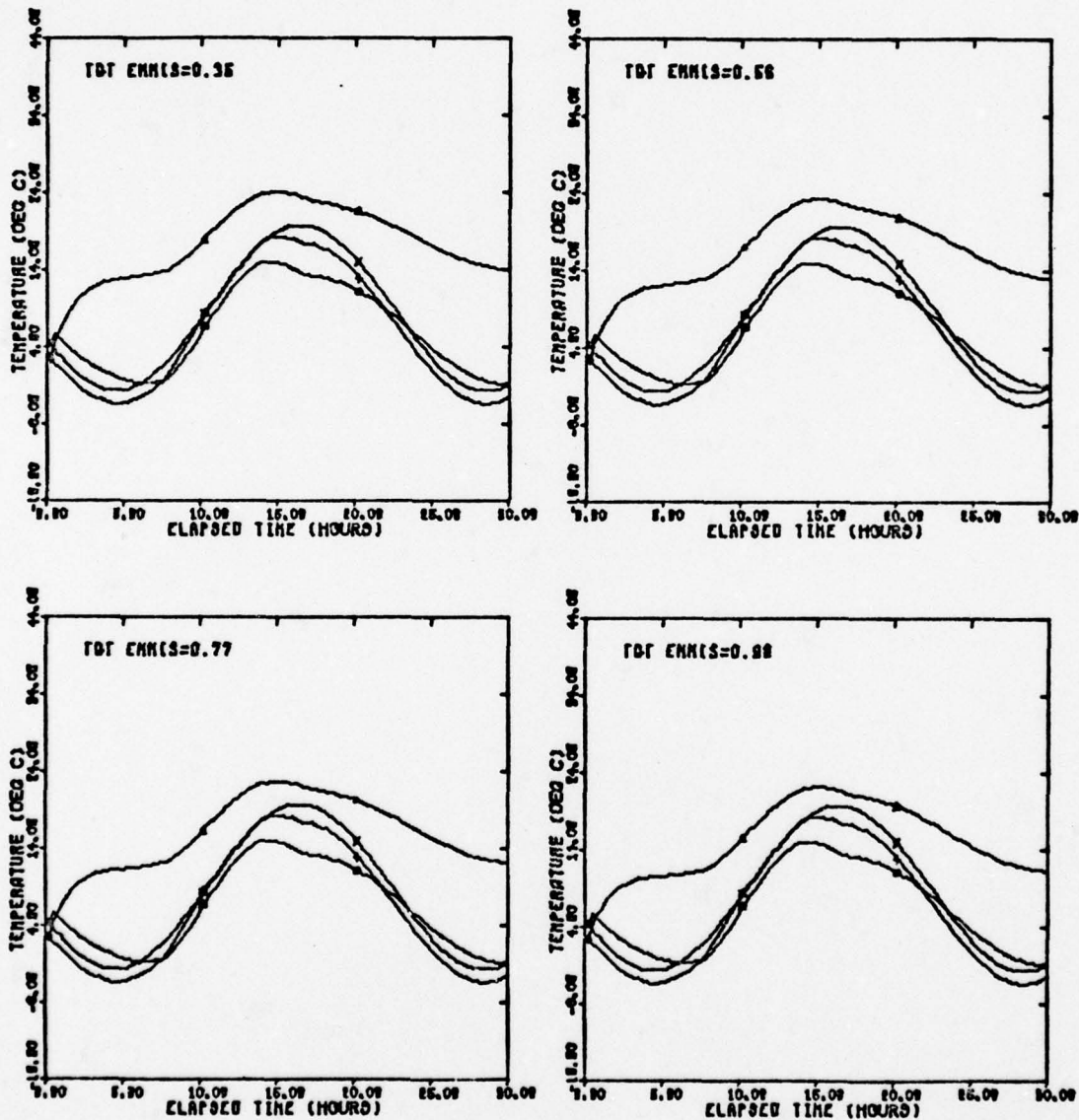


Fig. 33(e). Basic Temperature Plots of Target Emmissivity

PLOT SET 9/92/90

TGT EMISS RANGE  
0.95 TO 0.99

▲ - TANK  
● - GROUND  
+ - LEAF  
x - AIR

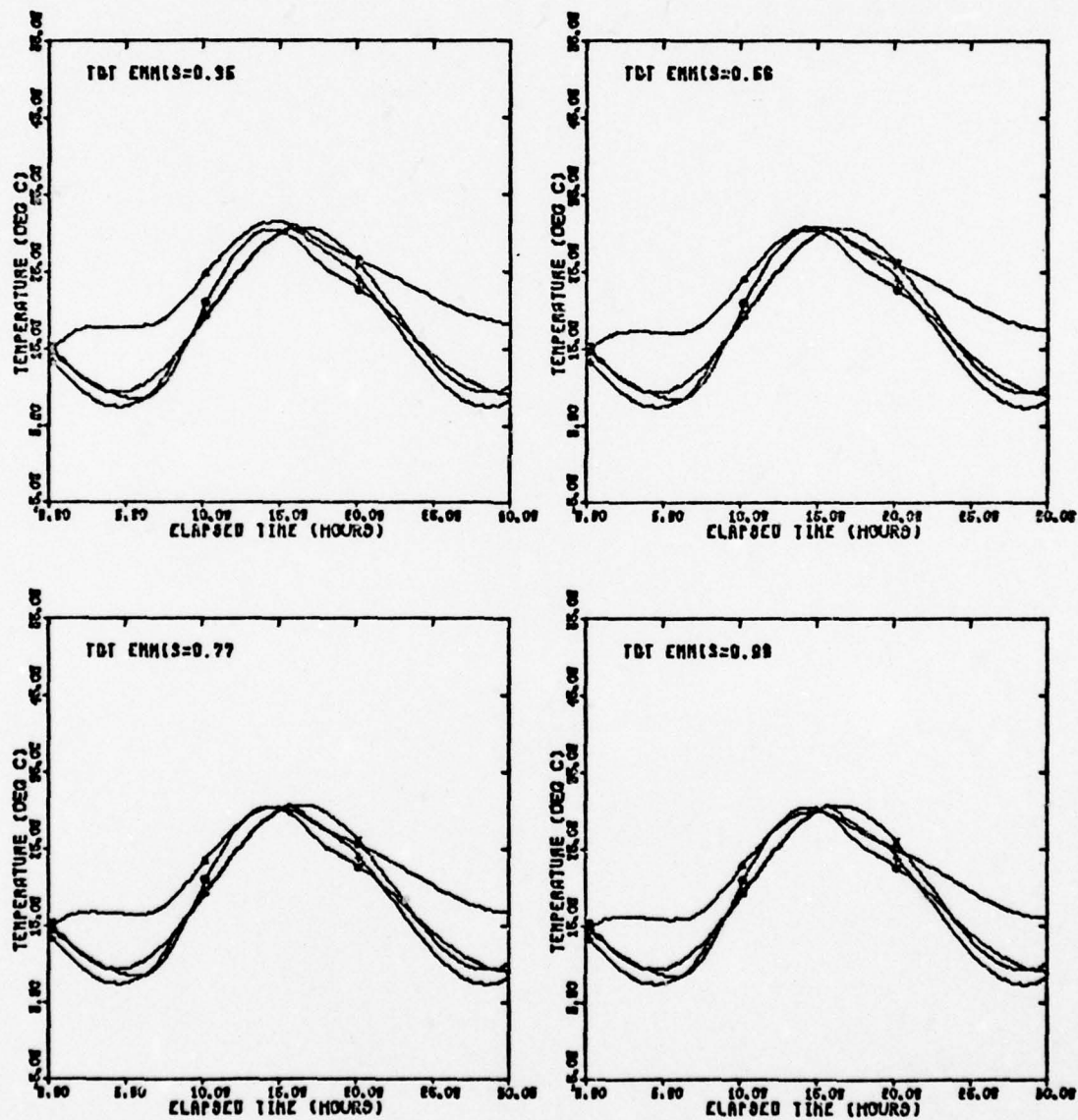


Fig. 33(f). Basic Temperature Plots of Target Emmissivity

PLOT SET 9/32/180

TOT EMISS RANGE  
0.35 TO 0.98

▲ - TRNK  
○ - GROUND  
+ - LEAF  
x - AIR

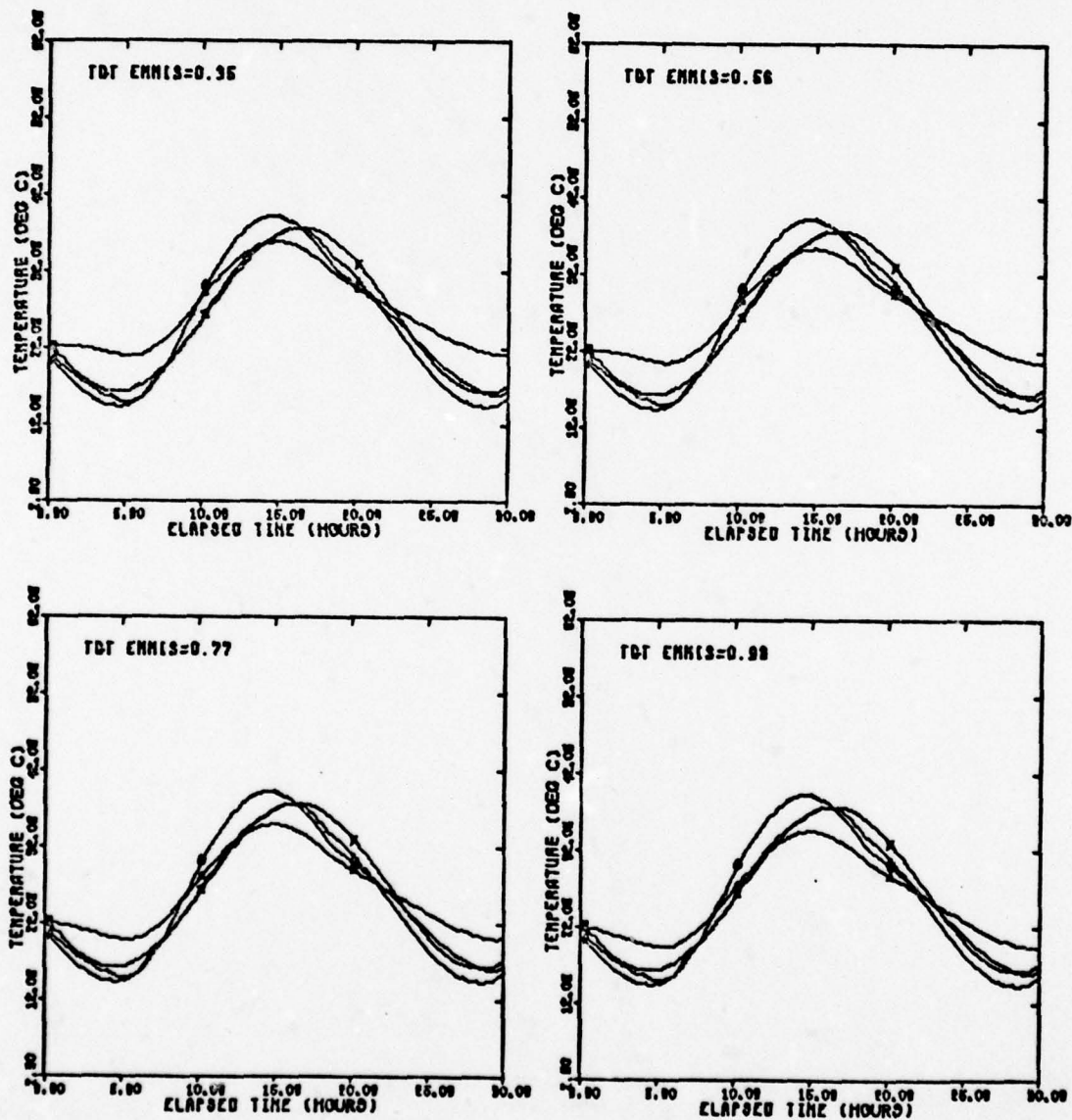


Fig. 33(g). Basic Temperature Plots of Target Emmissivity



PLOT SET 9/50/18

TGT EMIS RANGE  
0.35 TO 0.95

Δ - TRNK  
□ - GRND  
+ - LEAF  
X - AIR

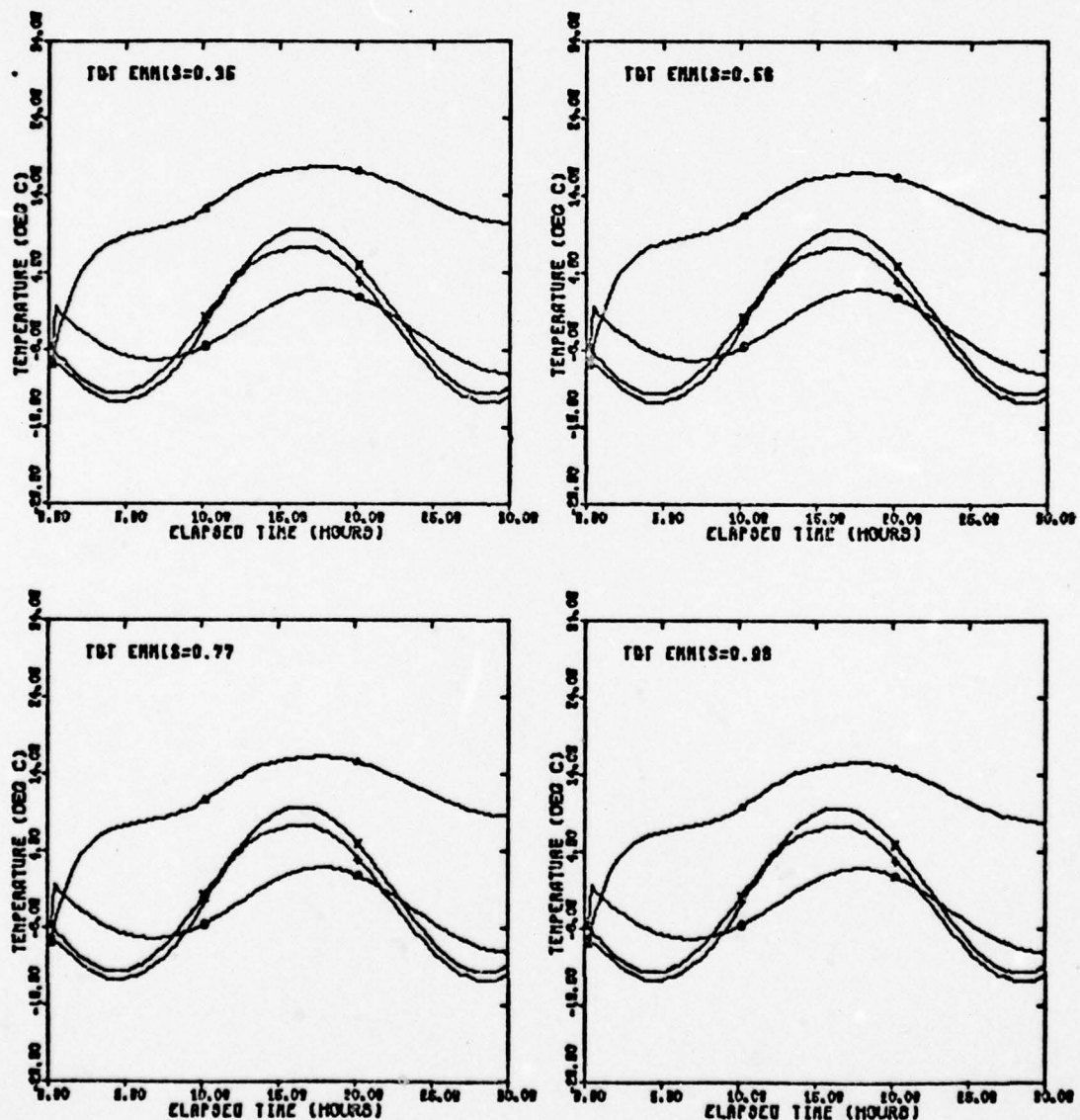


Fig. 33(h). Basic Temperature Plots of Target Emmissivity



PLOT SET 9/60/1

TOT EMIS RANGE  
0.35 TO 0.99

▲ - TANK  
○ - GROUND  
+ - LEAF  
X - AIR

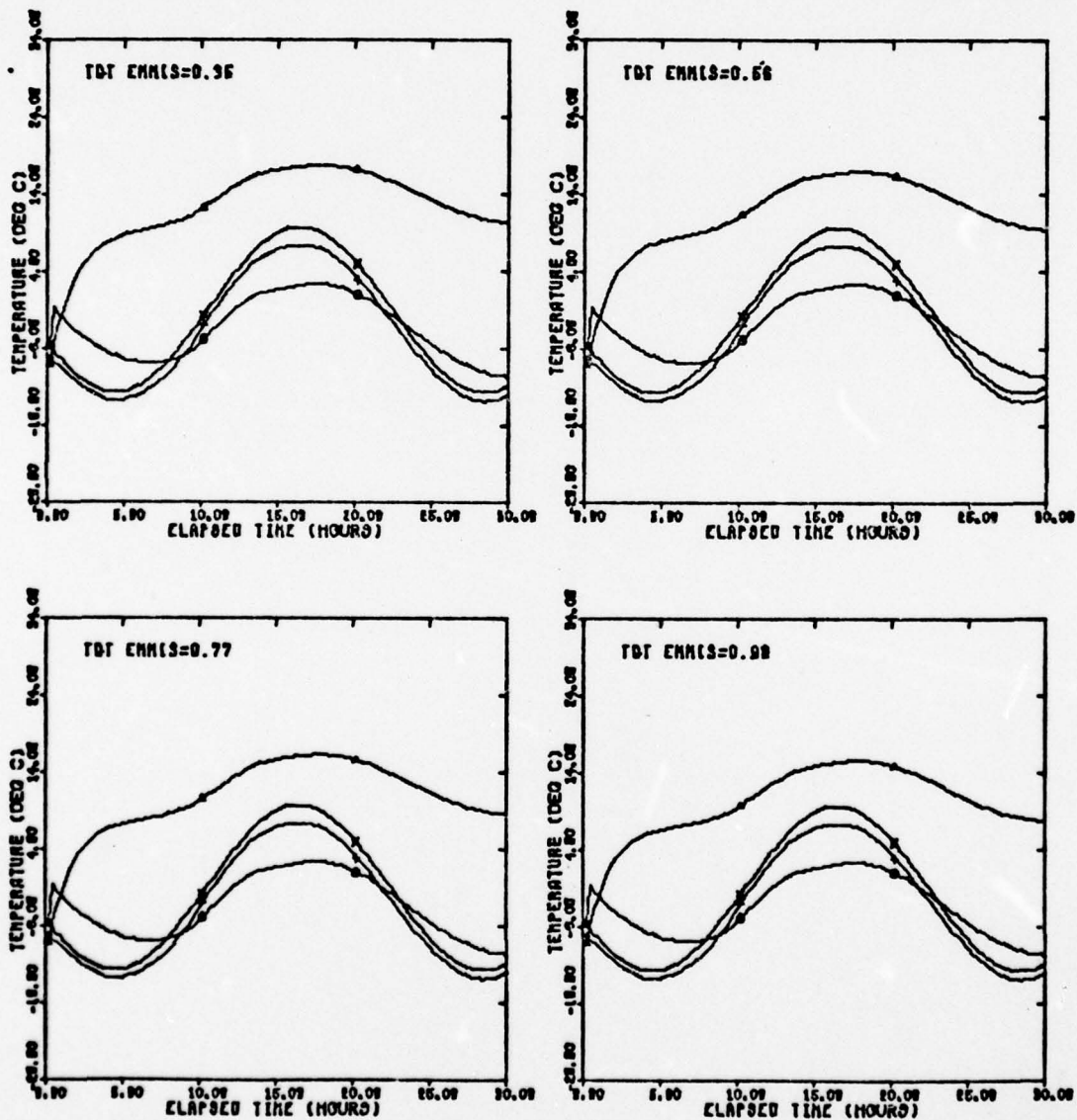


Fig. 33(1). Basic Temperature Plots of Target Emmissivity

PLOT SET 9/60/90

TGT EMISS RANGE  
0.35 TO 0.98

A - TANK  
O - GROUND  
+ - LEAF  
X - AIR

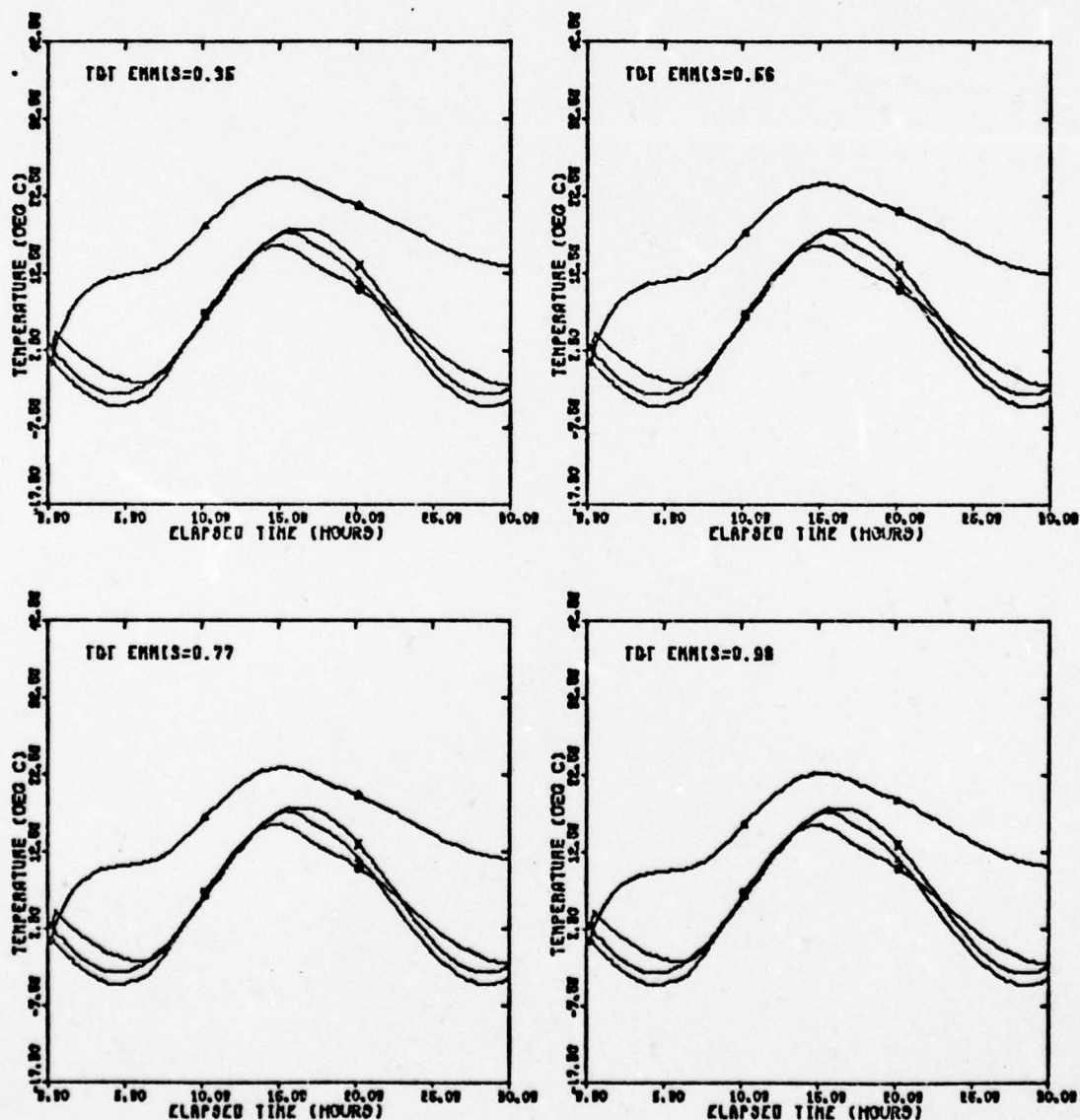


Fig. 33(j). Basic Temperature Plots of Target Emmissivity

PLOT SET 9/60/180

TOT ENNIS RANGE  
0.35 TO 0.98

A - TRNK  
O - GROUND  
+ - LEAF  
X - AIR

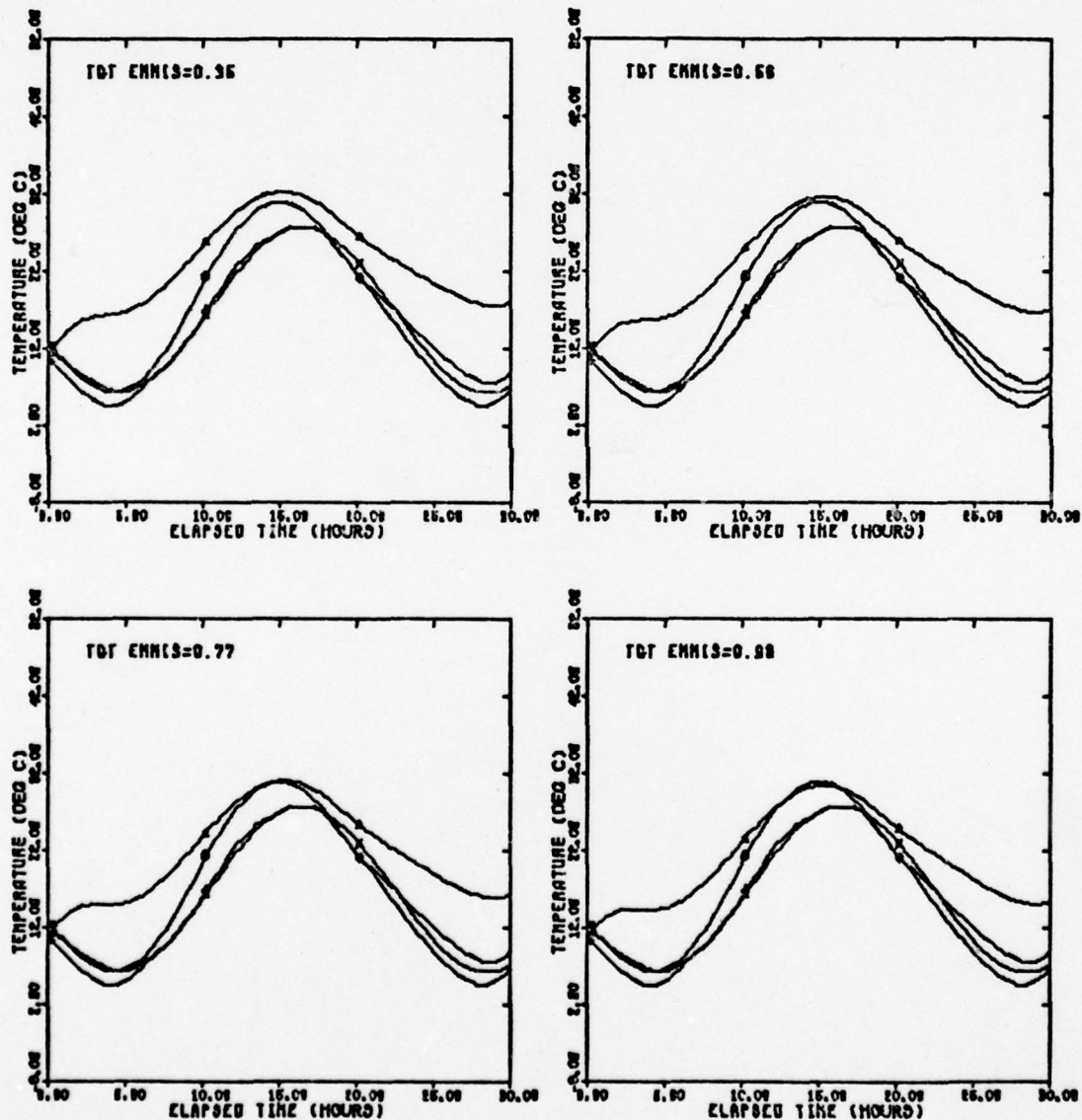


Fig. 33(k). Basic Temperature Plots of Target Emmissivity



PLOT SET 10/20/1

TGT THICK. RANGE  
1.50 TO 9.50 CM

▲ - TANK  
○ - GROUND  
+ - LEAF  
X - AIR

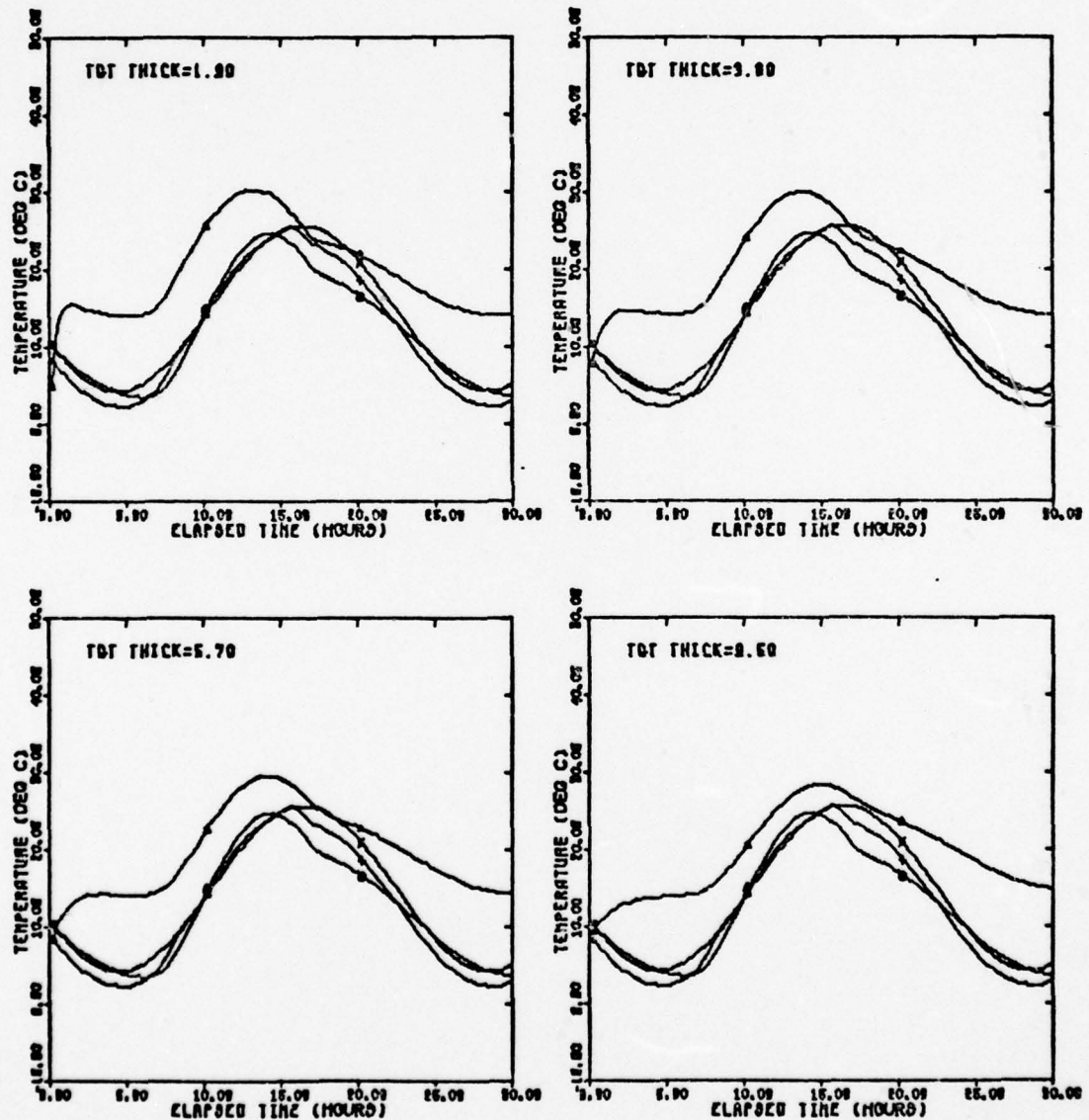


Fig. 34(a). Basic Temperature Plots of Target Thickness



PLOT SET 10/20/90

TOT THICK. RANGE  
1.90 TO 9.60 CM

▲ - TANK  
○ - DRUM  
+ - LEAF  
x - AIR

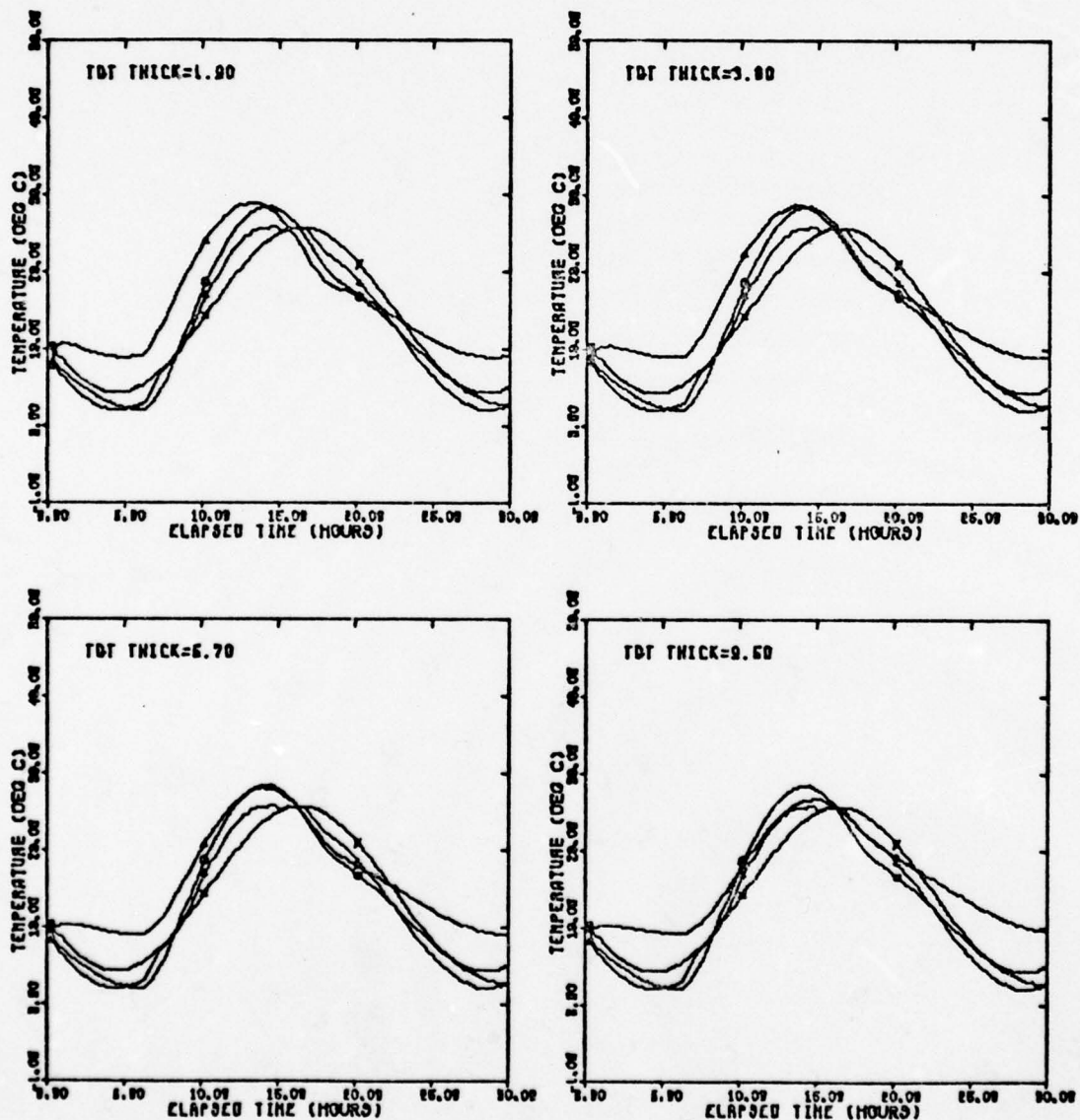


Fig. 34(b). Basic Temperature Plots of Target Thickness

PLOT SET 10/20/180

TOT THICK RANGE  
1.80 TO 8.60 CM

▲ - TANK  
○ - DRUM  
+ - LEAF  
X - AIR

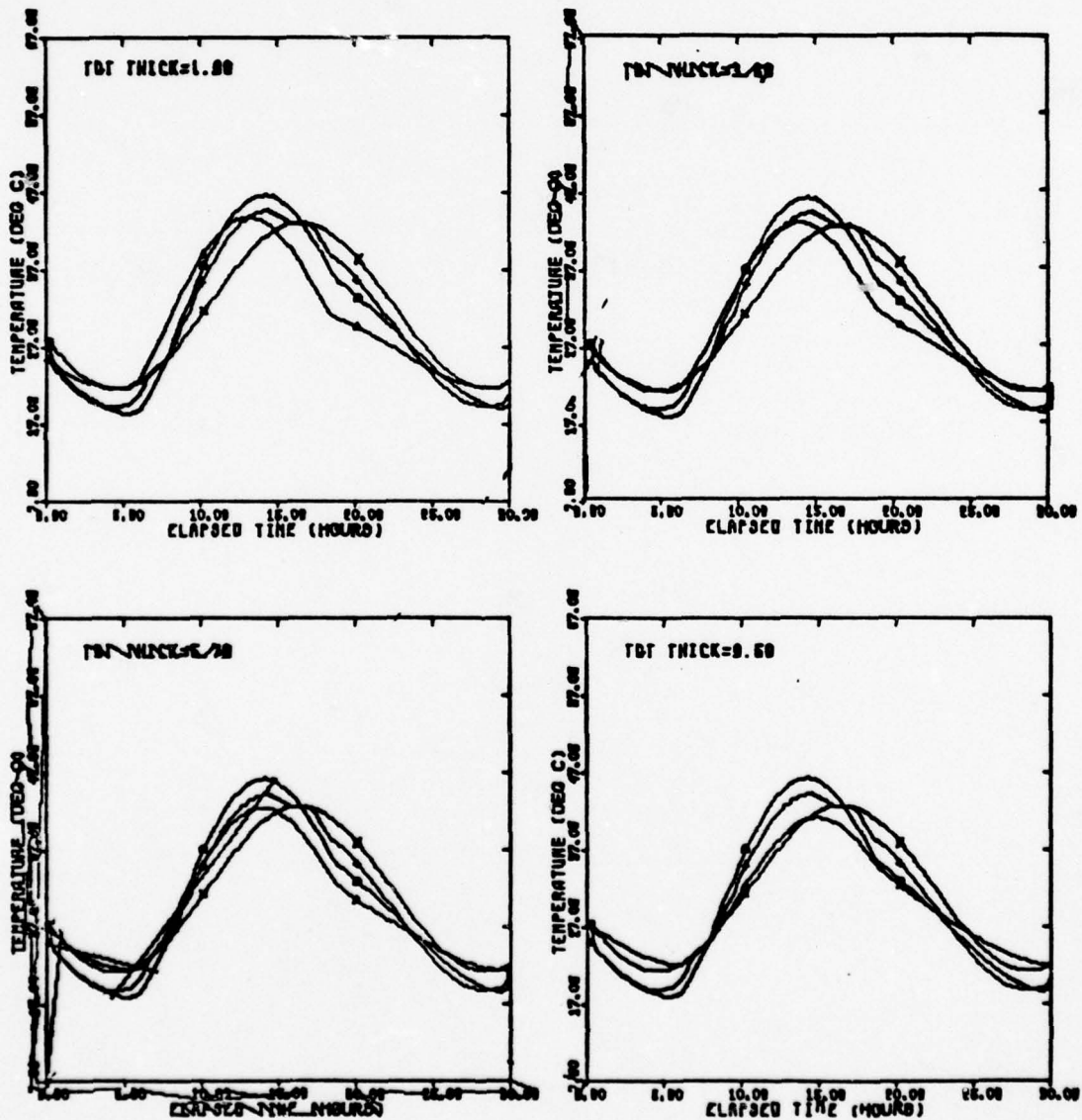


Fig. 34(c). Basic Temperature Plots of Target Thickness

PLOT SET 10/92/18

TOT THICK. REMOVED  
1.80 TO 9.60 CM

Δ - TRNK  
○ - DRUM  
+ - LEAF  
X - AIR

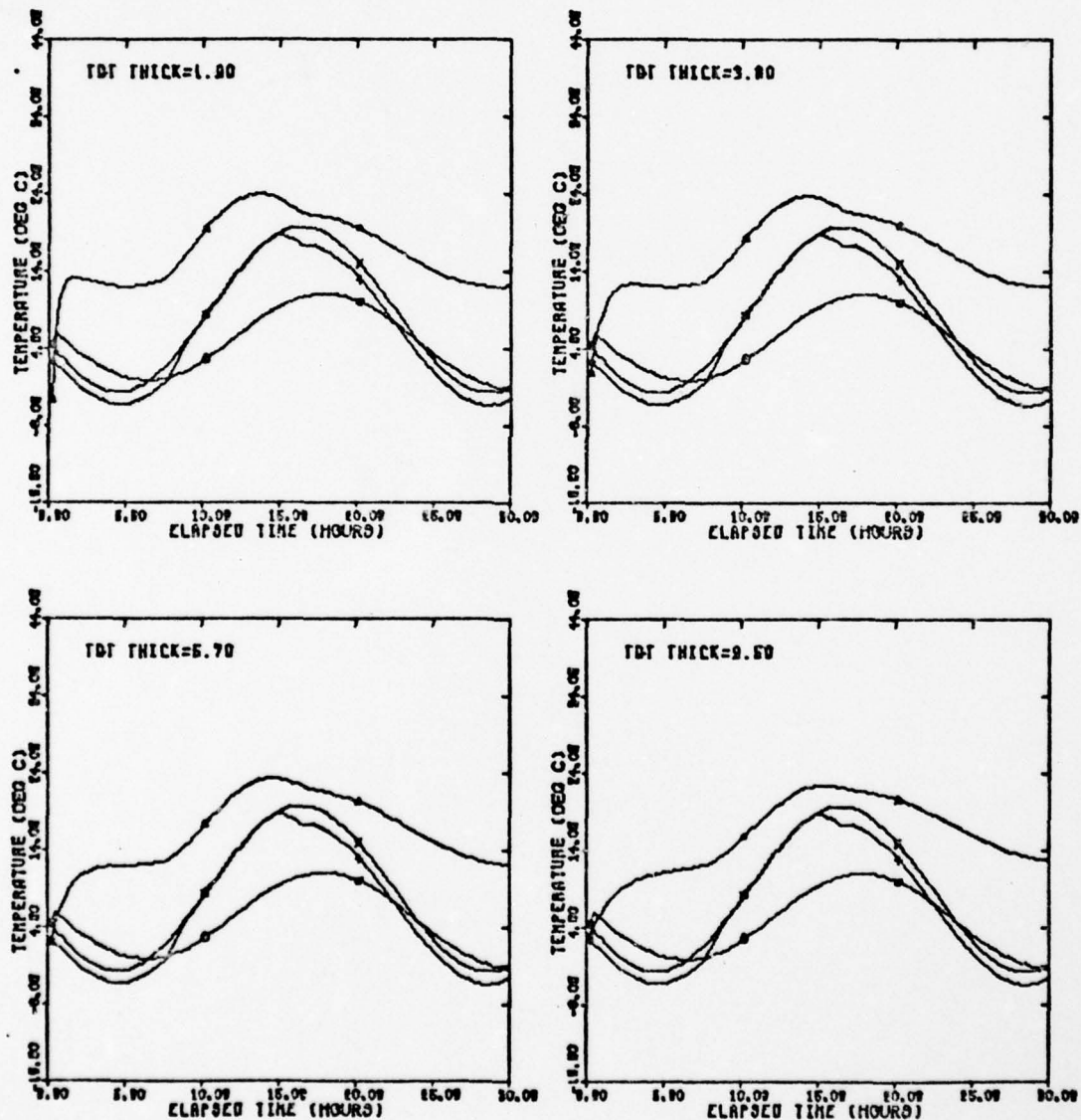


Fig. 34(d). Basic Temperature Plots of Target Thickness

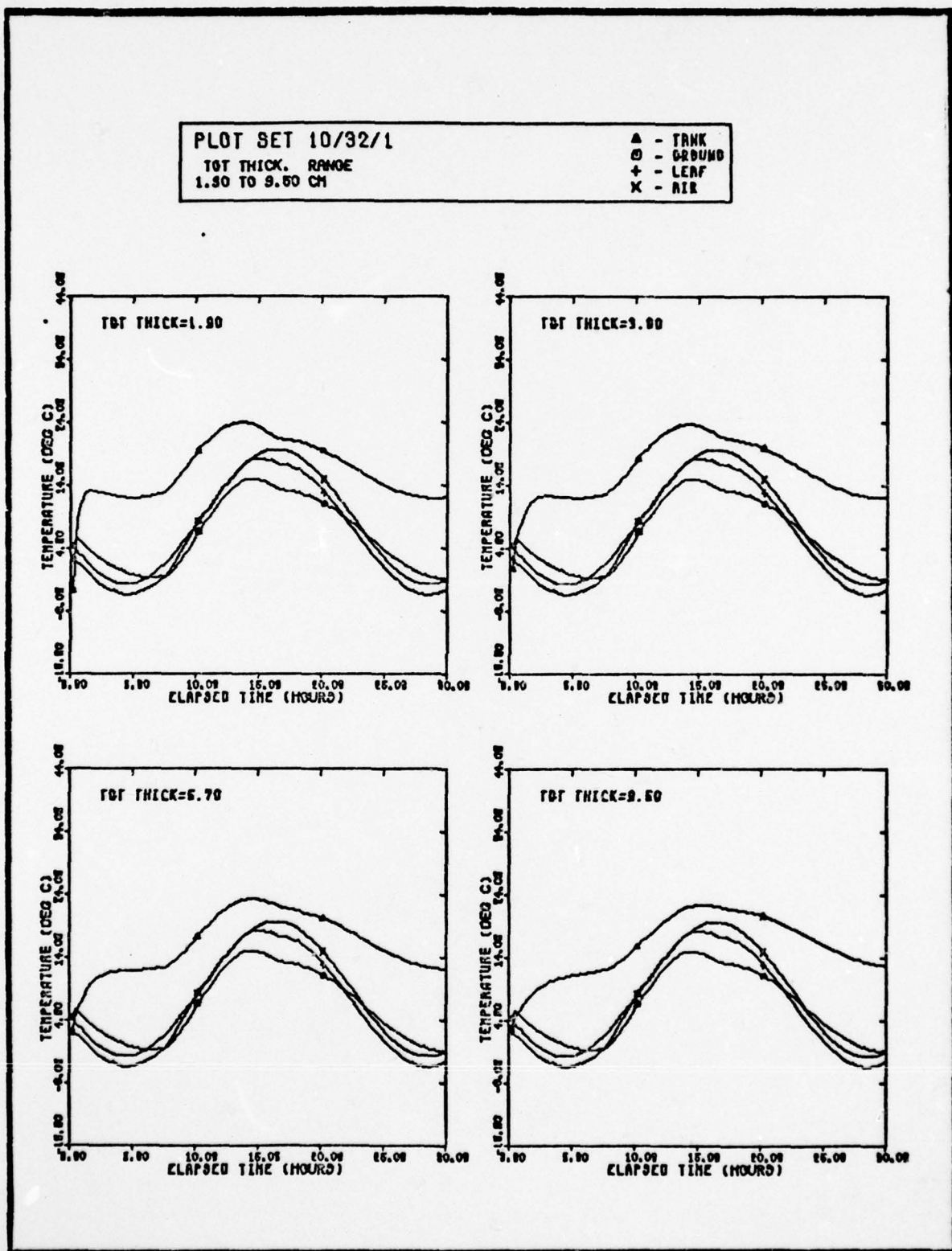


Fig. 34(e). Basic Temperature Plots of Target Thickness



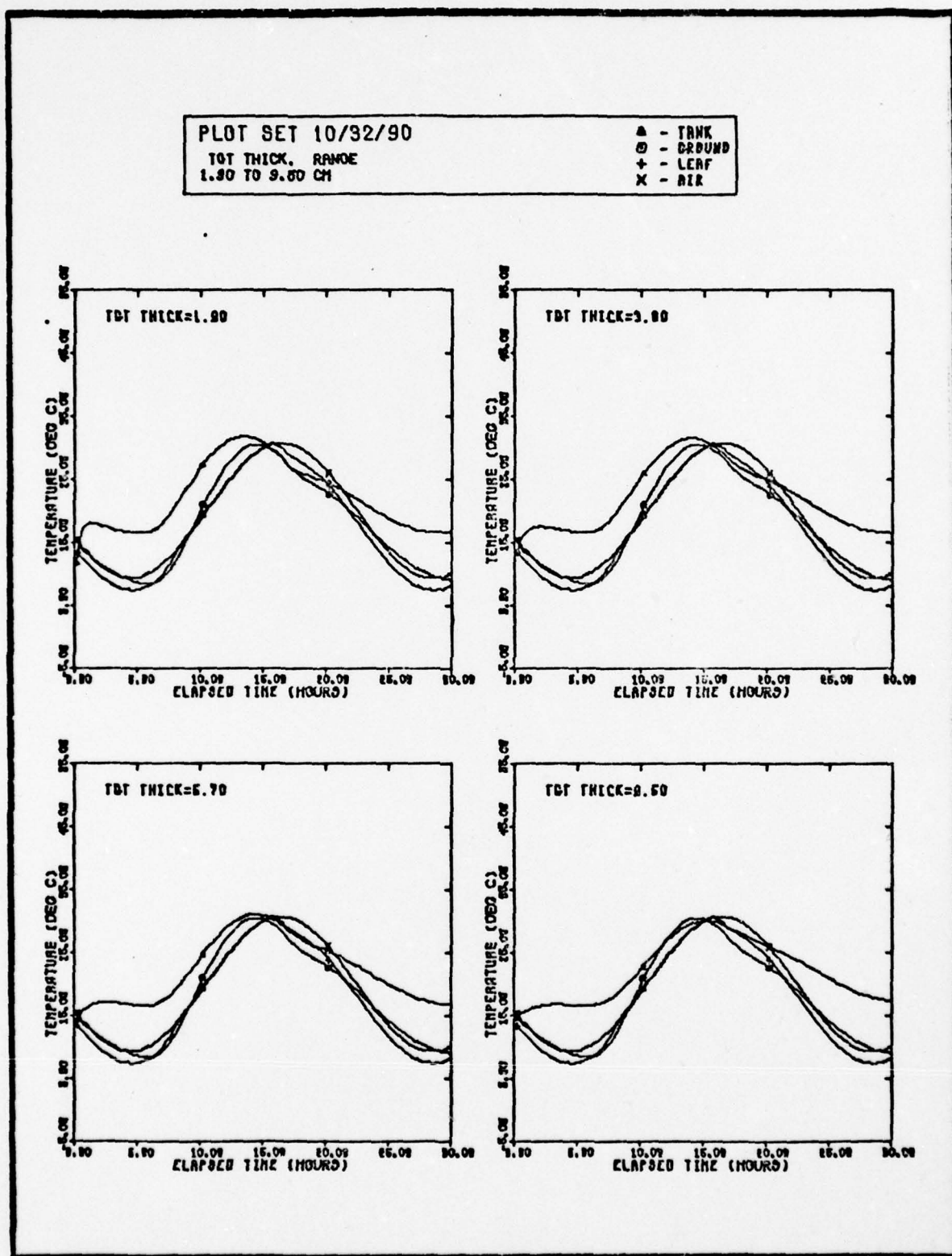


Fig. 34(f). Basic Temperature Plots of Target Thickness

PLOT SET 10/32/180

TOT THICK RANGE  
1.50 TO 9.50 CM

Δ - TANK  
○ - GROUND  
+ - LEAF  
X - AIR

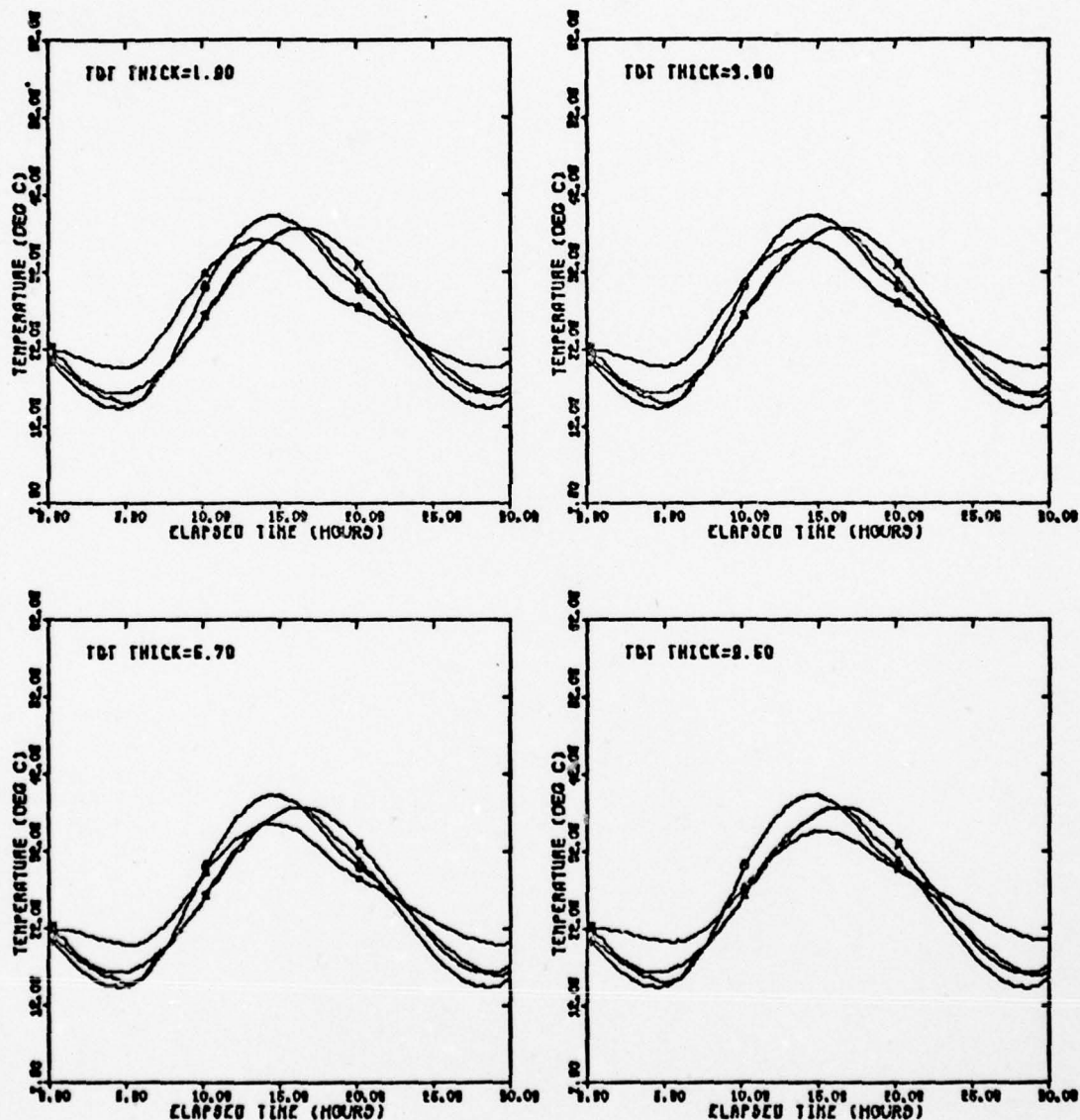


Fig. 34(g). Basic Temperature Plots of Target Thickness

PLOT SET 10/50/18

TGT THICK. RANGE  
1.50 TO 9.50 CM

△ - TANK  
○ - GROUND  
+ - LEAF  
x - AIR

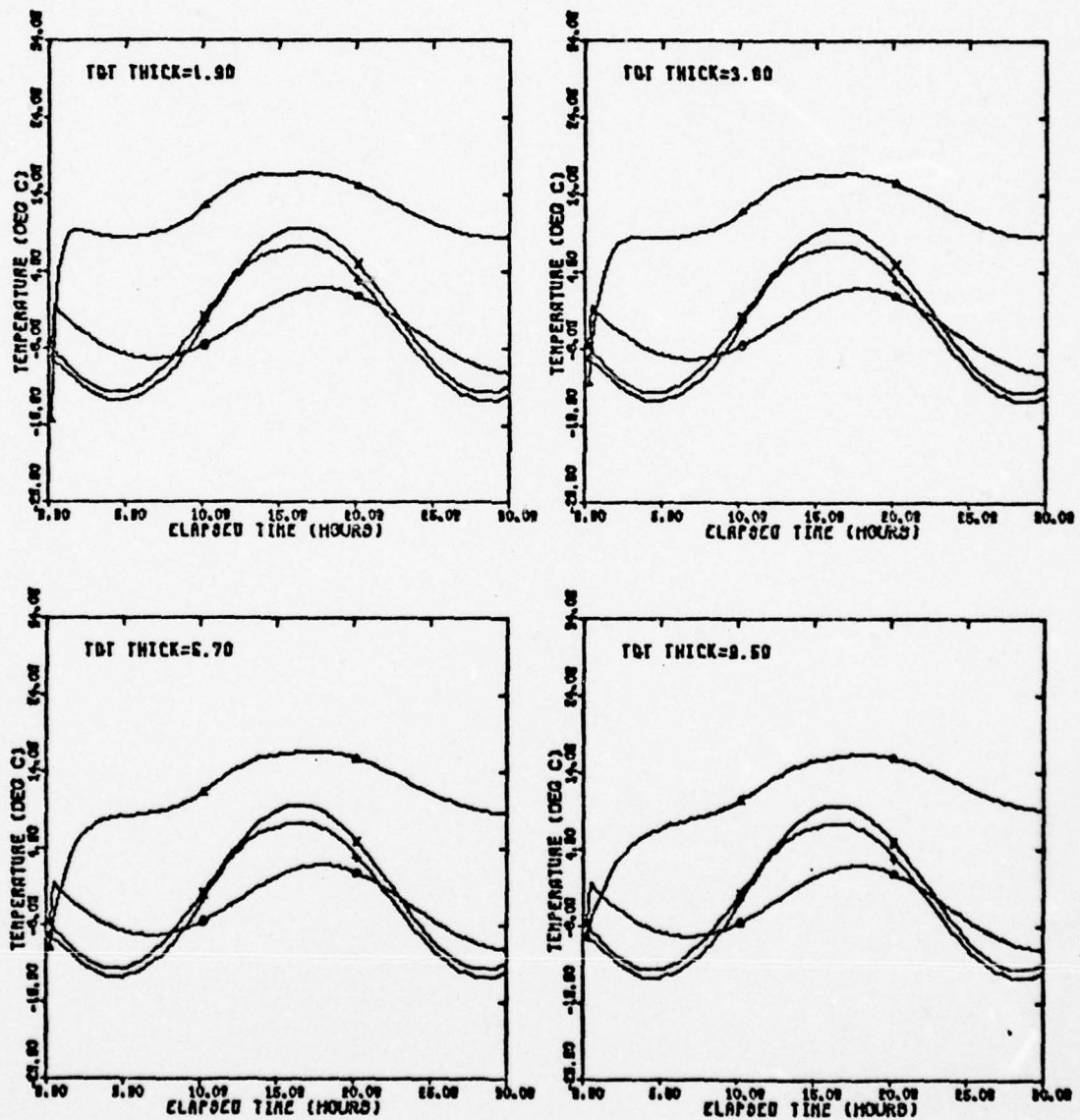


Fig. 34(h). Basic Temperature Plots of Target Thickness



PLOT SET 10/60/1

TGT THICK. RANGE  
1.50 TO 9.50 CM

▲ - TANK  
○ - GROUND  
+ - LEAF  
x - AIR

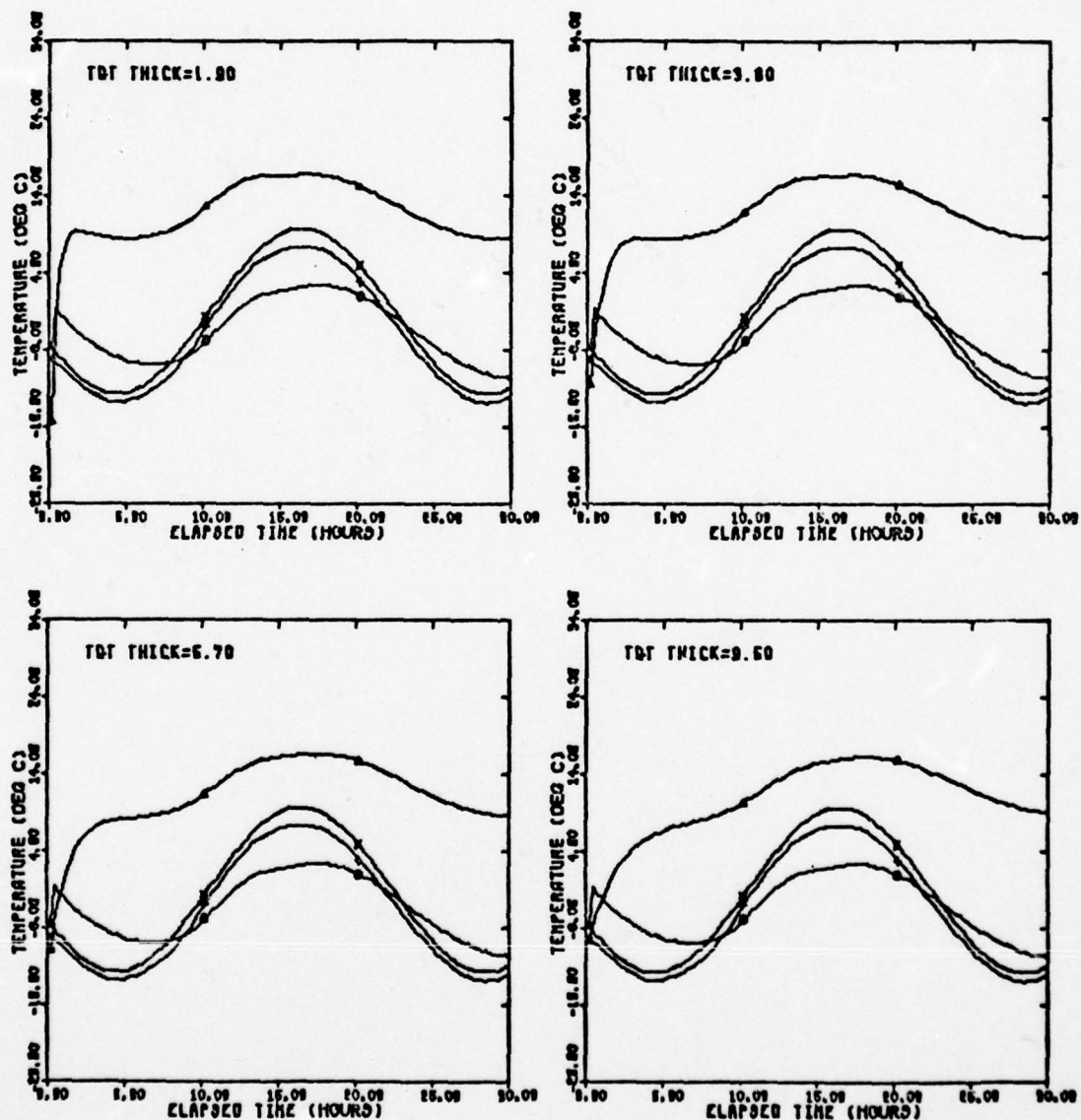


Fig. 34(1). Basic Temperature Plots of Target Thickness



PLOT SET 10/60/90

TGT THICK. RANGE  
1.90 TO 9.60 CM

Δ - TANK  
○ - GROUND  
+ - LEAF  
x - AIR

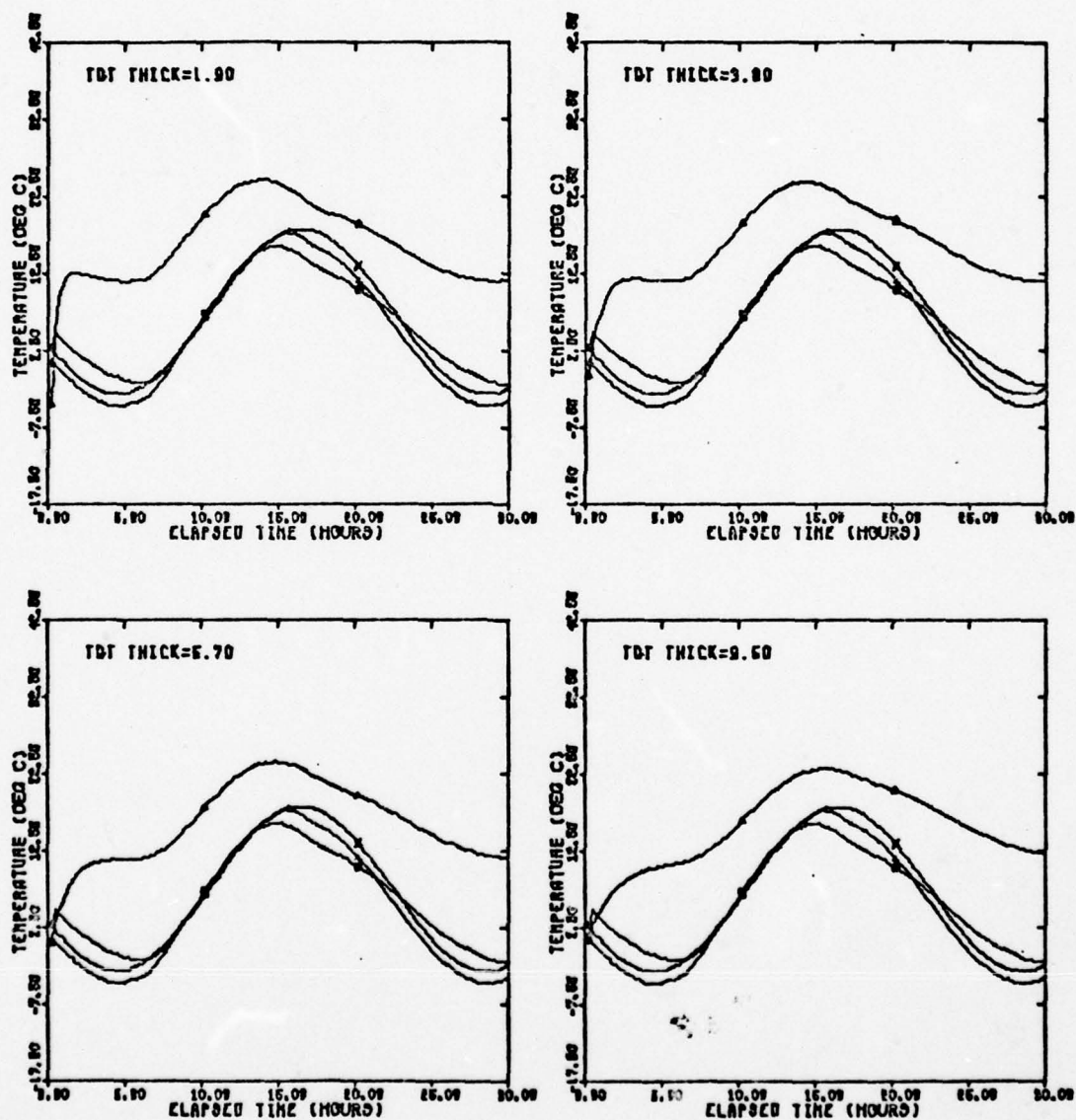


Fig. 34(j). Basic Temperature Plots of Target Thickness

PLOT SET 10/60/180

TOT THICK RANGE  
1.50 TO 9.50 CM

Δ - TANK  
○ - DRUM  
+ - LEAF  
X - AIR

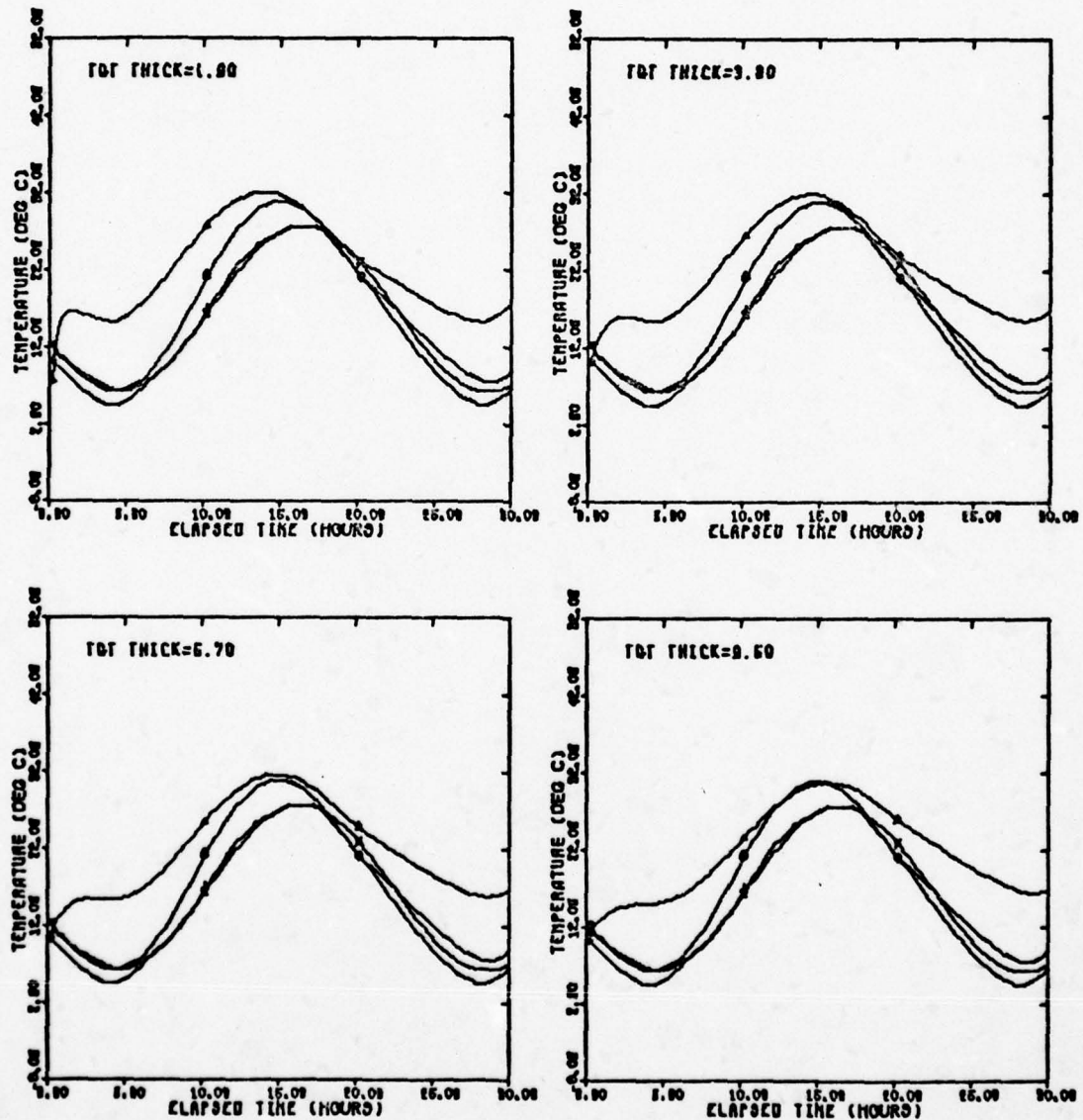


Fig. 34(k). Basic Temperature Plots of Target Thickness

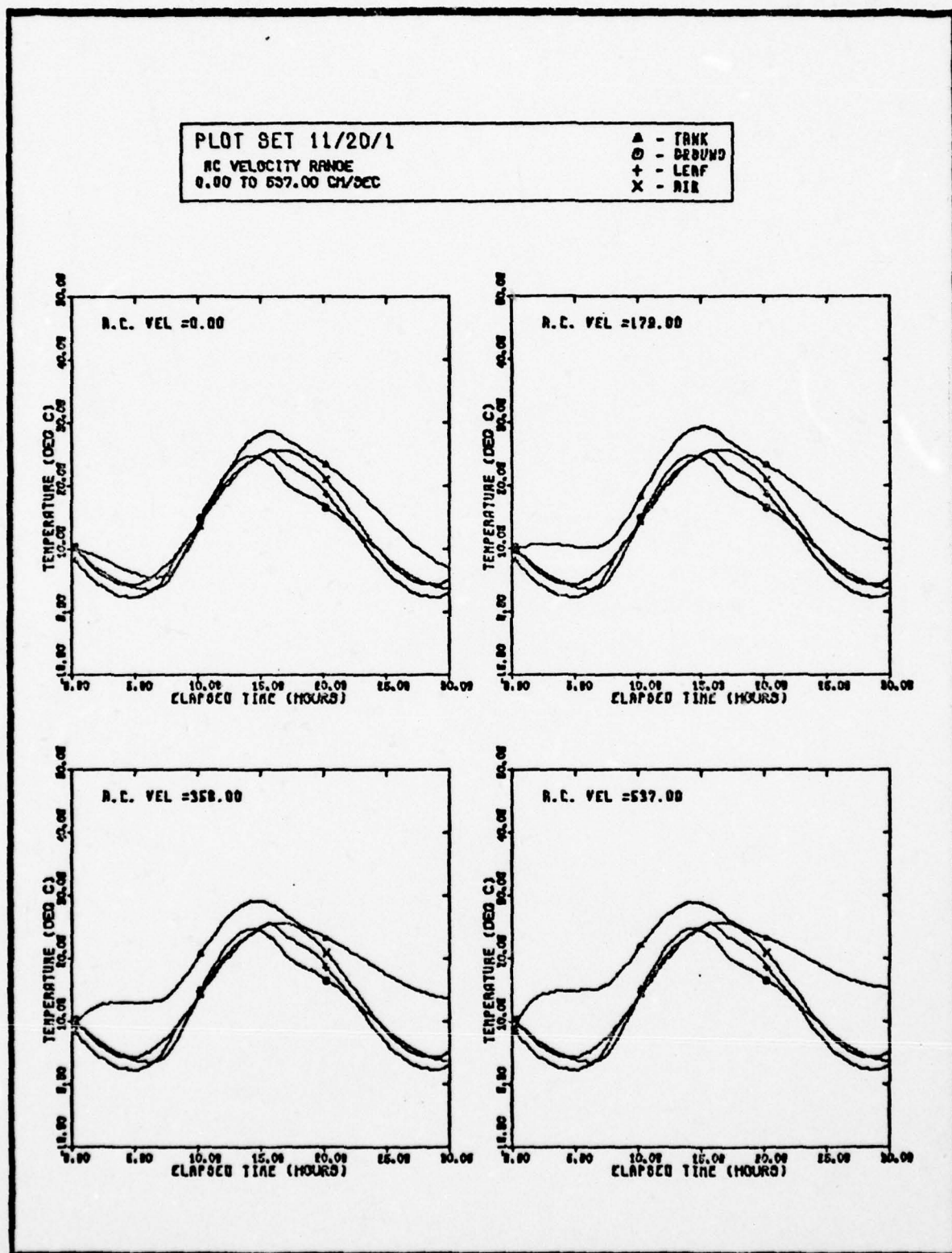


Fig. 35(a). Basic Temperature Plots of A.C. Velocity



PLOT SET 11/20/90

AC VELOCITY RANGE  
0.00 TO 537.00 CM/SEC

▲ - TRUNK  
○ - DRUM  
+ - LEAF  
x - AIR

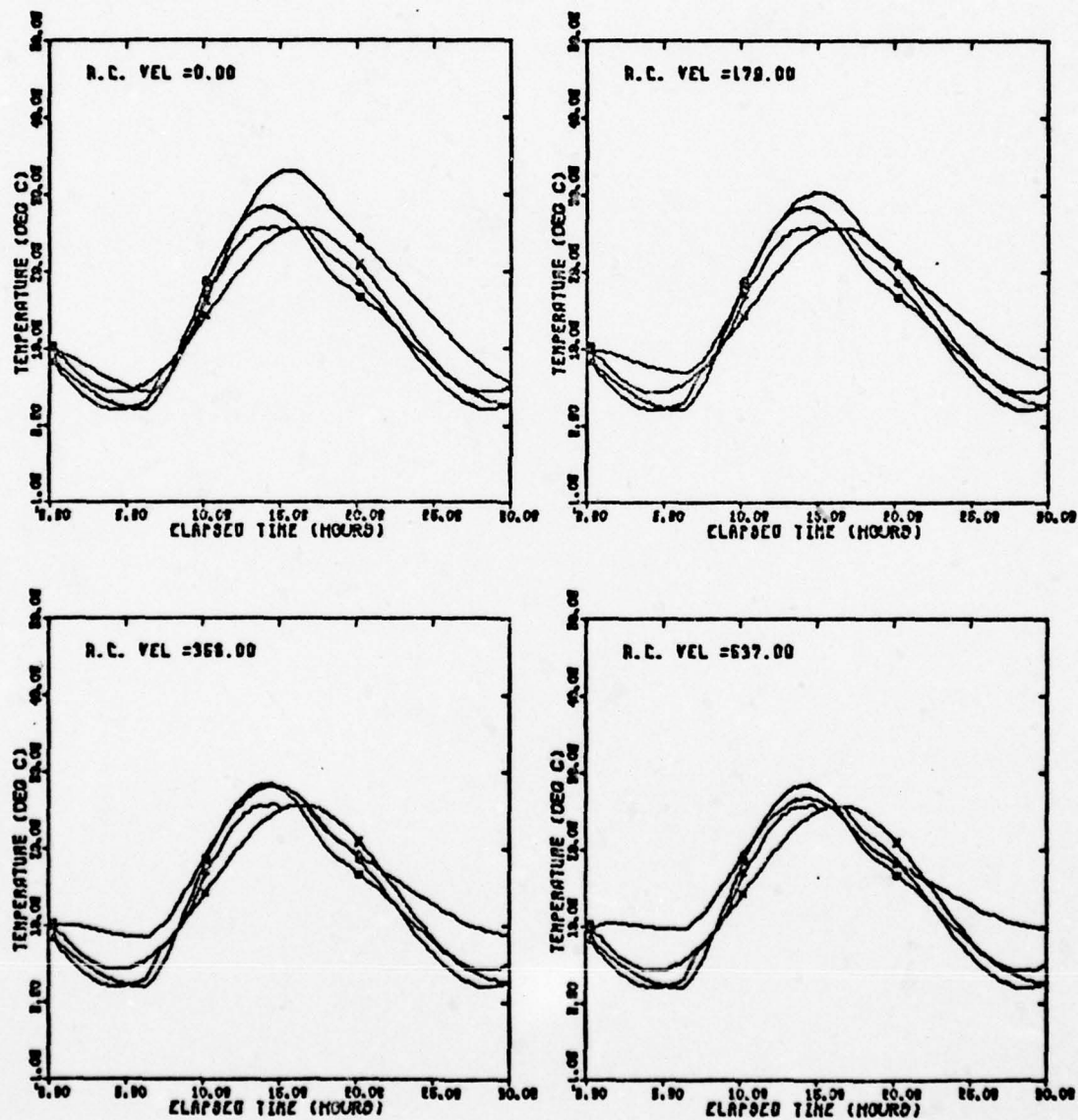


Fig. 35(b). Basic Temperature Plots of A.C. Velocity



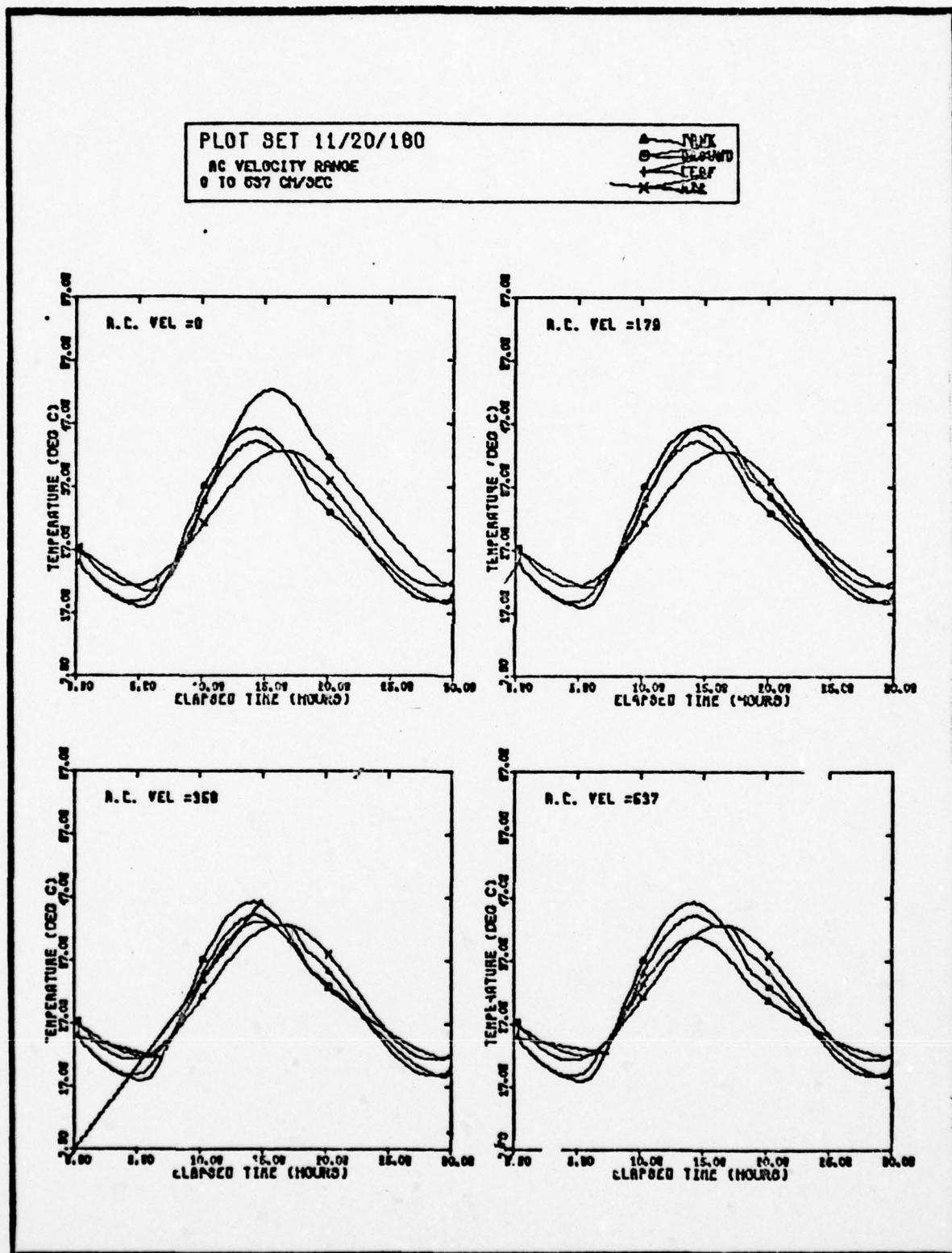


Fig. 35(c). Basic Temperature Plots of A.C. Velocity

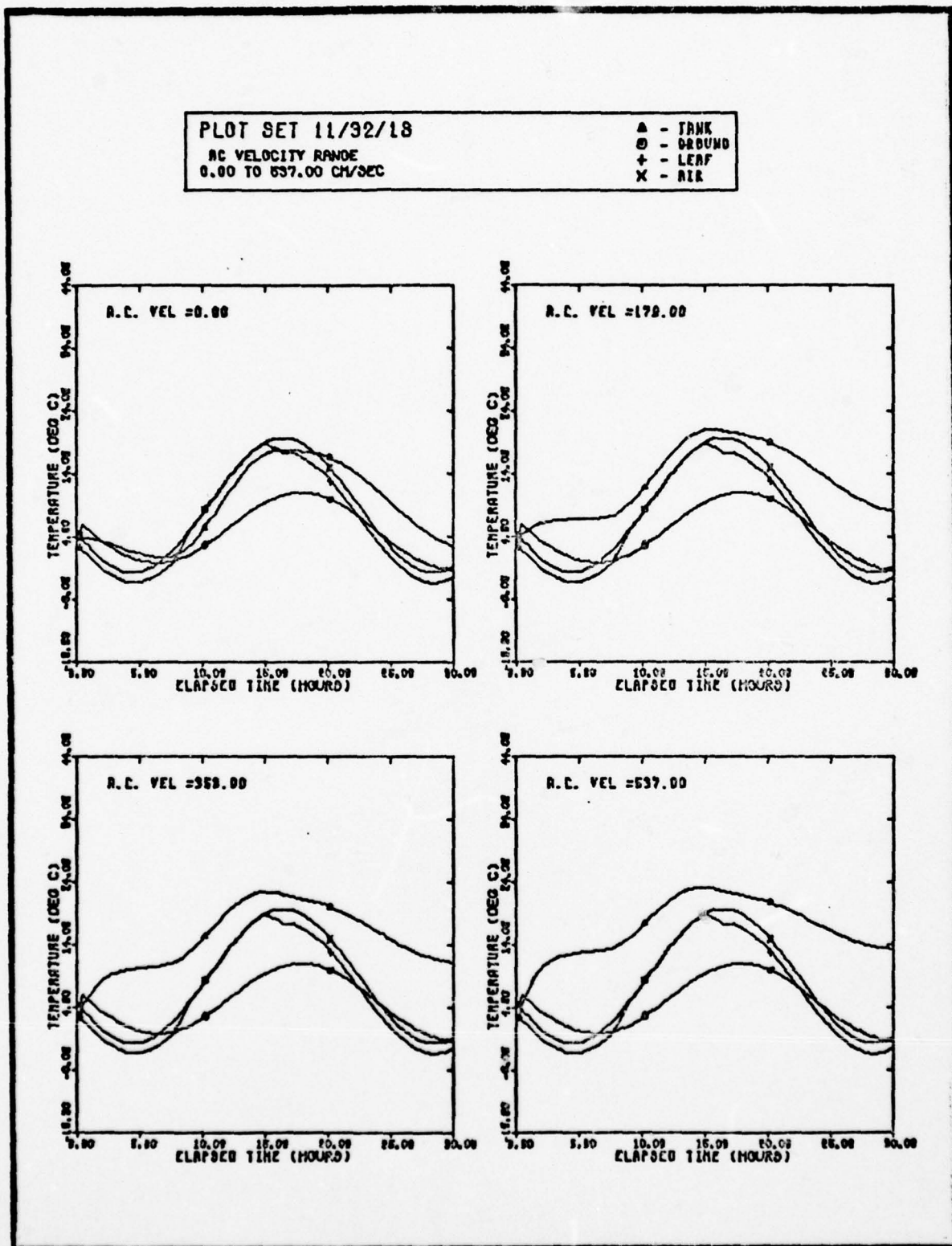


Fig. 35(d). Basic Temperature Plots of A.C. Velocity

PLOT SET 11/32/1

AC VELOCITY RANGE  
0.00 TO 537.00 CM/SEC

▲ - TANK  
○ - DRUM  
+ - LEAF  
X - AIR

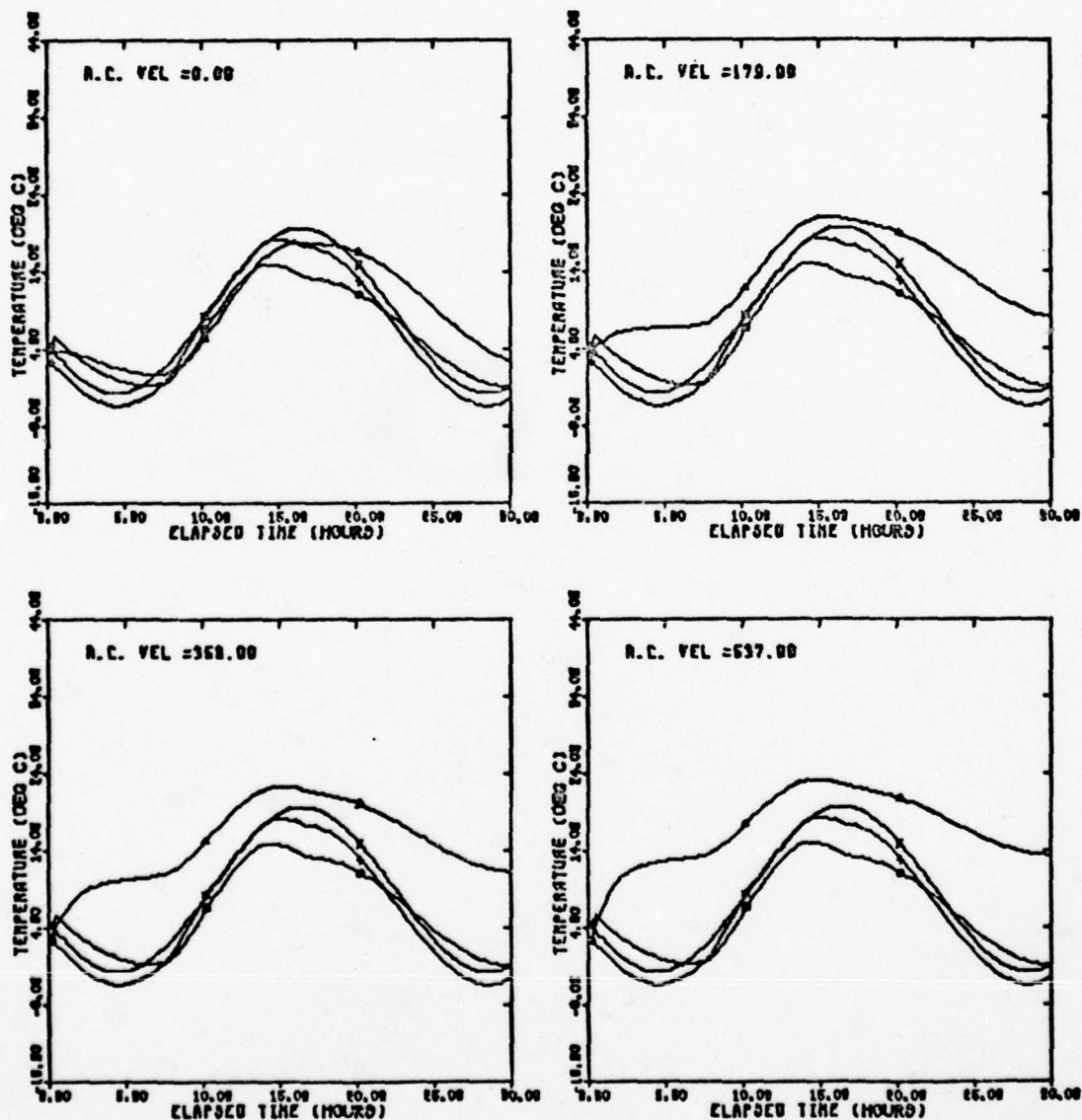


Fig. 35(e). Basic Temperature Plots of A.C. Velocity

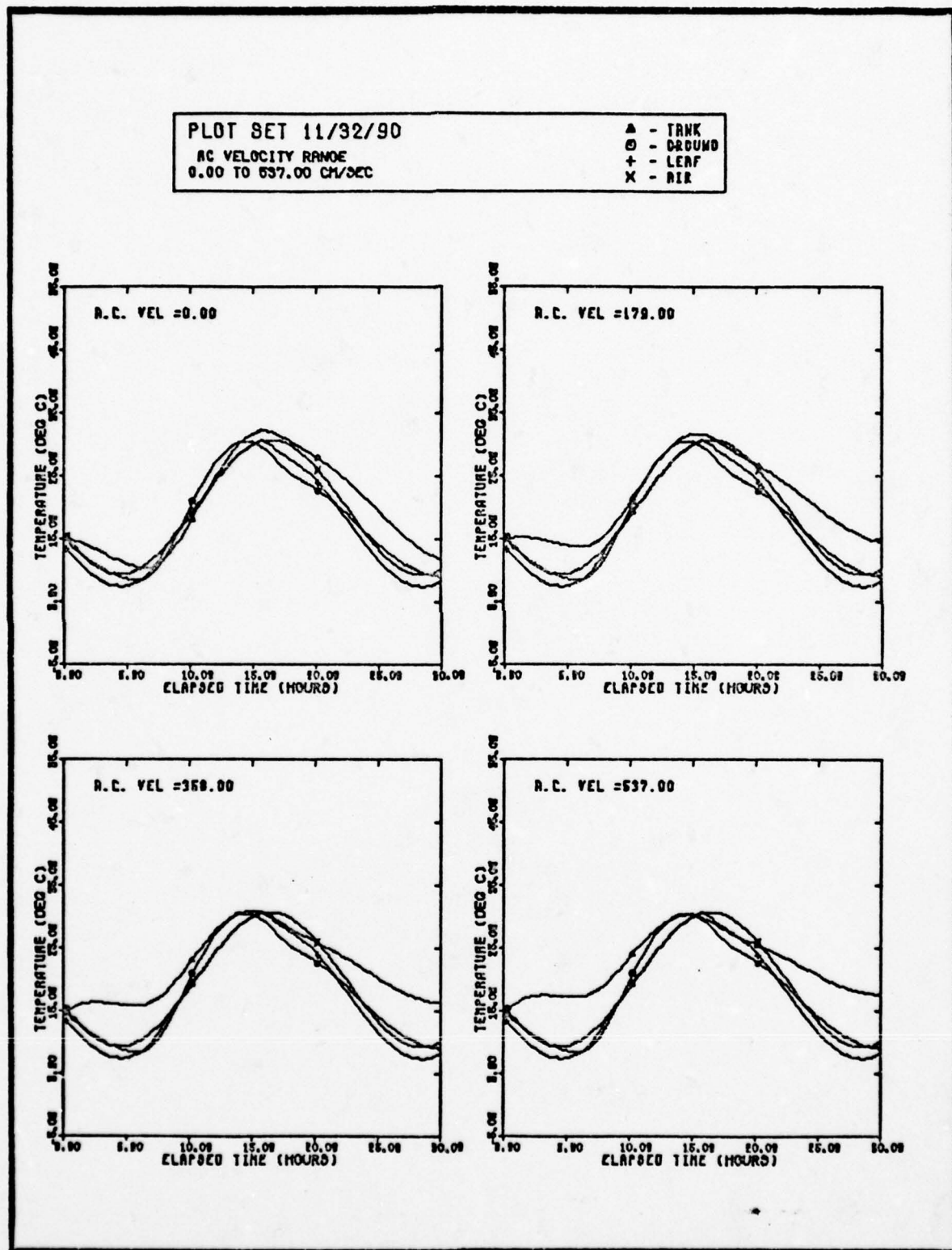


Fig. 35(f). Basic Temperature Plots of A.C. Velocity



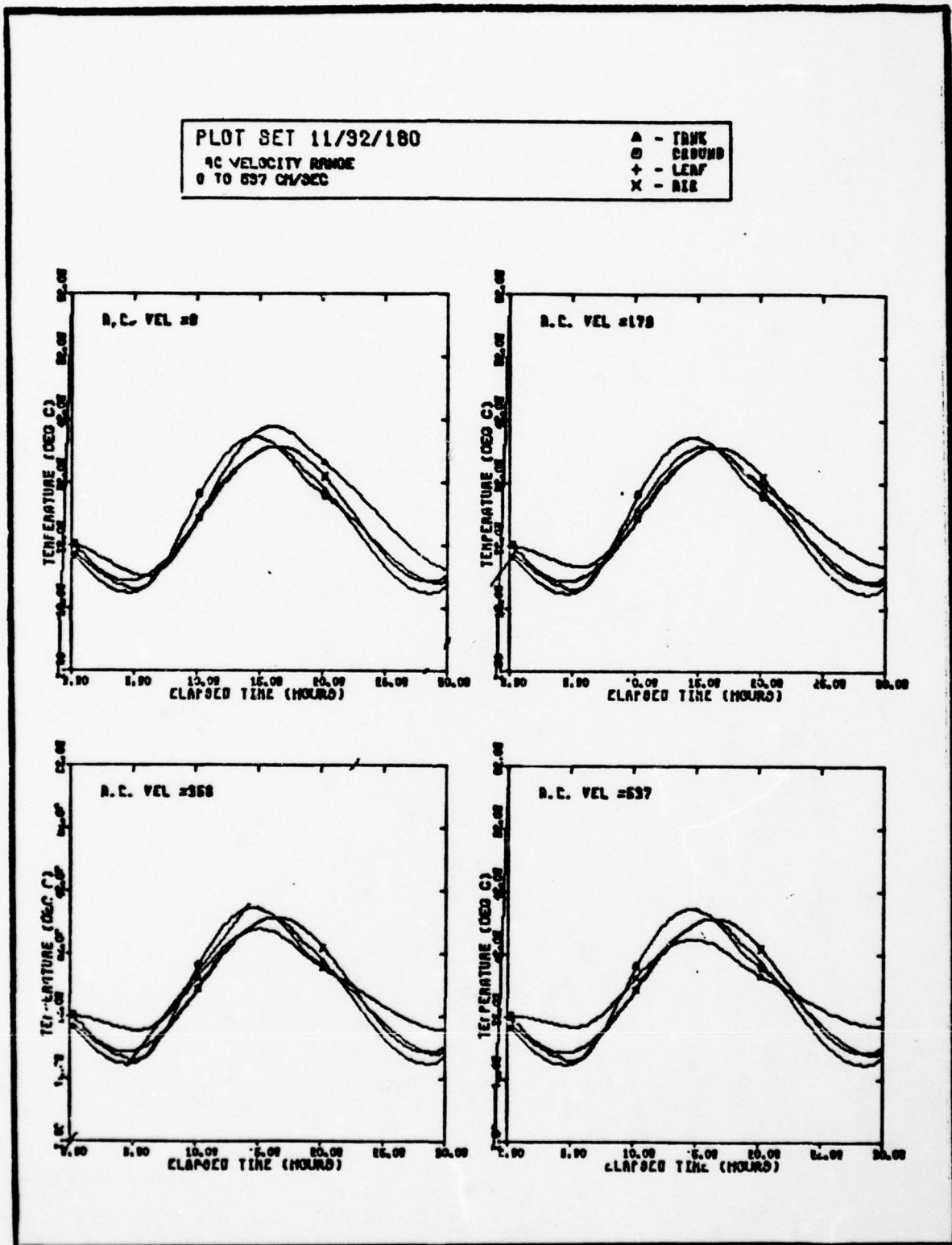


Fig. 35(g). Basic Temperature Plots of A.C. Velocity

PLOT SET 11/50/L

AC VELOCITY RANGE  
0.00 TO 537.00 CM/SEC

Δ - TRNK  
○ - GROUND  
+ - LEAF  
x - AIR

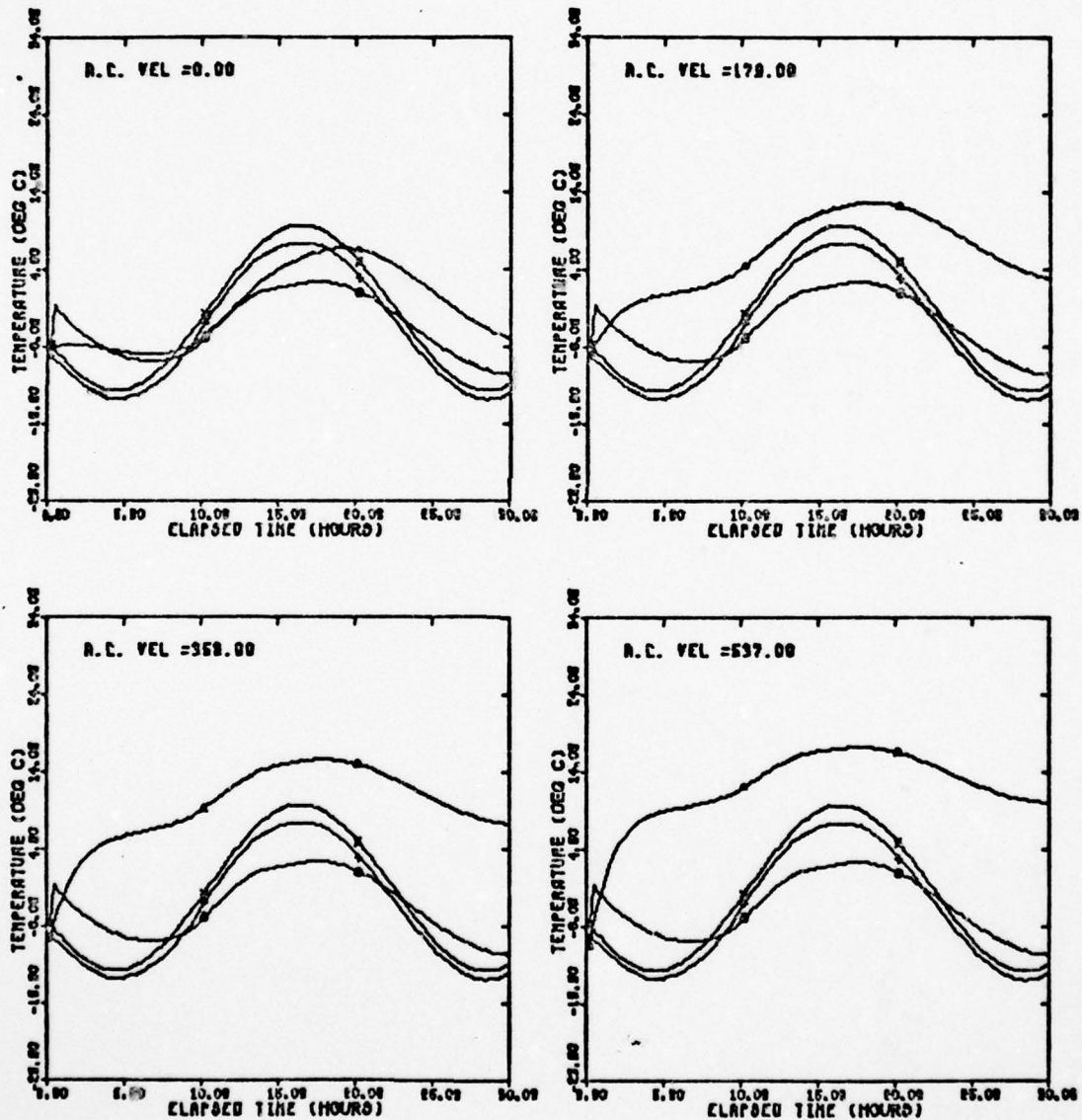


Fig. 35(h). Basic Temperature Plots of A.C. Velocity

PLOT SET 11/60/18

AC VELOCITY RANGE  
0.00 TO 537.00 CM/SEC

▲ - TANK  
○ - GROUND  
+ - LEAF  
X - AIR

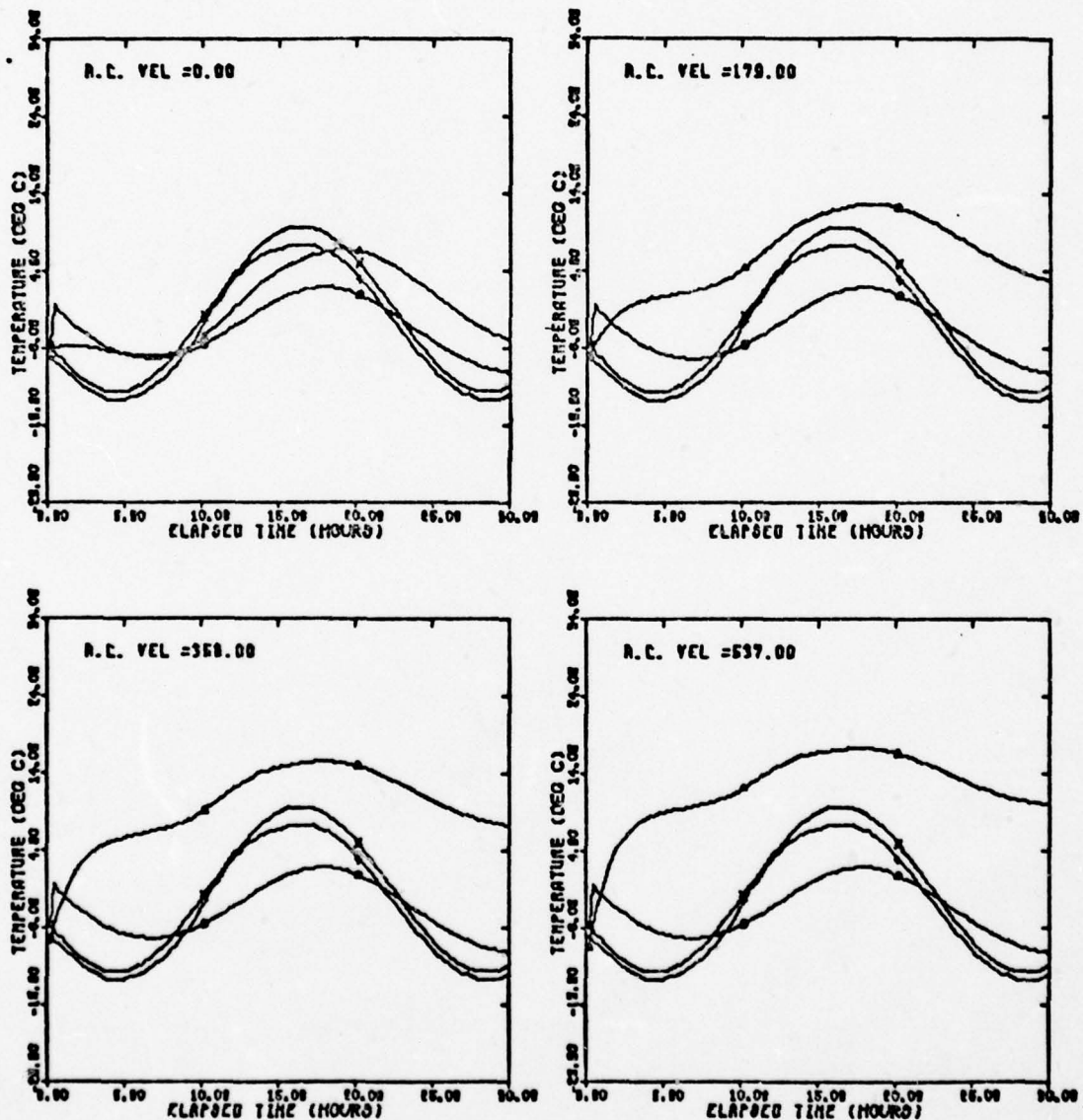


Fig. 35(1). Basic Temperature Plots of A.C. Velocity

PLOT SET 11/60/90

AC VELOCITY RANGE  
0.00 TO 637.00 CM/SEC

△ - TRNK  
○ - DRUMD  
+ - LEAF  
X - AIR

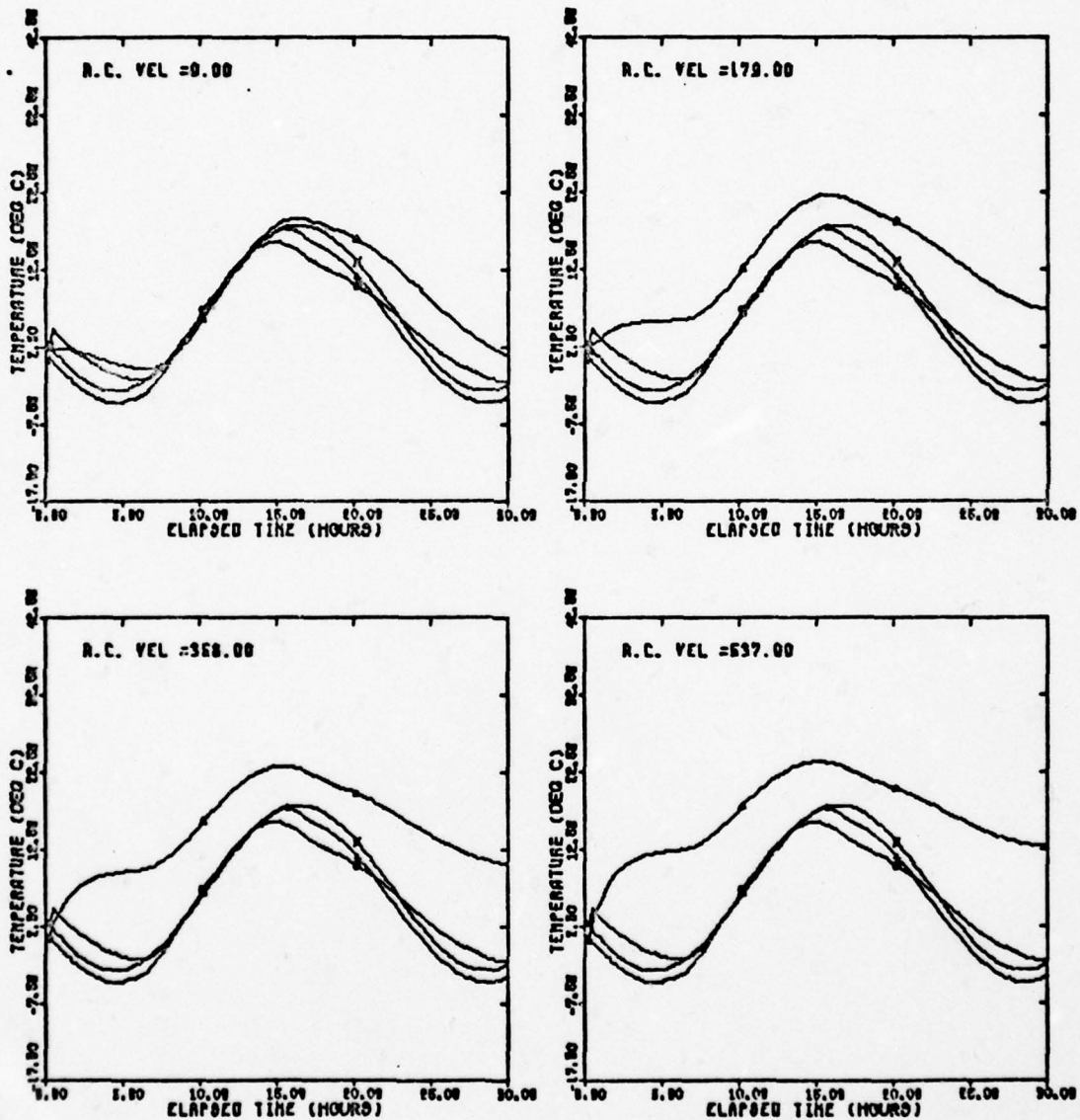


Fig. 35(j). Basic Temperature Plots of A.C. Velocity



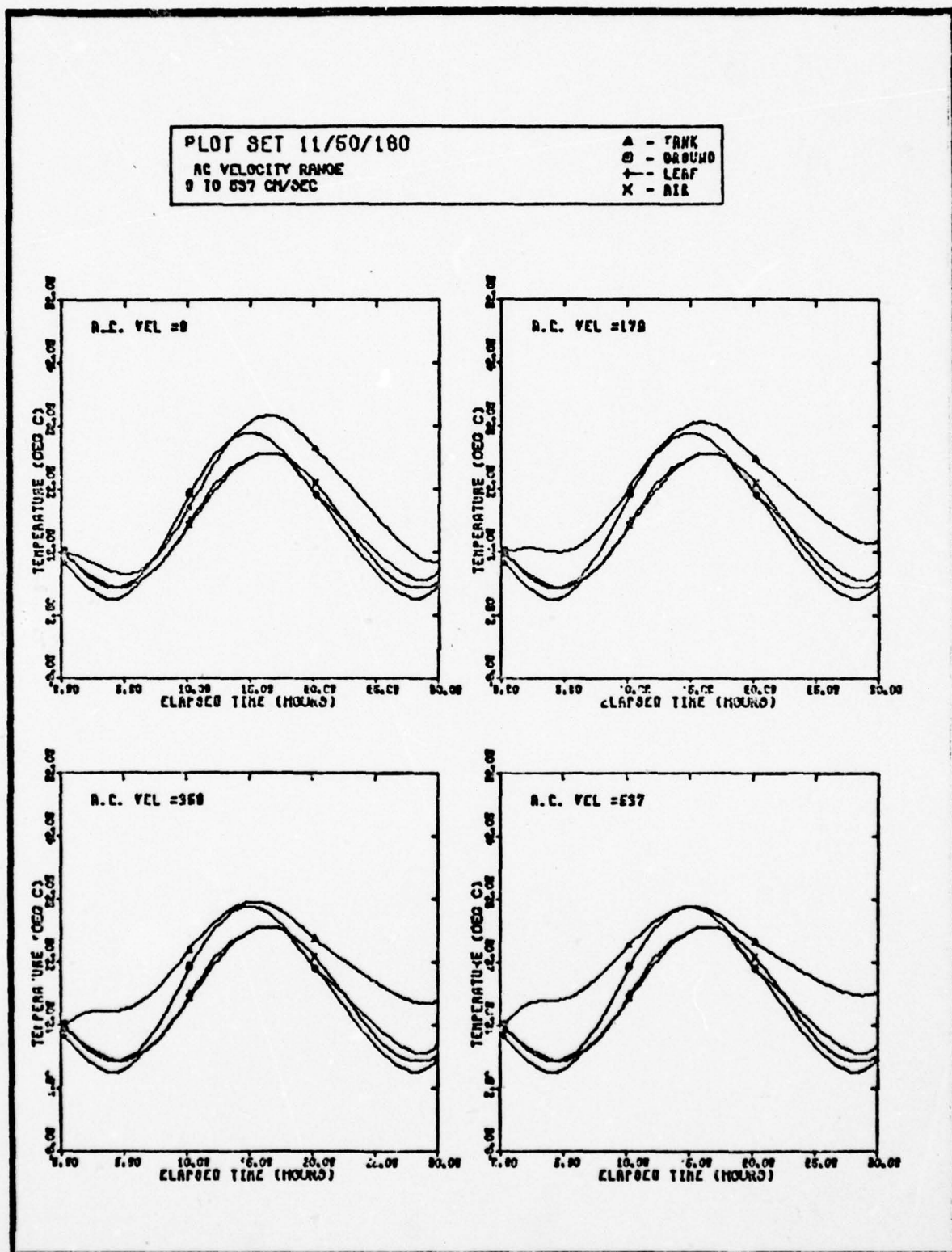


Fig. 35(k). Basic Temperature Plots of A.C. Velocity

## Appendix D

### Plots from Program DELTA for all Parameters

Figs. 36(a)-36(d) are plots of the parameter Mean Temperature. Figs. 37(a)-37(d) are plots of the parameter Absolute Humidity. Figs. 38(a)-38(d) are plots of the parameter Wind. Figs. 39(a)-39(d) are plots of the parameter Sun Strength. Figs. 40(a)-40(d) are plots of the parameter Ground Reflectivity. Figs. 41(a)-41(d) are plots of the parameter Ground Emmissivity. Figs. 42(a)-42(d) are plots of the parameter Ground Diffusivity. Figs. 43(a)-43(d) are plots of the parameter Target Reflectivity. Figs. 44(a)-44(d) are plots of the parameter Target Emmissivity. Figs. 45(a)-45(d) are plots of the parameter Target Thickness. Figs. 46(a)-46(d) are plots of the parameter Internal Air Conditioning Velocity.

DELTA-T (TARGET-GROUND)  
PARAMETER-MEANTEMP JULIAN DAY-18

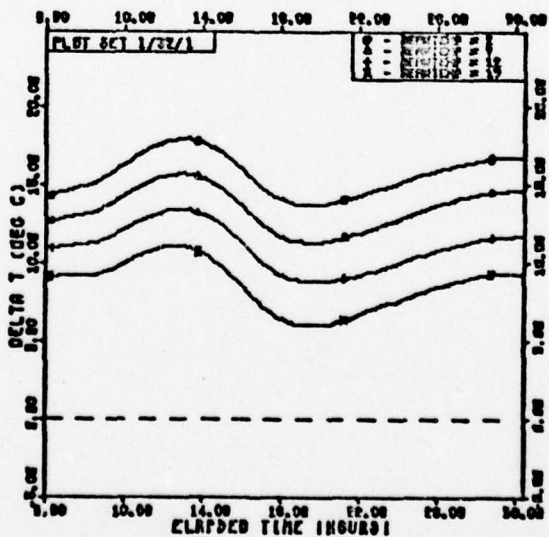
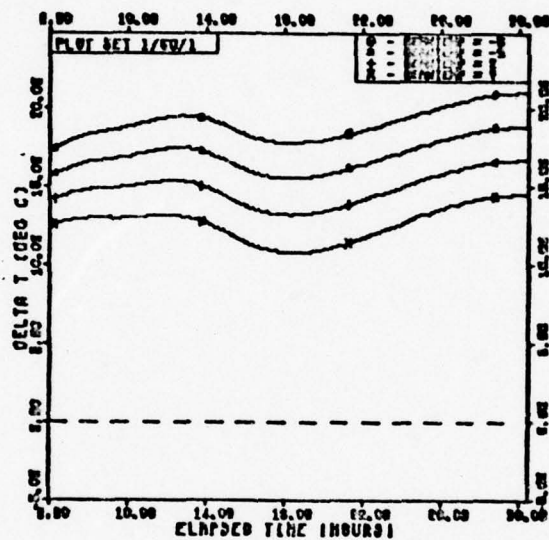


Fig. 36(a). Delta-T Plots for Meantemp

DELTA-T (TARGET-GROUND)  
PARAMETER-MEANTEMP JULIAN DAY-1

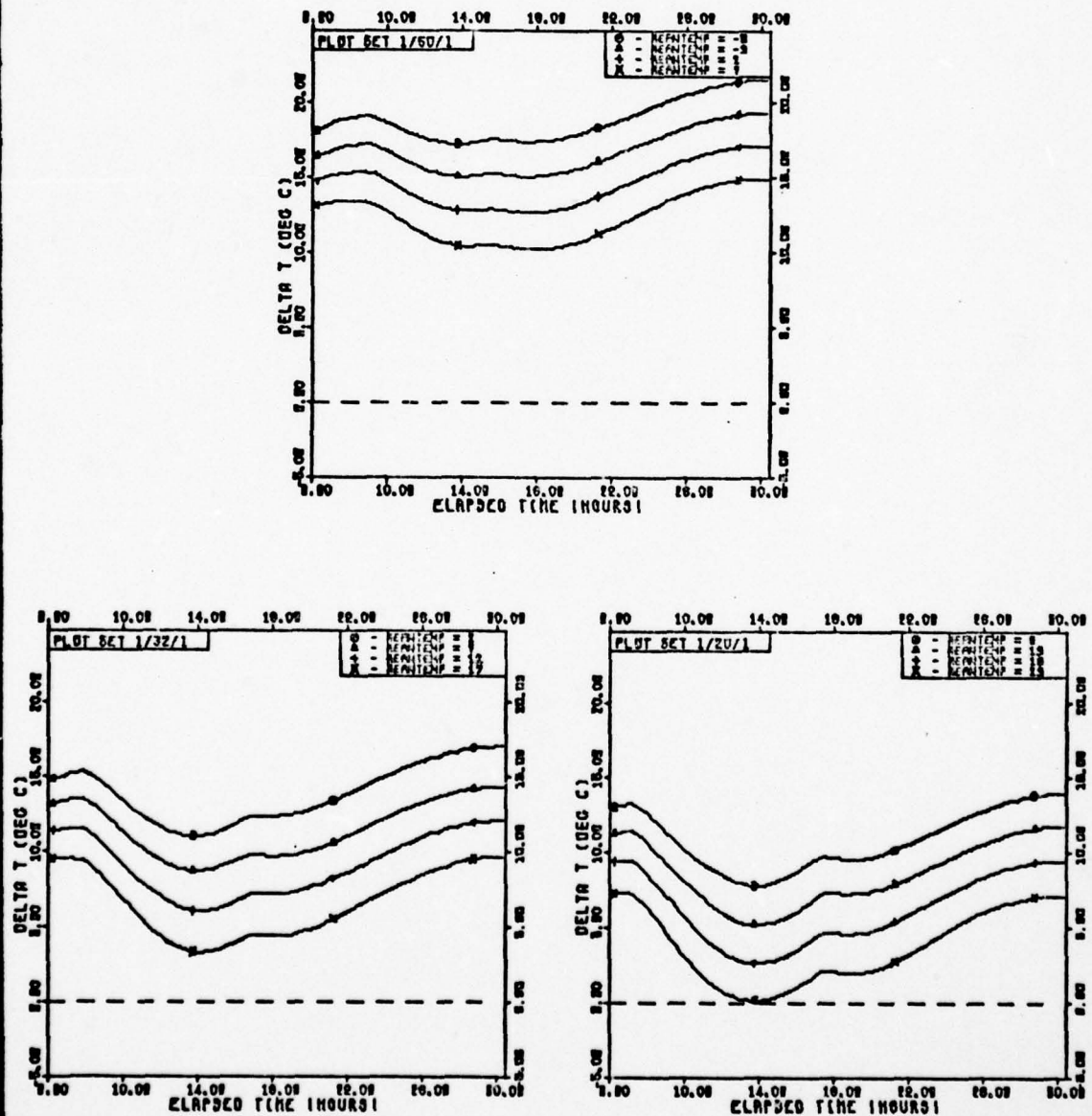
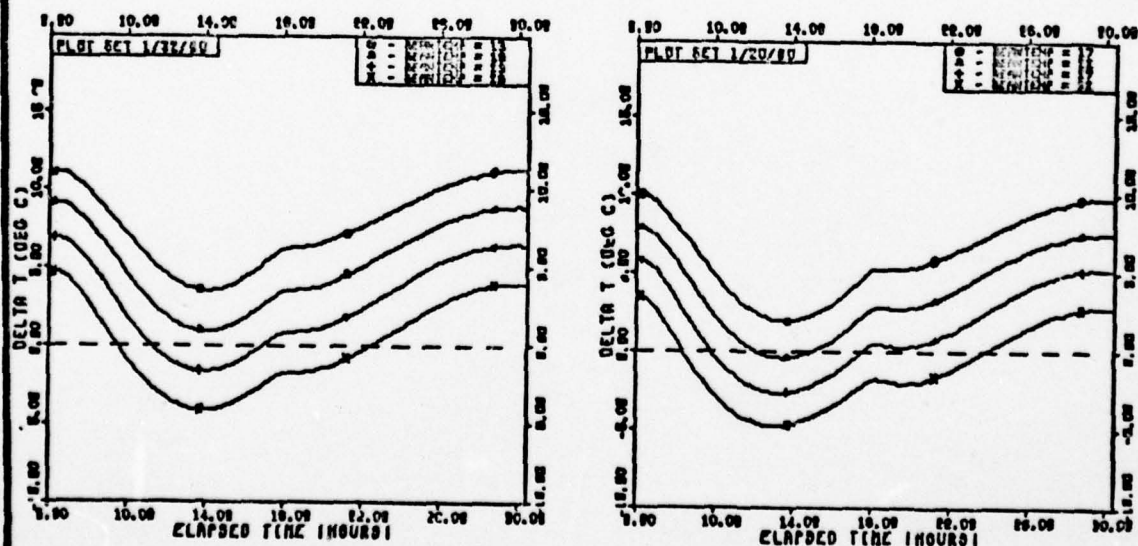


Fig. 36(b). Delta-T Plots for Meantemp



## JULIAN DAY-90



212

DELTA-T (TARGET-GROUND)  
PARAMETER-MEANTEMP JULIAN DAY-180

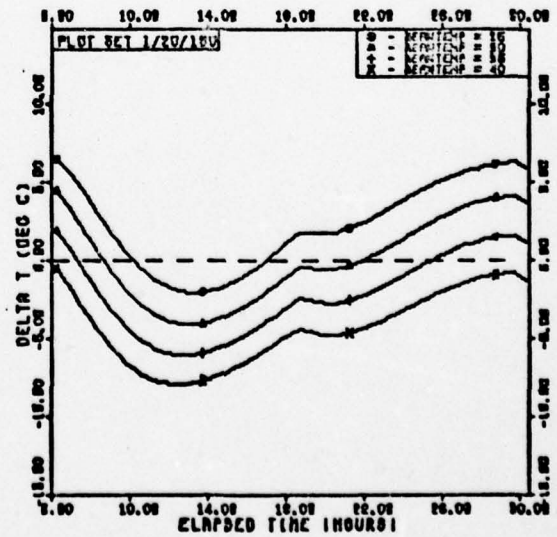
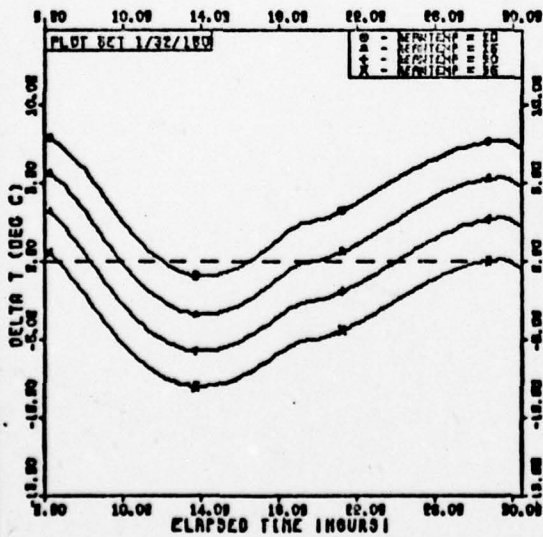
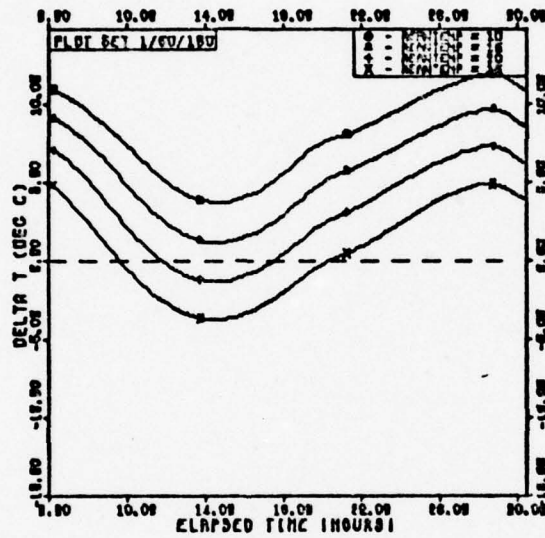
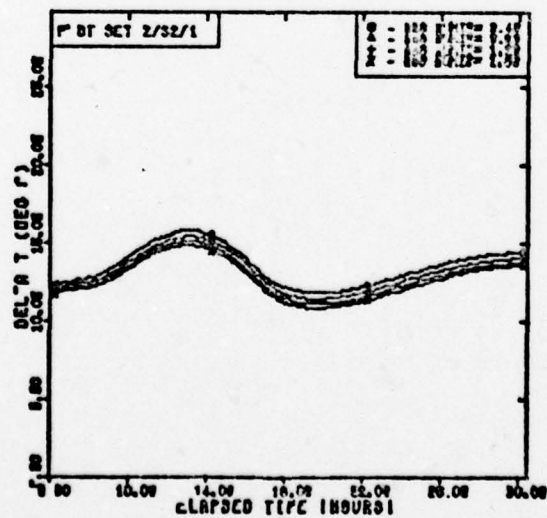
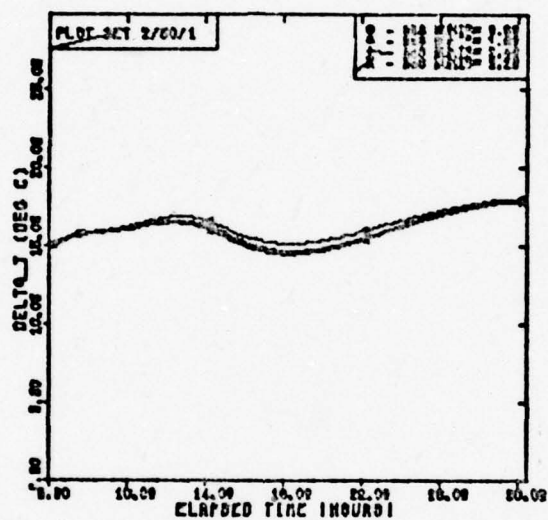


Fig. 36(d). Delta-T Plots for Meantemp

## PARAMETER-ABS. NUM. JULIAN DAY 18



DELTA-T (TARGET-GROUND)  
 PARAMETER-ABS. HUM. JULIAN DAY-1

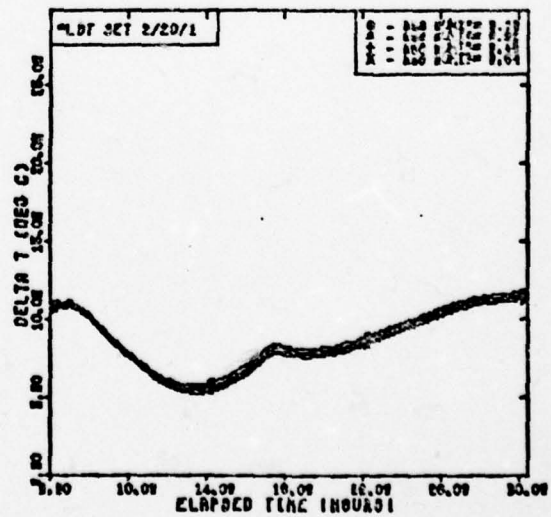
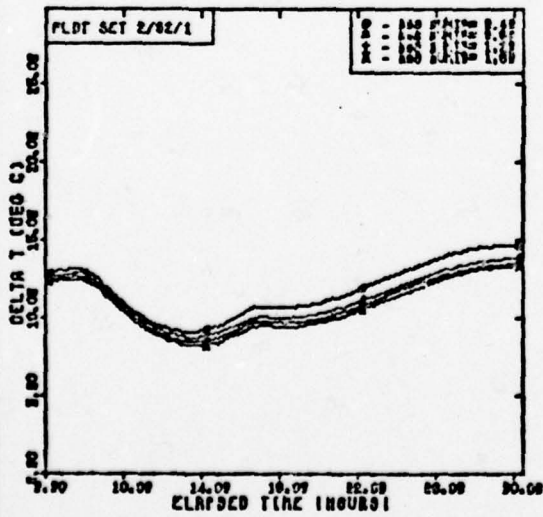
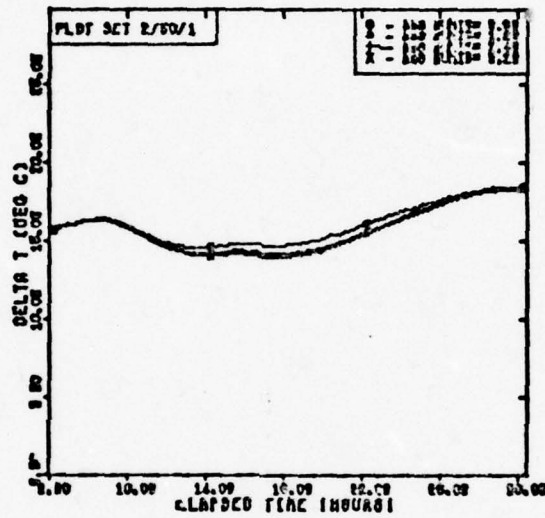


Fig. 37(b). Delta-T Plots for Absolute Humidity



DELTA-T (TARGET-GROUND)  
PARAMETER-ABS. HUM. JULIAN DAY-00

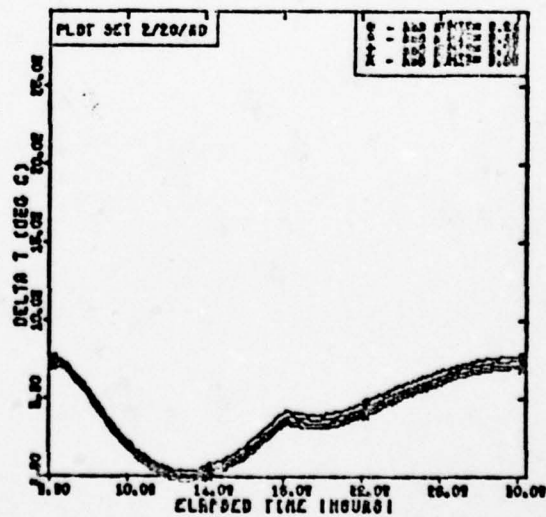
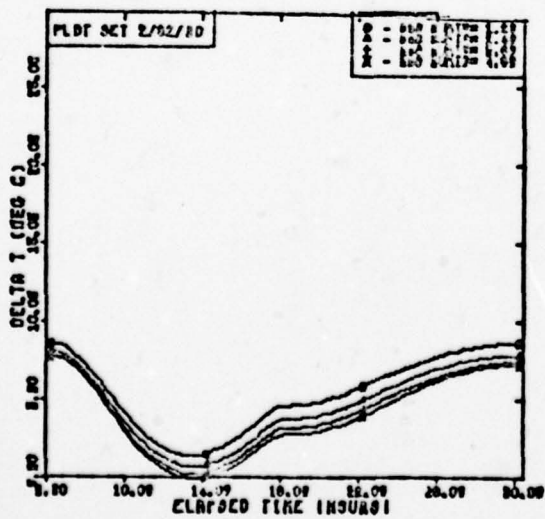
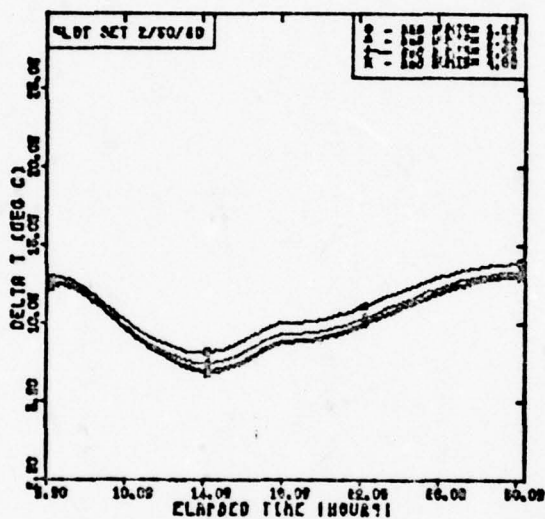


Fig. 37(c). Delta-T Plots for Absolute Humidity

DELTA-T (TARGET-GROUND)  
 PARAMETER-ABS. HUM. JULIAN DAY-180

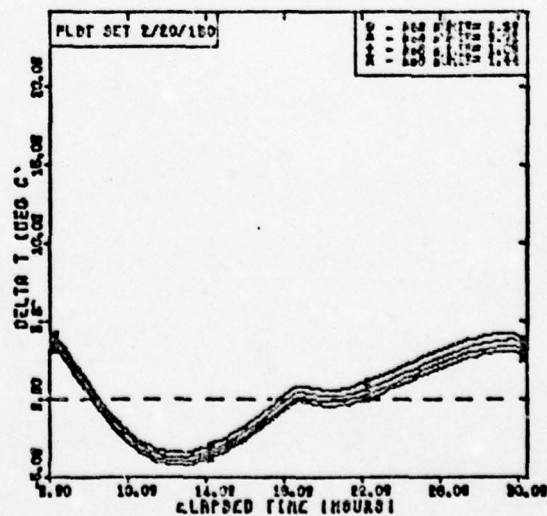
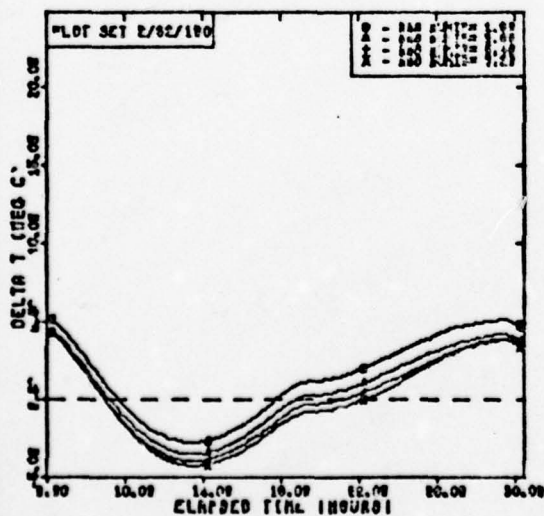
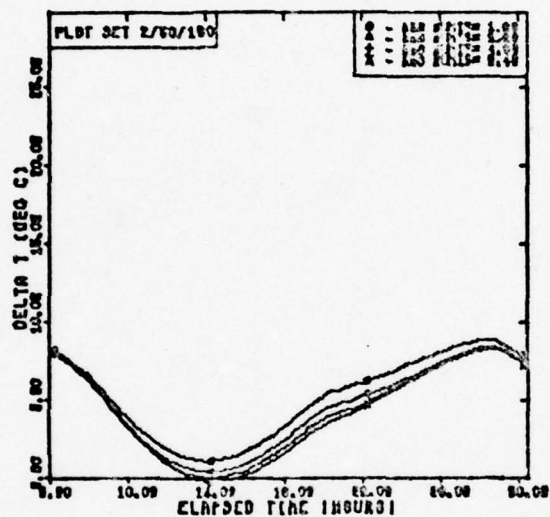


Fig. 37(d). Delta-T Plots for Absolute Humidity

DELTA-T (TARGET-GROUND)  
 PARAMETER- WIND JULIAN DAY-15

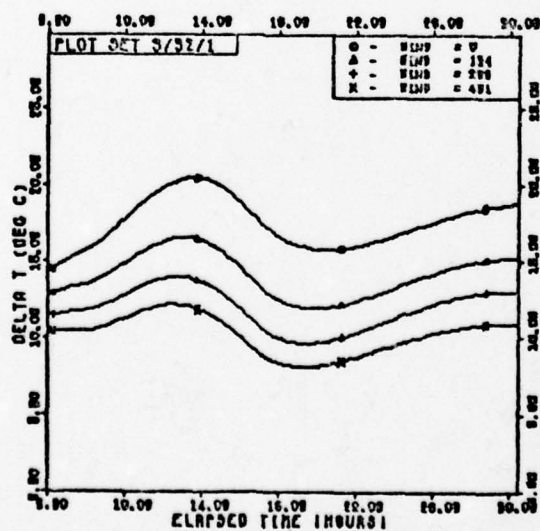
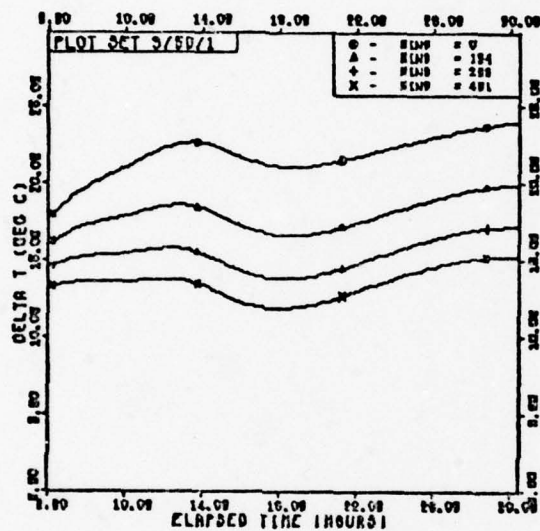


Fig. 38(a). Delta-T Plots for Wind

DELTA-T (TARGET-GROUND)  
 PARAMETER- WIND JULIAN DAY-1

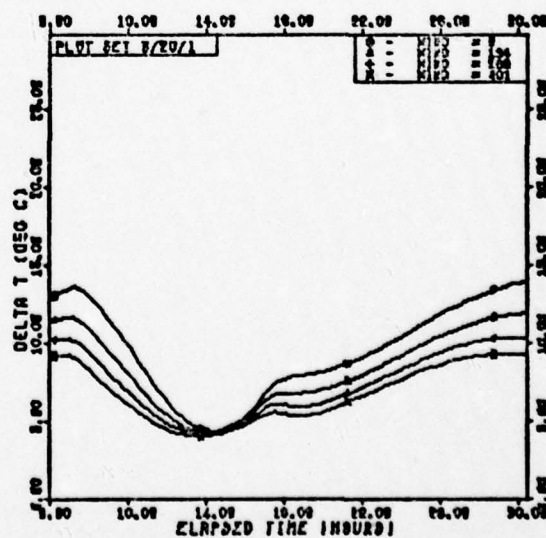
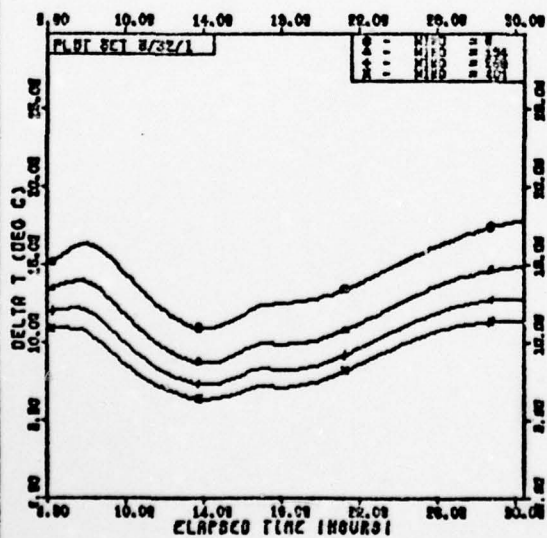
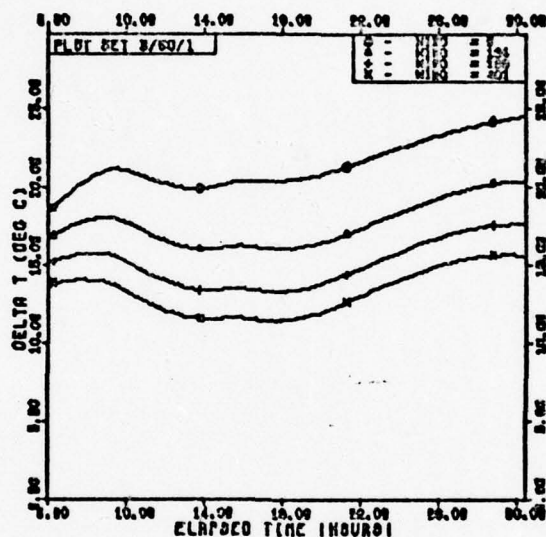


Fig. 38(b). Delta-T Plots for Wind



DELTA-T (TARGET-GROUND)  
 PARAMETER- WIND JULIAN DAY-00

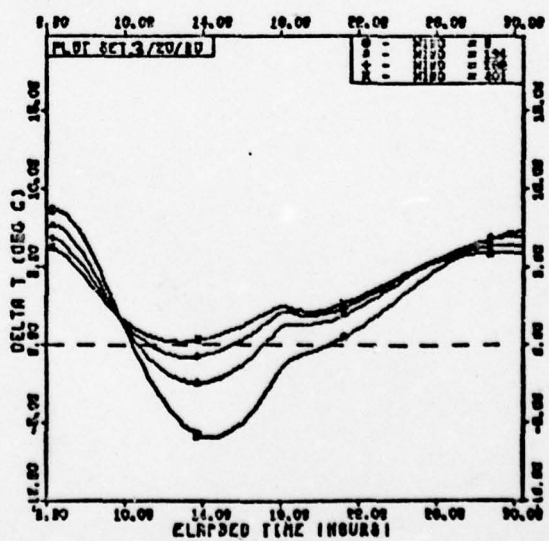
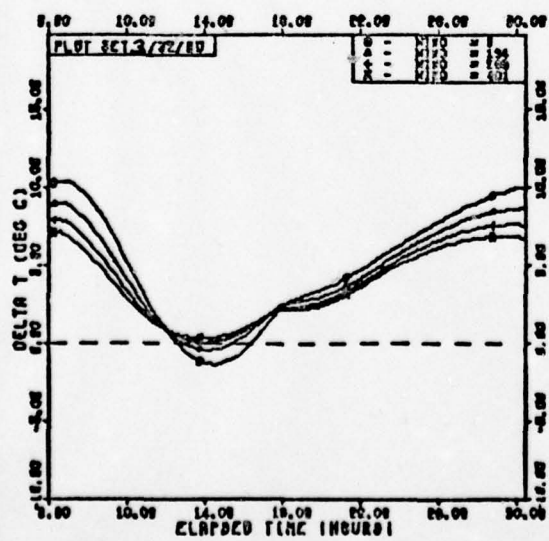
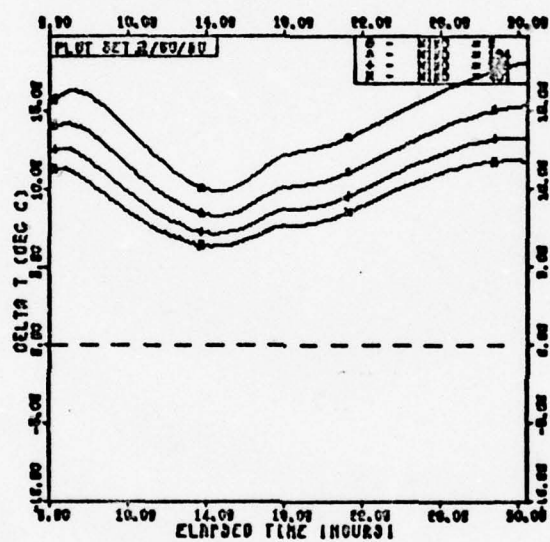


Fig. 38(c). Delta-T Plots for Wind

PARAMETER- MIND

**JULIAN DAY-180**

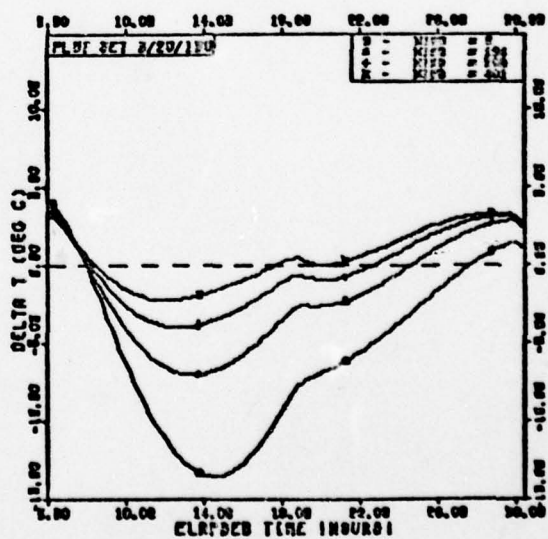
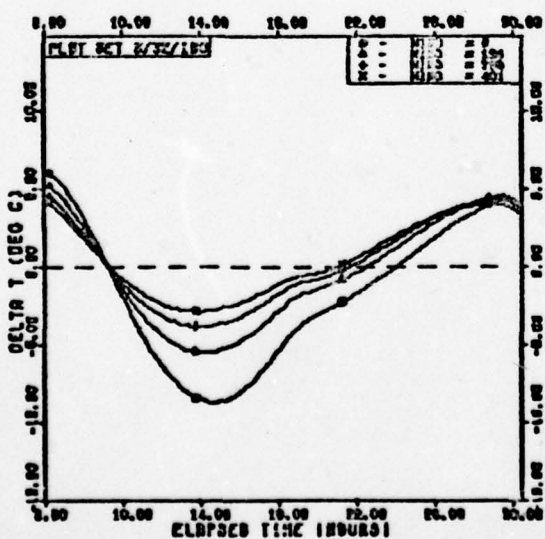
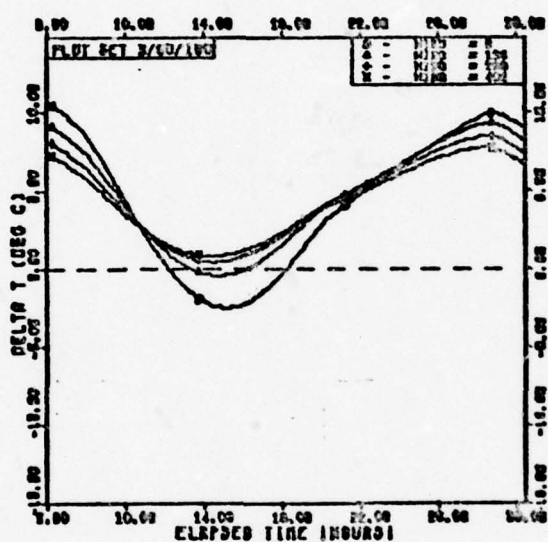


Fig. 38(d). Delta-T Plots for Wind

DELTA-T (TARGET-GROUND)  
PARAMETER-SUN STRENGTH JULIAN DAY-18

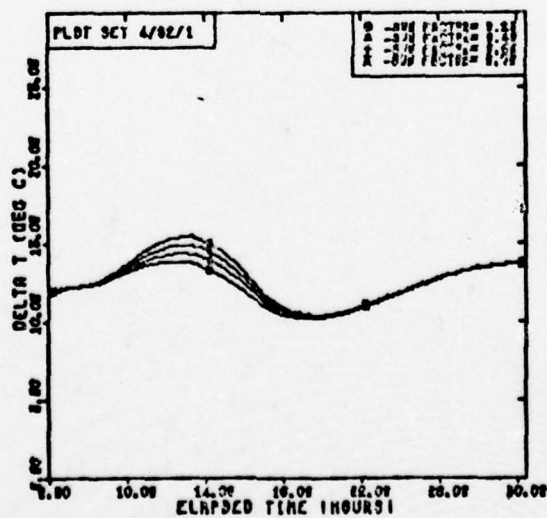
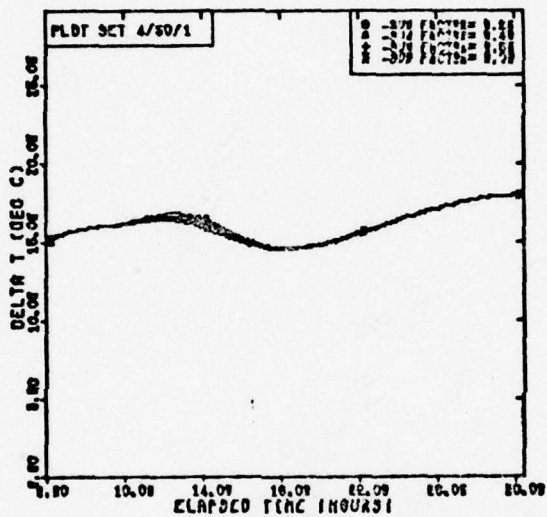


Fig. 39(a). Delta-T Plots for Sun Strength

DELTA-T (TARGET-GROUND)  
PARAMETER-SUN STRENGTH JULIAN DAY-1

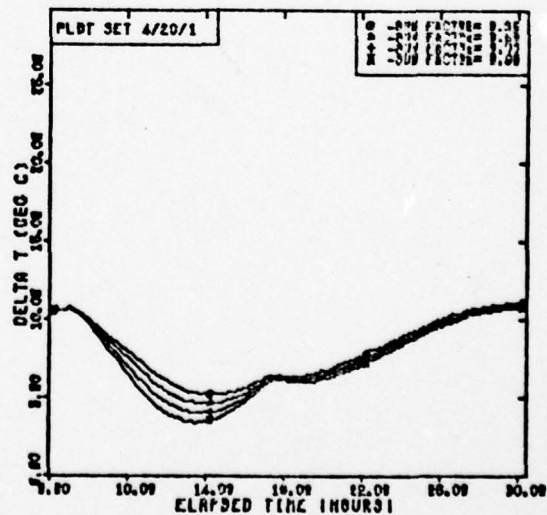
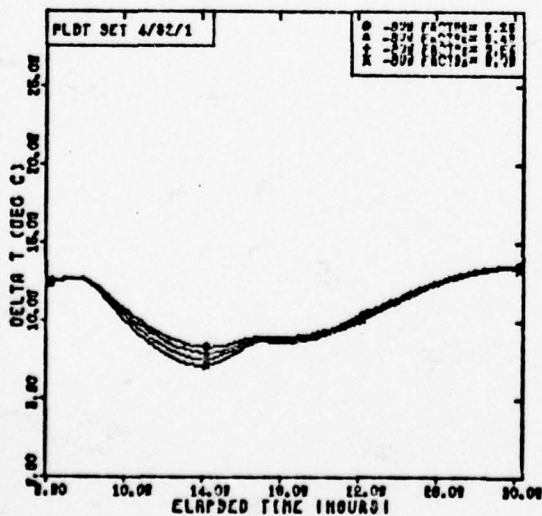
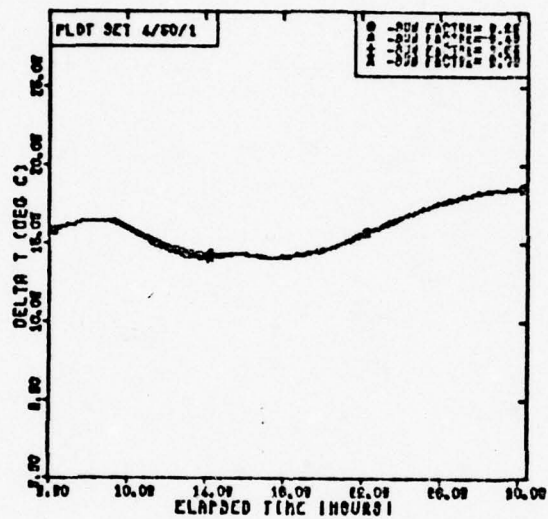


Fig. 39(b). Delta-T Plots for Sun Strength



DELTA-T (TARGET-GROUND)  
PARAMETER-SUN STRENGTH JULIAN DAY-90

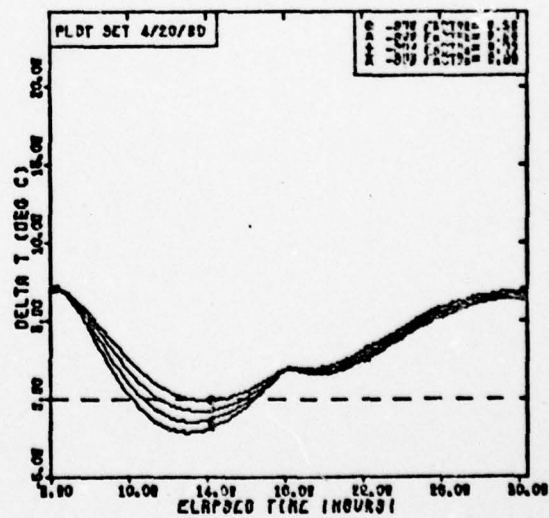
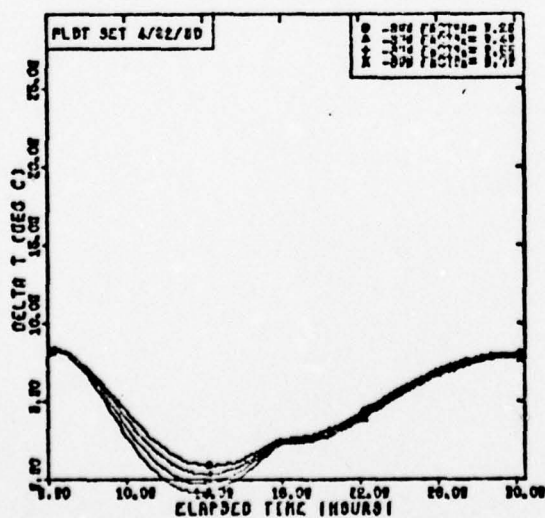
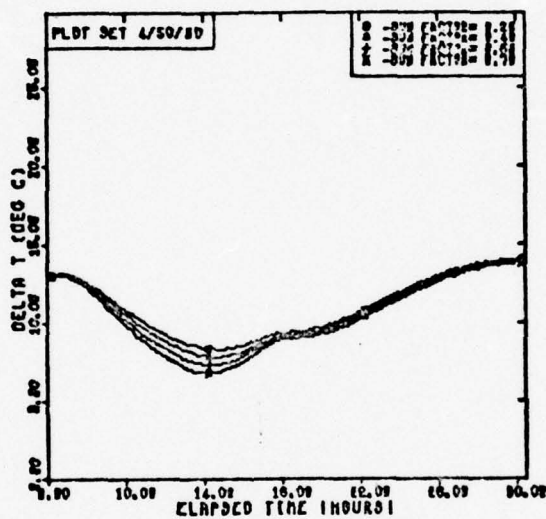


Fig. 39(c). Delta-T Plots for Sun Strength

DELTA-T (TARGET-GROUND)  
PARAMETER-SUN STRENGTH JULIAN DAY-180

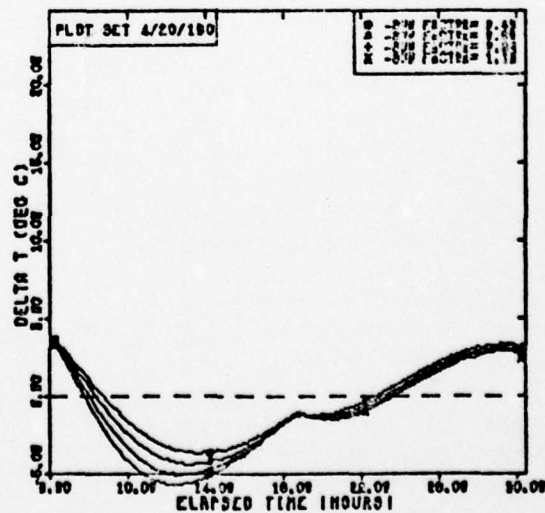
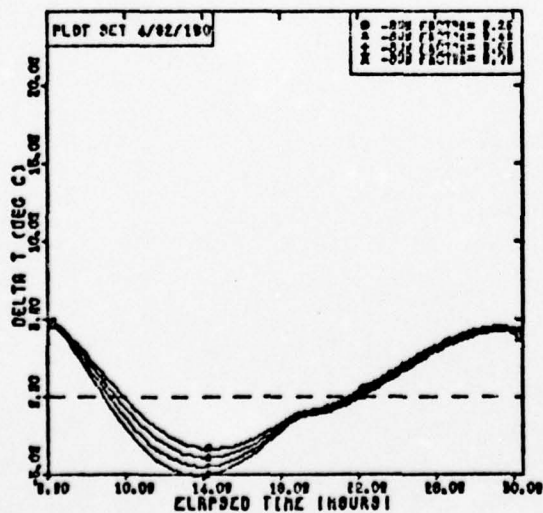
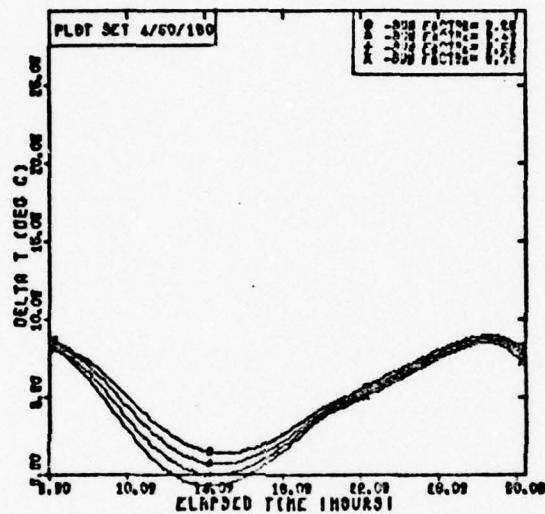


Fig. 39(d). Delta-T Plots for Sun Strength

DELTA-T (TARGET-GROUND)  
PARAMETER-ORND REFL JULIAN DAY-18

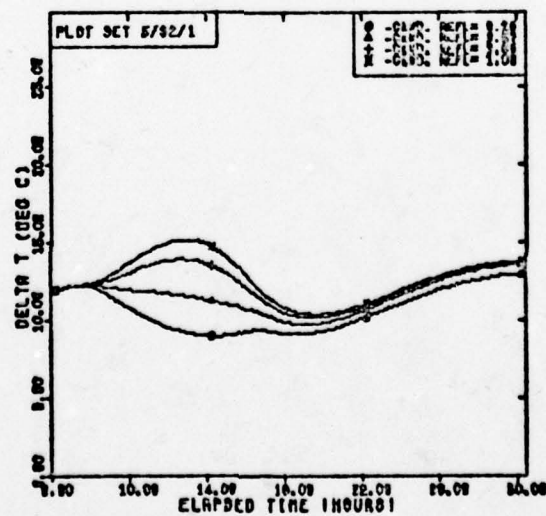
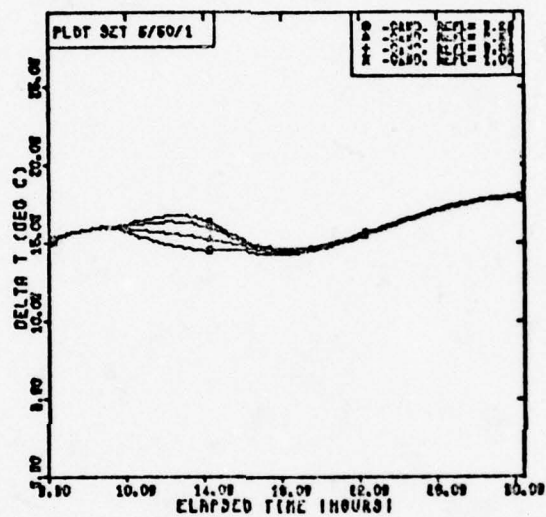


Fig. 40(a). Delta-T Plots for Ground Reflectivity

DELTA-T (TARGET-GROUND)  
PARAMETER-ORND REFL JULIAN DAY-1

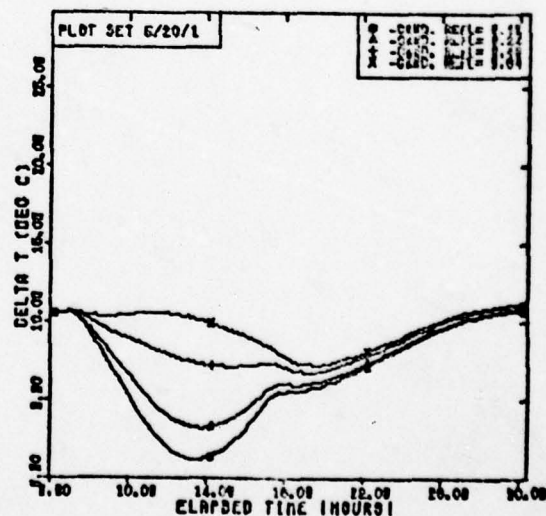
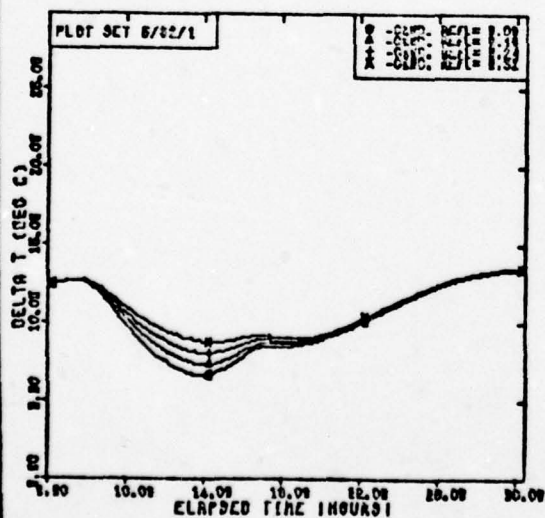
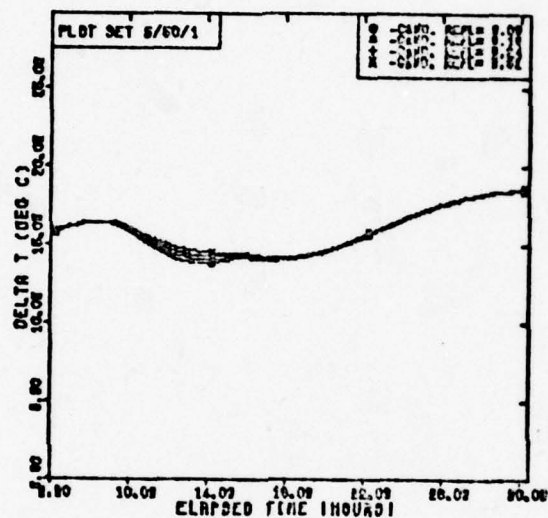


Fig. 40 (b). Delta-T Plots for Ground Reflectivity



DELTA-T (TARGET-GROUND)  
 PARAMETER-GRND REFL JULIAN DAY-00

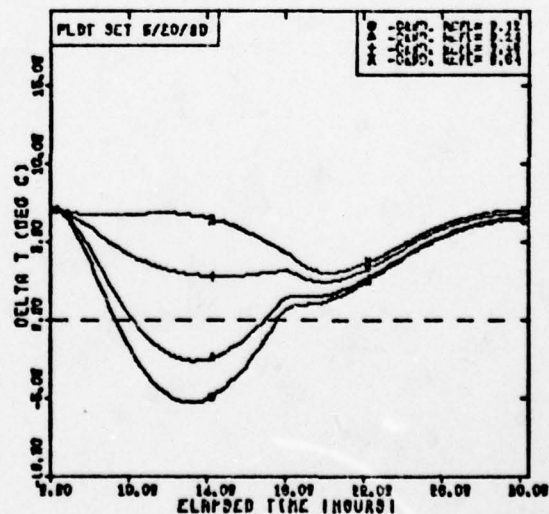
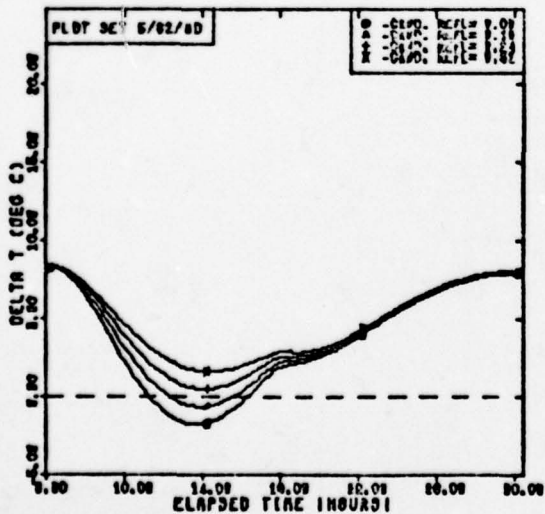
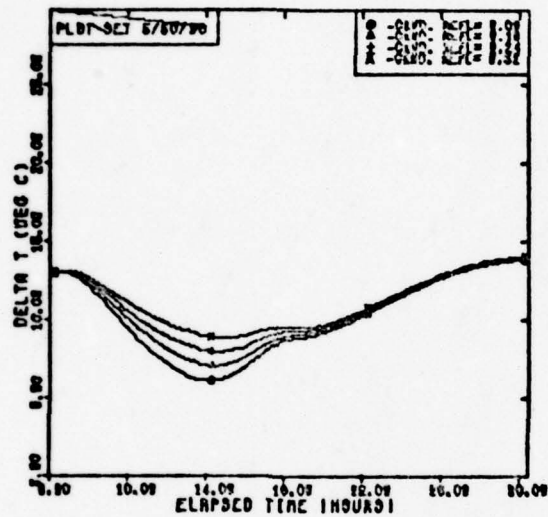


Fig. 40(c). Delta-T Plots for Ground Reflectivity

DELTA-T (TARGET-GROUND)  
PARAMETER-ORND REFL JULIAN DAY-180

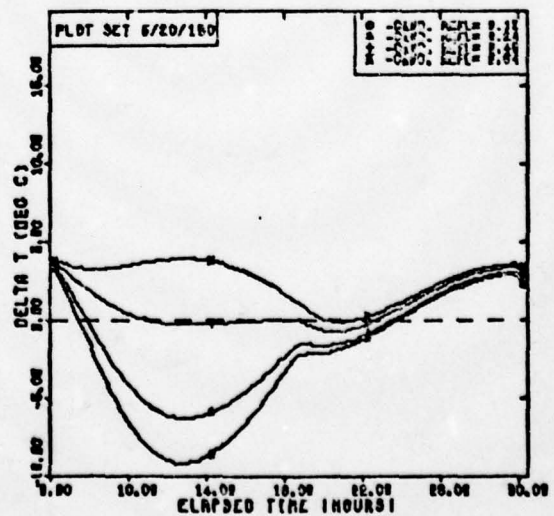
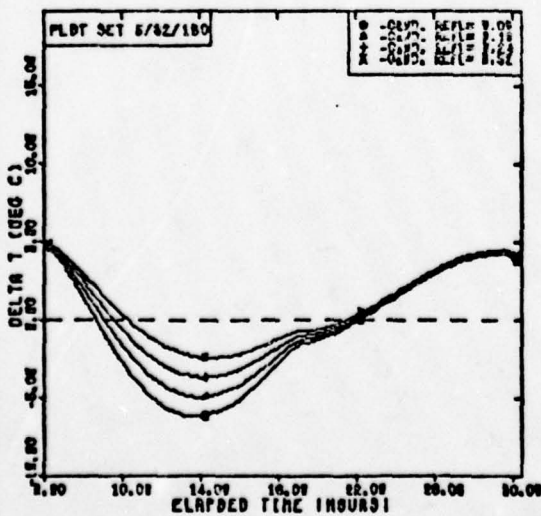
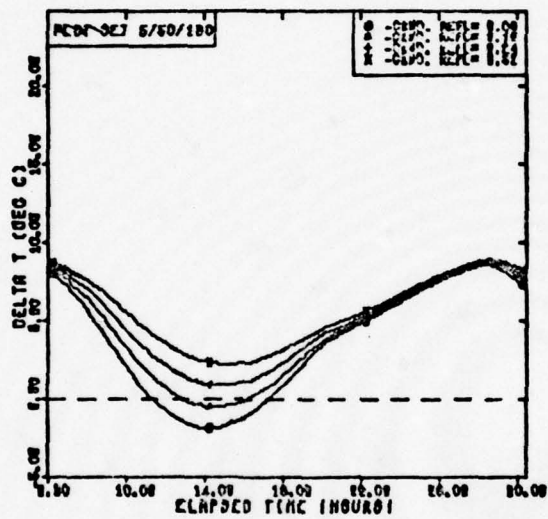


Fig. 40(d). Delta-T Plots for Ground Reflectivity

DELTA-T (TARGET-GROUND)  
 PARAMETER- ORND EM JULIAN DAY-18

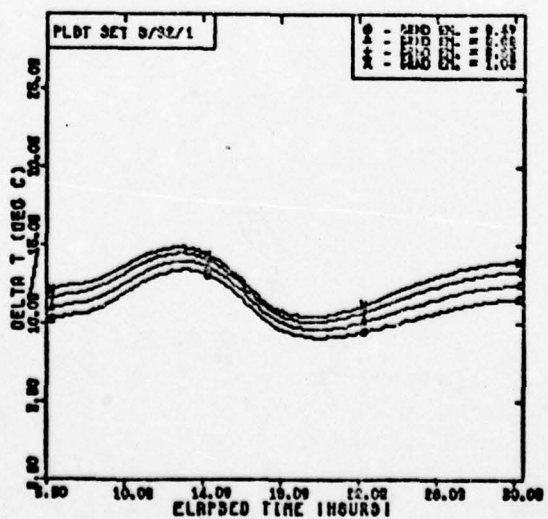
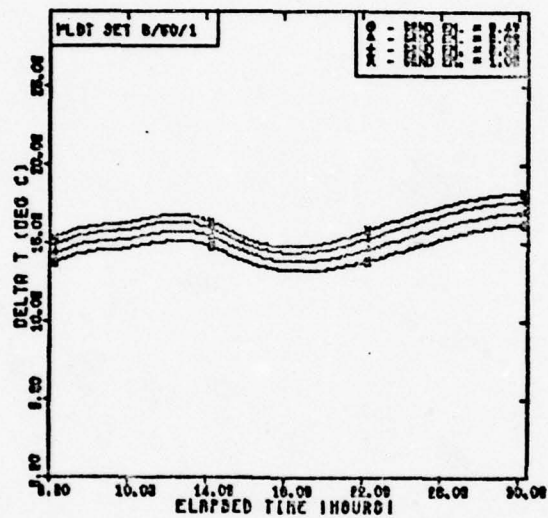
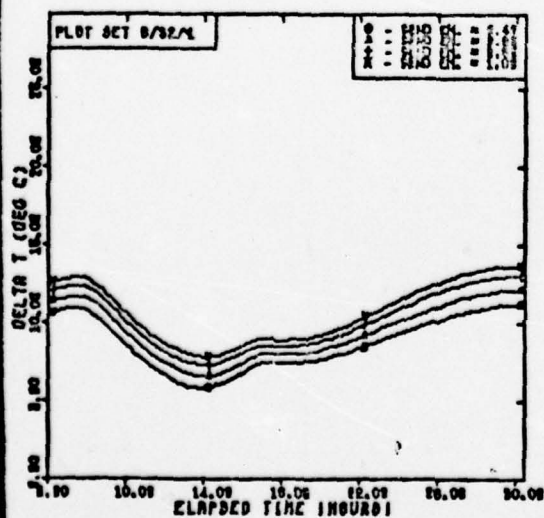
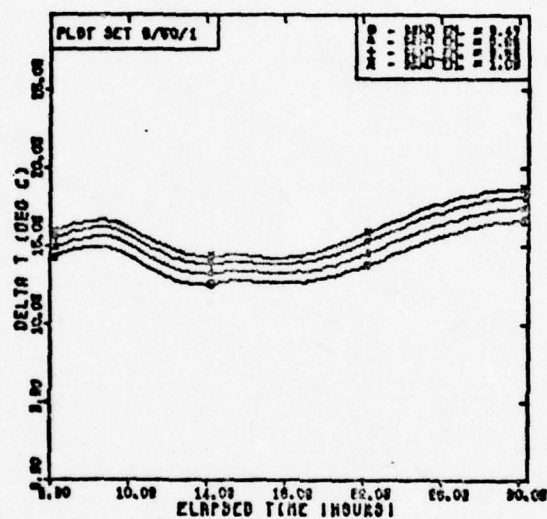


Fig. 41(a). Delta-T Plots for Ground Emmissivity

DELTA-T (TARGET-GROUND)  
 PARAMETER- ORND EM JULIAN DAY-1





DELTA-T (TARGET-GROUND)  
PARAMETER- GRND EM JUNEAN DAY-00

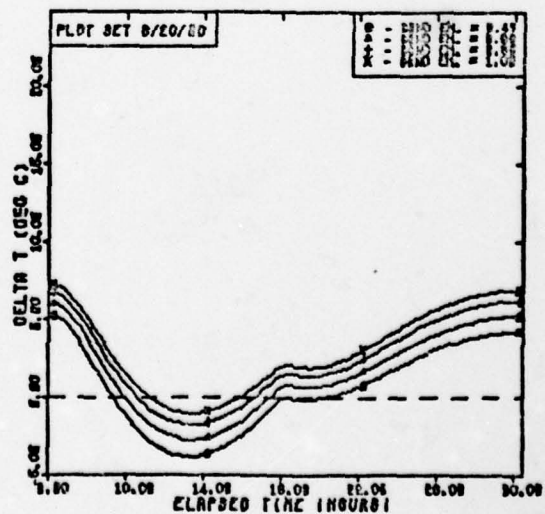
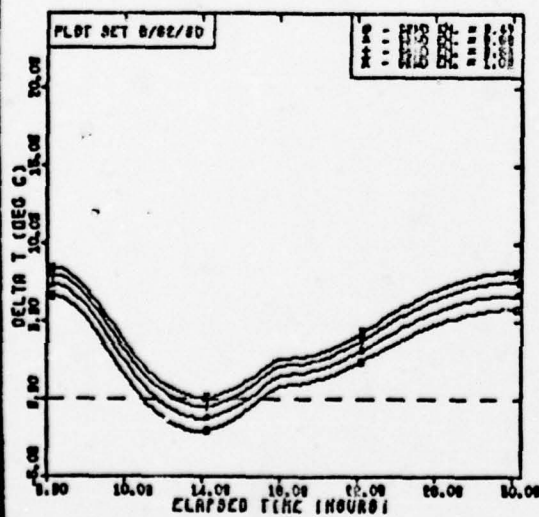
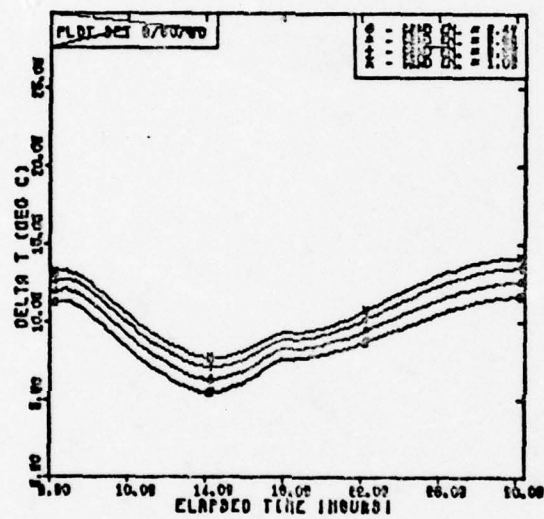


Fig. 41(c). Delta-T Plots for Ground Emmissivity

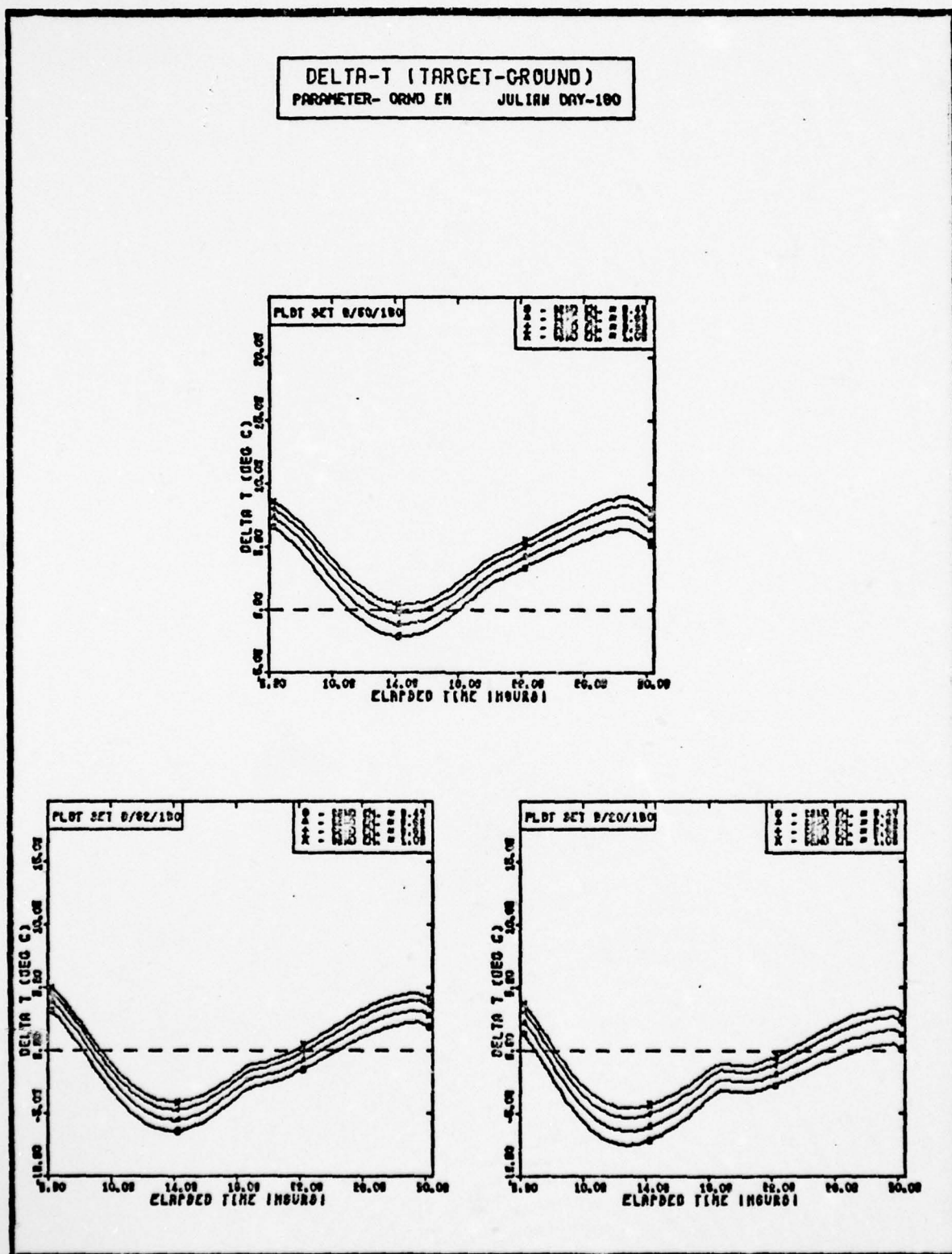


Fig. 41(d). Delta-T Plots for Ground Emmissivity

DELTA-T (TARGET-GROUND)  
PARAMETER-GRND DIFF JULIAN DAY-18

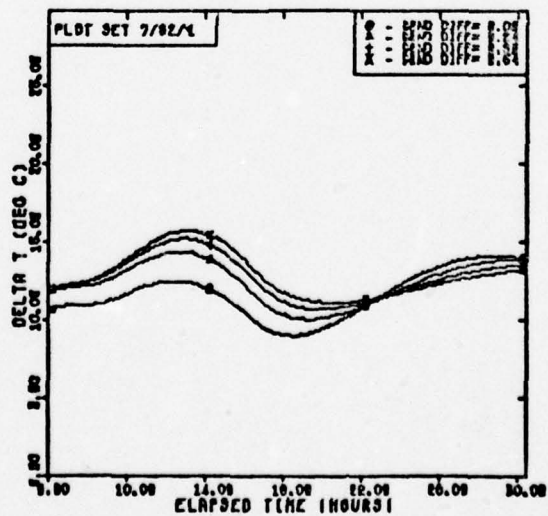
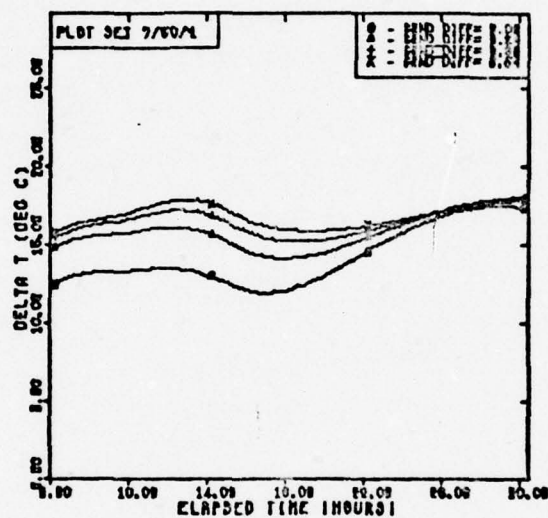


Fig. 42(a). Delta-T Plots for Ground Diffusivity

DELTA-T (TARGET-GROUND)  
PARAMETER-ORND DIFF JULIAN DAY-1

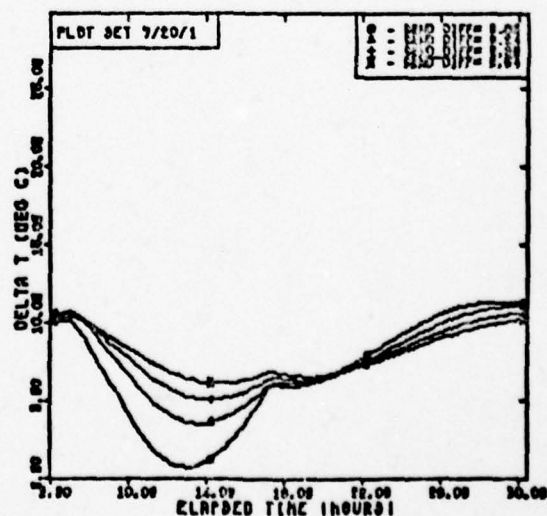
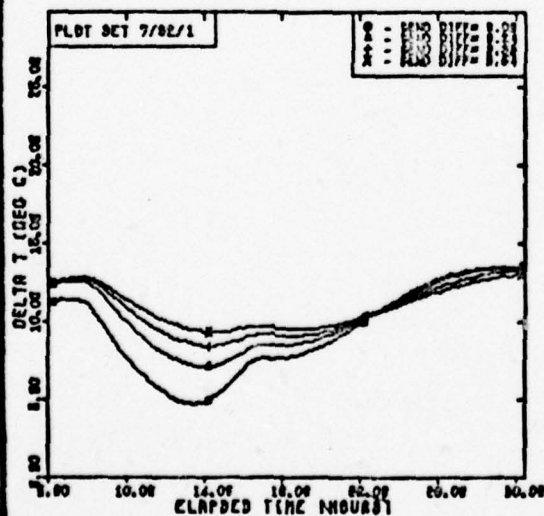
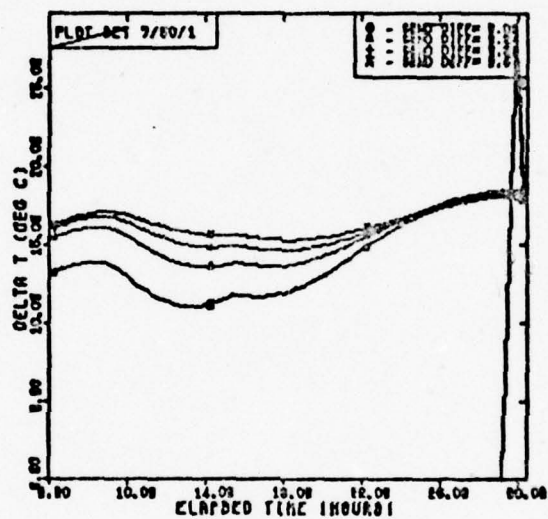


Fig. 42(b). Delta-T Plots for Ground Diffusivity



DELTA-T (TARGET-GROUND)  
PARAMETER-GRND DIFF JULIAN DAY-00

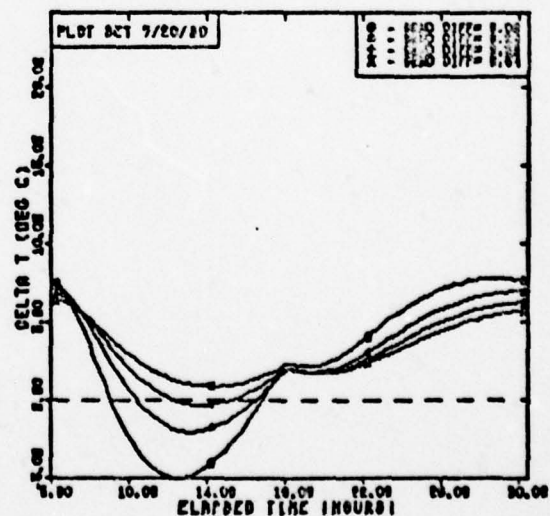
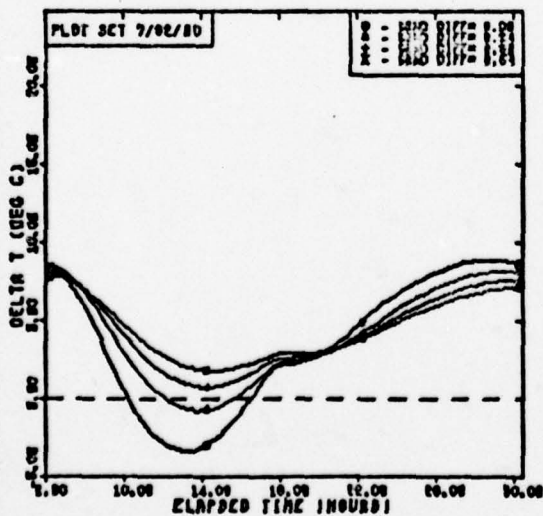
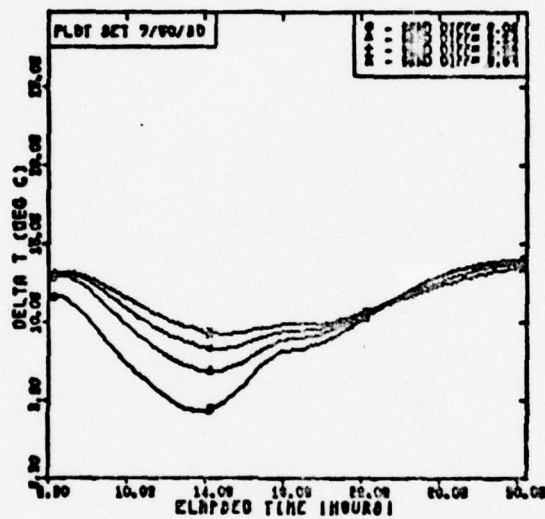


Fig. 42(c). Delta-T Plots for Ground Diffusivity

DELTA-T (TARGET-GROUND)  
PARAMETER-GRND DIFF JULIAN DAY-180

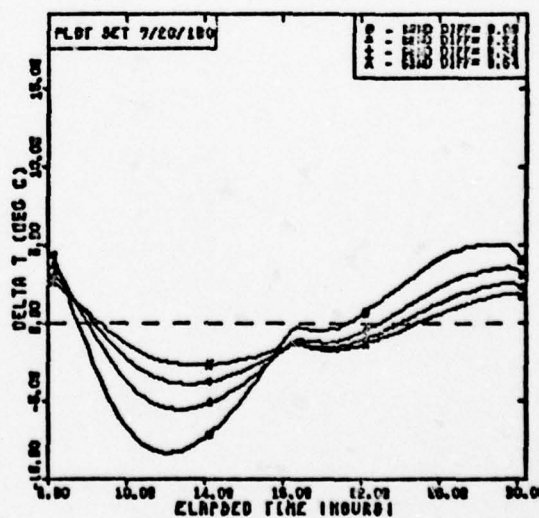
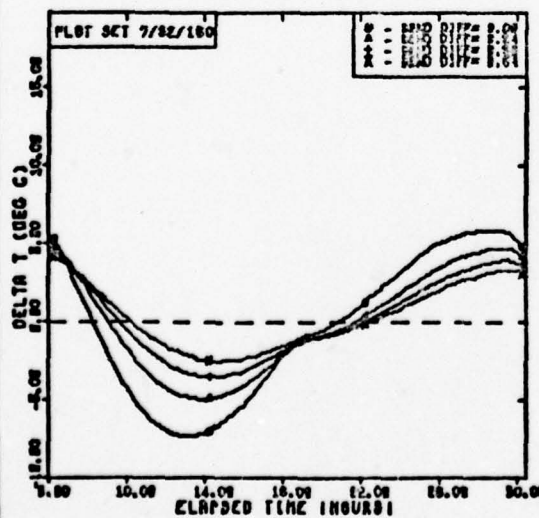
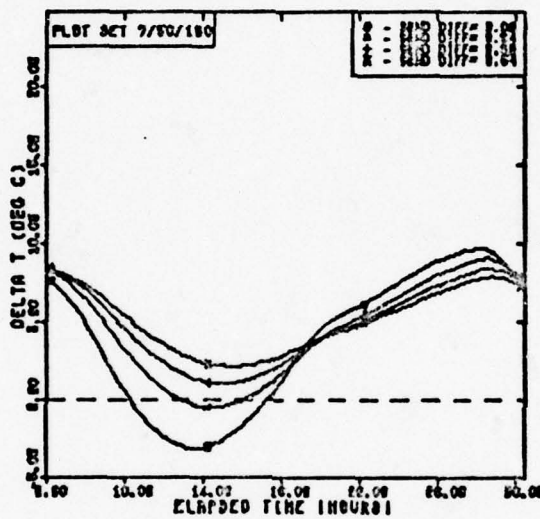


Fig. 42(d). Delta-T Plots for Ground Diffusivity

DELTA-T (TARGET-GROUND)  
 PARAMETER-TOT REF/6 JULIAN DAY-18

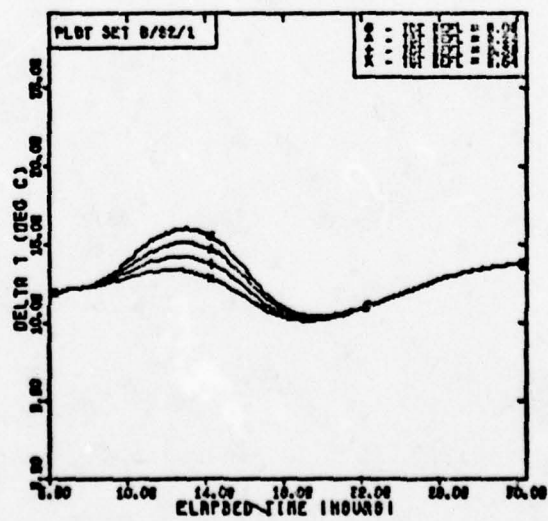
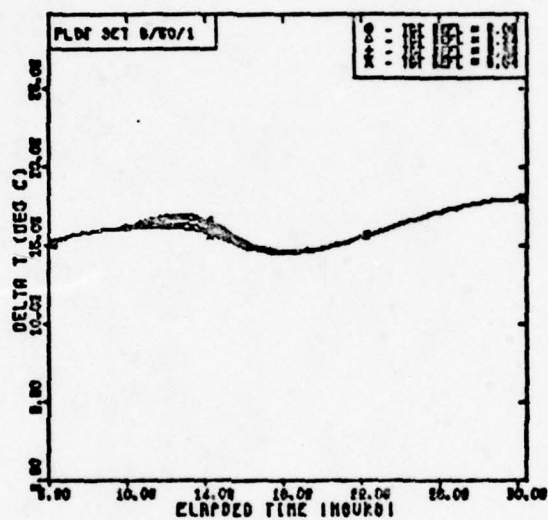


Fig. 43(a). Delta-T Plots for Target Reflectivity

DELTA-T (TARGET-GROUND)  
PARAMETER-TOT REFL. JULIAN DAY-1

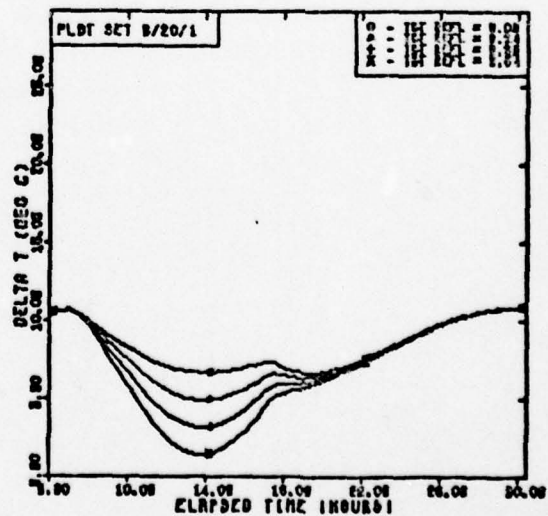
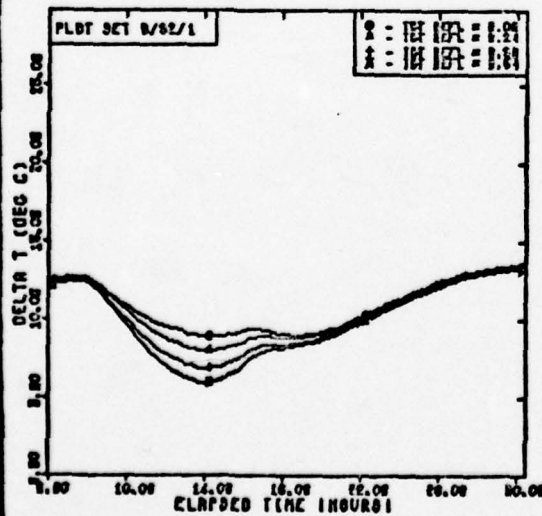
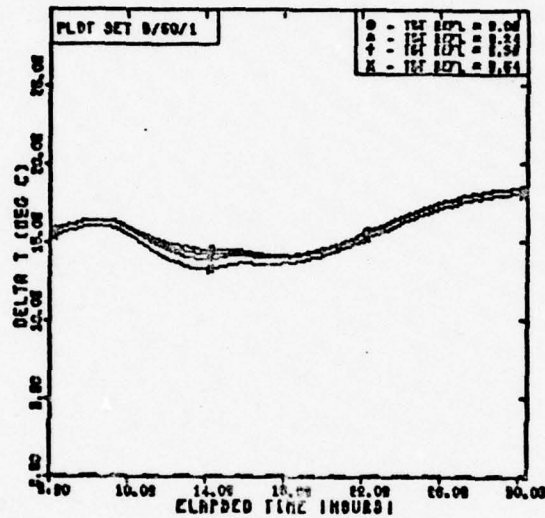


Fig. 43(b). Delta-T Plots for Target Reflectivity



DELTA-T (TARGET-GROUND)  
PARAMETER-TOT REFL. JULIAN DAY-00

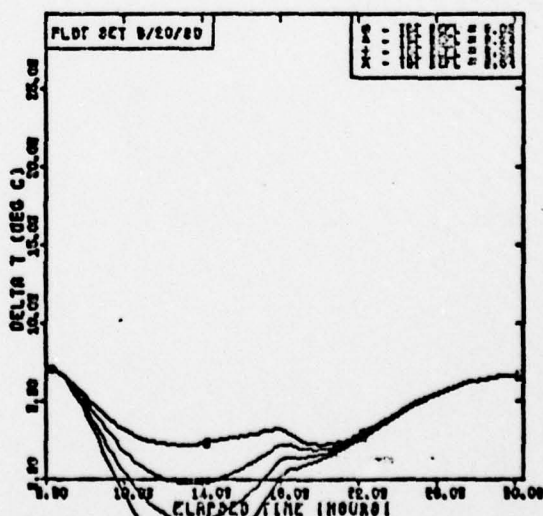
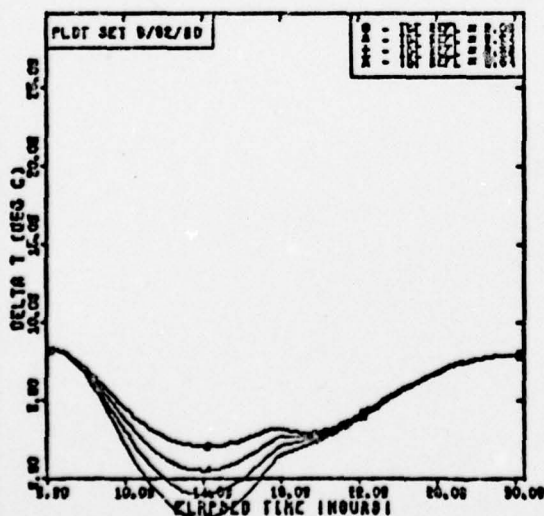
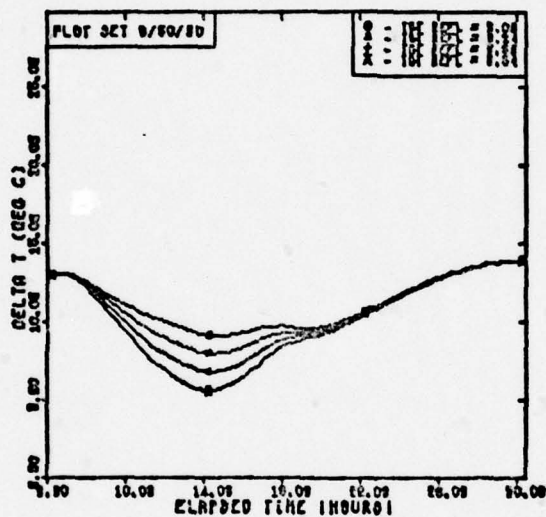


Fig. 43(c). Delta-T Plots for Target Reflectivity

DELTA-T (TARGET-GROUND)  
PARAMETER-TOT REFL. JULIAN DAY-180

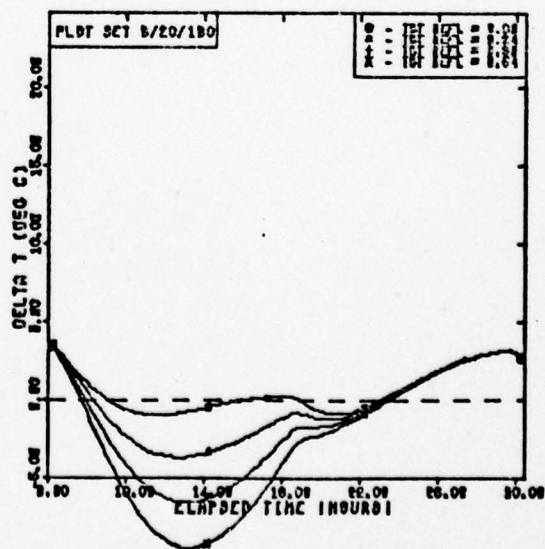
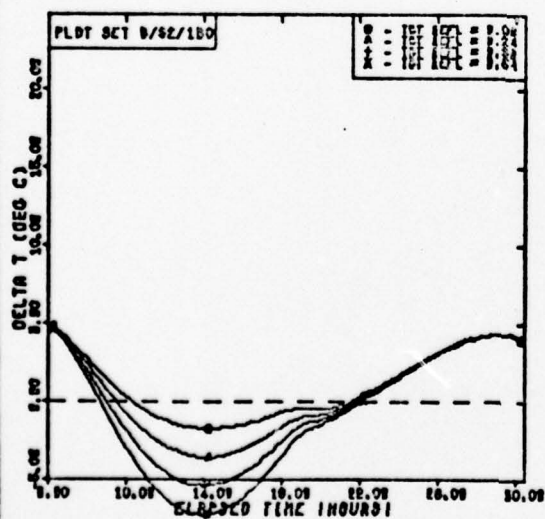
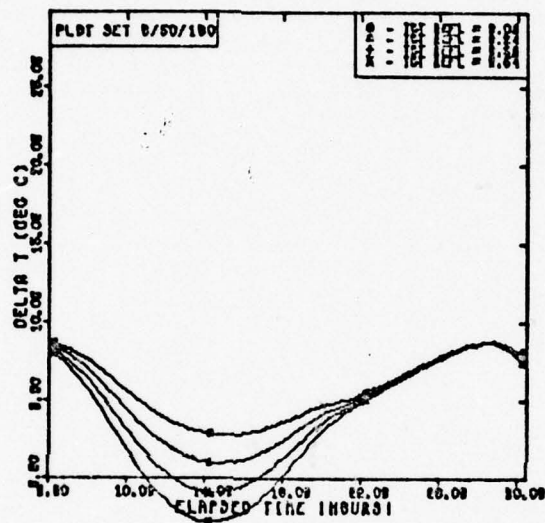


Fig. 43(d). Delta-T Plots for Target Reflectivity

DELTA-T (TARGET-GROUND)  
 PARAMETER-TOT EMISS JULIAN DAY-18

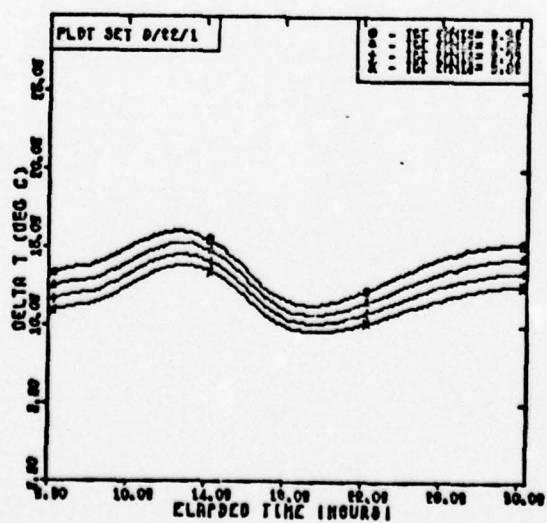
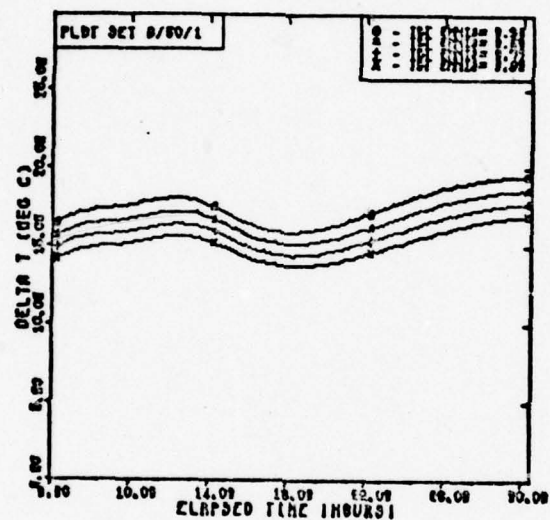


Fig. 44(a). Delta-T Plots for Target Emmissivity

DELTA-T (TARGET-GROUND)  
PARAMETER-TOT ENHIB JULIAN DAY-1

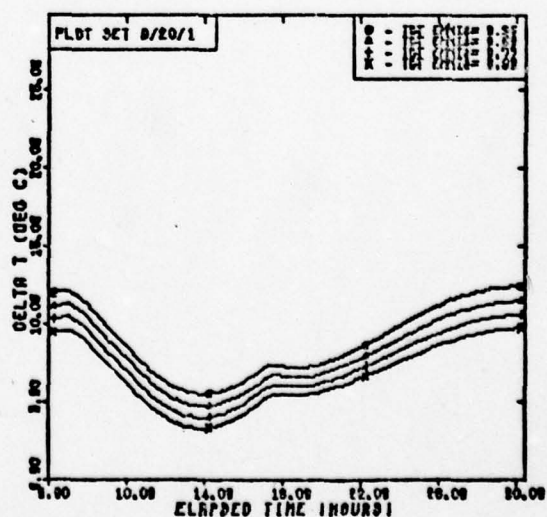
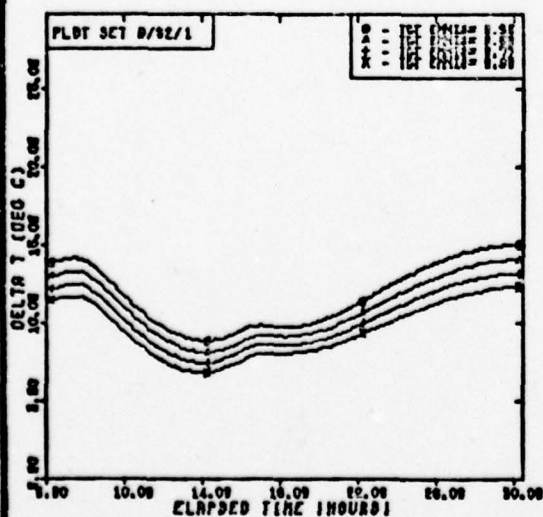
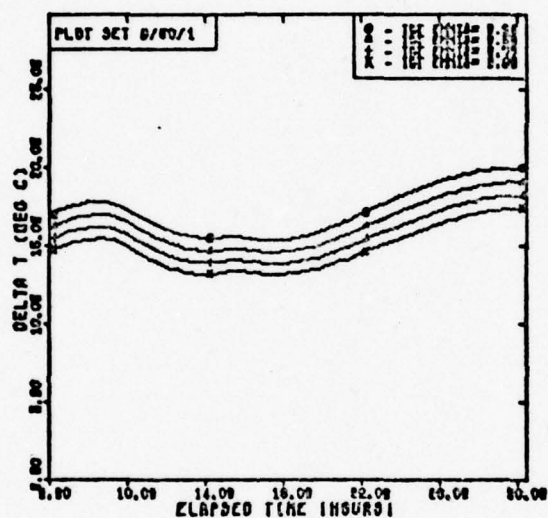


Fig. 44(b). Delta-T Plots for Target Emmissivity



DELTA-T (TARGET-GROUND)  
PARAMETER-TOT ENMI9 JULIAN DAY-00

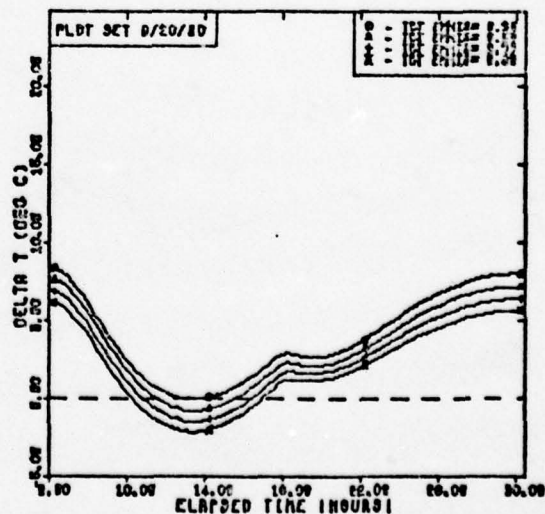
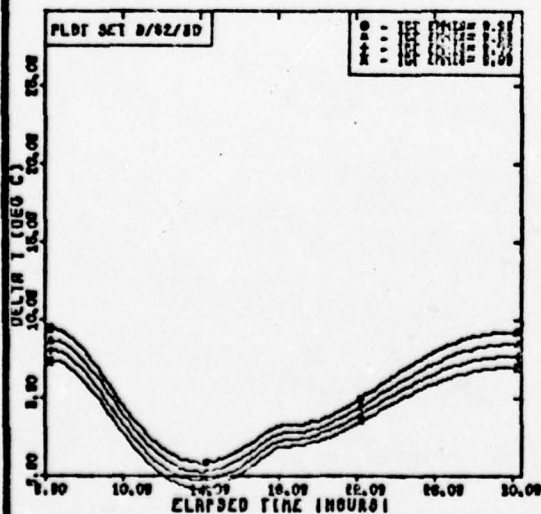
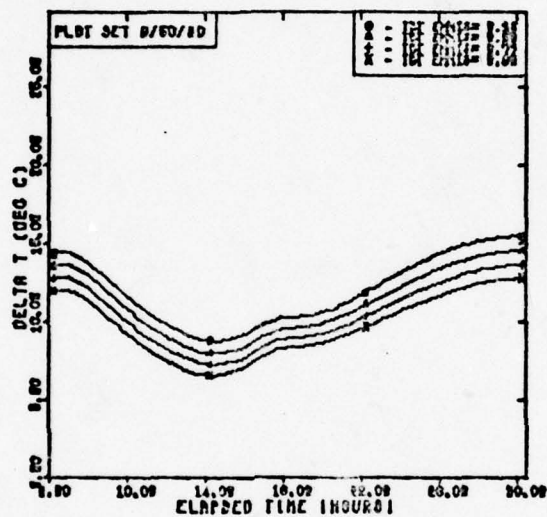


Fig. 44(c). Delta-T Plots for Target Emmissivity

DELTA-T (TARGET-GROUND)  
PARAMETER-TOT ENNIS JULIAN DAY-190

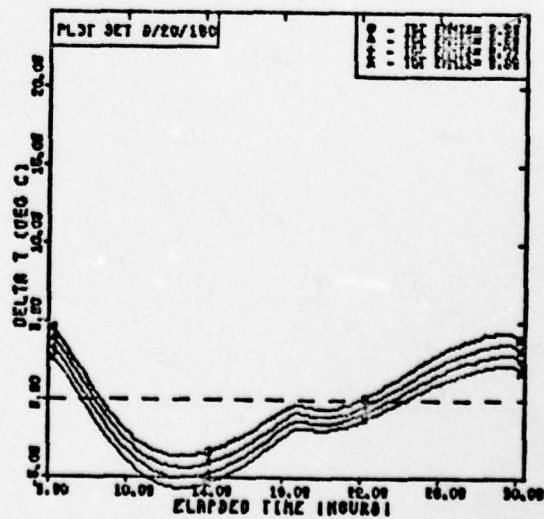
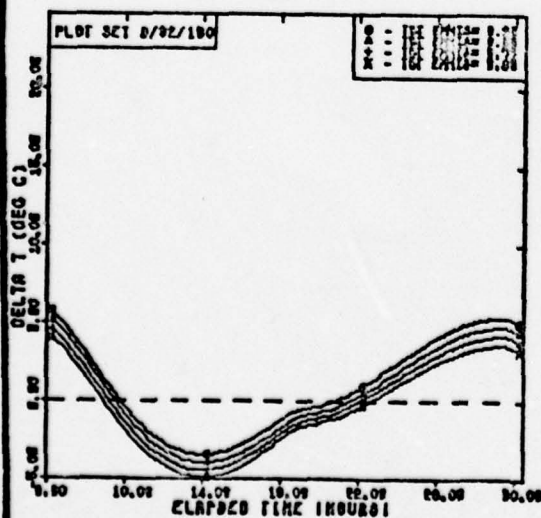
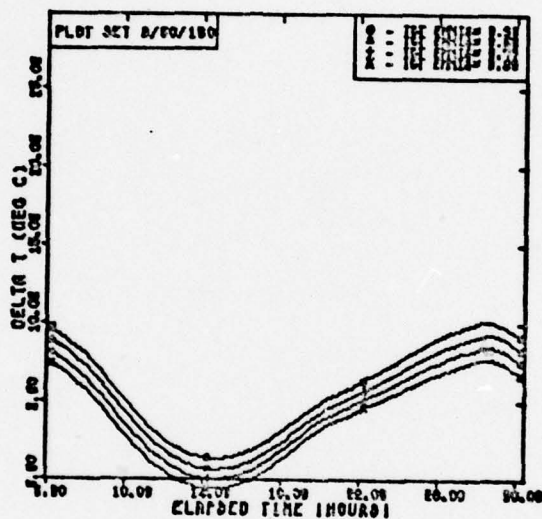


Fig. 44(d). Delta-T Plots for Target Emmissivity

DELTA-T (TARGET-GROUND)  
PARAMETER-TOT THICK JULIAN DAY-10

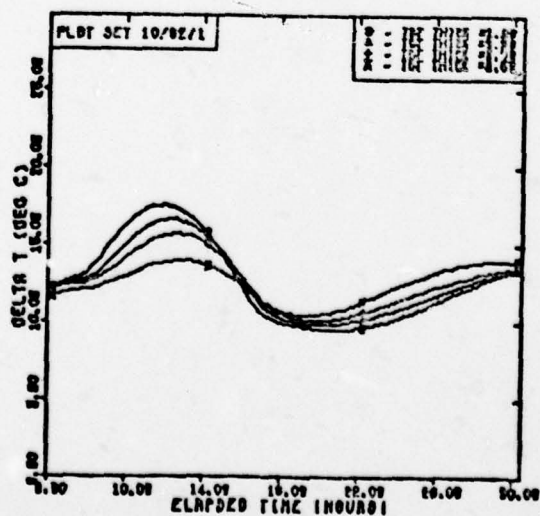
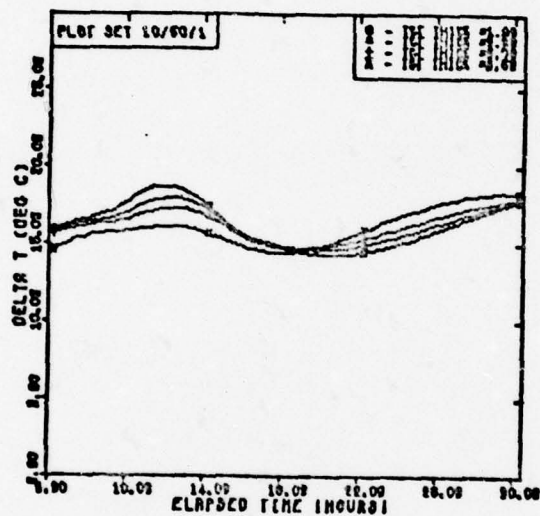


Fig. 45(a). Delta-T Plots for Target Thickness

DELTA-T (TARGET-GROUND)  
PARAMETER-TOT THICK JULIAN DAY-1

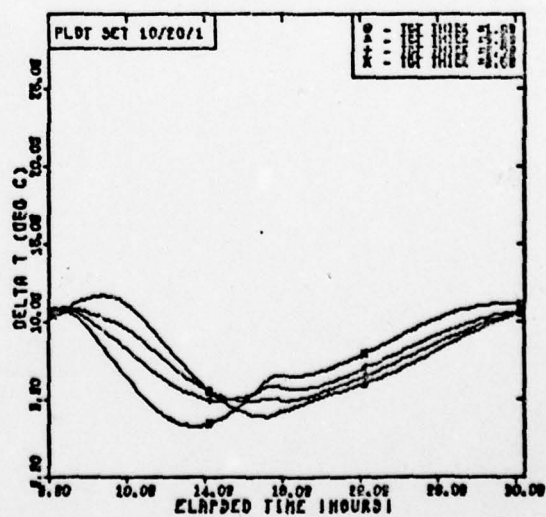
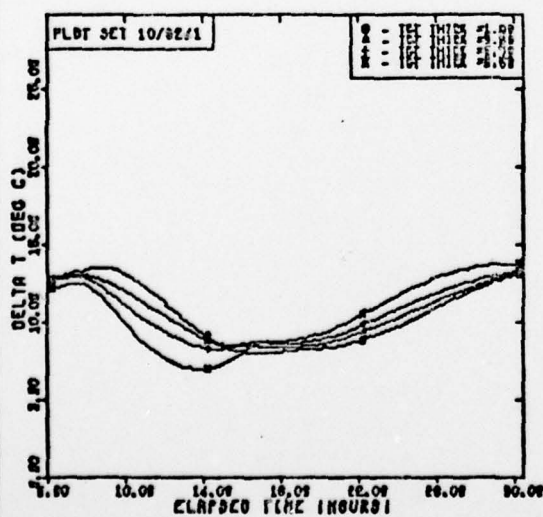
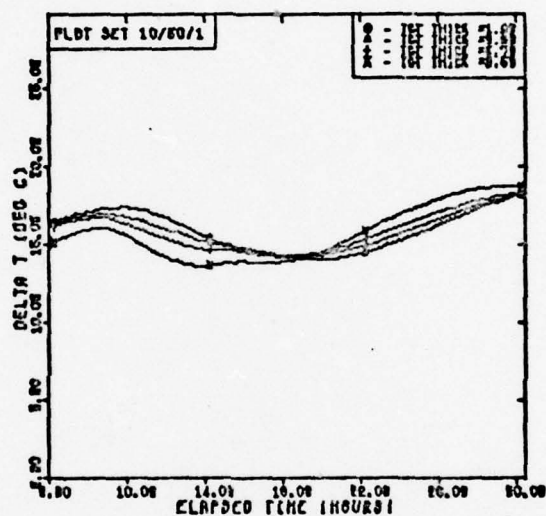


Fig. 45(b). Delta-T Plots for Target Thickness



DELTA-T (TARGET-GROUND)  
PARAMETER-TOT THICK JULIAN DAY-90

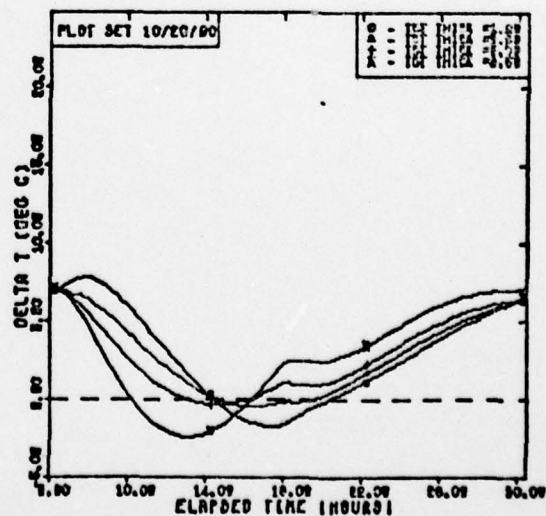
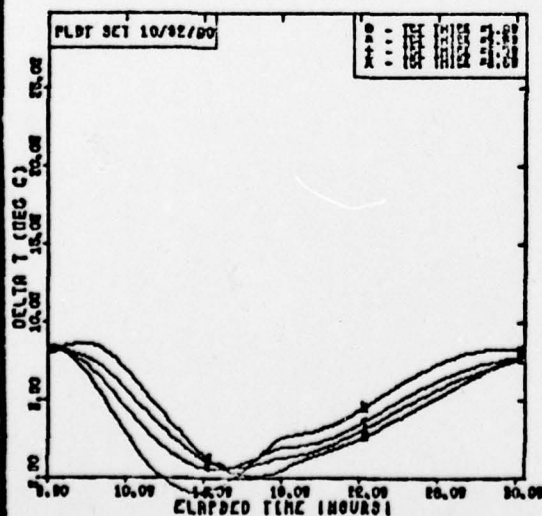
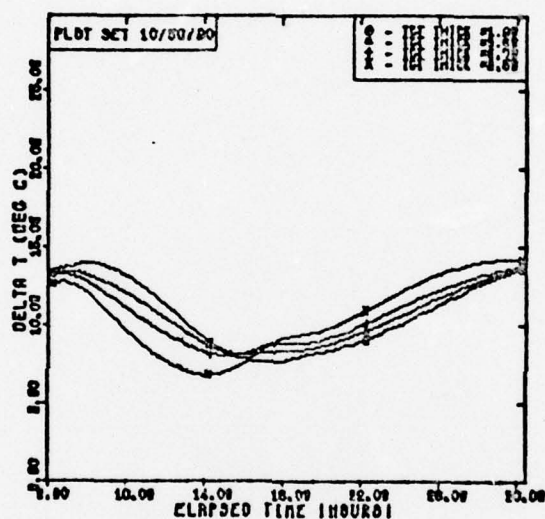


Fig. 45(c). Delta-T Plots for Target Thickness

DELTA-T (TARGET-GROUND)  
 PARAMETER-TOT THICK JULIAN DAY-100

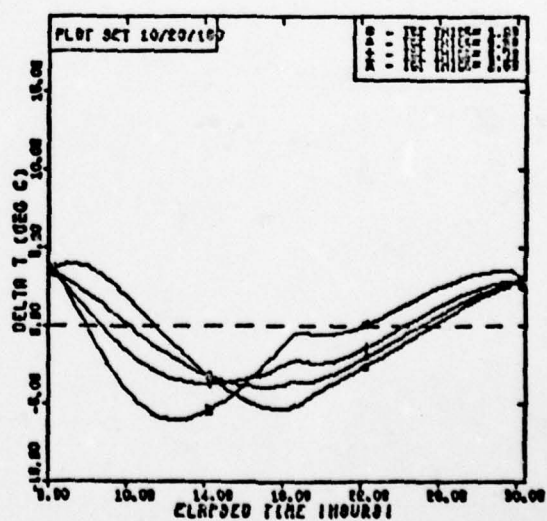
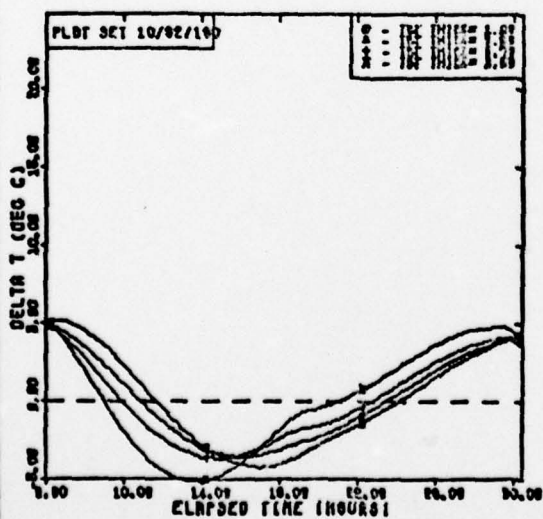
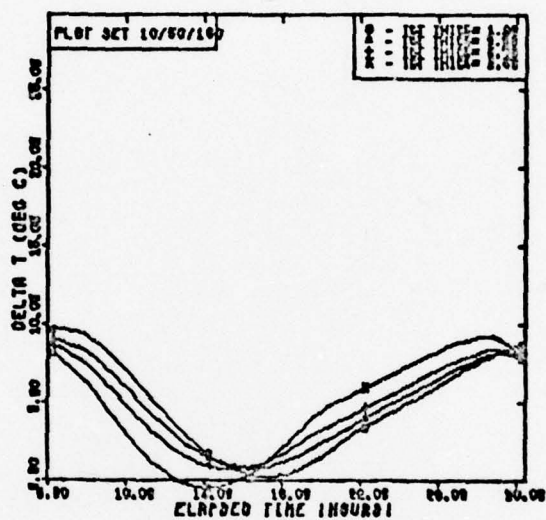


Fig. 45(d). Delta-T Plots for Target Thickness

DELTA-T (TARGET-GROUND)  
PARAMETER-A.C. VEL. JULIAN DAY-18

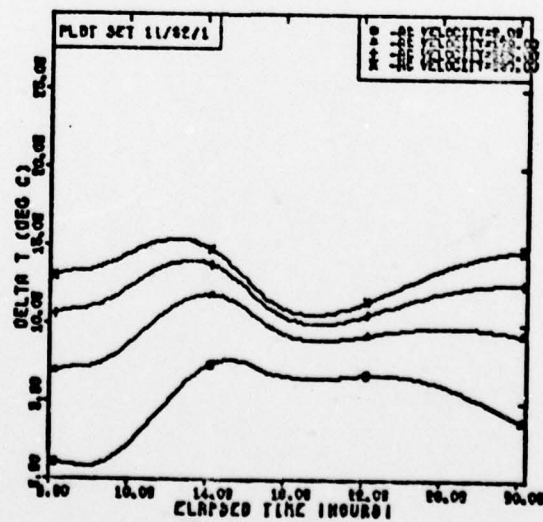
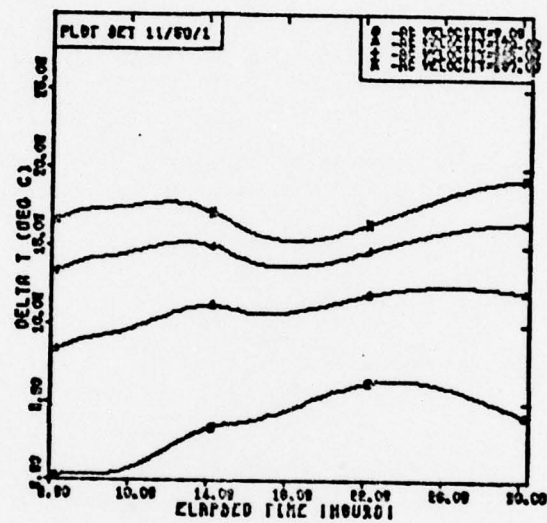


Fig. 46(a). Delta-T Plots for A.C. Velocity

DELTA-T (TARGET-GROUND)  
PARAMETER-A.C. VEL. JULIAN DAY-1

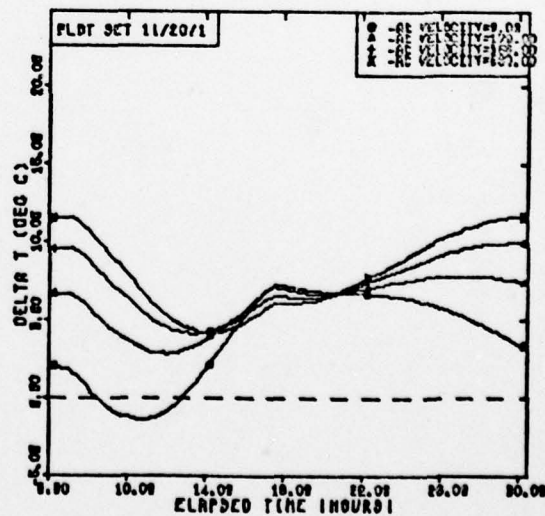
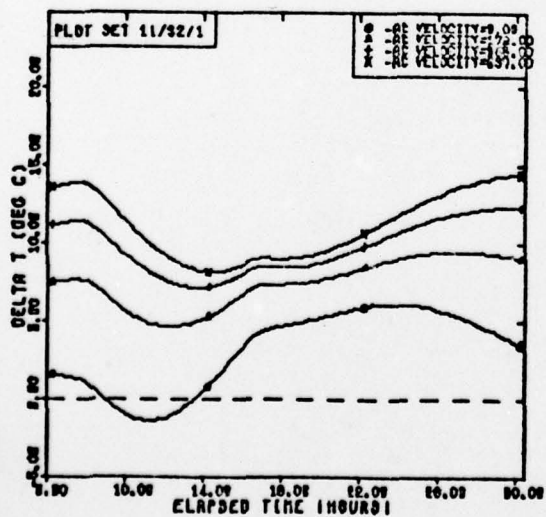
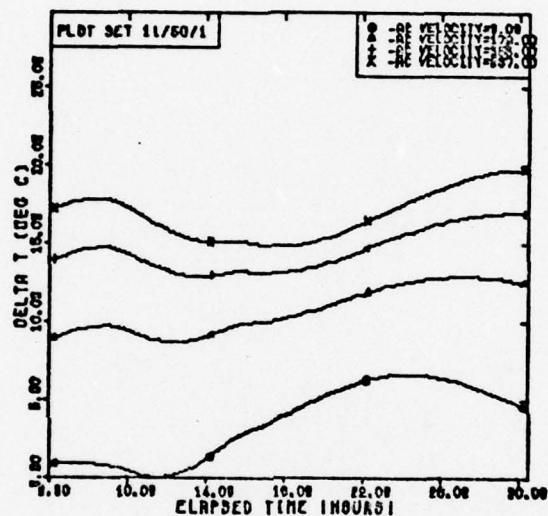


Fig. 46(b). Delta-T Plots for A.C. Velocity



DELTA-T (TARGET-GROUND)  
PARAMETER-A.C. VEL. JULIAN DAY-00

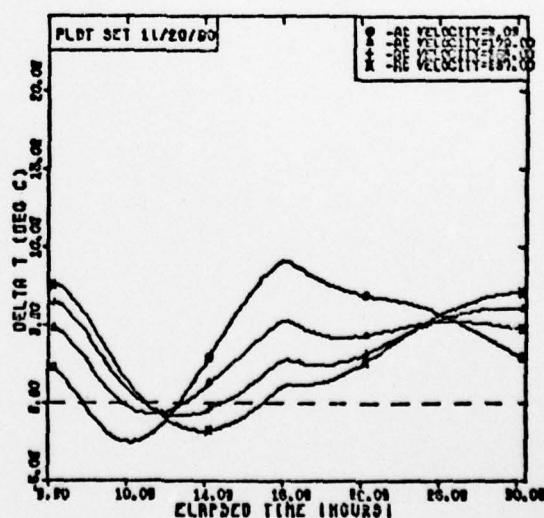
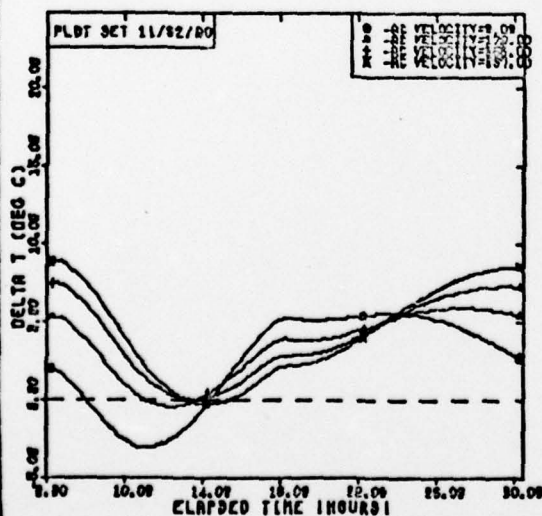
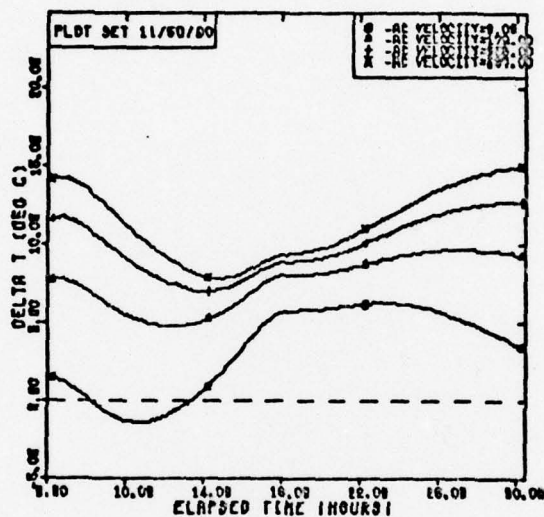


Fig. 46(c). Delta-T Plots for A.C. Velocity

DELTA-T (TARGET-GROUND)  
PARAMETER-A.C. VEL. JULIAN DAY-180

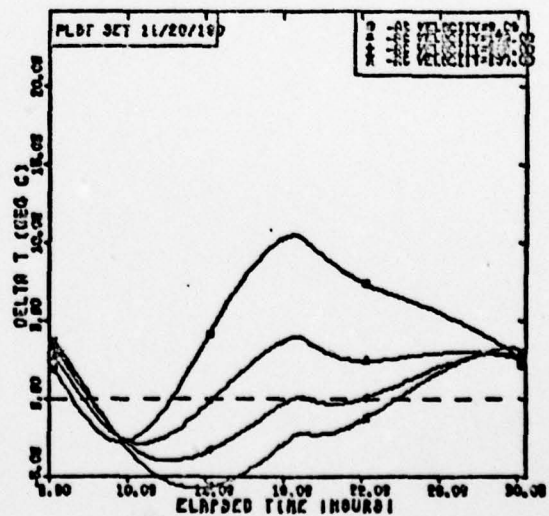
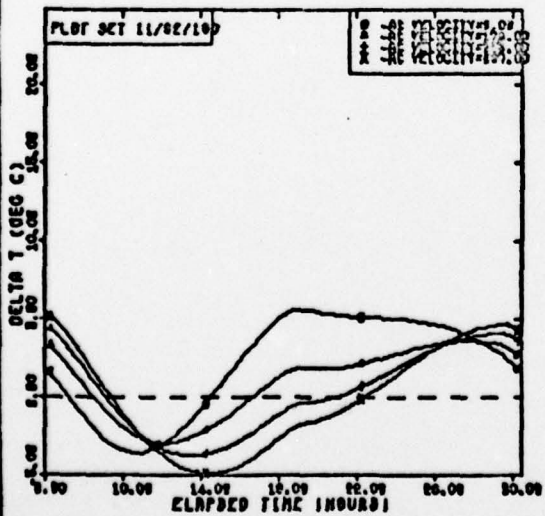
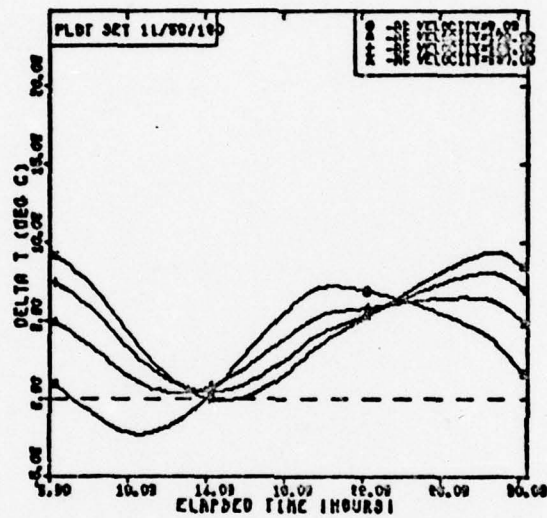


Fig. 46(d). Delta-T Plots for A.C. Velocity

## Appendix E

### Sample Target/Background Physical Characteristics

Table VI is a listing of some of the physical characteristics of the targets and backgrounds used in this report, they are from a variety of references, listed in the Bibliography. Figure 47, taken from McClatchey (Ref 29:75) shows the variation of the reflectivities of some natural objects in the range of .4 to 14 microns.



Table VII

## Sample Target/Background Characteristics

Characteristic	Substance	Value	Reference
Reflectivity	Soil(Wet)	.05	Ref 14:14
	Soil(Dry)	.16	"
	Sand(Wet)	.008	"
	Sand(Dry)	.087	"
	"Terrain"	.2	Ref 14:8
	Oxidised Iron	.1	Ref 27
	Brown Paint	.01	"
	Olive Drabe Paint	.06 - .07	"
	Oak Leaf	.1 - .45	"
	Maple Leaf	.1 - .4	"
(Albedo)	Grass	.25	Ref 26:14
Diffusivity	Soil(Dry)	.01 ft <sup>2</sup> /hr(.15 cm <sup>2</sup> /min)	Ref 16:594
	Soil(Wet)	.0031 cm <sup>2</sup> /sec(.186 cm <sup>2</sup> /min)	Ref 28:143
	Soil(Avg)	.0046 cm <sup>2</sup> /sec(.276 cm <sup>2</sup> /min)	Ref 21:497
	Soil(Sandy,Dry)	.002 cm <sup>2</sup> /sec(.12 cm <sup>2</sup> /min)	"
	Soil(8% H <sub>2</sub> O)	.0033 cm <sup>2</sup> /sec(.198 cm <sup>2</sup> /min)	"
	Soil(Damp)	.005 cm <sup>2</sup> /sec(.3 cm <sup>2</sup> /min)	Ref 28:143
	Sandstone	.0113 cm <sup>2</sup> /sec(.678 cm <sup>2</sup> /min)	"
	"	.011 cm <sup>2</sup> /sec(.66 cm <sup>2</sup> /min)	Ref 21:497
	"	.045 ft <sup>2</sup> /hr(.7 cm <sup>2</sup> /min)	Ref 15:508
	Limestone	.017 ft <sup>2</sup> /hr(.26 cm <sup>2</sup> /min)	Ref 16:594
	"	.007 cm <sup>2</sup> /sec(.42 cm <sup>2</sup> /min)	Ref 21:497
	"	.0081 cm <sup>2</sup> /sec(.49 cm <sup>2</sup> /min)	Ref 28:143
	Rock(Avg)	.0118 cm <sup>2</sup> /sec(.71 cm <sup>2</sup> /min)	Ref 21:497
	Rock	.0118 cm <sup>2</sup> /sec(.71 cm <sup>2</sup> /min)	Ref 28:143
	Snow	.005 cm <sup>2</sup> /sec(.3 cm <sup>2</sup> /min)	Ref 21:497
	Snow(Fresh)	.0033 cm <sup>2</sup> /sec(.198 cm <sup>2</sup> /min)	Ref 28:143
	Water	.00144 cm <sup>2</sup> /sec(.084 cm <sup>2</sup> /min)	Ref 21:497
	Ice	.0115 cm <sup>2</sup> /sec(.68 cm <sup>2</sup> /min)	"



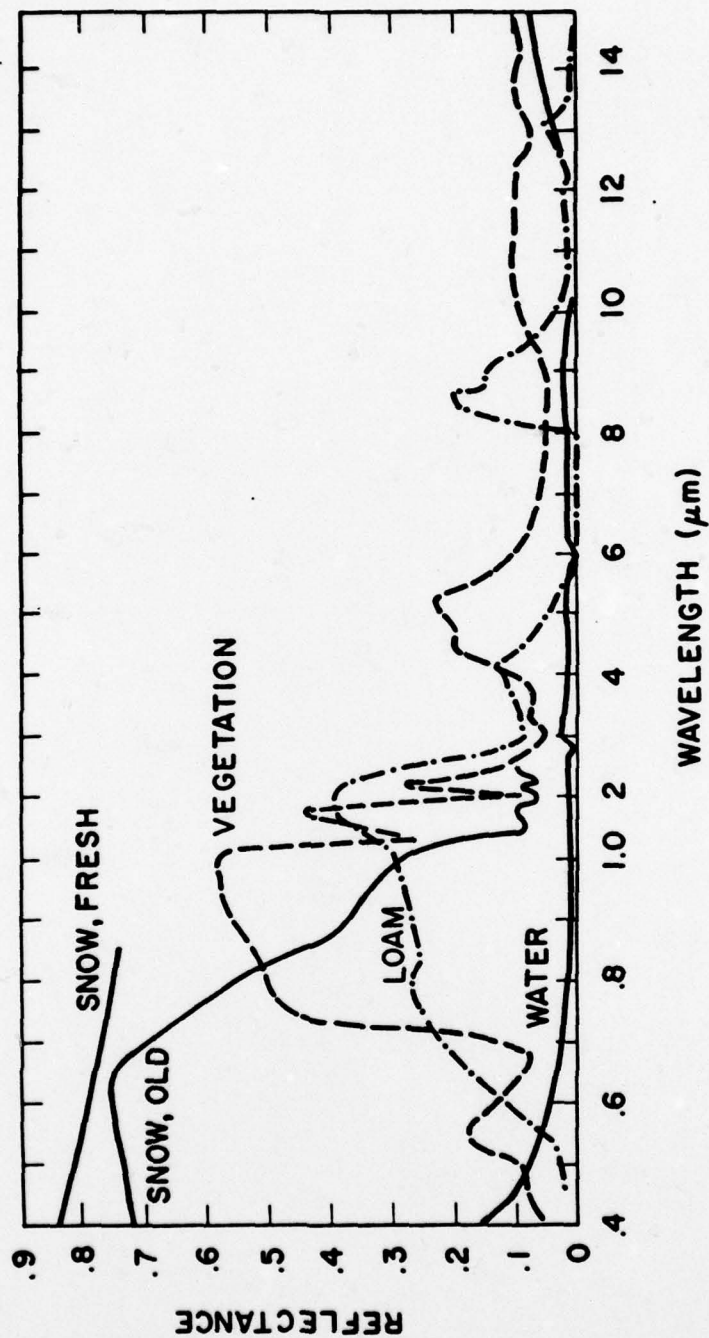


Fig. 47 Typical Reflectance of Water Surface, Snow, Dry Soil, and Vegetation. (Ref 29:75)

## VITA

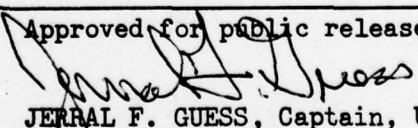
John Thomas Small, Jr. Was born on 16 June 1947 in Rochester, Minnesota. He graduated from Rothesay Collegiate School, Rothesay, New Brunswick, Canada in 1964, then attended McGill University, Montreal, Canada and Rockford College, Rockford, Illinois, receiving a Bachelor of Arts degree in Zoology from the latter in May 1968. Upon graduation, he entered Officer Training School and was commissioned in the USAF in February 1969. He completed pilot training at Vance Air Force Base, Oklahoma and received his wings in March 1970. He then served as a C-130 pilot in the 345th Tactical Airlift Squadron, Ching Chuan Kang Air Force Base, Taiwan. From there he was transferred to fly B-52G aircraft at Loring Air Force Base, Maine, and while there, he served a temporary duty tour flying the B-52G over Southeast Asia from Anderson Air Force Base, Guam under Operation Bullet Shot. In June 1975, he entered the Air Force Institute of Technology as an undergraduate student in Engineering Sciences, and later as a graduate student in Engineering Physics.

Permanent address: 851 So. Logan St.

Denver, Colorado 80209

Unclassified

SECURITY CLASSIFICATION OF THIS PAGE (When Data Entered)

REPORT DOCUMENTATION PAGE		READ INSTRUCTIONS BEFORE COMPLETING FORM
1. REPORT NUMBER GEP/PH/77-12	2. GOVT ACCESSION NO.	3. RECIPIENT'S CATALOG NUMBER
4. TITLE (and Subtitle) A THEORETICAL ANALYSIS OF CHANGES IN THERMAL SIGNATURES CAUSED BY PHYSICAL AND CLIMATOLOGICAL FACTORS		5. TYPE OF REPORT & PERIOD COVERED MS Thesis
		6. PERFORMING ORG. REPORT NUMBER
7. AUTHOR(s) John T. Small, Jr. Captain		8. CONTRACT OR GRANT NUMBER(s)
9. PERFORMING ORGANIZATION NAME AND ADDRESS Air Force Institute of Technology (AFIT-EN) Wright-Patterson AFB, Ohio 45433		10. PROGRAM ELEMENT, PROJECT, TASK AREA & WORK UNIT NUMBERS
11. CONTROLLING OFFICE NAME AND ADDRESS		12. REPORT DATE December 1977
		13. NUMBER OF PAGES 257
14. MONITORING AGENCY NAME & ADDRESS (if different from Controlling Office) Lt Col Carl T. Case Headquarters AF/SAGF Washington, D.C. 20330		15. SECURITY CLASS. (of this report) Unclassified
		15a. DECLASSIFICATION/DOWNGRADING SCHEDULE
16. DISTRIBUTION STATEMENT (of this Report) Approved for public release; distribution unlimited		
17. DISTRIBUTION STATEMENT (of the abstract entered in Block 20, if different from Report)		
18. SUPPLEMENTARY NOTES Approved for public release; IAW AFR 190-17  JERRAL F. GUESS, Captain, USAF Director of Information		
19. KEY WORDS (Continue on reverse side if necessary and identify by block number) Diurnal Cycle      Tank Signatures Energy Balance      Temperature Model Infrared Signatures      Thermal Signature Mathematical Thermal Model      Tree Modeling Plants (Botany)		
20. ABSTRACT (Continue on reverse side if necessary and identify by block number) An investigation of the thermal signatures of natural objects is undertaken. Using the principle of energy balance, diurnal temperature models are developed for the ground, a vehicle (such as a tank), and the leaves of a tree. These models are included in a computer program designed to simulate daily variations in conductive, radiative, and convective heat transfer processes. Environmental conditions are changed by altering the program inputs, which include; latitude, day, wind speed, mean air temperature, cloud type, total insolation, absolute and relative humidity, atmospheric pressure, and particulate con-		

DD FORM 1 JAN 73 1473

EDITION OF 1 NOV 65 IS OBSOLETE

Unclassified

SECURITY CLASSIFICATION OF THIS PAGE (When Data Entered)



Unclassified

SECURITY CLASSIFICATION OF THIS PAGE(When Data Entered)

centration. The program is iterated for several values of a single parameter such as one of the environmental inputs, or one of 21 physical characteristics of the models (for example; ground reflectivity, tank thickness, or leaf transpiration rate). There are two types of output from the program; simultaneous plots of the temperatures of all the models for a 30-hour period, and curves representing 24-hour periods of the temperature difference (Delta-T) between the tank and the ground. The effects of changing a parameter are analyzed by comparing the various Delta-T curves.

In this study, 11 scenarios (representing three geographical locations and a variety of climatic conditions) are used to examine the following parameters; mean temperature, absolute humidity, wind speed, cloud cover, ground/target reflectivity and emissivity, ground diffusivity, target thickness, and tank air conditioning velocity. Analysis of the Delta-T curves indicates that overall, the ground emissivity appears to affect the temperatures the most, while the amount of insolation affects them the least.

Unclassified

SECURITY CLASSIFICATION OF THIS PAGE(When Data Entered)